POLYMERIC-BASED MEMBRANES FOR HYDROGEN ENRICHMENT AND NATURAL GAS SWEETENING

LOW BEE TING

NATIONAL UNIVERSITY OF SINGAPORE

2009

POLYMERIC-BASED MEMBRANES FOR HYDROGEN ENRICHMENT AND NATURAL GAS SWEETENING

LOW BEE TING

(B.Eng., National University of Singapore, Singapore)

A THESIS SUBMITTED

FOR THE DEGREE OF DOCTOR OF PHILOSOPHY

DEPARTMENT OF CHEMICAL AND BIOMOLECULAR ENGINEERING

NATIONAL UNIVERSITY OF SINGAPORE

2009

ACKNOWLEDGEMENTS

The journey to the accomplishment of a PhD degree is certainly full of challenges. As my time as a graduate student draws to a close, I would like to acknowledge the people who made this endeavor a wonderful and rewarding experience. First and foremost, I wish to thank my family and friends for their constant support and love throughout my candidature. My academic advisor, Professor Chung Tai-Shung, Neal is an enthusiastic membrane scientist who has bestowed numerous opportunities and well-equipped research facilities for me to excel in my research playground. Over the past three years, he has pushed me to achievements beyond what I ever imagine and nurtured me as an independent researcher. I wish to express my sincere appreciation to Professor Chung for his teaching and guidance.

My mentor, Dr. Xiao Youchang has been a constant source of advice, inspiration and encouragement. He is an exceptionally creative and intelligent researcher, without whom a significant portion of the work described herein may have been unattainable. It is indeed a true blessing to have the opportunity to work with him. Thanks are given to my buddy, Dr. Widjojo Natalia who has guided me in my research from the first day I embarked on this tough research expedition. She has showered me with love and joy, and has made my life as a graduate student colorful and enjoyable. Thank you both for always being there for me and for telling me what I need to hear and not what I want to hear at the critical moments.

I would like to convey my appreciation to Dr. Shao Lu and Dr Wang Kaiyu for their valuable advice to my work, and for sharing their knowledge and technical expertise with me. Special thanks are dedicated to Professor Donald R. Paul from the University of Texas at Austin and Professor Maria R. Coleman from the University of Toledo for their professional and constructive suggestions. My gratitude extends to Ms Chng Mei Lin for her helpful assistance in the daily operations of my experiments and for being a great friend. Thanks are due to the fun-loving members of Professor Chung's group, the resourceful and helpful laboratory technologists and all who have assisted me in one way or another.

I gratefully acknowledge the research scholarship by the National University of Singapore. I would like to thank the Singapore National Research Foundation (NRF) for the support on the Competitive Research Programme for the project "Molecular Engineering of Membrane Materials: Research and Technology for Energy Development of Hydrogen, Natural Gas and Syngas" (grant number R-279-000-261-281) and A*Star support for the project "Polymeric Membrane Development for CO_2 Capture from Flue Gas" (grant number R-398-000-058-305).

TABLE OF CONTENTS

SUMMARY

The volatile and escalating oil prices, combined with concerns about the environmental consequences of anthropogenic carbon dioxide emissions, have led to the growing interest in the development of alternative energy sources. The world energy consumption continues to be at the core of the climate change debate and the use of natural gas and hydrogen is recommended to alleviate global warming. Membrane technology is a promising purification technique for hydrogen enrichment and natural gas sweetening. Polymeric membranes remain the most viable commercial choice and substantial research works on the design of polymers with improved gas separation performance and physicochemical properties are in progress. Various approaches have been utilized by membrane scientists to overcome the bottlenecks and to achieve this goal.

Due to the undesirable coupling of high H_2 diffusivity and CO_2 solubility, it is an exceptionally challenging task to separate H_2 and CO_2 by polymeric membranes. Majority of the polymers display inferior H_2/CO_2 selectivity and the current state of the art remains inadequate for industrial applications. For CO_2/CH_4 separation, polymers with good CO_2/CH_4 selectivity and CO_2 permeability are available. Hence, greater emphasis must be placed on strategies to suppress CO_2-induced plasticization. In this study, the diamine modification of polyimide dense membranes is investigated for enhancing the intrinsic H_2/CO_2 selectivity. The critical parameters that determine the effectiveness of the modification approach are comprehensively examined. Commercially, asymmetric hollow fiber membranes are of greater significance compared to dense films. Therefore, the

fabrication of polyimide/polyethersulfone dual-layer hollow fiber membranes and the post-treatment with an aliphatic diamine are studied for H_2/CO_2 separation. A synthetic approach that involves the in-situ preparation of a pseudo interpenetrating polymer network (IPN) comprising of an azido-containing monomer and a polyimide is explored. The CO_2/CH_4 separation performance and the CO_2-plasticization behavior of the pseudo-IPNs are evaluated. The key results and conclusions obtained from this study are presented as follows.

The surface modifications of copoly(4,4'-diphenyleneoxide/1,5-naphthalene-2,2'-bis(3,4-dicarboxylphenyl) hexafluoropropane diimide (6FDA-ODA/NDA) dense membranes are performed using aliphatic diamines of different spacer lengths i.e. ethylenediamine (EDA), 1,3-diaminopropane (PDA) and 1,4-diaminobutane (BuDA). Chemical grafting, crosslinking and polymer main chain scission occurs simultaneously on the film surface during the modification. The extent of each reaction depends on the nucleophilicity and molecular dimensions of the diamines, which are computed using molecular simulation. The small molecular dimensions and high nucleophilicity of EDA result in severe polymer main chain scission. PDA provides the greatest degree of cross-linking and this is attributed to its favorable kinetic property and appropriate nucleophilicity. The ideal H_2/CO_2 permselectivity increases from 2.3 to a remarkable value of 64 after PDA modification for 90 min. This promising result is re-confirmed by the binary gas tests showing a H_2/CO_2 permselectivity of 45 at 35 ºC. In a nutshell, appropriate selections of the diamino reagent and modification duration are required to crosslink the polymer

chains substantially while maintaining the main chain rigidity, thereby giving the desired gas separation performance of the membrane.

The effectiveness of the diamine modification approach is also dependent on the inherent properties of the polyimides. The integration of molecular design with diamine modification generates synergistic effects for enhancing and fine tuning the molecular sieving potential of polyimide membranes. Polymer free volume and rigidity represent crucial conformational parameters that influence the effectiveness of diamine modification for elevating the H_2/CO_2 permselectivity of polyimide membranes. Experimental and molecular dynamics simulation results suggest that polyimides with higher intrinsic free volume and rigidity are ideal for diamine treatment, yielding greater increment in H_2/CO_2 selectivity. A series of 6FDA-ODA/NDA copolyimide membranes are modified with PDA. 6FDA-NDA has the highest free volume and rigidity, thus exhibiting impressive improvement in ideal H_2/CO_2 selectivity from 1.8 to 120 after PDA modification. Conversely, 6FDA-ODA which is deficient in terms of free volume and rigidity, demonstrates a much lower increment in H_2/CO_2 selectivity from 2.5 to 8.2. The inherent heterogeneity of the PDA modified polyimide films results in thickness-dependent gas permeability and selectivity. The potential of merging macromolecular tailoring with diamine networking to enhance the H_2/CO_2 separation performance of polyimide membranes is evident.

In view of the promising H_2/CO_2 separation performance of the PDA-modified dense films, we have developed functional 6FDA-NDA/polyethersulfone (PES) dual layer

hollow fiber membranes and studied their performance for H_2/CO_2 separation before and after PDA modification. The effects of air gap on gas transport properties of as-spun hollow fiber membranes are investigated. For the first time, we have observed that the optimal air gap for maximizing the ideal permselectivity is strongly dependent on the kinetic diameters of gas pair molecules. A higher air gap diminishes the population of Knudsen pores in the apparently dense outer skin layer and induces greater elongational stresses on polymer chains. The latter enhances polymer chain alignment and packing which possibly result in the shift and sharpening of the free volume distribution. Due to the influence of methanol swelling and the high initial diffusion rates of diamines, the chemical modification occurs throughout the polyimide outer layer. This densifies the asymmetric structure of the pristine 6FDA-NDA outer layer and creates additional resistance to gas transport, which hinders the enhancement in H_2/CO_2 permselectivity that can be reaped. At higher temperature, the H_2 permeance of the PDA-modified fibers increases with negligible decrease in the H_2/CO_2 permselectivity. The diamine modification of 6FDA-NDA/PES dual layer hollow fiber membranes effectively suppresses the CO_2-induced plasticization.

In the last part of this study, a novel synthetic strategy to fine tune the cavity size and free volume distribution of polyimide membranes via the formation of homogenous pseudo-interpenetrating polymer networks (IPN) is explored. The transformation in the free volume characteristics of the pseudo-IPN can be effectively exploited for achieving enhanced gas transport properties. The molecular construction of the pseudo-IPNs entails the in-situ polymerization of azido-containing monomers with multi-reactive sites within

rigid polyimide molecular scaffolds. The intrinsic free volume of the host polyimide and the dimensions of the azido-containing monomer predominantly influence the mean cavity size of the semi-IPN. The pseudo-IPNs assembled using fluorinated polyimides and 2,6-bis(4-azidobenzylidene)-4-methylcyclohexanone (azide) display improved CO_2/CH_4 separation performance. The alterations in the gas permeability and gas pair permselectivity of the semi-IPNs are adequately mapped to the variation in the free volume distributions characterized by the positron annihilation lifetime spectroscopy. Depending on the functionalities of the host polyimides, chemical cross-links are formed between the azide network and the pre-formed linear polyimide. The chemical bridges in conjunction with the interpenetrating network restrict the mobility of the polymer chains and suppress CO_2-induced plasticization.

In summary, polymeric membranes with enhanced H_2/CO_2 selectivity via the diamine modification of polyimides have been developed. The chemistry and key parameters for optimizing of the diamine modification approach are identified and established. This modification technique is demonstrated on asymmetric hollow fiber membranes which are of greater commercial importance. In addition, polyimide/azide pseudo-interpenetrating polymer networks with promising CO_2/CH_4 separation performance and enhanced anti-plasticization properties against CO_2 are discovered. The applicability of polymeric membranes for hydrogen enrichment and natural gas sweetening are evident. This motivates one to work towards the realization of membrane technology for clean energy applications and recommendations for the future research directions are highlighted.

NOMENCLATURE

A	Effective membrane area
A_d	Penetrant dependent parameter (Fujita FFV model)
A^*	Constant (Cohen and Turnbull model)
B_d	Penetrant dependent parameter (Fujita FFV model)
b	Langmuir affinity constant
b_0	Pre-exponential factor for b
C	Local penetrant concentration in the membrane
C_m	Material-dependent constant (0.001-0.003 for polymers)
C_D	Gas concentration at the Henry sites
C_H	Gas concentration at the Langmuir sites
C_H'	Langmuir capacity constant
c	Polymer dependent parameter (Brandt's model)
D	Diffusivity
D_D	Diffusion coefficient at the Henry sites
D_H	Diffusion coefficient at the Langmuir sites
D_{app}	Apparent diffusion coefficient
D_{avg}	Average diffusion coefficient
D_f	Self-diffusion coefficient
D_0	Pre-exponential factor for D
d	Average d-spacing of polymer chains
d_k	Kinetic diameter

dp/dt	Rate of pressure increase at steady state
E_D	Activation energy for diffusion
E_p	Activation energy for gas permeability
F	Ratio of D_H to D_D
f	Polymer dependent parameter (Brandt's model)
I_3	Intensity
k	Boltzmann's constant
K	$C_H'b/k_D$
k_D	Henry law constant
k_{D0}	Pre-exponential factor for k_D
L_T	Total membrane thickness
L_1	Thickness of modified layer
L_2	Thickness of unmodified layer
l	Membrane thickness
M_W	Gas molecular weight
M_{WA}	Molecular weight of gas A
M_{WB}	Molecular weight of gas B
M_i	Polymer-penetrant interaction parameter
M_0	Original mass of the crosslinked film
M_1	Mass of the insoluble fraction of the crosslinked film
N	Steady-state gas flux through the membrane
N_c	Constant 0.023 K^{-1}
P	Gas permeability

P_0	Pre-exponential factor for P
P_1	Gas permeability of modified layer
P_2	Gas permeability of unmodified layer
P/l	Gas permeance
p	Pressure
p_1	Downstream pressure
p_2	Upstream pressure
R	Universal gas constant
r_3	Mean free-volume radius
S	Solubility
T	Temperature
T_c	Critical temperature
T_g	Glass transition temperature
V	Downstream volume
V_W	Van der Waals volume
V_e	Equilibrium volume of polymer
V_{sp}	Specific volume of polymer
V_0	Occupied volume of polymer
v_f	Average free volume per molecule
v_{f3}	Mean free volume of a cavity
w_0	Mass of the sample in air
w_1	Mass of the sample in ethanol
x	Gas molar fraction in the feed

y	Gas molar fraction in the permeate
$\alpha_{A/B}$	Permselectivity for component A relative to component B
$\alpha_{K,A/B}$	Knudsen selectivity for gas A to gas B
β_{AB}	Parameter for the upper bound
γ	Constant (Cohen and Turnbull model)
ΔH_D	Sorption enthalpy for Henry sites
ΔH_H	Sorption enthalpy for Langmuir sites
Δh	Thickness of hollow fiber membrane
Δr	An empirical constant (1.656 Å)
ε	Potential energy well depth parameter
ε/k	Lennard-Jones temperature
η	Gas viscosity
θ	Time lag
λ	Mean free path of a gas molecule
λ_{AB}	Parameter for the upper bound
ρ	Polymer density
$\rho_{ethanol}$	Density of ethanol
σ_c	Collision diameter
σ_{eff}	Effective diameter
τ_3	Parameter for determining the average cavity size in the polymer
ν^*	Minimum required volume of the void

LIST OF TABLES

LIST OF FIGURES

CHAPTER 1

INTRODUCTION

Parts of this chapter are published in the following review articles

Lu Shao, **Bee Ting Low**, Tai Shung Chung, Alan R. Greenberg, Polymeric membranes for the hydrogen economy: Contemporary approaches and prospects for the future, *J. Membr. Sci.* 327 (2009) 18-31.

Youchang Xiao, **Bee Ting Low**, Seyed Saeid Hosseini, Tai Shung Chung, Donald Ross Paul, The strategies of molecular architecture and modification of polyimide-based membranes for CO_2 removal from natural gas-A review, *Prog. Polym. Sci.* 34 (2009) 561-580.

1.1 The quest for clean fuels to curb global warming and the energy crisis

In the latest International Energy Outlook 2009 report by the US Department of Energy, it is anticipated that the world marketed energy consumption will increase by 44 percent over the 2006 to 2030 time frame [1]. The current economic recession leads to a temporary reduction in energy demand but the world energy usage is projected to grow as the economy recovers in the long run. Despite the increased attention to a wide range of renewable and non-renewable energy sources, liquid fuels continue to dominate the energy consumption as demonstrated in Figure 1.1 (a). The extensive oil usage generates substantial greenhouse gases that cause irreversible and detrimental effects on the climate. In fact, CO_2 emission from the combustion of liquid fuels contributes 39 percent of the total emission in 2006 [1]. The persistent demand for oil and its gradual depletion result in highly volatile and escalating oil prices as depicted in Figure 1.1 (b). There is an urgent need to shift the world's reliance on oil as an energy source to alternative fuels.

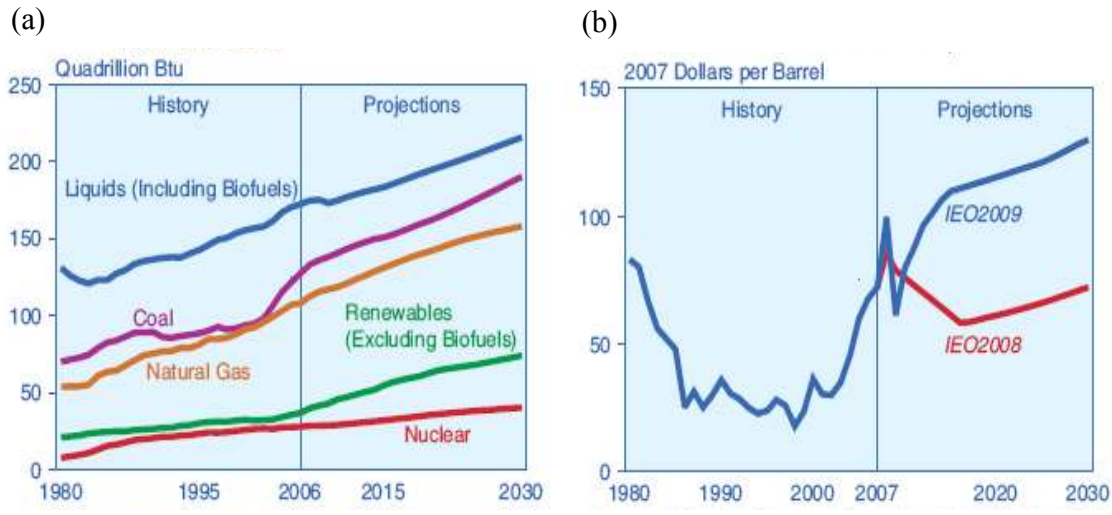

Figure 1.1 (a) World marketed energy use by fuel type and (b) world oil prices from year 1890 to 2030 [1]

The ideal solution to secure global sustainability is the complete utilization of renewable resources for power generation and transportation. Inevitably, there is a transition phase of uncertain duration, as the world progresses towards this model. During the changeover period, the use of non-renewable fossil fuels other than oil becomes prevalent. Natural gas, a less carbon intensive (i.e. lower CO_2 emission) fuel is increasingly being used for electricity generation and as a transportation fuel. Despite the growing demand for natural gas, the gas reserves have remained relatively constant since 2004, implying that producers have been able to replenish the drained reserves with new resources over time [1]. The forecast for the natural gas consumption worldwide is from 104 trillion cubic feet in 2006 to 153 trillion cubic feet in 2030. In the absence of stringent regulations and efforts to control greenhouse gas emissions, a significant portion of the increase in energy demand is expected to be meet by coal. The world coal consumption is likely to increase from 127 quadrillion Btu in 2006 to 190 quadrillion Btu in 2030. Coal is a highly carbon intensive fossil fuel and the CO_2 emission contributed by coal combustion may hit 45 percent in 2030.

Among these non-renewable fossil fuels, natural gas has the advantages of lower CO_2 emission, stable supply and low fuel costs because of its relatively abundant supply. Nevertheless, it would be favorable to eliminate the carbon source prior to fuel consumption. Pre-combustion CO_2 capture from a point source is more efficient than post-combustion, in particular for the consumption of fuel in the transportation sector. An approach to attain this is the conversion of methane to hydrogen, a “green” fuel (i.e. the only combustion product is water) which creates zero environmental or ecological

damage [2]. Generally, large-scale hydrogen production occurs via the steam methane reforming (SMR) followed by the water-gas shift (WGS) reaction which are represented by equations (1-1) and (1-2), respectively [3-5]. Coal is typically used for the generation of electricity and the treatment of the emitted flue gas is an example of post-combustion CO_2 capture. To extend the usage of coal, it can similarly be gasified to produce hydrogen which can be utilized as a green energy source.

$$C_nH_m + nH_2O \leftrightarrow nCO + \frac{m}{2+n}H_2 \quad (1\text{-}1)$$

$$CO + H_2O \leftrightarrow CO_2 + H_2 \quad (1\text{-}2)$$

Following the launch of Agenda 21 by the United Nations, several projects related to the production and treatment of hydrogen by economically-viable and environmentally-friendly approaches were initiated [6]. For instance, a $1.2 billion Hydrogen Fuel Initiative was announced in the United States in 2003 for developing commercially feasible hydrogen fuel cells [6]. The U.S. Department of Energy commenced the "Vision 21" project that aims to establish multi-purpose power plants that couple fuel processing (H_2 production) with CO_2 sequestration technologies [6]. In Australia, the "Coal 21" project was initiated to explore novel green technologies for hydrogen production via coal gasification [6].

Natural gas and hydrogen (derived from natural gas and coal) emerge as the vital alternative fuels to lessen greenhouse gas emission and global warming in the

aforementioned transition phase faced by the global energy consumption pattern. The larger reserves of natural gas with relatively constant fuel price provide a more reliable supply of energy source. Due to the lack of infrastructure for the storage and distribution of hydrogen, natural gas is often seen as a bridging fuel source towards a hydrogen-based economy. The projected growth in the demand for hydrogen and natural gas drives the development and advancement of gas separation technologies with outstanding process efficiency.

1.2 Membrane technology as an emerging tool for gas purification

The hydrogen product stream exiting the WGS reactor contains CO_2 as the key contaminant and H_2O and CO in trace amounts. Therefore, the effective separation of H_2 and CO_2 is of great significance. The required H_2 purity varies for different applications. For instance, high-purity hydrogen (minimum 99.99 %) is essential for fuel cell technology while hydrogen as a feedstock for hydro-cracking requires only 70-80% purity [7]. Conventional industrial techniques for hydrogen enrichment include pressure swing adsorption (PSA) and cryogenic distillation [8-9]. PSA is a matured industrial process for producing high-purity hydrogen of up to 99.99 %. The adsorption process operates at a high pressure of larger than 10 MPa and utilizes suitable adsorbents such as activated carbon and zeolites [10]. In a cryogenic distillation process, the gas mixture is frozen and separated based on the difference in the boiling points of the gases [9]. Cryogenic distillation produces hydrogen with moderate purity of $\leq$ 95 %. Both PSA and cryogenic distillation are highly energy and capital intensive processes.

For natural gas, methane is the key constituent in the presence of varying amounts of impurities including H_2O, CO_2, N_2, H_2S and other hydrocarbons. The removal of acid gases (i.e. CO_2 and H_2S) is an important processing step in natural gas treatment. Natural gas sweetening is necessary for increasing the fuel heating value, decreasing the volume of gas to be transported, preventing pipeline corrosion within the gas distribution network and reducing atmospheric pollution [11]. The traditional means for acid gas removal are absorption in basic solvents (e.g. amine or hot aqueous potassium carbonate solutions) and PSA [12]. There are several drawbacks of a gas absorption process, namely the need for solvent regeneration, large footprint for offshore applications and lack of robustness towards different feed compositions. Similarly, PSA is highly capital intensive and requires significant energy usage.

Conversely, membrane technology shows great potential for the hydrogen (H_2/CO_2) and natural gas (CO_2/CH_4) purification markets. Typically, a membrane-based separation exhibits the following advantages: (1) higher energy efficiency, (2) simplicity in operation, (3) compactness and portability and (4) environmentally friendly [13-15]. From the economic point of view, membrane technology appears more advantageous for small-to-medium scale separations where the product purity requirement is less stringent. Moreover, membrane technology can be coupled with other gas-processing steps to achieve higher hydrogen throughput. For example, H_2-selective membranes can be utilized to increase the hydrogen yield in WGS reactors by driving the chemical equilibrium in favor of the forward reaction. Despite the advantages of membrane technology for hydrogen purification and natural gas sweetening, its widespread

application on the industrial scale is limited. The effective industrial implementation of the membrane technology for gas separation is largely dependent on the constructive integration of membrane material advancement, membrane configuration and module design, and process optimization [16-19].

1.3 Diversity of membrane materials

1.3.1 Polymers

Polymers are the leading materials for fabricating gas separation membranes because of the ease of processability, good physicochemical properties and reasonable production costs [6,16]. Substantial research works have been conducted to design new polymers with enhanced gas transport properties. Despite the increasing polymer database that is available, only a small group of polymers have been commercialized and among those that are marketed, less than 10 are currently in use for industrial gas separations. This is because majority of the engineered polymers are costly and the separation performance under field conditions falls below expectations. Table 1.1 summarizes the gas transport properties of the polymers which are of practical importance for large-scale applications [19].

There are several considerations in the selection of polymeric membranes for H_2/CO_2 and CO_2/CH_4 separations. The primary factor is a good compromise between the gas

permeability and gas pair permselectivity. The membranes should display thermal, chemical and mechanical robustness toward harsh operating conditions and aggressive feeds. The similarity in the use of glassy polymeric membranes for hydrogen enrichment and natural gas sweetening is that both involve the presence of condensable gas species, e.g. CO_2 which results in plasticization and possible deterioration of the separation performance. One point to highlight here is the current research on the design of polymers for H_2/CO_2 and CO_2/CH_4 separation is progressing at different stages. For H_2/CO_2, the search is on for polymers with improved permselectivity while for CO_2/CH_4, polymers with excellent separation performance have been discovered and the next challenge is to overcome the undesirable plasticization effects.

Table 1.1 Gas transport properties of commercial polymers used for fabricating gas separation membranes [19]

Commercial polymer	**Permeability at 30 ^oC (Barrer)**				
	H_2	**N_2**	**O_2**	**CH_4**	**CO_2**
Cellulose acetate	2.63	0.21	0.59	0.21	6.3
Ethyl cellulose	87	3.2	11	19	26.5
Polycarbonate, brominated	-	0.18	1.36	0.13	4.23
Polydimethylsiloxane	550	250	500	800	2700
Polyimide (Matrimid®)	28.1	0.32	2.13	0.25	10.7
Polymethylpentene	125	6.7	27	14.9	84.6
Polypheynleneoxide	113	3.81	16.8	11	75.8
Polysulfone	14	0.25	1.4	0.25	5.6
Polyetherimide	7.8	0.047	0.4	0.035	1.32

Polymeric membranes for H_2/CO_2 separation can be selective for H_2 or CO_2. H_2-selective polymeric membranes are generally fabricated using glassy polymers while CO_2-selective membranes are usually derived from rubbery polymers. For membrane-based natural gas purification, it is desirable to select polymers which selectively remove CO_2 from the mixtures, thereby maintaining CH_4 at or near feed pressure and to avoid costly gas recompression. Among the studied materials, it was noted that polyimides with excellent intrinsic properties have attracted much attention in the academia and industries [20]. Du Pont Co. (USA) and Ube Industries (Japan) were the pioneers in the commercial application of polyimides for separation processes [20].

Supported-liquid membrane belongs to a special category where a polymeric support is impregnated with suitable carriers that interact favorably with one component in the gas mixture [3,21]. The separation is attained based on the interactions between the gas molecules and the carrier. This is unlike the conventional polymeric membranes which utilize the structural properties of the polymers and the interactions between the gas penetrants and the macromolecules to achieve a separation. Basic or CO_2-reactive carriers can be used to significantly enhance CO_2 solubility and the resultant membranes are exceptionally selective for CO_2 [3]. Nevertheless, the long-term stability of this membrane remains uncertain and the separation performance may deteriorate due to carrier saturation. A detailed description of facilitated transport membranes for CO_2 removal is beyond the scope of this work and can be obtained elsewhere [21].

1.3.2 Inorganics (metallic and non-metallic)

A wide array of inorganic materials can be used for membrane fabrication, including metals and metal alloys, silica, ceramic, carbon, zeolite and oxides [22-37]. Inorganic membranes typically display superior gas separation performance, excellent chemical resistance and thermal stability. However, inorganic membranes may not be commercially attractive because of their inherent brittleness, high production costs and the challenges faced in large scale production. Further technological breakthroughs in the processing and manufacturing of inorganic membranes are needed.

Dense palladium membranes are highly selective for H_2, and in fact the theoretical selectivity for H_2 is infinite. The transport of H_2 across Pd membranes occurs in seven consecutive steps: (1) movement of H_2 molecules to the membrane surface facing the feed, (2) dissociation of H_2 into H^+ and electrons, (3) adsorption of H^+ in the membrane, (4) diffusion of H^+ across the membrane, (5) desorption of H^+ from the membrane, (6) reassociation of H^+ and electrons to form H_2, and (7) diffusion of H_2 from the permeate side of the membrane [3]. Attempts have been made by Athayde et al. and Mercea et al. to fabricate "sandwich membrane" whereby the metals are deposited on one or both sides of a polymeric support [38-39]. Pd membranes are not practical for commercialization due to the considerable cost of precious Pd metal and the difficulty in fabricating thin and defect-free Pd membranes. In addition, Pd membranes suffer from hydrogen enbrittlement, cracking during thermal cycling and surface contamination by sulfur-containing species.

Silica membranes represent another type of inorganic membranes that can be utilized for gas separation. Compared to metallic membranes, silica membranes are relatively less expensive and easier to fabricate [3]. Gas transport in silica membranes occurs by the site-hopping diffusion within the microporous network. Typically, silica membrane takes the form of composite structure with distinct selective, intermediate and support layers. At high pressure operations, disruptive stresses may be formed between the layers and structural changes may occur in the highly porous inorganic membranes [3]. Zeolite membranes have extremely uniform pore size and narrow pore-size distribution which result in excellent gas separation efficiency. Nonetheless, it is difficult to produce thin and defect-free zeolite membranes for practical gas separation applications.

Carbon molecular sieve membranes (CMSMs) derived from polymeric precusors belong to a sub-category of the family of carbon membranes [30-35]. The gas separation performance of a CMSM is strongly dependent on precursor selection and treatment, pyrolysis conditions and post-treatments [30]. The pore size and pore size distribution of the CMSMs governs the gas transport. It has been reported that CMSMs derived from polyimides exhibit excellent CO_2/CH_4 selectivity and high gas permeability [30-32]. However, the apparently superior gas separation performance is bound to deteriorate in the presence of moisture or other hydrocarbons. The poor mechanical strength of free-standing CMSM and the high cost of production deter its applications on the industrial scale.

1.3.3 Organic-inorganic hybrids

Organic-inorganic hybrid membrane or mixed matrix membrane consists of a polymer as the continuous phase and inorganic particles as the dispersed phase. The key motivation is to combine the processability of polymers with the superior gas separation properties of inorganic materials. The preparation of organic-inorganic hybrid membranes can be classified into two categories based on the state of the inorganic fillers prior to membrane formation. One involves the direct addition of pre-formed fillers to a polymer solution while the other approach entails the in-situ formation of fillers in a polymer phase. In the latter approach, the size of the inorganic fillers typically falls in the nano range and a good dispersion of the fillers within the polymeric matrix can be obtained [40]. Based on the nature and functional role of the inorganic particles, the fillers can be classified as (1) non-porous inert, (2) non-porous activated, (3) high affinity with polymers and (4) porous nanoparticles. Figure 1.2 depicts the gas transport mechanisms occurring in mixed matrix membranes containing different types of inorganic fillers.

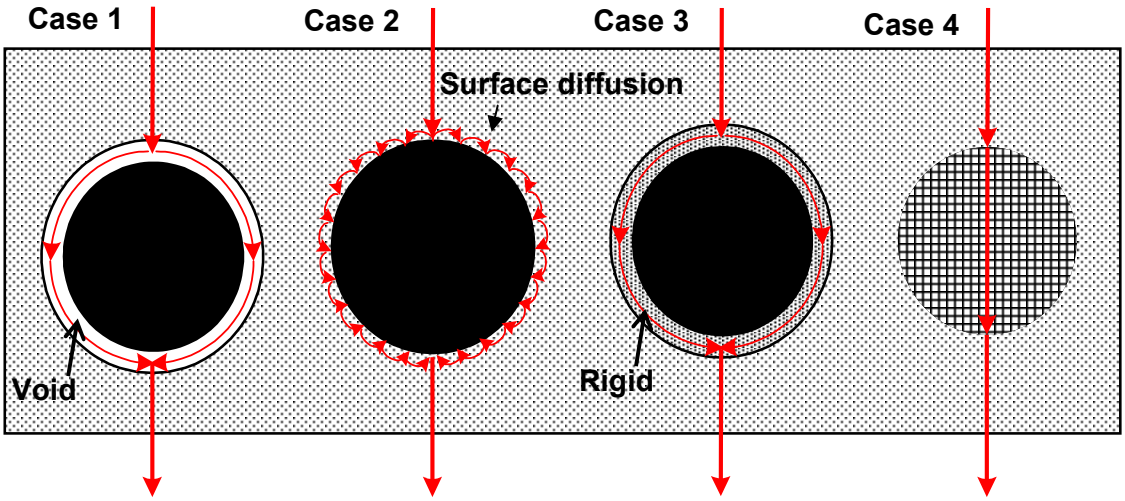

Figure 1.2 Different gas transport routes through hybrid polymeric membranes

Fume silica and C60 are examples of non-porous inert nanoparticles [41-42]. The weak interaction between these inert particles and the polymer chains disrupts chain packing and creates interfacial voids between the two phases. Enhanced surface flow may occur at the interfacial voids, thereby increasing the overall gas permeability [43]. Activated carbon particles belong to the group of non-porous activated nanoparticles [44]. The favorable interactions between the gas molecules and the activated fillers may improve the gas sorption. Some examples of nanoparticles with high affinity to the polymers are metal, metal oxides and surface modified zeolites [45-47]. The high affinity of these particles with the polymers hinders the mobility of the polymer chains and this "rigidification effect" may improve the gas pair selectivity of the membrane. Porous nano-size particles such as zeolites [48-50] and carbon molecular sieves [51] have the potential to combine the high diffusivity selectivity of inorganic molecular sieves and the good processability of polymeric material. A detailed documentation on organic-inorganic hybrid membranes can be found elsewhere [52].

1.4 Gas transport mechanisms

1.4.1 Solution diffusion

For most dense polymeric membranes, the solution diffusion mechanism is accountable for the selective transport of gases. Thomas Graham proposed the solution-diffusion model for explaining the gas transport and it comprises three distinct steps. With reference to Figure 1.3, the first step involves the sorption of gas molecules upon the

upstream boundary. The gas molecules then diffuse across the membrane and eventually desorb at the downstream side. The gas pressure at the upstream is higher than at the downstream which provides the key driving force for attaining a separation. The permeability, *P* of a membrane to a gas penetrant is defined as [53]:

$$P = \frac{Nl}{(p_2 - p_1)} \tag{1-3}$$

where N is the steady-state gas flux through the membrane, p_1 and p_2 are the downstream and upstream pressures, respectively and *l* is the membrane thickness. The permeability of a membrane is generally expressed in Barrer (1 Barrer $=10^{-10}$ cm^3 (STP)-cm /cm^2 sec cm Hg).

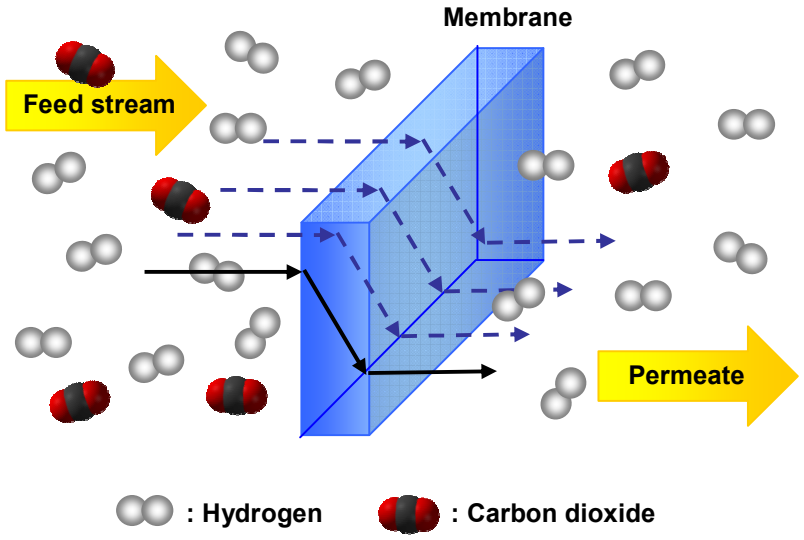

Figure 1.3 Solution diffusion mechanism for a H_2-selective polymeric membrane

Based on the solution-diffusion model, the permeability (P) of a gas across the membrane is a product of the diffusivity (D) and solubility (S) coefficients.

$$P = D \times S \tag{1-4}$$

The diffusion coefficient is a kinetic parameter that measures the overall mobility of the penetrant molecules in the membrane. The gas diffusivity depends on various factors, including (1) the size and shape of the gas molecules, (2) the cohesive energy density of the polymer, (3) the mobility of the polymer chains and (4) the free volume size and distribution of the polymer [54]. The solubility coefficient is a thermodynamic parameter and is influenced by (1) the condensability of the penetrant gases, (2) the nature of interactions between the polymer and the penetrants and (3) the chain packing density in glassy polymers [55]. The units for the diffusivity and solubility coefficients are 10^{-10} cm^2/s and $cm^3(STP)/cm^3$-cmHg, respectively.

For a binary gas mixture permeating across a membrane, the ideal permselectivity for component A relative to component B, $\alpha_{A/B}$ is represented by equation (1-5).

$$\alpha_{A/B} = P_A / P_B \tag{1-5}$$

Factoring the gas permeability into the respective diffusivity and solubility terms, the ideal selectivity is expressed as

$$\alpha_{A/B} = \left(\frac{D_A}{D_B}\right) \times \left(\frac{S_A}{S_B}\right) \tag{1-6}$$

where $\frac{D_A}{D_B}$ is the diffusivity selectivity and $\frac{S_A}{S_B}$ is the solubility selectivity. Therefore, both the solubility selectivity and diffusivity selectivity should complement each other in

order to obtain a high gas pair permselectivity. In the separation of non-polar gases using glassy polymers, diffusivity is considered as the factor that determines the overall gas permeability while a limited role is seen for solubility [56]. However, for gas separation involving highly condensable gases such as carbon dioxide, the role of solubility with regards to the separation performance should not be neglected.

1.4.2 Poiseuille flow, Knudsen diffusion and molecular sieving

In porous membranes, Poiseuille flow and/or Knudsen diffusion govern the overall gas transport. As shown in Figure 1.4 (a), Poiseuille flow is present when the pore radius (r) of the membrane is larger than the mean free path (λ) of the gas molecule. The mean free path (λ) refers to the distance traversed by a gas molecule during collision and is represented by equation 1-7 [57]. Poiseuille flow, also known as viscous flow, takes place when the pore diameter is larger than 10 μm [58].

$$\lambda = \frac{3\eta}{2p}\left(\frac{\pi RT}{2M_w}\right)^{1/2} \qquad (1\text{-}7)$$

where η is the gas viscosity, p is the pressure, T is the temperature, M_W is the gas molecular weight and R is the universal gas constant.

As the pore size decreases to 50-100 Å, Knudsen diffusion occurs and the permeation of each gas molecule is independent of neighboring molecules [58]. The Knudsen diffusion coefficient is inversely proportional to the square root of the gas molecular weight. Hence, if Knudsen diffusion accounts for the transport of an equimolar gas feed

comprising of two components across the membrane, the Knudsen selectivity for gas A to gas B ($\alpha_{K,A/B}$) is shown by equation (1-8).

$$\alpha_{K,A/B} = \sqrt{\frac{M_{WB}}{M_{WA}}} \tag{1-8}$$

where M_{WA} and M_{WB} are the molecular weights of gas A and B, respectively.

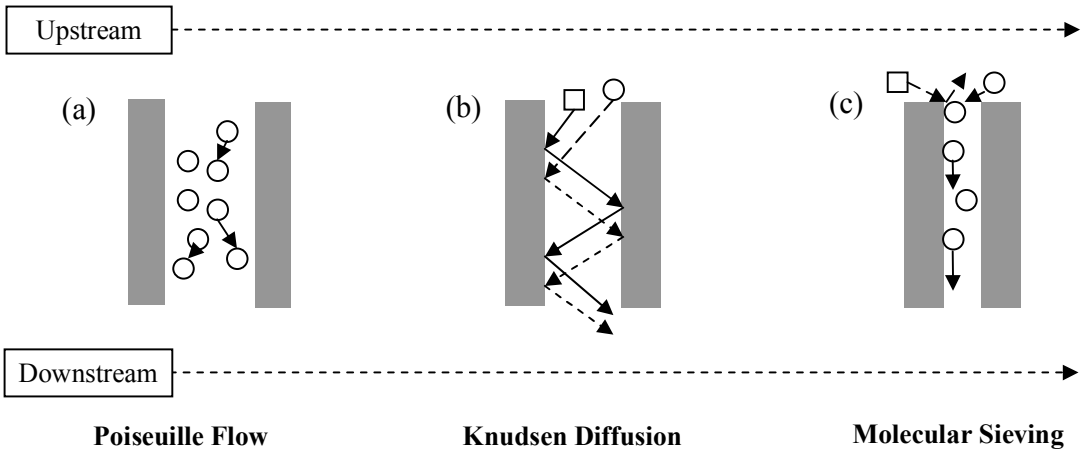

Figure 1.4 Schematics of (a) Poiseuille flow, (b) Knudsen diffusion and (c) molecular sieving

The ratio of r to λ indicates the relative contributions of Poiseuille flow and Knudsen diffusion across the membrane. A large r/λ ratio means that the frequency of collisions between the gas molecules is higher than the collisions between the gas molecules and the pore wall i.e. Poiseuille flow is dominant. If the r/λ ratio is significantly less than 1, the frequency of gas-wall collisions is higher than gas-gas collisions, i.e. Knudsen diffusion governs the gas transport.

Molecular sieving is the governing gas transport mechanism in pores which are generally lesser than 7 Å in diameter. This type of gas transport is particularly important in inorganic membranes e.g. carbon molecular sieves and zeolites. With reference to Figure 1.4 (c), the smaller gas molecules with higher diffusion rates are able to permeate readily through the ultra-micropores while the passageways of the larger molecules are hindered [59].

1.5 Membrane fabrication and structures

Membranes can be fabricated by various techniques including solution casting, hollow fiber spinning, melt extrusion, compression molding, track etching, sol-gel process, spin coating, etc. The membrane fabrication technique subsequently influences the structure of the membranes. For instance, the structure of the membrane prepared by solution casting may be dense or asymmetric. If the polymer solution is cast on a substrate and controlled evaporation of the solvent in the absence of moisture occurs, the resultant membrane structure is dense and homogenous as shown in Figure 1.5 (a). Dense membranes are often used for the fundamental investigations of the polymer intrinsic separation properties and physicochemical characteristics. The preliminary studies conducted using dense membranes provide valuable information for the subsequent fabrication of asymmetric membranes which are of greater commercial importance.

If the as-cast membrane is immersed into a non-solvent coagulant, the membrane is formed via phase inversion and the membrane structure is likely to be asymmetric (Figure

1.5 (b)). Hollow fiber membranes prepared by wet-spinning (both with and without air gap) are similarly asymmetric. Phase inversion is a phenomenon where a molecularly homogeneous and thermodynamically stable polymer solution undergoes a transition into a heterogeneous system [61]. The occurrence of liquid-liquid demixing between the solvent and non-solvent during phase inversion results in polymer-rich and polymer-poor regions. Depending on the mechanisms (i.e. nucleation and growth or spinodal decomposition) in play, the resultant membrane morphology may be dense or porous (close or open cell).

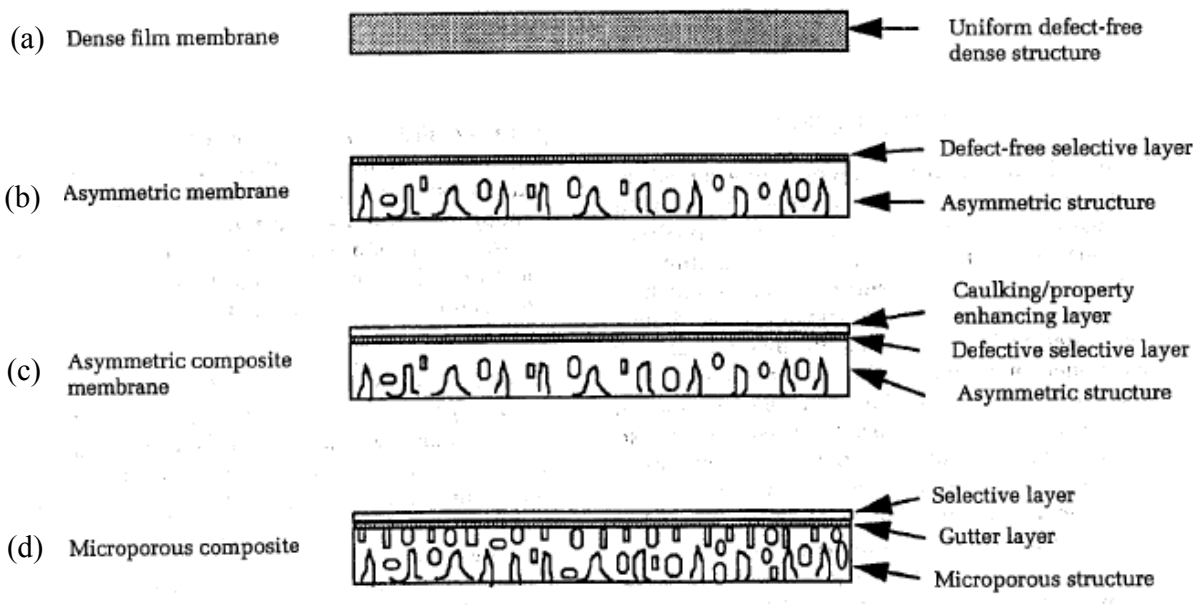

Figure 1.5 Types of membrane structures [60]

The selective layer of functional gas separation membranes must be defect-free and it is certainly non-trivial to fabricate defect-free membranes. If an asymmetric membrane with a defect-free skin layer is not attainable upon optimizing the phase inversion conditions, a commonly used approach is to seal the pin-holes with silicone rubber. This silicone

rubber coating technique was invented by Henis and Tripodi [62]. The membrane configuration after coating can be represented by Figure 1.5 (c). In some cases, the selective layer and the microporous substrate may be incompatible with each other and the use of another material is needed for the adhesion of the two layers (Figure 1.5 (d)).

Compared to the relatively simple and straight forward process of preparing a dense membrane by solution casting, the fabrication of hollow fiber membrane by phase inversion is more complex. Conventionally, hollow fiber membrane is spun using one material and the resultant membrane structure is asymmetirc and single layer. The discovery of the co-extrusion approach from a triple-orifice spinneret enables the fabrication dual layer hollow fiber membrane [63-67]. An evaluation of both the single- and dual- layer hollow fiber membrane configurations reveals that the latter possesses more advantages. The dual-layer hollow fiber configuration enables the use of materials with high performance but poor mechanical properties as the outer selective layer and substantial savings on the material costs of expensive polymers can be reaped [65-67]. Moreover, it eliminates the additional step of depositing a functional layer on single layer hollow fiber membranes [66]. Generally, the role of the outer selective layer is to attain a separation while the inner layer provides the mechanical support for the outer layer. The dual layer hollow fiber membrane technology is a double-edged sword. Although it has more advantages, it is also more challenging to produce functional dual-layer hollow fiber membranes due to the greater complexities that are encountered in the process.

There are several rules-of-thumb that guide the fabrication of functional dual-layer hollow fibers. From the gas separation performance aspect, the two requirements are the formation of a dense selective skin with a reasonable thickness and no substructure resistance (i.e. (1) absence of dense interface between the two layers and (2) porous support layer with an open-cell structure) [66-68]. It has been shown that a higher polymer concentration in the dope significantly reduces the formation of defects on the outer selective skin [65-67].There exists a critical polymer concentration, beyond which, the dope viscosity increases dramatically. This is attributed to the varying extent of polymer chain entanglement [65-66]. The preferred concentration to fabricate hollow fiber membranes with near defect-free outer selective layer is at or above the critical concentration [65-66]. To attain high gas permeation rates, the dense selective skin thickness should preferably falls in the range of 0.1 to 5 μm or less [69]. Taking into account the operational concerns, for the dual-layer hollow fibers to maintain the mechanical integrity when subjected to high pressures, the essential characteristics are (1) concentricity, (2) delamination-free, (3) macrovoids-free and (4) the ratio of the fiber outer diameter (OD) to twice the fiber thickness (Δh) should be approximately 2 [66-67]. The problem of delamination can be solved by choosing an appropriate inner layer dope formulation. Based on the work by Li et al., delamination-free membrane structure can be obtained if the inner and outer layers exhibit a comparable degree of shrinkage [66]. Therefore, it is certainly non-trivial to fabricate dual-layer hollow fiber membranes with these desirable properties.

1.6 Types of membrane module configurations

Depending on the application, membranes can be packed into modules of different designs, namely plate-and-frame, spiral wound, hollow fiber, tubular and capillary. Majority of the membranes for gas separation are in the form of hollow fiber modules and less than 20% are of spiral wound configuration [69]. Figures 1.6 (a) and (b) show the schematics of a hollow fiber and spiral wound membrane modules, respectively. The advantages of hollow fiber module are higher membrane packing density and lower module production costs. Hollow fiber membrane modules cost about \$2-5/m^2 while membrane modules in the form of spiral wound cost \$10-100/m^2 [69].

(a)

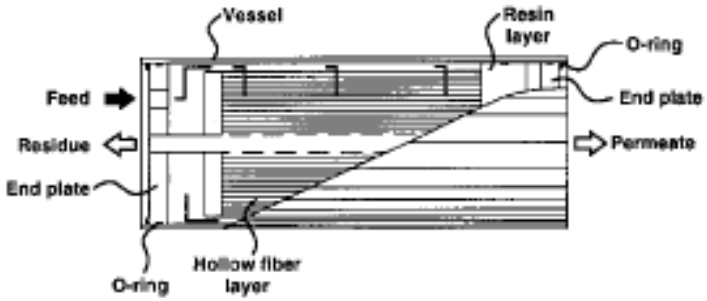

(b)

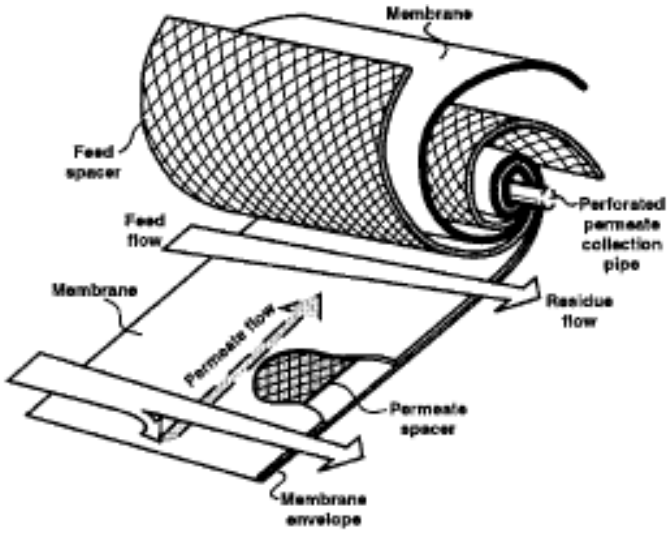

Figure 1.6 (a) Hollow fiber and (b) spiral wound membrane modules [69]

However, hollow fiber modules may not be the best choice for all types of gas separation. Hollow fiber modules with cross-flow configuration and high pressure feed entering from the shell side is suitable for hydrogen enrichment. Conversely, it is not advisable for use in natural gas purification where membrane fouling by the condensable vapors and particulates is a concern. Good pretreatment of natural gas may be required before feeding into a hollow fiber membrane module and this implies larger processing costs. The use of spiral wound membrane modules is recommended for natural gas sweetening as it gives more reliable long term operations [69].

1.7 Process and cost optimization

Ultimately, regardless of how fantastic the gas separation performance of the membrane modules is, the incorporation of the membrane separator with other unit operations must yield considerable economic returns. An optimized membrane unit may be running at minimum capital and operating costs. However, if the cost savings acquired from the membrane unit less than compensate for the increase in the costs of running other units, the use of membrane technology is unjustifiable. For hydrogen enrichment using a one-stage membrane separator, the hydrogen purity of the permeate stream may be < 95%. To further increase the hydrogen purity to meet product requirements, using a two-stage membrane separator or coupling a one-stage membrane reactor with a PSA unit may be required. H_2S in raw natural gas is difficult to be effectively removed by polymeric membranes. Thus, integrating a H_2S scrubber with a membrane unit is a more realistic hybrid process for use in natural gas treatment. For the separation of nitrogen and

methane in natural gas streams, the combination of cryogenic distillation with membrane separation as shown in Figure 1.7 may be offer more cost savings and better overall process efficiency [69]. In the dehydration of natural gas, the use of a counter-current flow membrane module effectively reduces the methane loss as depicted in Figure 1.8 [69]. The small footprint of a membrane separator facilitates its integration with other process units in a chemical plant or refinery.

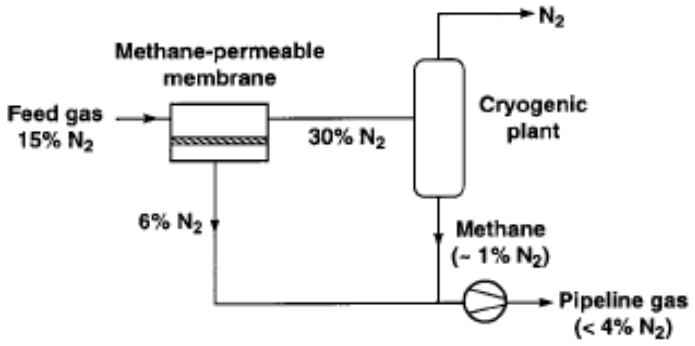

Figure 1.7 Coupling of membrane reaction with cryogenic distillation for N_2/CH_4 separation [69]

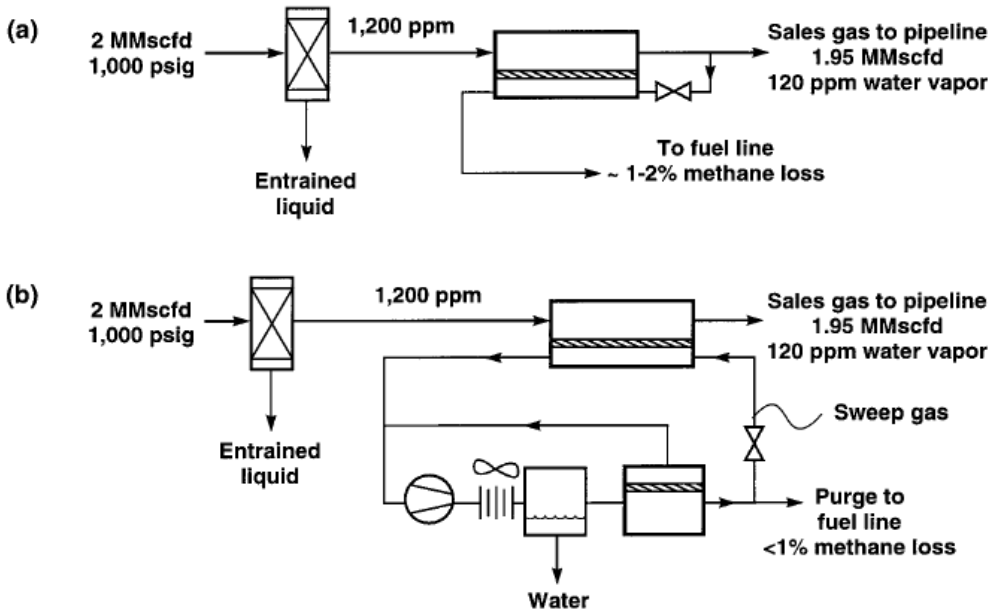

Figure 1.8 Use of counter-current flow hollow fiber membrane module to reduce methane loss during natural gas dehydration [69]

1.8 Research objectives and organization of dissertation

The preceding sections illustrate the anticipated growth in the hydrogen and natural gas energy consumption markets and the potential use of membrane technology for gas purifications. Polyimides are attractive materials for fabricating gas separation membranes because of the good processability and physicochemical properties. The core of this research study is to perform fundamental investigations on the diamine modification of polyimide membranes for improving the H_2/CO_2 separation performance. The intrinsic properties of aliphatic diamines and polyimides in relation to the enhancement in the H_2/CO_2 selectivity are explored systematically. An attempt to scale up the diamine modification approach to commercially useful hollow fiber membranes will be presented. Another objective of this work is to design new materials comprising of pseudo-interpenetrating polymer networks with improved anti-CO_2 plasticization properties for CO_2/CH_4 separation.

This dissertation is organized and structured into nine chapters and a brief description of the coverage in each chapter is as follows.

Chapter 1: A review on the importance of utilizing hydrogen and natural gas as alternative clean fuels in the transition phase of the global consumption pattern is presented. This chapter highlights the gaining significance and relevance of membrane technology in hydrogen and natural gas purifications. The determining factors (i.e. membrane material, structure and configuration, module design and process optimization)

for the effective commercial implementation of membrane technology are discussed. The research objectives of this work are emphasized.

Chapter 2: The current state of the art on polymeric membranes for hydrogen enrichment and natural gas sweetening are surveyed. This chapter describes the approaches used by membrane scientists in the pursuit of membrane materials with enhanced gas separation properties. The current challenges encountered and the future prospects in using polymeric membranes for hydrogen enrichment and natural gas separation are discussed.

Chapter 3: The theoretical background underlying the transport of gas molecules across dense glassy polymeric membranes is presented in this chapter. The concepts of plasticization and aging which leads to time-dependent gas separation are discussed.

Chapter 4: The materials used and the membrane preparation protocols for both dense film and asymmetric dual-layer hollow fiber membrane are documented. This chapter includes detailed descriptions of the characterization techniques used to determine the physicochemical and gas transport properties of the membranes.

Chapter 5: The effects of using different aliphatic diamines and modification durations on the H_2/CO_2 separation performance of diamine modified polyimide membranes are investigated. The types and extent of the chemical reactions occurring during the modification process are discussed. A simplified resistance model to describe the diamine-modified membrane is proposed.

Chapter 6: In this chapter, the influence of the polyimide intrinsic free volume and chain rigidity on the enhancement in the H_2/CO_2 selectivity of diamine modified membrane is explored. Molecular dynamics simulation is used in conjunction with the experimental data to reveal the dominating forces in play at the molecular level.

Chapter 7: The fabrication of polyimide/polyethersulfone dual-layer hollow fiber membranes and the subsequent modification with 1,3-diaminopropane are investigated. The effect of air gap on the resultant gas pair permselectivities of the pristine fibers is examined and hypotheses are proposed to explain the observed peculiar trends. A comparison of H_2/CO_2 transport properties before and after the diamine modification is presented.

Chapter 8: This chapter reports the use of a pseudo-interpenetrating polymer network (IPN) comprising of a rigid polyimide and a network formed by the in-situ polymerization of azide monomers for CO_2/CH_4 separation. The physicochemical properties of the pseudo-IPN membranes are characterized and the CO_2 plasticization behaviors of the membranes are investigated.

Chapter 9: A summary of the key conclusions derived from this study is presented and the future research directions are highlighted.

1.9 References

[1] International energy outlook 2009, Energy Information Administration, U.S. Department of Energy, May 2009

[2] G. Marban, T. Valdes-Solis, Towards the hydrogen economy?, Int. J. Hydrog. Energy 32 (2007) 1625-37.

[3] N. W. Ockwig, T. M. Nenoff, Membranes for hydrogen separation, Chem. Rev. 107 (2007) 4078.

[4] J. G. Xu, G. F. Froment, Methane steam reforming, methanation and water-gas shift. 1. Intrinsic kinetics, AIChE J. 35 (1989) 88.

[5] N. Muradov, Hydrogen via methane decomposition: an application for decarbonization of fossil fuels, Int. J. Hydrog. Energy 26 (2001) 1165.

[6] L. Shao, B. T. Low, T. S. Chung, A. R. Greenberg, Polymeric membranes for the hydrogen economy: Contemporary approaches and prospects for the future, J. Membr. Sci. 327 (2009) 18.

[7] J. A. Turner, A realizable energy future, Science 285 (1999) 687.

[8] S. I. Yang, D. Y. Choi, S. C. Jang, S. H. Kim, D. K. Choi, Hydrogen separation by multi-bed pressure swing adsorption of synthesis gas, Adsorption 14 (2008) 583.

[9] A. B. Hinchliffe, K. E. Porter, A comparison of membrane separation and distillation, Chem. Eng. Res. Des. 78 (2000) 255.

[10] S. Sircar, T. C. Golden, Purification of hydrogen by pressure swing adsorption, Sep. Sci. Technol. 35 (2000) 667.

[11] B. D. Bhide, A. Voskericyan, S. A. Stern, Hybrid processes for the removal of acid gases from natural gas, J. Membr. Sci. 140 (1998) 27.

[12] A. L. Kohl, R. Nielson, Gas purification, Gulf Publishing, Houston, Texas, 1997.

[13] W. J. Koros, G. K. Fleming, Membrane-based gas separation, J. Membr. Sci. 83 (1993) 1.

[14] J. D. Perry, K. Nagai, W. J. Koros, Polymer membranes for hydrogen separations, MRS Bull 31 (2006) 745.

[15] K. Scott. Handbook of industrial membranes, Elsevier Advanced Technology, United Kingdom, 1995.

[16] Y. Xiao, B. T. Low, S. S. Hosseini, T. S. Chung, D. R. Paul, The strategies of molecular architecture and modification of polyimide-based membranes for CO_2 removal from natural gas-A review, Prog. Polym. Sci. 34 (2009) 561.

[17] J. Lemanski, G. Lipscomb, Effect of shell-side flows on hollow-fiber membrane device performance, AIChE J. 41 (1995) 2322.

[18] B. D. Bhide, S. A. Stern, Membrane processes for the removal of acid gases from natural gas. II. Effects of operating conditions, economic parameters, and membrane properties, J. Membr. Sci. 81 (1993) 239.

[19] V. Abetz, T. Brinkmann, M. Dijkstra, K. Ebert, D. Fritsch, K. Ohlrogge, D. Paul, K. V. Peinemann, S. P. Nunes, N. Scharnagl, M. Schossig, Developments in membrane research: from material via process design to industrial application, Adv. Eng. Mater. 8 (2006) 328.

[20] H. Ohya, V. V. Kudryavtsev, S. I. Semenova, Polyimide membranes: applications, fabrications and properties, Gordon and Breach Publishers, Tokyo, 1996.

[21] M. B. Hagg, R. Quinn, Polymeric facilitated transport membranes for hydrogen purification, MRS Bull 31 (2006) 750.

[22] S. N. Paglieri, J. D. Way, Innovations in Palladium membrane research. Sep. Purif. Meth. 31 (2002) 1.

[23] P. P. Mardilovich, Y. She, Y. H. Ma, Defect-free palladium membranes on porous stainless-steel support, AIChE J. 44 (1998) 310.

[24] J. Tong, Y. Kashima, R. Shirai, H. Suda, Y. Matsumura, Thin Defect-Free Pd Membrane Deposited on Asymmetric Porous Stainless Steel Substrate, Ind. Eng. Chem. Res. 44 (2005) 8025.

[25] K. Kusakabe, F. Shibao, G. Zhao, K. I. Sotowa, K. Watanabe, T. Saito, Surface modification of silica membranes in a tubular-type module, J. Membr. Sci. 215 (2003) 321.

[26] Y. Iwamoto, K. Sato, T. Kato, T. Inada, Y. Kubo, A hydrogen-permselective amorphous silica membrane derived from polysilazane. J. Eur. Ceram. Soc. 25 (2005) 257.

[27] J. C. Diniz da Costa, G. Q. Lua, V. Rudolph, Y. S. Lin, Novel molecular sieve silica (MSS) membranes: characterization and permeation of single-step and two-step sol-gel membranes, J. Membr. Sci. 198 (2002) 9.

[28] U. Balachandran, T. H. Lee, L. Chen, S. J. Song, J. J. Picciolo, S. E. Dorris, Hydrogen separation by dense cermet membranes, Fuel 85 (2006) 150.

[29] Y. F. Gu, S. T. Oyama, High molecular permeance in a poreless ceramic membrane, Adv. Mater. 19 (2007) 1636.

[30] P. S. Tin, Y. Xiao, T. S. Chung, Polyimide-carbonized membranes for gas separation: structural, composition, and morphological control of precursors, Sep. Purif. Rev. 35 (2006) 285.

[31] Y. Xiao, Y. Dai, T. S. Chung, M. D. Guiver, Effects of brominating Matrimid polyimide on the physical and gas transport properties of derived carbon membranes, Macromolecules 38 (2005) 10042.

[32] L. Shao, T. S. Chung, K. P. Pramoda, The evolution of physicochemical and transport properties of 6FDA-durene toward carbon membranes: from polymer, intermediate to carbon, Microporous Mesoporous Mat. 84 (2005) 59.

[33] H. B. Park, Y. K. Kim, J. M. Lee, Y. M. Lee, Relationship between chemical structure of aromatic polyimides and gas permeation properties of their carbon molecular sieve membranes, J. Membr. Sci. 229 (2004) 117.

[34] K. M. Steel, W. J. Koros, An investigation of the effects of pyrolysis parameters on gas properties of carbon materials, Carbon 43 (2005) 1843.

[35] H. Hatori, Y. Yamada, M. Shiraishi, H. Nakata, S. Yoshitomi, Carbon molecular sieve films from polyimide, Carbon 30 (1992) 305.

[36] G. P. Fotou, Y. S. Lin, S. E. Pratsinis, Hydrothermal stability of pure and modified microporous silica membranes, J. Mater. Sci. 30 (1995) 2803.

[37] A. L. Ahmad, M. R. Othman, H. Mukhtar, H_2 separation from binary gas mixture using coated alumina-titania membrane by sol-gel technique at high-temperature region, Int. J. Hydrog. Energy 29 (2004) 817.

[38] A. L. Athayde, R. W. Baker, P. Nguyen, Metal composite membranes for hydrogen separation, J. Membr. Sci. 94 (1994) 299.

[39] P. Mercea, L. Muresan, V. Mecea, Metal composite membranes for hydrogen separation, J. Membr. Sci. 24 (1985) 297.

[40] H. Cong, M. Radosz, B. F. Towler, Y. Shen, Polymer-inorganic nanocompostie membranes for gas separation, Sep. Purif. Technol. 55 (2007) 281.

[41] M. Moaddeb, W. J. Koros, Gas transport properties of thin polymeric membranes in the presence of silicon dioxide particles, J. Membr. Sci. 125 (1997) 143.

[42] T. S. Chung, S. S. Chan, R. Wang, Z. Lu, C. He, Characterization of permeability and sorption in Matrimid/C_{60} mixed matrix membranes, J. Membr. Sci. 211 (2003) 91.

[43] T. C. Merkel, B. D. Freeman, R. J. Spontak, Z. He, I. Pinnau, Ultrapermeable, reverse-selective nanocomposite membranes, Science 296 (2002) 519.

[44] M. Anson, J. Marchese, E. Garis, N. Ochoa, C. Pagliero, ABS copolymer-activated carbon mixed matrix membrane for CO_2/CH_4 separation, J. Membr. Sci. 243 (2004) 19.

[45] S. Yoda, A. Hasegawa, H. Suda, Preparation of a platinum and palladium/polyimide nanocomposite film as a precursor of metal-doped carbon molecular sieve membrane via supercritical impregnation, Chem. Mat. 16 (2004) 2363.

[46] Q. Hu, E. Marand, S. Dhingra. D. Fritsch, J. Wen, G. Wilkes, Poly(amide-imide)/TiO_2 nano-composite gas separation membranes: fabrication and characterization, J. Membr. Sci. 135 (1997) 65.

[47] Y. Li, H.M. Guan, T.S. Chung, S. Kulprathipanja, Effects of novel silane modification of zeolite surface on polymer chain rigidification and partial pore

blockage in polyethersulfone (PES) – zeolite A mixed matrix membranes, J. Membr. Sci. 275 (2006) 17.

[48] S. Kulprathipanja, R. W. Neuzil, N. N. Li, Separation of fluids by means of mixed matrix membranes, US patent 4740219, 1988.

[49] R. Mahajan, W.J. Koros, Mixed matrix membrane materials with glassy polymers. Part 1, Polym. Eng. Sci. 42 (2002) 1420.

[50] Y. Li, T.S. Chung, S. Kulprathipanja, Novel Ag^{+}-zeolite/polymer mixed matrix membranes with a high CO_2/CH_4 selectivity, AIChE J. 53 (2007) 610.

[51] D. Q. Vu, W. J. Koros, S. J. Miller, Mixed matrix membranes using carbon molecular sieves. I. Preparation and experimental results, J. Membr. Sci. 211 (2003) 311.

[52] T. S. Chung, L. Y. Jiang, Y. Li, S. Kulprathipanja, Mixed matrix membranes (MMMs) comprising organic polymers with dispersed inorganic fillers for gas separation, Prog. Polym. Sci 4 (2007) 483.

[53] K. Ghosal, B. D. Freeman, Gas separation using polymer membrane: an overview. Polym. Adv. Technol. 5 (1994) 673.

[54] A. Singh-Ghosal, W. J. Koros, Energetic and entropic contributions to mobility selectivity in glassy polymers for gas separation membranes, Ind. Eng. Chem. Res. 38 (1999) 3647.

[55] B. D. Bhide, A. Voskericyan, S. A. Stern, Hybrid processes for the removal of acid gases from natural gas, J. Membr. Sci. 140 (1998) 27.

[56] W. J. Koros, G. K. Fleming, S. M. Jordan, T. H. Kim, H. H. Hoehn, Polymeric membrane materials for solution-diffusion based permeation separations, Prog. Polym. Sci. 13 (1988) 339.

[57] M. Mulder, Basic principles of membrane technology. Dordrecht: Kluwer Academic Publishers, 1996.

[58] P. S. Tin, Membrane materials and fabrication for gas separation, Ph. D. Dissertation, National University of Singapore, 2004.

[59] W. J. Koros, K. G. Fleming, Membrane-based gas separation, J Membr Sci 83 (1993) 1.

[60] T. S. Chung, A review of microporous composite polymeric membrane technology for air-sepration, Polymer and polymer composites 4 (1996) 269.

[61] J. Xiong, Architecture of polymeric nanophase materials – From understanding to fabrication, Ph.D. Dissertation, National University of Singapore, 2005.

[62] J. M. Henis, M. K. Tripodi, The developing technology of gas separating membranes, Science 220 (1983) 11.

[63] O. M. Ekiner, R. A. Hayes, P. Manos, Novel multicomponent fluid separation membranes, U.S. patent 5085676, E.I. Du Pont de Nemours and Company, 1992.

[64] H. Suzuki, K. Tanaka, H. Kita, K. Okamoto, H. Hoshino, T. Yoshinaga, Y. Kusuki, Preparation of composite hollow fiber membranes of poly(ethylene oxide)-containing polyimide and their CO_2/N_2 separation properties, J. Membr. Sci. 146 (1998) 31.

[65] D. F. Li, T. S. Chung, R. Wang, Y. Liu, Fabrication of fluoropolyimide/ polyethersulfone dual-layer asymmetric hollow fiber membranes for gas separation, J. Membr. Sci. 198 (2002) 211.

[66] D. F. Li, T. S. Chung, R. Wang, Morphological aspects and structure control of dual-layer asymmetric hollow fiber membranes formed by a simultaneous co-extrusion approach, J. Membr. Sci. 243 (2004) 155.

[67] N. Widjojo, S. D. Zhang, T. S. Chung, Y. Liu, Enhanced gas separation performance of dual-layer hollow fiber membranes via substructure resistance reduction using mixed matrix materials, J. Membr. Sci. 306 (2007) 147.

[68] I. Pinnau, W. J. Koros, Relationship between substructure resistance and gas separation properties of defect-free integrally skinned asymmetric membranes, Ind. Eng. Chem. Res. 30 (1991) 1837.

[69] R. W. Baker, Future directions of membrane gas separation technology, Ind. Eng. Chem. Res. 41 (2002) 1393.

CHAPTER 2

LITERATURE REVIEW

Parts of this chapter are published in the following review articles

Lu Shao, **Bee Ting Low**, Tai Shung Chung, Alan R. Greenberg, Polymeric membranes for the hydrogen economy: Contemporary approaches and prospects for the future, *J. Membr. Sci.* 327 (2009) 18-31.

Youchang Xiao, **Bee Ting Low**, Seyed Saeid Hosseini, Tai Shung Chung, Donald Ross Paul, The strategies of molecular architecture and modification of polyimide-based membranes for CO_2 removal from natural gas-A review, *Prog. Polym. Sci.* 34 (2009) 561-580.

2.1 Membrane material design guidelines for hydrogen and natural gas purifications

Polymers are popular materials for fabricating gas separation membranes. Before we examine and evaluate the different approaches that have been used by membrane scientists in the design of polymeric-based materials for hydrogen and natural gas separations, it is essential to establish an understanding of the basic design principles. The gas diffusivity and solubility across a polymeric membrane are strongly related to the inherent gas and polymer properties. Table 2.1 summaries the key physical properties of H_2, CO_2 and CH_4 [1].

Table 2.1 Physical properties of H_2, CO_2 and CH_4 [1]

Properties	**H_2**	**CO_2**	**CH_4**
Kinetic diameter, d_k (Å)	2.98	3.30	3.80
Collision diameter, σ_c (Å)	2.92	4.00	3.82
Effective diameter, σ_{eff} (Å)	2.90	3.63	3.81
Critical temperature, T_c (K)	33.3	304.2	190.7

First, let us consider the separation of H_2 and CO_2 using dense polymeric membranes. The kinetic diameter of H_2 is slightly smaller than CO_2 which means H_2 displays larger gas diffusivity. Conversely, the critical temperature of CO_2 is almost ten times higher than H_2. This implies that CO_2 is more easily condensable than H_2. The opposing effects resulting from the undesirable coupling of high H_2 diffusivity and CO_2 condensability is the key reason behind the poor permselectivity of numerous polymeric membranes toward this gas pair.

Based on the inherent properties of H_2 and CO_2, both the H_2/CO_2 diffusivity selectivity and CO_2/H_2 solubility selectivity are greater than unity i.e. the former is kinetically favorable and the latter is thermodynamically favorable [2]. Generally, glassy polymers are preferred for fabricating H_2 selective membranes and the separation performance can be improved by amplifying D_{H2}/D_{CO2} while limiting S_{CO2}/S_{H2}. On the other hand, rubbery polymers are typically used for fabricating CO_2-selective membranes and the design rule is reversed i.e. increasing S_{CO2}/S_{H2} and minimizing D_{H2}/D_{CO2}.

The scenario is rather different for the separation of CO_2 from CH_4. In fact, it is feasible to utilize polymeric membranes for CO_2/CH_4 separation because of the intrinsic gas properties. Considering this gas pair, CO_2 possesses both higher diffusivity (i.e. smaller kinetic diameter) and solubility (i.e. higher critical temperature) than CH_4. In other words, the preferential transport of CO_2 across polymeric membranes can be easily achieved because of favorable kinetic and thermodynamic factors i.e. D_{CO2}/D_{CH4} and S_{CO2}/S_{CH4} are larger than one. There are many polymers, in particular polyimides which display recommendable CO_2/CH_4 separation performance.

In the following sections, a critical review of the various methods that have been used by membrane researchers to design polymeric-based membranes with enhanced H_2/CO_2, CO_2/H_2 and CO_2/CH_4 separation performance is presented.

2.2 Molecular design of polymers

2.2.1 Homopolymers and random copolymers

The molecular design of polymers represents one of the most conventional approaches to create polymers with better gas separation properties [3-9]. To date, it has been extremely challenging to improve the H_2/CO_2 separation performance by utilizing novel polymer designs. The development of H_2-selective polymeric membranes via this technique has generated rather disappointing results and most glassy polymers show poor H_2/CO_2 selectivity [10-16]. It is difficult to control the polymer free volume within a narrow distribution and to tune the *d*-spacing between 2.89 and 3.30 Å for effective H_2/CO_2 separation based on size discrimination. Although the molecular design of glassy polymers is not a promising approach for improving H_2/CO_2 selectivity, it is excellent for altering the CO_2/CH_4 separation performance. Among the different polymers, polyimides exhibit a good compromise between high CO_2/CH_4 selectivity and CO_2 permeability.

Polyimides are extensively investigated as potential materials for fabricating gas separation membranes [10-18]. Aromatic polyimides comprising of hexafluoro substituted carbons in the polymer backbone are of particular interest and an example of a widely used dianhydride containing the $C(CF_3)_2$ linkage is hexafluoroisopropylidene-diphthalic anhydride (6FDA) [17-18]. The gas transport properties of the polymer are strongly dependent on the inherent chemical structure which influences the polymer free volume and chain rigidity. Generally, a polymer with high free volume and chain

flexibility results in large gas permeability and poor permselectivity, and vice versa. In order to achieve a good balance between gas permeability and permselectivity, the increase in the inter-chain spacing (i.e. free volume) should be coupled with backbone stiffness [19]. The polymer free volume can be increased with the incorporation of bulky pendant groups and designing polyimides with para linkages in the polymer backbone [19]. The polymer chain rigidity can be enhanced by (1) integrating polar side groups that improve the interactions between neighboring chains, (2) including bridging groups that have higher energy barrier, thereby inhibiting rotations and (3) incorporating aromatic rings with more rigid structures compared to aliphatic and cyclic configurations [19].

The design of polyimides by varying the monomers (i.e. dianhydrides and diamines) fails to generate polymers with impressive H_2/CO_2 selectivity but the approach works elegantly for CO_2/CH_4 separation. A comprehensive literature survey on engineered polyimides that are reported in the past two decades is conducted and the H_2/CO_2 and CO_2/CH_4 separation performances are plotted against the Robeson trade off lines as shown in Figures 2.1 and 2.2, respectively [19-22]. With reference to Figure 2.1, the H_2/CO_2 permselectivity of polyimide membranes is in the range of 2 to 6 while the H_2 permeability is between 20 and 80 Barrer. The poor intrinsic H_2/CO_2 selectivity deters the application of polymeric membranes for hydrogen enrichment. In the design of random copolyimides, a minor increment in the H_2/CO_2 selectivity is often achieved at the expense of a significant drop in the H_2 permeability. For instance, Liu et al. investigated the gas transport properties of 6FDA-durene/sulfone-containing diamine (3,3'-DDS) copolyimides and found that increasing the 3,3'-DDS content from 25 to 75 mol%

improves the H_2/CO_2 selectivity from 2.3 to 5.5 but decreases the corresponding H_2 permeability from 85 to 5 [23].

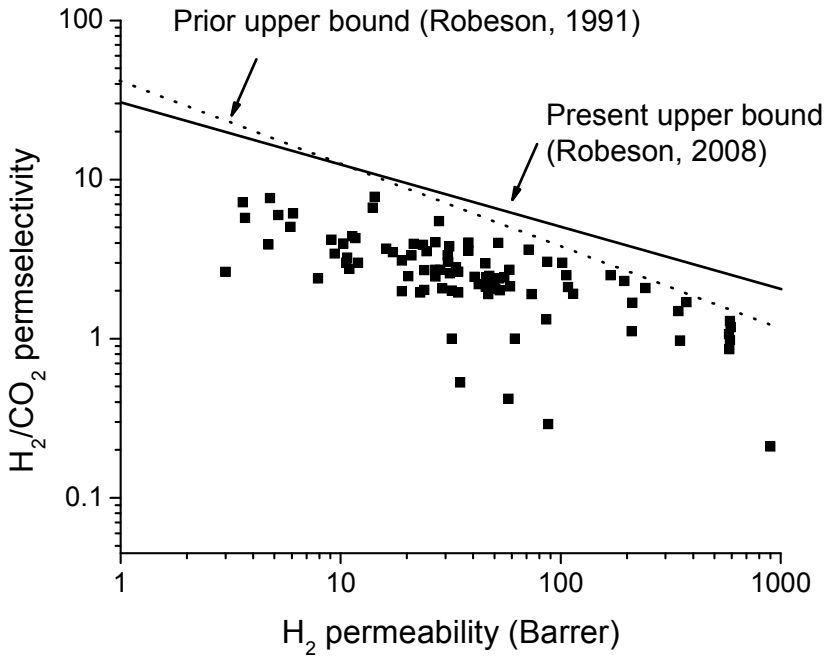

Figure 2.1 H_2/CO_2 separation performance of tailored polyimides

In contrast to the use of tailored polyimides for H_2/CO_2 separation, this category of polymer exhibits promising CO_2/CH_4 separation performance as depicted in Figure 2.2. Majority of the engineered polyimides display high CO_2/CH_4 selectivity in the range of 30 to 70 and satisfactory CO_2 permeability between 15 and 80 Barrer. Vast research works on polyimide gas separation membranes have been conducted for CO_2/CH_4 separation and approximately 50 % of the studies are based on 6FDA-polyimides. As shown in Figure 2.2, for polyimides displaying similar CO_2/CH_4 selectivity, the CO_2 permeability of 6FDA-polyimides is significantly higher than others. Despite the good CO_2/CH_4 separation performance of 6FDA-polyimides, they are not used for fabricating

commercial gas separation membranes. One of the main reasons is the susceptibility of these materials to CO_2-induced plasticization. Moreover, the long term performance of the polyimide membranes when subjected to real industrial feeds has yet been established. The higher cost of 6FDA-polyimides as compared to other polymers like cellulose acetate and polysulfone makes it less attractive from the economical aspect. However, this is a less pressing issue compared to the operational concerns since the price of the polymer will be determined by the demand-supply relationship i.e. greater demand leads to lower price.

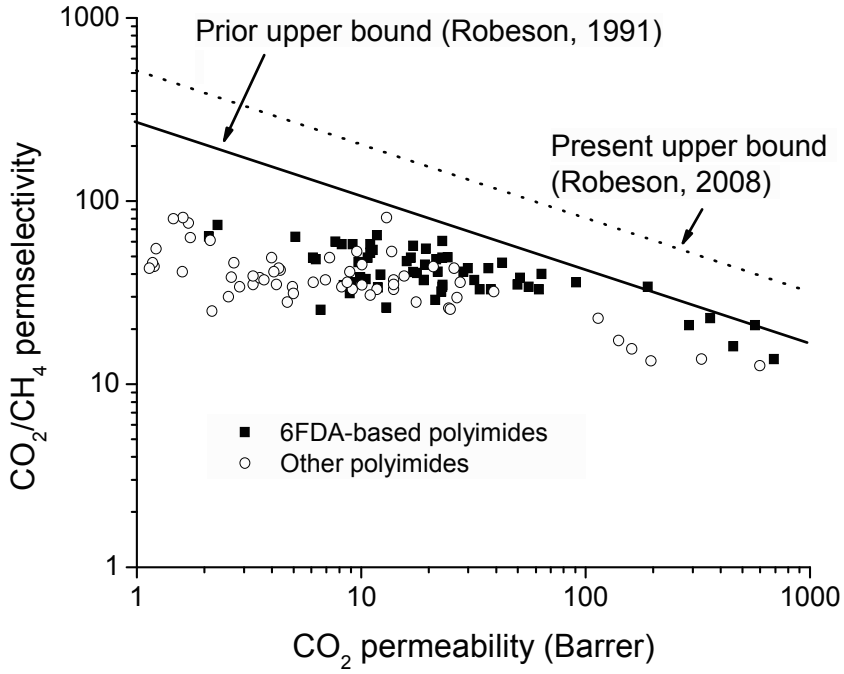

Figure 2.2 CO_2/CH_4 separation performance of tailored polyimides

Another variant of polyimides that has been studied for H_2/CO_2 and CO_2/CH_4 separations is poly(imide-siloxane) copolymers. Generally, these materials are prepared by the

condensation, imidization, and sol-gel reaction of hybrid poly(amicacid-siloxane) solutions. Smaihi et al. investigated a series of poly(imide siloxane) copolymers and concluded that the nature of the coupling agent and the proportion of siloxane significantly affects the gas permeabilities [24]. In their study, the use of aminopropylmethyldiethoxysilane for the formation of the silica network produces membranes with good H_2/CO_2 separation performance. At a temperature of 190 ^oC, the membrane exhibits a H_2/CO_2 selectivity of 7.8 and a corresponding H_2 permeability of 102 Barrer. When aminopropyltrimethoxysilane was used, the resultant poly(imide siloxane) membrane displays a higher H_2/CO_2 selectivity of 12 and a lower H_2 permeability of 21 Barrer. In another work by Hibshman et al., the gas transport properties of a series of poly(imide siloxane) copolymers fabricated from different silane-compounds were investigated [25]. For the poly(imide siloxane) comprising of 15 wt% methyltrimethoxysilane, annealing the membrane at 400 ^oC leads to the simultaneous increment in the CO_2/CH_4 selectivity and CO_2 permeability, and the separation performance falls above the Robeson upper bound. The increase in permeability is due to the quenching of the membrane after thermal annealing while the higher permselectivity is attributed to the greater extent of crosslinking that occurred during the heat treatment.

In addition to polyimides, membrane scientists have synthesized other novel polymers for inhibiting the chain-packing of glassy polymers and optimizing the free volume distribution. In some cases, the molecular architecture of novel polymers enhances D_{H2}/D_{CO2} but fails to minimize S_{CO2}/S_{H2}. For instance, Xu et al. examined the gas transport properties of fluorene-containing poly(arylene ether) with large and bulky

diphenylfluorene moieties [26]. The membranes exhibit notable H_2/CO_2 diffusivity selectivity of approximately 100 but the highly unfavorable H_2/CO_2 solubility selectivity of 0.017 leads to a poor overall H_2/CO_2 permselectivity. In a work by Camacho-Zuñiga et al., a series of cardo poly(aryl ether ketone) with side phthalide groups and aryl ether ketones of varying lengths was investigated [27]. Similarly, the membrane shows impressive D_{H2}/D_{CO2} of 320 but the unfavorable S_{H2}/S_{CO2} of 0.018 suppresses the H_2/CO_2 permselectivity. Compared to polyimides, the CO_2/CH_4 separation performance of these tailored poly(arylene ether) and poly(aryl ether ketone) are much inferior

Although majority of the glassy polymers are H_2-selective, there are some which are highly permeable to CO_2 and becomes reverse-selective. A well known example is poly(1-trimethylsilyl-1-propyne) (PTMSP), a stiff chain, glassy polymer with exceptionally high free volume for gas transport. Due to the large size and quantity of free volume cavities in PTMSP, the molecular sieving ability of the polymer is poor and the difference in gas solubility dominates the separation. The CO_2 permeability of PTMSP is 18200 Barrer and the CO_2/H_2 selectivity is 1.5 [28]. Another glassy polymer that displays comparable gas transport properties to PTMSP is poly(4-methyl-2-pentyne) (PMP) [29]. PMP membrane has a large CO_2 permeability of 11000 Barrer but a poor CO_2/H_2 selectivity of 1.8 [29]. The high gas permeability of PMP is attributed to the high free volume and interconnectivity of the free-volume-elements. The large intrinsic CO_2 permeability of PTMSP and PMP membranes allows room for further modification and to enhance the gas-pair selectivity. Rubbery homopolymers that are selective for CO_2 over H_2 have been investigated. For example, the gas transport properties of a series of

polyphosphazenes with 2-(2-methoxyethoxy) ethanol moiety were studied by Orme et al [30]. Increasing the proportion of 2-(2-methoxyethoxy) ethanol enhances both the CO_2 permeability and CO_2/H_2 solubility selectivity of the membrane. The highest CO_2/H_2 selectivity is 10 with a corresponding CO_2 permeability of 250 Barrer.

2.2.2 Block copolymer with hard and soft segments

In the design of CO_2-selective polymer, a feasible approach for increasing CO_2 solubility and CO_2/H_2 selectivity is to introduce functional groups that enhance the affinity of CO_2 with the polymer. A particularly effective approach is the incorporation of rubbery domains with glassy segments in the form of block copolymer systems as depicted in Figure 2.3 [19]. The hard segments, usually formed by a glassy polymer are expected to provide the main structural framework while the soft rubbery segments usually govern the gas transport. Due to the favorable interactions between ethylene oxide units and CO_2, a popular choice for the soft segment is poly(ethylene oxide) (PEO) while polyimide, polyamide, polyurea and polyurethane have been employed as the hard segments.

Poly(amide-6-b-ethyleneoxide) with the commercial name of Pebax® was first introduced as a material for gas separation membranes by Membrane and Technology Research (MTR) Inc., USA in 1990 [31]. Kim et al. explored the use of Pebax® membranes for gas separation and discovered that polarizable gases (e.g. CO_2 and SO_2) display higher permeability [32]. The CO_2/H_2 separation factor is 6.1 and the CO_2 permeability is 130

Barrer at 25 ^{0}C. Bondar et al. investigated another series of Pebax® polymers and the highest CO_2/H_2 selectivity is 10 at 35 ^{0}C [33]. At high pressures, the CO_2 permeability of Pebax® membranes increases while the H_2 permeability decreases. Therefore, an improvement in the CO_2/H_2 separation performance of Pebax® membranes is achievable at higher pressures.

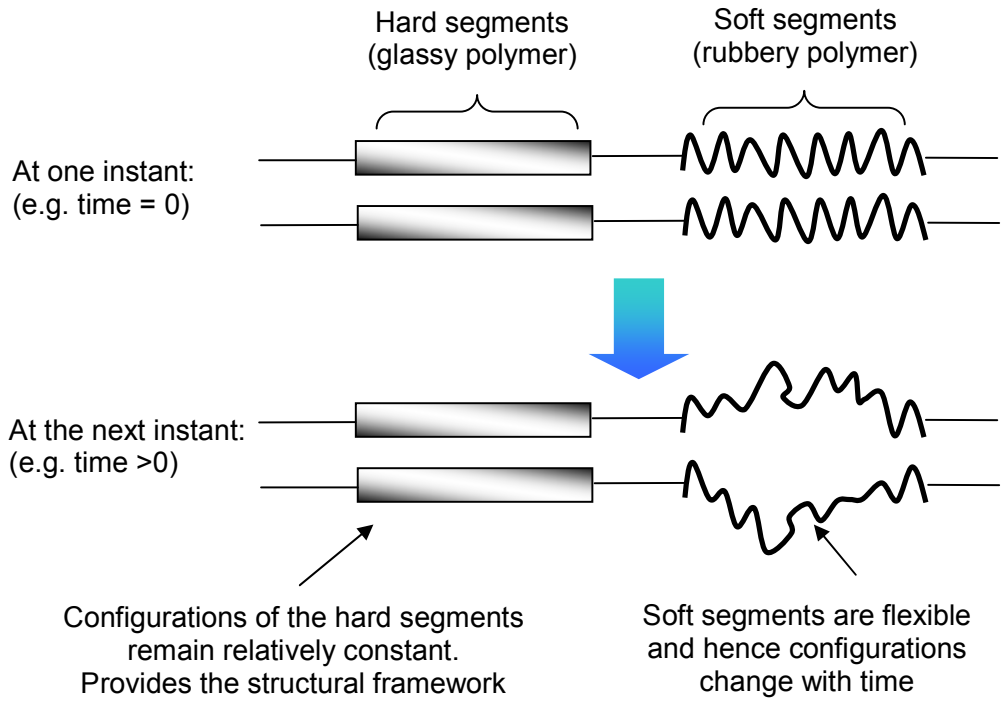

Figure 2.3 Synthetic strategy for copolymer systems with soft and hard segments

Simmons synthesized a series of poly(ether-urethane) and poly(ether-urea) block copolymers that contain polypropylene glycol (PPG) or polyethylene glycol (PEG) units [34]. The CO_2/H_2 selectivity of the synthesized materials (highest value of 7.7) is comparable to PEBAX but the CO_2 permeability is much larger (590 Barrer). In a subsequent work by Simmons, the gas transport properties of novel polyester-polyether

block copolymers containing PEG were investigated. The membrane displays a CO_2/H_2 selectivity of 13 and CO_2 permeability of 220 Barrer at 35 °C [35]. The presence of PEO or PEG units accounts for the preferential transport of CO_2 across these rubbery polymeric membranes.

Okamoto and co-workers employed a series of PEO-containing polyimides for CO_2/N_2 separations [36]. The block copolymers exhibit good CO_2/N_2 selectivity and CO_2 permeability, possibly due to the high CO_2 solubility in the PEO segments. The CO_2/H_2 separation performance of the PEO-polyimide membrane has not been reported. However, it is anticipated that the gas transport properties should be comparable to PEO-polyamide (e.g. Pebax®) membranes. Generally, the block copolymers with soft and hard segments work well for the separation of gases with significant difference in the gas condensability (i.e. CO_2/H_2 and CO_2/N_2) since the separation is dominated by the gas solubility. Therefore, these block copolymers are not commonly investigated for CO_2/CH_4 separation and it is likely that the polymers show poor CO_2/CH_4 selectivity.

2.3 Polymer blends

2.3.1 Linear polymer blends

The blending of linear polymers synergistically combines the advantages of different materials. One important consideration in the selection of polymers for the blend system

is their miscibility. A miscible polymer blend system indicates good interactions between the constituent polymers, and ensures homogeneity and reproducibility of the resultant membranes. Although there are numerous polymers, miscible polymer pairs are rather difficult to come by. The selection of the appropriate polymer pair for blending is critical in determining the gas transport properties of the resultant blend system, which is not simply the summation of the gas transport behaviors of the respective components.

Acharya et al. studied polysulfone/polycarbonate blend membranes for H_2/CO_2 separation [37]. Increasing the polycarbonate content from 0 to 50 % doubles the H_2 permeability from 13.5 to 25 Barrer but the corresponding H_2/CO_2 selectivity decreases by 50 % from 2.5 to 1.2. The gas transport properties of a polyimide/polyaniline blend system were investigated by Su et al [38]. The H_2 permeabilities of the pure polyimide and polyaniline are 3.3 and 4.6 while the H_2/CO_2 selectivities are 3.4 and 5.5, respectively. A polyimide/polyaniline (50:50) blend displays an enhanced H_2 permeability of 7.4 while maintaining the H_2/CO_2 selectivity at 5.5. This polymer blend system shows an impressive CO_2/CH_4 selectivity of 85 but a low CO_2 permeability of 1.3

In a recent work by Hosseini et al., Matrimid®/polybenzimidazole (PBI) blends were examined for its potential use in H_2/CO_2 and CO_2/CH_4 separations [39]. Both Matrimid® and PBI exhibit intrinsic H_2/CO_2 selectivity of approximately 3.8, but blending the two components in the ratio of 1:3 results in a selectivity of 9.4. The gain in H_2/CO_2 selectivity is probably attributed to the formation of hydrogen bonds between PBI and Matrimid® that reduces the inter-chain spacing. However, the improvement in H_2/CO_2

selectivity of the Matrimid®/PBI blend is obtained at the expense of lower gas permeability. Higher CO_2/CH_4 selectivity is achievable by increasing the PBI content but similarly, this increment is accompanied by lower CO_2 permeability. Maeda and Paul explored the use of miscible poly(phenylene oxide)/polysulfone blends in gas separation [40]. The CO_2/CH_4 selectivity of the polymer blend supersedes the separation factor that can be reaped from the respective pristine polymers. A higher percentage of poly(phenylene oxide) in the polymer blend results in greater CO_2 permeability. The improvement in the gas transport properties of the poly(phenylene oxide)/polysulfone blends is probably the result of stronger polymer-polymer interactions between the components.

In addition to improving the gas separation performance, polymer blending may enhance the integrity of polymeric membranes in the presence of condensable gas species e.g. CO_2. It has been demonstrated by Kapantaidakis et al. that the Matrimid®/polysulfone blends exhibit better anti-plasticization properties against carbon dioxide as compared to the neat Matrimid® membrane [41]. The enhanced anti-swelling property is due to the addition of polysulfone which has lower tendency to be plasticized by CO_2. In another related study by Bos and co-workers, the CO_2/CH_4 transport behavior of a polymer blend system comprising of Matrimid® and P84® copolyimide was studied [42]. The Matrimid®/P84® films show better anti-CO_2 plasticization characteristics with reasonably good CO_2/CH_4 separation performance.

The polymer blending approach can be exploited in the design of CO_2-selective membranes for hydrogen enrichment. In a work by Car et al., the blending of low molecular weight polyethylene glycol (PEG) with commercially available Pebax® improves the gas transport properties [43]. Increasing the PEG content enhances the polymer chain mobility and gives rise to greater CO_2 permeability and CO_2/H_2 permselectivity. An optimal CO_2 permeability of 150 Barrer and CO_2/H_2 selectivity of 11 is obtained by using a blend composition of 50 wt% PEG in Pebax®. The Pebax® membrane has a CO_2 permeability of 73 Barrer and a CO_2/H_2 selectivity of 9. The incorporation of PEG with Pebax® doubles the CO_2 permeability while maintaining the CO_2/CH_4 selectivity.

2.3.2. Interpenetrating polymer networks

An interpenetrating polymer network (IPN) consists of two different polymer networks that only physically interact with each other [44-50]. If a network polymer is combined with a linear polymer, a pseudo- or semi- IPN results [44]. A pseudo-IPN is produced either by (1) the polymerization of the precursors of a branched polymer in the presence of a pre-formed linear polymer or (2) the formation of a straight-chain polymer within a pre-existing network. IPNs are novel and versatile composite materials for many applications, including their prospective use as a barrier material for gas separation. However, there are limited studies that report the use of IPN materials for gas separation membranes.

Rezac and Schoberl incorporated an acetylene-terminated monomer which is capable of forming a polymer network, with a polyetherimide to form a semi-IPN [51]. The effect of curing temperature on the resultant gas transport behavior of the semi-IPNs has been reported. Compared to the linear polyetherimide, the addition of 9 wt% acetylene-terminated monomer followed by curing at 230 ^{o}C increases the H_2/CO_2 selectivity marginally from 5.9 to 7.0 and decreases the H_2 permeability from 6 to 5.7 Barrer. The semi-IPN has lower CO_2/CH_4 selectivity and CO_2 permeability. Although the formation of the semi-IPN does not improve the gas transport properties, these membranes display better chemical resistance as proven by the high gel content of the cured films in methylene chloride.

Bos et al. fabricated a series of pseudo-IPNs with different compositions of Matrimid® and Thermid FA-700 [52]. Thermid FA-700 is a polyimide oligomer with three aminophenylacetylene end caps that reacts and forms a network polymer when it is subjected to thermal treatment. The Matrimid®/Thermid semi-IPNs effectively suppress the CO_2-induced plasticization and the CO_2/CH_4 selectivity is higher than the neat Matrimid® film. These are attributed to the restricted chain mobility brought about by the favorable physical interconnections between the linear Matrimid® polymer and the crosslinked Thermid oligomers. The H_2/CO_2 transport properties of the Matrimid®/Thermid semi-IPNs have not been reported.

Kurdi and Kumar have done substantial works on a series of semi-IPNs based on bismaleimide (BMI) [53]. The network polymer is formed by the ethoxylation reaction

followed by the formation of anionic and proton radicals, and lastly the anionic polymerization of BMI. Polysulfone and polyetherimide (PEI) were used as the linear polymers to form the semi-IPNs with the BMI network. For these semi-IPNs, only the O_2 and N_2 transport properties were tested. Therefore, the applicability of these materials to hydrogen enrichment and natural gas sweetening remains unknown. Subsequently, Saimani and Kumar investigated the CO_2/N_2 transport properties of pseudo-IPNs made up of PEI and crosslinked polyethylene glycol diacrylate (PEGDA) [54]. A higher concentration of PEGDA results in a significant enhancement in CO_2 permeability but lowers the CO_2/N_2 selectivity. The PEI/PEGDA semi-IPNs may be suitable materials for fabricating CO_2-selective membranes for hydrogen purification.

2.4 Chemical modification

2.4.1 Diamine crosslinking of polyimides

Hayes introduced a cross-linking method by immersing polyimide membranes in a solution containing diamine [55-56]. To date, the diamino modification method is one of the most promising strategies that generates significant enhancement in the intrinsic H_2/CO_2 selectivity of polyimide membranes. This approach utilizes the spontaneous reactions between the amine and imide groups which is applicable to all polyimides. Chung et al. utilized a series of aliphatic diamines, i.e. ethylenediamine (EDA), 1,3-diaminopropane (PDA) and 1,4-diaminobutane (BuDA), to modify dense polyimide membranes for H_2/CO_2 separation [3]. The ideal H_2/CO_2 selectivity of the 6FDA-durene

membrane increases dramatically from 1 to 100 at 35 °C after crosslinking with PDA for 10 min [3]. Nevertheless, the diamine modification considerably reduces the H_2 permeability of the resultant membranes [3,57]. The significant alteration to the H_2/CO_2 transport properties may be due to (1) the optimization of the free-volume distribution by the space filling effects of diamines, (2) the enhanced polymer chain rigidity and (3) the presence of hydrogen bonds within the crosslinked/network structure. The diamine modification scheme can be similarly employed to polymer blend systems containing polyimides. For instance, Hosseini et al. modified Matrimid®/PBI (1:3) blend with p-xylylene diamine and the H_2/CO_2 selectivity increases from 9.4 to 26 [39]. In another work by Zhao et al., the amino-terminated PEG was used to modify Matrimid® membranes via the chemical reaction between the amine and imide groups [58]. Due to the favorable interactions between PEG and CO_2, a significant increment in CO_2 permeability from 5.4 Barrer for the neat Matrimid® film to 115 Barrer for the PEG modified membrane is obtained. The pristine membrane exhibits a H_2/CO_2 selectivity of 3.3 while the amino-PEG modified membrane (i.e. 50:50 Matrimid®/PEG) shows a CO_2/H_2 selectivity of 7.3.

The modification of polyimides with diamines similarly increases CO_2/CH_4 selectivity. Chemical modifications of 6FDA-durene dense membranes were performed using ethylenediamine (EDA) and 1,3-cyclohexanebis(methylamine) (CHBA) by Shao et al. [59-60]. With appropriate modification duration, the EDA-modified polyimide membrane shows higher CO_2/CH_4 permselectivity and lower permeability. The diamine modification approach improves the plasticization resistance of 6FDA-durene membranes i.e.

plasticization pressure increases from 300 to more than 720 psia. For the CHBA-modified films with thermal treatment, the enhancement in CO_2/CH_4 permselectivity is greater. The combined effects of diamine-induced cross-linking and thermal annealing accelerate the formation of charge transfer complexes which densifies the polyimide membrane structure. Liu et al., Cao et al. and Ren et al. used *p*-xylylenediamine as a cross-linking agent to modify different polyimide hollow fiber membranes at ambient temperature [61-64]. Similar enhancements in the CO_2/CH_4 permselectivity and anti-swelling properties are achieved.

Chung, Xiao and their co-workers extended this approach by utilizing multi-amine compounds, polyamidoamine (PAMAM) dendrimers to modify 6FDA-durene polyimide films [65-68]. Due to the larger molecular size of the dendrimers, the cross-linking modification mainly occurs on the membrane surface. The modified polyimide films exhibit better CO_2/CH_4 separation performance because of the affinity between PAMAM dendrimer and CO_2. In a subsequent study, it was found that annealing the dendrimer-modified polyimide film at a mild temperature of 150 ^oC facilitates the amidization reaction and enhances the degree of cross-linking by the dendrimers [68].

Although the modification of polyimide membranes with amines improves H_2/CO_2 and CO_2/CH_4 permselectivity, the long term operational stability of the membranes at elevated temperatures is a concern. One major limitation of this approach is the reversible reaction between the amino-compounds and the imide groups at high temperatures which has been verified by Shao et al. and Powell et al. [59,69]. The applicability of the diamino

modification approach on polyimide membranes has been proven by the promising results reported in these studies. However, the types of chemical reactions occurring during the modification remain unclear. In addition, it would be interesting to investigate the effects of diamine and polyimide properties on the effectiveness of the modification method.

2.4.2 Diol crosslinking of polyimides containing carboxylic acid groups

Paul, Koros and their co-workers investigated the CO_2/CH_4 separation performance of a 6FDA-copolyimide with 2,4,6-trimethyl-1,3-diaminobenzene (DAM) and 3,5-diaminobenzoic acid (DABA) as the diamine moieties [70-75]. 6FDA-DAM/DABA contains carboxylic acid groups which undergo esterification reaction with hydroxyl groups. Wind et al. utilized a series of diol containing reagents (i.e. ethylene glycol (EG), butylene glycol (BG), 1,4-cyclohexanedimethanol (CHDM) and 1,4-benzenedimethanol (BDM)) to effect crosslinking of the polyimides [70-71]. In the presence of a large excess of the diol compound and using p-toluenesulfonic acid as the catalyst, the polyimide first undergoes monoesterification where the diol is grafted to the polymer chain via reaction with the carboxylic acid groups [70]. The grafted polyimide is used for fabricating membranes and the subsequent thermal annealing allows for transesterification to take place between the free –OH and –COOH groups i.e. crosslinking of the polyimide. The effect of crosslinking is related to the chemical structure of the diol-containing reagents and the annealing temperatures. The crosslinking of 6FDA-DAM/BADA with BG and thermal curing at 295 ^{o}C brings about an increase in CO_2 permeability without sacrificing the CO_2/CH_4 selectivity. This enhancement in gas permeability is possibly due to the

creation of additional free-volume from the removal of pendant diol groups during the transesterification or the inhibition of chain packing by the formation of chemical crosslinks between the chains. The crosslinked 6FDA-DAM/DABA membranes display superior CO_2 plasticization resistance for natural gas recovery.

Hillock and Koros extended this solid state crosslinking approach by exploring the use of 1,3-propanediol as the modification reagent [73]. The propanediol monoester cross-linkable (PDMC) polyimide membranes display significantly larger CO_2 permeability and slightly higher CO_2/CH_4 selectivity after transesterification and thermal annealing. The crosslinked PDMC dense films similarly show excellent anti-swelling properties against aggressive feed streams containing CO_2. This solid state crosslinking approach has been implemented on asymmetric hollow fiber membranes which are of greater commercial value. Omole et al. modified the esterification process by removing the water formed during esterification in order to synthesize high molecular weight polymer which is more favorable for the fabrication of hollow fiber membranes [74]. The as-spun hollow fibers are subjected to thermal annealing at 200 ^{o}C for transesterification and crosslinking to take place. The diol cross-linked polyimide hollow fiber membrane displays promising CO_2/CH_4 permselectivity of 43 and a CO_2 permeance of 46 GPU. The diol crosslinked 6FDA-DAM/DABA copolyimide membranes with excellent anti-swelling properties can be effectively used for CO_2/CH_4. However, this approach is only limited to polyimides containing carboxylic acid groups. The H_2/CO_2 separation property of this material has yet been reported and it may be worthwhile to explore the use of this material for hydrogen enrichment.

2.4.3 Rubbery polymers with crosslinked networks

Poly(ethylene oxide) (PEO) is a potential material to fabricate CO_2-selective membranes for hydrogen purification but the ease of crystallization and poor mechanical properties of PEO are highly undesirable [4,6,76-78]. One strategy to overcome the deficiencies of linear PEO membranes is to disrupt the alignment of polymer chains via crosslinked networks. Lin et al. synthesized highly branched and crosslinked PEO for fabricating high performance CO_2-selective membranes [4]. Decreasing the temperature leads to a significant improvement in the CO_2/H_2 separation performance i.e. the CO_2/H_2 selectivity increases from 9 to 31 as the temperature decreases from 35 to -20 ^oC at a CO_2 partial pressure of 17 atm. At a temperature of -20 ^oC, the CO_2 permeability elevates from less than 30 Barrer to 410 Barrer with increasing CO_2 partial pressure. Typically for glassy polymers, the membrane performance tends to deteriorates in the presence of condensable gas species. A notably reversed behavior is observed for this rubbery crosslinked PEO membrane where the CO_2 plastcization brings about simultaneous enhancement in CO_2/H_2 selectivity and CO_2 permeability. Superior CO_2/H_2 separation performance can be obtained even in the presence of other impurities like H_2S, H_2O and CO.

The CO_2/CH_4 separation performance of the crosslinked PEO membrane was investigated [78]. Similar to CO_2/H_2 separation, a higher CO_2/CH_4 selectivity can be obtained at lower operating temperatures. At a CO_2 partial pressure of 17 atm, the CO_2/CH_4 selectivity increases from 14 to 37 as the temperature decreases from 35 to –20 °C. However, in contrast to the increasing CO_2/H_2 selectivity at higher pressures, the increase in CO_2

partial pressure results in a decline in CO_2/CH_4 selectivity. This is attributed to the decrease in CO_2/CH_4 diffusivity selectivity at higher CO_2 partial pressures. For natural gas purification, the presence of higher hydrocarbons is unavoidable and usually leads to poor CO_2/CH_4 separation performance of glassy polymeric membranes. As the activity of butane in the feed increases, the CO_2/CH_4 selectivity of the crosslinked PEO membranes decreases marginally from 25 to 23 but the CO_2 permeability increases significantly from 200 to 300 Barrer.

Taniguchi et al. studied the immobilization of poly(amidoamine) (PAMAM) dendrimers within a PEG network by the photopolymerization of PEG dimethylcrylate [79]. A composite membrane with 50 wt % of PAMAM dendrimer and 50 wt% of PEG displays an impressive CO_2/H_2 selectivity of 500 and a CO_2 permeability of 3.65 x 10^3 Barrer. The excellent CO_2/H_2 separation performance is attributed to the enhanced CO_2 solubility brought about by the favorable interactions between CO_2 and the amine groups of the dendrimer. Moreover, the presence of the dendrimer possibly inhibits the crosslinking of the PEG oligomers and hence creates more free volume in the resultant membrane. In a recent work by Shao and Chung, the in-situ fabrication of crosslinked PEO-silica network was investigated and the membranes were tested for the CO_2/H_2 separation [80]. The incorporation of the silica network greatly reduces the crystallinity of the membranes and improves the mechanical properties of the rubbery polymer. An optimal CO_2/H_2 selectivity of 9 and CO_2 permeability of 318 Barrer is achievable by the PEO/Silica (90:10) composite film.

The promising CO_2/H_2 separation performance of PEO-based membranes motivates the exploration of poly(propylene oxide) (PPO) membranes for CO_2/H_2 separation. Despite the close similarity in the chemical structures of PPO and PEO, the gas separation performance of the former is less impressive. Raharjo et al. investigated a series of crosslinked PPO copolymers, and the highest CO_2/H_2 selectivity is 4.7 at 35 ^oC which is only 50% of what can be achieved by the crosslinked PEO copolymer i.e. CO_2/H_2 selectivity of 9.4 [81]. However, the crosslinked PPO membranes generally show higher CO_2 permeability than the crosslinked PEO membranes and this is due to the larger free volume created by the methyl appendages. The CO_2/CH_4 separation performance of crosslinked PPO membranes is also much lower than the crosslinked PEO membranes. Therefore, crosslinked PEO copolymers are better materials for fabricating high performance CO_2 selective membranes.

2.4.4 Halogenation, sulfonation and metal ion-exchange

The doping of conjugated polyaniline membranes with halogen ions for enhancing the gas separation performance has been studied [82-86]. Anderson et al. demonstrated a significant improvement in H_2/N_2 selectivity from 210 to 3600 after doping and undoping the polyaniline membranes with suitably-sized counterions (e.g. F^-, Cl^-, Br^-, I^-) [82]. This selectivity improvement is attributed to the morphological changes in polyaniline membranes resulting from the doping, undoping and redoping process. In a subsequent study by Anderson et al., the gas transport properties of polyaniline membranes treated with HCl were reported [83]. The redoped membranes exhibit an enhanced H_2/CO_2

selectivity of 9 and CO_2/CH_4 separation factor of 146. The corresponding H_2 and CO_2 permeabilities are 6.5 and 0.7 Barrer. Chang et al. highlighted a change in the *d*-spacing of the polyaniline dense film from 4.5Å to 3.5Å after doping with 1M HCl [84]. These results indicate that doping of polyanline improves the diffusivity selectivity of various gas pairs. Similar works on the doping of polyaniline films were conducted by Kaner et al. and Illing et al [85-86].

Alternatively, the benzene rings of polyimides can be used as functional sites for side group grafting via electrophilic aromatic substitution reactions. Guiver et al. performed the direct bromination of Matrimid® by electrophilic bromination [87]. The brominated polyimide displays an enhanced CO_2 permeability from 8 to 14 Barrer with a marginal decrease in CO_2/CH_4 selectivity from 36 to 33. The higher CO_2 permeability is due to presence of the Br substituent groups which reduce the polymer chain packing efficiency. In addition to polyimides, the aryl bromination of poly(phenylene oxide) was investigated by Chern et al [88]. It was found that increasing the degree of bromination brings about a considerable increase in CO_2 permeability from 50 to 70 Barrer while the CO_2/CH_4 selectivity increases from 17 to 20 at 20 atm. In a subsequent study by Story and Koros, the brominated poly(phenylene oxide) similarly exhibits an improved CO_2 permeability by a factor of 2.5 with nearly no change in the CO_2/CH_4 selectivity [89]. The bromine substituent group introduces steric hindrance which increases the diffusional jump length and the gas mobility. This accounts for the observed improvement in CO_2 permeability.

The aryl halogenation approach can be applied to aromatic polyesters as demonstrated in a work by Chern and Provan [90]. The presence of Br and Cl substituent groups in the aromatic polyester increases the CO_2 permeability due to the enhanced CO_2 sorption which more than compensates for the decrease in CO_2 diffusivity. Conversely, the lower gas diffusivity brought about by the reduced chain motion results in lower CH_4 permeability. Thus, simultaneous improvement in CO_2 permeability and CO_2/CH_4 selectivity was obtained. The results from this study seem to be in contrary to the brominated poly(phenylene oxide) membranes where the presence of the Br substituent group increases the gas diffusivity [89]. The brominated and chlorinated polyesters are more susceptible to CO_2-induced plasticization. The H_2 transport parameters of the polymers have not been reported.

The sulfonation of poly(phenylene oxide) was investigated by Sridhar et al [91]. The sulfonated polymer shows a higher CO_2/CH_4 selectivity from 12 to 27 while the CO_2 permeability decreases from 44 to 18 Barrer. Hamad et al. studied the sulfonation of brominated poly(phenylene oxide) and the effects on the gas transport properties of the material [92]. Increasing the extent of bromination leads to larger CO_2 permeability while higher sulfonation degree decreases the gas flux. Varying the bromination extent does not alter the CO_2/CH_4 selectivity but increasing the degree of sulfonation leads to higher separation factor. Therefore, the combination of bromination and sulfonation is a good approach to achieve a compromise between gas permeability and gas pair selectivity. The sulfonated-brominated poly(phenylene oxide) membrane shows reasonably high CO_2 permeability of 76 Barrer and CO_2/CH_4 selectivity of 42. The H_2 transport properties of

these polymers have not been reported. Piroux et al. studied the H_2/CO_2 transport behavior of different sulfonated polyimides, including the cardo-type polymer [93]. The membranes show poor H_2/CO_2 selectivity that falls in the range of 1.0 to 2.7. The CH_4 transport property of the sulfonated polyimide has not been reported.

The effect of metal ion substitution on the gas transport characteristics of the polymer has been investigated. Hamad et al. explored the use of divalent (i.e. Mg^{2+}, Ca^{2+} and Ba^{2+}) and trivalent (i.e. Al^{3+}) metal cations [94]. It was found that Mg^{2+}-sulfonated poly(phenylene oxide)/polyethersulfone thin film composite membranes display the best gas separation performance i.e. CO_2 permeance of 1.5 GPU and CO_2/CH_4 permselectivity of 67. The differences in the gas separation performance of the ion-exchanged sulfonated poly(phenylene oxide) membranes are attributed to the varying hindrance effect, electronegativity and crosslinking strength of the metal cations. Kruczek and Matsuura reported the CO_2/CH_4 transport properties of the sulfonated poly(phenylene oxide) with Na^+, Mg^{2+} and Al^{3+} ions [95]. The Mg^{2+}-sulfonated poly(phenylene oxide) membranes yield the highest CO_2/CH_4 selectivity of 54 and a corresponding CO_2 permeability of 12 Barrer. The sulfonation and metal ion exchange of polyethersulfone dense membranes were investigated by Li and Chung [96]. The sulfonated polyethersulfone membranes have poor H_2/CO_2 selectivity. Among the cations used, Zn^{2+}-sulfonated polyethersulfone membranes displays the highest CO_2/CH_4 selectivity of 47 but a relatively low CO_2 permeability of 1.4 Barrer. The ion-exchanged membranes have enhanced anti-CO_2 plasticization properties.

2.5 Mixed matrix membranes

The concept of mixed matrix membranes (MMM) has been developed to combine the processability of polymers with the better separation performance of inorganic materials. A significant challenge that is faced in the fabrication of mixed matrix membranes is the elimination of interfacial voids between the organic and inorganic phases. Attempts have been made to chemically graft the inorganic fillers to the polymer chains via organic reactions. In a work by Guiver et al., a silane coupling agent was used to react with the hydroxyl groups on the surface of zeolite 3A molecular sieves and to introduce amine groups on the particle surface [97]. Composite membranes are made with the modified zeolite 3A and aldehyde-functionalized polysulfone. The grafting of zeolite 3A particles occurs via the favorable reactions between the amine and aldehyde groups. The H_2/CO_2 selectivity is only 1.6 for the neat polysulfone membrane and the polysulfone/zeolite 3A MMM exhibits an impressive H_2/CO_2 selectivity of 72 and a corresponding H_2 permeability of 7.1 Barrer.

Mixed matrix membranes with zeolites as the dispersed inorganic phase have been used for CO_2/CH_4 separation. Husain and Koros altered the hydrophobicity of HSSZ-13 zeolite particles by a Grignard reagent and this improves the interactions between the fillers and the Ultem® polyetherimide [98]. This mixed matrix membrane in the form of hollow fiber has a CO_2/CH_4 selectivity of 47 and CO_2 permeance of 7 GPU. Hillock et al. incorporated SSZ-13 zeolite into crosslinkable 6FDA-DAM/DABA polyimide membranes [99]. Simultaneous enhancements in CO_2/CH_4 selectivity from 58 to 67 and

CO_2 permeability from 37 to 50 Barrer are obtained. The increase in separation factor is brought about by the molecular sieving effects of the well-adhered silanated zeolites to the polymer matrix. Conversely, the increase in gas permeability is due to the presence of leaky surfaces caused by a fraction of the zeolite particles that have poor adhesion with the organic phase. Li and Chung investigated the CO_2 and CH_4 transport properties of AgA zeolite/polyethersulfone mixed matrix membranes [100]. The presence of Ag^+ ions brings about the facilitated transport of CO_2 and the zeolite pore accounts for the molecular sieving effects. The AgA zeolite/PES dense film exhibits a CO_2/CH_4 selectivity of 44 and CO_2 permeance of 1.2 Barrer compared to the neat PES film which has a CO_2/CH_4 selectivity of 35 and CO_2 permeance of 1 Barrer.

The addition of inorganic fillers may be utilized to enhance the physical properties of polymeric membranes and this is particularly applicable to rubbery polymers with relatively poor mechanical properties. PEO is a popular material for fabricating CO_2-selective membranes but this polymer generally displays poor mechanical integrity at high testing pressures. Chemically crosslinked poly(ethylene glycol diacrylate) (PEGda) oligomers and their nanocomposites were investigated by Patel et al [101-102]. The PEGda membranes display attractive CO_2 permeability and CO_2/H_2 selectivity. The incorporation of fumed silica in the PEGda membranes enhances the mechanical strength of the membrane without adversely affecting CO_2/H_2 selectivity.

In addition to zeolites and fumed silica which are widely used for fabricating mixed matrix membranes, other inorganic fillers like carbon molecular sieves (CMS), metal-

organic-frameworks (MOF) and metal oxides have also been investigated [103-105]. In a study by Vu et al., Matrimid® dense films were pyrolyzed and the carbonized films were crushed into small particle sizes, silanated and added to Ultem® or Matrimid® polymer matrix [103]. For both commercial polymers, the incorporation of CMS particles enhances the CO_2/CH_4 selectivity and CO_2 permeability. Perez et al. studied the use of MOF-5 as the inorganic filler to form mixed matrix membranes with Matrimid® as the continuous polymer phase [104]. With increasing MOF loading from 0 to 30 %, the H_2 permeability increases from 24 to 54 Barrer while the H_2/CO_2 permselectivity remains relatively constant at 2.7. Despite MOF being a good storage material for hydrogen, the addition of MOF in the mixed matrix membranes does not improve the H_2/CO_2 selectivity. This is possibly due to the effects of competitive gas sorption. Conversely, the CO_2/CH_4 selectivity of the MOF-5/Matrimid® membranes exhibits an up-and-down trend with an optimal separation factor of 51 at 10% MOF loading. The CO_2 permeability increases with increasing MOF content. The CO_2/CH_4 selectivity first increases because the increase in CO_2 solubility is more important than the increase in CH_4 diffusivity. With further increase in the MOF loadings, the higher CH_4 diffusivity brings about a decrease in CO_2/CH_4 separation factor. Hosseini et al. investigated the CO_2/CH_4 separation performance of MgO/Matrimid® dense films that are treated with silver nitrate [105]. The Ag^+-modified MgO/Matrimid® MMM shows higher CO_2/CH_4 selectivity due to the facilitated transport function of the silver ions to CO_2. The partial blockage of the MgO pores with Ag^+ ions results in lower CO_2 permeability.

2.6 Challenges and future prospects

It is often difficult to achieve the best of both worlds and similarly for gas separation using polymeric membranes, a trade off relationship usually exists between permeability and permselectivity. Most polymeric membranes which are highly permeable typically show inferior permselectivity and vice versa. Good selectivity and permeability are not the only considerations in the selection of appropriate materials for hydrogen enrichment and natural gas sweetening. Other critical factors include the thermal, mechanical and chemical robustness of the membranes in the presence of aggressive feeds and harsh operating conditions. Of course, obtaining a membrane with good gas separation performance typically outweighs other parameters but the priority of the membrane material research needs to be amended accordingly to the current situations.

To date, it is nevertheless an exceptionally challenging task to separate H_2 and CO_2 using polymeric membranes. Recently, the revised upper bound relationship by Robeson reveals that majority of the polymeric membranes show unfavorable H_2/CO_2 separation performance despite the efforts by researchers in the exploration of new membrane materials [21]. As shown in the preceding sections, different approaches are investigated in order to overcome the bottlenecks and improve H_2/CO_2 selectivity. All the design strategies have their merits and limitations. The search for polymeric-based materials to be used in hydrogen enrichment is still progressing since the current state of the art is perhaps inadequate for industrial applications. There exists considerable opportunities for improving the H_2/CO_2 separation performance of polymeric membranes.

For the separation of CO_2/CH_4 using polymeric membranes, the current situation as reflected by the upper bound appears more optimistic [21]. In fact, a growing number of polymers exhibit CO_2/CH_4 separation performance above the 1991 trade-off line and this considerably shift the position of the upper bound line towards the high permeability and permselectivity region. Recently, thermally rearranged polymers were discovered and these polymers exhibit promising CO_2/CH_4 separation performance that falls well above the present upper bound. The research on membrane materials for CO_2/CH_4 separation has somewhat attained a stage whereby greater emphasis needs to be placed on the strategies to suppress CO_2-induced plasticization rather than on increasing the CO_2/CH_4 separation factor. A literature survey on the research works done on gas separation membranes show that only a minority of the studies addresses the issues of CO_2-induced plasticization, long term separation performance and multi-component feed mixtures.

There is no doubt to the potential benefits of membrane technology over conventional techniques for hydrogen and natural gas purifications. However, membrane technology has not been extensively utilized for real industrial gas separations and this is an indication of the shortcomings of the past and current membrane research work. A severe deficiency comes from the fact that most of the membranes are tested with mild feed and operating conditions at the bench-scale and the membrane separation performance in real industrial applications remains unknown. In the selection of a suitable membrane for gas purification, the operating temperature and pressure are of paramount importance since they directly affect the separation efficiency of the membrane. Moreover, the composition of the gas mixture to be separated, the material and fabrication costs of the membranes

and the overall process design must be addressed. Ultimately, the incorporation of a membrane unit to the overall process must reap considerable cost and energy savings. This is attainable only with stronger collaborations between the academia and the industries.

2.7 References

[1] S. L. Liu, R. Wang, Y. Liu, M. L. Chng, T. S. Chung, The physical and gas permeation properties of 6FDA-durene/ 2,6 diaminotoluene copolyimides, Polymer 42 (2001) 8847.

[2] B. D. Freeman, Basis of permeability/selectivity tradeoff relations in polymeric gas separation membranes, Macromolecules 32 (1999) 375.

[3] T. S. Chung, L. Shao, P. S. Tin, Surface modification of polyimide membranes by diamines for H_2 and CO_2 separation, Macromol. Rapid Commun. 27 (2006) 998.

[4] H. Lin, E. Van Wagner, B. D. Freeman, L. G. Toy, R. P. Gupta, Plasticization-enhanced hydrogen purification using polymeric membranes, Science 311 (2006) 639.

[5] J. Qiu, J. M. Zheng, K. V. Peinemann, Gas transport properties of poly(trimethylsilylpropyne) and ethylcellulose filled with different molecular weight trimethylsilylsaccharides: Impact on fractional free volume and chain mobility, Macromolecules 40 (2007) 3213.

[6] H. Lin, B. D. Freeman, Materials selection guidelines for membranes that remove CO_2 from gas mixtures, J. Mol. Struct. 739 (2005) 57.

[7] A. Car, C. Stropnik, W. Yave, K. V. Peinemann, PEG modified poly(amide-b-ethylene oxide) membranes for CO_2 separation, J. Membr. Sci. 307 (2008) 88.

[8] T. C. Merkel, B. D. Freeman, R. J. Spontak, Z. He, I. Pinnau, P. Meakin, A. J. Hill, Ultrapermeable, reverse-selective nanocomposite membranes, Science 296 (2002) 519.

[9] N. P. Patel, M. A. Hunt, S. Lin-Gibson, S. Bencherif, R. J. Spontak, Tunable CO_2 transport through mixed polyether membranes, J. Membr. Sci. 251 (2005) 51.

[10] K. Tanaka, H. Kita, K. Okamoto, A. Nakamura, Y. Kusuki, Gas permeability and permselectivity in polyimides based on 3,3',4,4'-biphenyltetracarboxylic dianhydride, J. Membr. Sci. 47 (1989) 203.

[11] M. Al-Masri, H. R. Kricheldorf, D. Fritsch, New polyimides for gas separation 1. Polyimides derived from substituted terphenylenes and 4,4‘-(hexa fluoroisopropylidene) diphthalic anhydride, Macromolecules 32 (1999) 7853.

[12] C. Staudt-Bickel, W. J. Koros, Improvement of CO_2/CH_4 separation characteristics of polyimides by chemical crosslinking, J. Membr. Sci. 155 (1999) 145.

[13] S. Shishatskiy, C. Nistor, M. Popa, S. P. Nunes, K. V. Peinemann, Polyimide asymmetric membranes for hydrogen separation: Influence of formation conditions on gas transport properties, Adv. Eng. Mater. 8 (2006) 390.

[14] J. Hao, K. Tanaka, H. Kita, K. I. Okamoto. Synthesis and properties of polyimides from thianthrene-2,3,7,8-tetracarboxylic dianhydride-5,5,10,10-tetraoxide, J. Polym Sci.: Part A: Polym Chem 36 (1998) 485.

[15] S. A. Stern, R. Vaidyanathan, J. R. Pratt, Structure/permeability relationships of silicon containing polyimides, J. Membr. Sci. 49 (1990) 1.

[16] S. A. Stern, Y. Mi, H. Yamamoto, Structure/permeability relationships of polyimide membranes. Applications to the separation of gas mixtures, J. Polym. Sci: Part B: Polym. Phys. 27 (1989) 1887.

[17] M. R. Coleman, W. J. Koros, The transport properties of polyimide isomers containing hexafluoroisopropylidene in the diamine residue, J. Polym. Sci.: Part B: Polym. Phy. 32 (1994) 1915.

[18] Y. Liu, R. Wang, T. S. Chung, Chemical cross-linking modification of polyimide membranes for gas separation, J. Membr. Sci. 189 (2001) 231.

[19] Y. Xiao, B. T. Low, S. S. Hosseini, T. S. Chung, D. R. Paul, The strategies of molecular architecture and modification of polyimide-based membranes for CO_2 removal from natural gas-A review, Prog. Polym. Sci. 34 (2009) 561.

[20] L. Shao, B. T. Low, T. S. Chung, A. R. Greenberg, Polymeric membranes for the hydrogen economy: Contemporary approaches and prospects for the future, J. Membr. Sci. 327 (2009) 18.

[21] L. M. Robeson, The upper bound revisited, J. Membr. Sci., 320 (2008) 390.

[22] L. M. Robeson, Correlation of separation factor versus permeability for polymeric membranes, J. Membr. Sci., 62 (1991) 165.

[23] S. L. Liu, R. Wang, T. S. Chung, M. L. Chng, Y. Liu, R. H. Vora, Effect of diamine composition on the gas transport properties in 6FDA-durene/3,3'-diaminodiphenyl sulfone copolyimides, J. Membr. Sci. 202 (2002) 165.

[24] M. Smaihi, J.-C. Schrotter, C. Lesimple, I. Prevost, C. Guizard, Gas separation properties of hybrid imide–siloxane copolymers with various silica contents, J. Membr. Sci. 161 (1999) 157.

[25] C. Hibshman, C.J. Cornelius, E. Marand, The gas separation effects of annealing polyimide–organosilicate hybrid membranes, J. Membr. Sci. 211 (2003) 25.

[26] Z. K. Xu, C. Dannenberg, J. Springer, S. Banerjee, G. Maier. Gas separation properties of polymers containing fluorene moieties, Chem. Mater. 14 (2002) 3271.

[27] C. Camacho-Zuniga, F. A. Ruiz-Trevino, M. G. Zolotukhin, L. F. del Castillo, J. Guzman, J. Chavez, Gas transport properties of new aromatic cardo poly(acryl ether ketone)s, J. Membr. Sci. 283 (2006) 393.

[28] T. C. Merkel, R. P. Gupta, B. S. Turk, B. D. Freeman, Mixed-gas permeation of syngas components in poly(dimethylsiloxane) and poly(1-trimethylsilyl-1-propyne) at elevated temperatures, J. Membr. Sci. 191 (2001) 85.

[29] A. Morisato, I. Pinnau, Synthesis and gas permeation properties of poly(4-methyl-2-pentyne), J. Membr. Sci. 121 (1996) 243.

[30] C. J. Orme, M. K. Harrup, T. A. Luther, R. P. Lash, K. S. Houston, D. H. Weinkauf, Characterization of gas transport in selected rubbery amorphous polyphosphazene membranes, J. Membr. Sci. 186 (2001) 249.

[31] I. Blume, I. Pinnau, Composite membrane, method of preparation and use, US patent 4963165, 1990.

[32] J. H. Kim, S. Y. Ha, Y. M. Lee, Gas permeation of poly(amide-6-b-ethylene oxide) copolymer, J. Membr. Sci. 190 (2001) 179.

[33] V. I. Bondar, B. D. Freeman, I. Pinnau, Gas transport properties of poly(ether-b-amide) segmented block copolymers, J. Polym. Sci. Part B Polym. Phys. 38 (2000) 2051.

[34] J.W. Simmons, Block polyurethane-ether and polyurea-ester gas separation membranes, US patent 6843829, 2005.

[35] J.W. Simmons, Block polyester-ether gas separation membranes, US patent 6860920, 2005.

[36] K. Okamoto, M. Fujii, S. Okamyo, H. Suzuki, K. Tanaka, H. Kita, Gas permeation properties of poly(ether imide) segmented copolymers. Macromolecules 28 (1995) 6950.

[37] N. K. Acharya, V. Kulshrestha, K. Awasthi, A. K. Jain, M. Singh, Y. K. Vijay, Hydrogen separation in doped and blend polymer membranes, Int. J. Hydrog. Energy 33 (2008) 327.

[38] T. M. Su, I. J. Ball, J. A. Conklin, S. C. Huang, R. K. Larson, S. L. Nguyen, Polyaniline/polyimide blends for pervaporation and gas separation studies, Synthetic Met. 84 (1997) 801.

[39] S. S. Hosseini, M. M. Teoh, T. S. Chung, Hydrogen separation and purification in membranes of miscible polymer blends with interpenetration networks, Polymer 49 (2008) 1594.

[40] Y. Maeda, D. R. Paul, Selective gas transport in miscible PPO-PS blends, Polymer 26 (1985) 2055.

[41] G. C. Kapantaidakis, S. P. Kaldis, X. S. Dabou, G. P. Sakellaropoulos, Gas permeation through PSF-PI miscible blend membranes, J. Membr. Sci. 110 (1996) 239.

[42] A. Bos, I. Punt, H. Strathmann, M. Wessling, Suppression of gas separation membrane plasticization by homogeneous polymer blending, AIChE J. 47 (2001) 1088.

[43] A. Car, C. Stropnik, W. Yave, K.V. Peinemann, PEG modified poly(amide-b-ethyleneoxide) membranes for CO_2 separation, J. Membr. Sci. 307 (2008) 88.

[44] I. Gitsov, C. Zhu, Novel functionally grafted pseudo semi-interpenetrating networks constructed by reactive linear-dendritic copolymers, J. Am. Chem. Soc. 125 (2003) 11228.

[45] J. M. Meseguer Dueñas, D. Torres Escuriola, G. Gallego Ferrer, M. Monleón Pradas, J. L. Gómez Ribelles, P. Pissis, A. Kyritsis, Miscibility of poly(butyl acrylate)−poly(butyl methacrylate) sequential interpenetrating polymer networks, Macromolecules 2001, 34, 5525.

[46] S. B. Pandit, S. S. Kulkarni, V. M. Nadkarni, Interconnected interpenetrating polymer networks of polyurethane and polystyrene. 2. Structure-property relationships, Macromolecules 27 (1994) 4595.

[47] T. Tamai, A. Imagawa, Q. Tran-Cong, Semi-interpenetrating polymer networks prepared by in situ photo-crosslinking of miscible polymer blends, Macromolecules 27 (1994) 7486.

[48] C. Leger, Q. T. Nguyen, J. Neel, C. Streicher, Level and kinetics of PVP extraction from blends, interpenetrating polymer blends and semiinterpenetrating polymer networks, Macromolecules 28 (1995) 143.

[49] M. Wang, K. P. Pramoda, S. H. Goh, Mechanical behavior of pseudo-semi-interpenetrating polymer networks based on double-C60-end-capped poly(ethylene oxide) and poly(methyl methacrylate), Chem. Mater. 16 (2004) 3452.

[50] A. Izuka, H. H. Winter, T. Hashimoto, Self-similar relaxation behavior at the gel point of a blend of a cross-linking poly(ε-caprolactone) diol with a poly(styrene-co-acrylonitrile), Macromolecules 30 (1997) 6158.

[51] M. E. Rezac, B. Schoberl, Transport and thermal properties of poly (ether imide)/ acetylene-terminated monomer blends, J. Membr. Sci. 156 (1999) 211.

[52] A. Bos, I. G. M. Punt, M. Wessling, H. Strathmann, Suppression of CO_2-plasticization by semiinterpenetrating polymer network formation, J. Polym. Sci. Part B Polym. Phys. 36 (1998) 1547.

[53] J. Kurdi, A. Kumar, Formation and thermal stability of BMI-based interpenetrating polymers for gas separation membranes, J. Membr. Sci. 280 (2006) 234.

[54] S. Saimani, A. Kumar, Semi-IPN asymmetric membranes based on polyether imide (ULTEM) and polyethylene glycol diacrylate for gaseous separation, J. Appl. Polym. Sci. 110 (2008) 3606.

[55] R.A. Hayes, Polyimide gas separation membranes, US patent 4717393, 1988.

[56] R.A. Hayes, Amine-modified polyimide membranes, US patent 4981497, 1991.

[57] L. Shao, L. Liu, S. X. Cheng, Y. D. Huang, J. Ma, Comparison of diamino cross-linking in different polyimide solutions and membranes by precipitation observation and gas transport, J. Membr. Sci. 312 (2008) 174.

[58] H. Y. Zhao, Y. M. Cao, X. L. Ding, M. Q. Zhou, J. H. Liu, Q. Yuan, Poly(ethylene oxide) induced cross-linking modification of Matrimid membranes for selective separation of CO_2, J. Membr. Sci. 320 (2008) 179.

[59] L. Shao, T. S. Chung, S. H. Goh, K. P. Pramoda, Polyimide modification by a linear aliphatic diamine to enhance transport performance and plasticization resistance, J. Membr. Sci. 256 (2005) 46.

[60] L. Shao, T. S. Chung, S. H. Goh, K. P. Pramoda, The effects of 1,3-cyclohexanebis(methylamine) modification on gas transport and plasticization resistance of polyimide membranes, J. Membr. Sci. 267 (2005) 78.

[61] Y. Liu, R. Wang, T. S. Chung, Chemical cross-linking modification of polyimide membranes for gas separation, J. Membr. Sci. 189 (2001) 231.

[62] C. Cao, T. S. Chung, Y. Liu, R. Wang, K. P. Pramoda, Chemical cross-linking modification of 6FDA-2,6-DAT hollow fiber membranes for natural gas separation, J. Membr. Sci. 216 (2003) 257.

[63] Y. Liu, T. S. Chung, R. Wang, D. F. Li, M. L. Chng, Chemical cross-linking modification of polyimide/poly(ether sulfone) dual-layer hollow-fiber membranes for gas separation, Ind. Eng. Chem. Res. 42 (2003) 1190.

[64] J. Ren, R. Wang, T. S. Chung, D. F. Li, Y. Liu, The effects of chemical modifications on morphology and performance of 6FDA-ODA/NDA hollow fiber membranes for CO_2/CH_4 separation, J. Membr. Sci. 222 (2003) 133.

[65] T. S. Chung, M. L. Chng, K. P. Pramoda, Y. Xiao, PAMAM Dendrimer Induced Cross-linking Modification of Polyimide Membranes, Langmuir 20 (2004) 2966.

[66] L. Shao, T. S. Chung, S. H. Goh, K. P. Pramoda, Transport properties of cross-linked polyimide membranes induced by different generations of diaminobutane (DAB) dendrimers, J. Membr. Sci. 238 (2004) 153.

[67] Y. Xiao, T. S. Chung, M. L. Chng, Surface characterization, modification chemistry and separation performance of polyimide and PAMAM dendrimer composites, Langmuir 20 (2004) 8230.

[68] Y. Xiao, L. Shao, T. S. Chung, D. A. Schiraldi, The effects of thermal treatments and dendrimer chemical structures on the properties of highly surface cross-linking polyimide films, Ind. Eng. Chem. Res. 44 (2005) 3059.

[69] C. E. Powell, X. J. Duthie, S. E. Kentish, Reversible diamine cross-linking of polyimide membranes, J. Membr. Sci. 291 (2007) 199.

[70] J. D. Wind, D. R. Paul , W. J. Koros, Natural gas permeation in polyimide membranes, J. Membr. Sci. 228 (2004) 227.

[71] J. D. Wind, C. Staudt-Bickel, D. R. Paul, W. J. Koros, Solid-state covalent cross-linking of polyimide membranes for carbon dioxide plasticization reduction, Macromolecules 36 (2003) 1882.

[72] J. D. Wind, S. M. Sirard, D. R. Paul, P. F. Green, K. P. Johnston, W. J. Koros, Carbon dioxide-induced plasticization of polyimide membranes: Pseudo-equilibrium relationships of diffusion, sorption, and swelling, Macromolecules 36 (2003) 6433.

[73] A. M. W. Hillock, W. J. Koros, Cross-linkable polyimide membrane for natural gas purification and carbon dioxide plasticization reduction, Macromolecules 40 (2007) 583.

[74] I. C. Omole, S. J. Miller, W. J. Koros, Increased molecular weight of a cross-linkable polyimide for spinning plasticization resistant hollow fiber membranes, Macromolecules 41 (2008) 6367.

[75] A. M. Kratochvil, W. J. Koros, Decarboxylation-induced cross-linking of a polyimide for enhanced CO_2 plasticization resistance, Macromolecules 41 (2008) 7920

[76] H. Lin, B. D. Freeman, S. Kalakkunnath, D. S. Kalika, Effect of copolymer composition, temperature, and carbon dioxide fugacity on pure- and mixed-gas permeability in poly(ethylene glycol)-based materials: Free volume interpretation, J. Membr. Sci. 291 (2007) 131.

[77] H. Lin, E. Van Wagner, J. S. Swinnea, B. D. Freeman, S. J. Pas, A. J. Hill, S. Kalakkunnath, D. S. Kalika, Transport and structural characteristics of crosslinked poly(ethylene oxide) rubbers, J. Membr. Sci. 276 (2006) 145.

[78] H. Lin, E. Van Wagner, R. Raharjo, B. D. Freeman, I. Roman, High-performance polymer membranes for natural-gas sweetening, Adv. Mater. 18 (2006) 39.

[79] I. Taniguchi, S. Duan, S. Kazama, Y. Fujioka, Facile fabrication of a novel high performance CO_2 separation membrane: immobilization of poly(amidoamine) dendrimers in poly(ethylene glycol) networks, J. Membr. Sci. 322 (2008) 277.

[80] L. Shao, T. S. Chung, In situ fabrication of cross-linked PEO/silica reverse-selective membranes for hydrogen purification, Int. J. Hydrog. Energy 34 (2009) 6492.

[81] R. D. Raharjo, H. Lin, D. F. Sanders, B. D. Freeman, S. Kalakkunnath, D. S. Kalika, Relation between network structure and gas transport in crosslinked poly(propylene glycol diacrylate), J. Membr. Sci. 283 (2006) 253.

[82] M. R. Anderson, B. R. Mattes, H. Reiss, R. B. Kaner, Conjugated polymer films for gas separations, Science 252 (1991) 1412.

[83] M. R. Anderson, B. R. Mattes, H. Reiss, R. B. Kaner, Gas separation membranes: A novel application for conducting polymers, Synthetic Met. 41 (1991)1151.

[84] M. J. Chang, Y. H. Liao, A. S. Myerson, T. K. Kwei, Gas transport properties of polyaniline membranes, J. Appl. Polym. Sci. 62 (1996) 1427.

[85] R. B. Kaner, R. Anderson, B. R. Mattes, H. Reiss, Membranes having selective permeability, US patent 5358556, 1994.

[86] G. Illing, K. Hellgardt, R. J. Wakeman, A. Jungbauer, Preparation and characterization of polyaniline based membranes for gas separation, J. Membr. Sci. 184 (2001) 69.

[87] M. D. Guiver, G. P. Robertson, Y. Dai, F. Bilodeau, Y. S. Kang, K. J. Lee, Structural characterization and gas-transport properties of brominated Matrimid polyimide, J. Polym. Sci. Part A: Polym. Chem. 40 (2003) 4193.

[88] R. T. Chern, F. R. Sheu, L. Jia, V. T. Stannett, H. B. Hopfenberg, Transport of gases in unmodified and aryl-brominated 2,6-dimethyl-1,4-poly(phenylene oxide), J. Membr. Sci. 35 (1987) 103.

[89] B. J. Story, W. J. Koros, Sorption and transport of CO_2 and CH_4 in chemically modified poly(phenylene oxide), J. Membr. Sci. 67 (1992) 191.

[90] R. T. Chern, C. N. Provan, The effects of aryl-halogenation on the gas permeabilities of poly (phenolphthalein terephthalate) and poly (bisphenol A phthalate), J. Membr. Sci. 59 (1991) 293.

[91] S. Sridhar, B. Smitha, M. Ramakrishna, T. M. Aminabhavi, Modified poly(phenylene oxide) membranes for the separation of carbon dioxide from methane, J. Membr. Sci. 280 (2006) 202.

[92] F. Hamad, T. Matsuura, Performance of gas separation membranes made from sulfonated brominated high molecular weight poly(2,4-dimethyl-l,6-phenyIene oxide), J. Membr. Sci. 253 (2005) 183.

[93] F. Piroux, E. Espuche, R. Mercier, M. Pinéri, G. Gebel, Gas transport mechanism in sulfonated polyimides - Consequences on gas selectivity, J. Membr. Sci. 209 (2002) 241.

[94] F. A. Hamad, G. Chowdhury, T. Matsuura, Sulfonated polyphenylene oxide–polyethersulfone thin-film composite membranes- Effect of counterions on the gas transport properties, J. Membr. Sci., 191 (2001) 71.

[95] B. Kruczek, T. Matsuura, Effect of metal substitution of high molecular weight sulfonated polyphenylene oxide membranes on their gas separation performance, J. Membr. Sci. 167 (2000) 203.

[96] Y. Li, T. S. Chung, Highly selective sulfonated polyethersulfone (SPES)-based membranes with transition metal counterions for hydrogen recovery and natural gas separation, J. Membr. Sci. 308 (2008) 128.

[97] M. D. Guiver, N. L. Thi, G.P. Robertson, Composite gas separation membranes, US patent 20,020,062,737, 2002.

[98] S. Husain, W. J. Koros, Mixed matrix hollow fiber membranes made with modified HSSZ-13 zeolite in polyetherimide polymer matrix for gas separation, J. Membr. Sci. 288 (2007) 195.

[99] A. M. W. Hillock, S. J. Miller, W. J. Koros, Crosslinked mixed matrix membranes for the purification of natural gas: Effects of sieve surface modification, J. Membr. Sci. 314 (2008) 193.

[100] Y. Li, T. S. Chung, K. Santi, Novel Ag^{+}-zeolite/polymer mixed matrix membranes with a high CO_2/CH_4 selectivity, AIChE J. 53 (2007) 610.

[101] N. P. Patel, A. C. Miller, R. J. Spontak, Highly CO_2-permeable and selective polymer nanocomposite membranes, Adv. Mater. 15 (2003) 729.

[102] N. P. Patel, A. C. Miller, R. J. Spontak, Highly CO_2-permeable and -selective membranes derived from crosslinked poly(ethylene glycol) and its nanocomposites, Adv. Funct. Mater. 14 (2004) 699.

[103] D. Q. Vu, W. J. Koros, S. J. Miller, Mixed matrix membranes using carbon molecular sieves I. Preparation and experimental results, J. Membr. Sci. 211 (2003) 311.

[104] E. V. Perez, K. J. Balkus Jr., J. P. Ferraris, I. H. Musselman, Mixed-matrix membranes containing MOF-5 for gas separations, J. Membr. Sci. 328 (2009) 165.

[105] S. S. Hosseini, Y. Li, T. S. Chung, Y. Liu, Enhanced gas separation performance of nanocomposite membranes using MgO nanoparticles, J. Membr. Sci. 302 (2007) 207.

CHAPTER 3

THEORETICAL BACKGROUND

Parts of this chapter are published in the following review article

Youchang Xiao, **Bee Ting Low**, Seyed Saeid Hosseini, Tai Shung Chung, Donald Ross Paul, The strategies of molecular architecture and modification of polyimide-based membranes for CO_2 removal from natural gas-A review, *Prog. Polym. Sci.* 34 (2009) 561-580.

3.1 Theory of gas transport in dense glassy polymeric membranes

3.1.1 Concept of polymer free volume

The concept of free volume in polymers is an extension of the postulation by Cohen and Turnbull that is used to explain the self-diffusion process in a liquid of hard spheres [1]. Figure 3.1 demonstrates a plot of specific volume against temperature for a typical glassy polymer which shows the presence of additional free volume at temperatures below the glass transition point (T_g). This is attributed to the non-equilibrium state of the polymeric matrix induced by the limited mobility and long relaxation times of entangled polymer chains [2-3]. The formation of irregular voids within a polymeric matrix has been proven by molecular modelling. This is due to the minimum barriers of each rotational bonds occurring at irregular intervals [4-5].

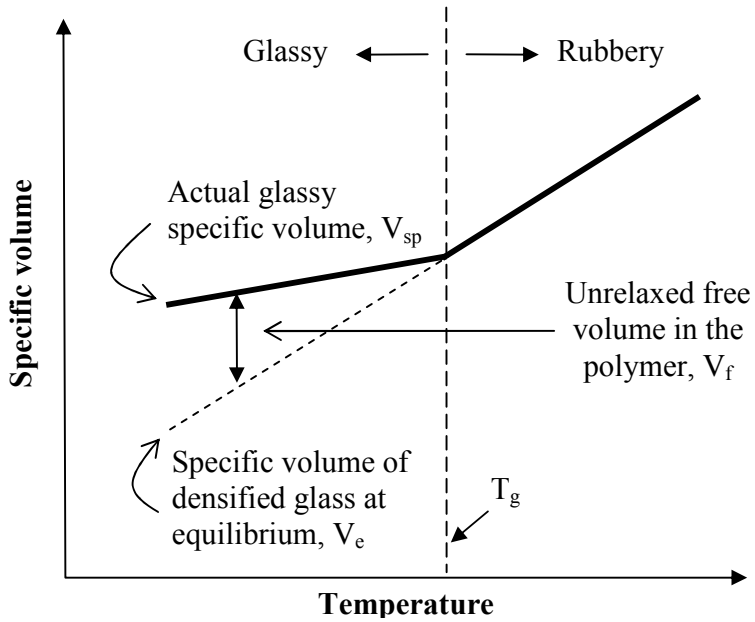

Figure 3.1 Specific volume of a polymer as a function of temperature

The polymer chains are in constant vibrational motion which leads to the occasional redistribution of free volume. The way in which the gas molecules transverse across the polymeric matrix is described by a series of diffusional jumps through the temporary channels created by the constantly vibrating polymer chains as shown in Figure 3.2. The diffusion of gas molecules within a polymer matrix is dependent on the size and shape of the penetrants, the ease of cavity formation resulting from the thermally induced motions of polymer chains and the quantity of free volume. Gas sorption is related to the gas condensability, interactions between the gas and polymers and the availability of sorption sites. Therefore, the size and distribution of free volume cavities are critical parameters that govern the overall gas transport.

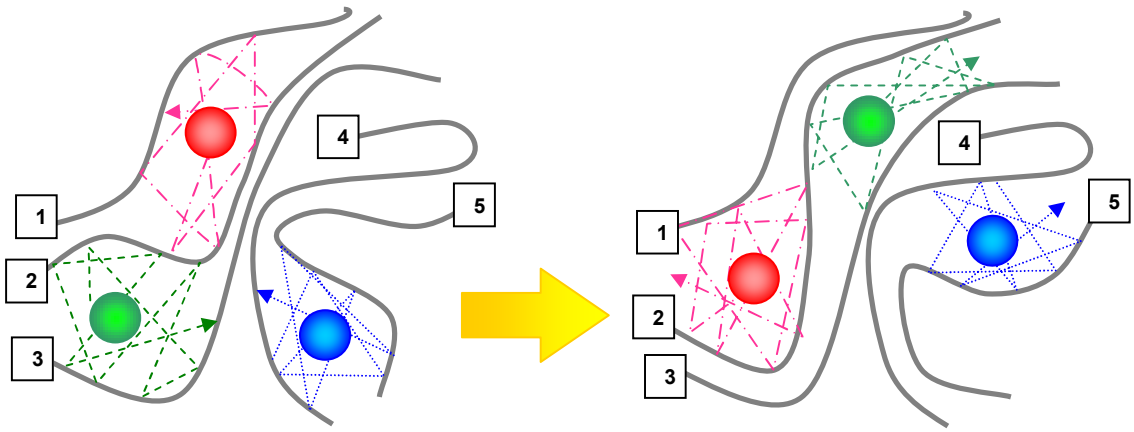

Figure 3.2 Motion of gas molecules within cavities via a series of diffusional jumps

Usually, the fractional free volume (FFV) of a polymer is expressed by equation (3-1) [7]

$$FFV = \frac{V_{sp} - V_0}{V_{sp}} \tag{3-1}$$

$$V_0 = 1.3V_W \tag{3-2}$$

$$V_{sp} = 1/\rho \qquad (3\text{-}3)$$

where V_{sp} is the specific volume of polymer film (cm^3/g), V_0 is the volume occupied by the chains (cm^3/g) and ρ represents the density (g/cm^3) of polymer films. The values of Van der Waals volumes (V_W) for individual polymers are calculated from the group contribution method by Van Krevelen [8]. Using the calculated Van der Waals volume as a basis, Bondi proposed equation (3-2) as an approximation for V_0 [9]. In Bondi's approach, the FFV of a polymer is not dependent on the gas type and a constant pre-factor of 1.3 is used for all polymers [9]. It has been revealed that the use of this model cannot fully account for all the experimentally determined results, especially for highly condensable gases [10]. Park and Paul have introduced a modified correlation to determine the FFV of a polymer whereby the universal parameter of 1.3 suggested by Bondi for all polymer types is replaced with an empirical constant that is dependent on the gas type and the chemical groups constituting the polymer [10].

Boehme and Cargill proposed an analogy between the free volume and the inter-chain spacing i.e. d-spacing [11]. The d-spacing can be experimentally determined by the wide angle x-ray diffraction. Recent investigations using molecular modelling tools have revealed that the X-ray scattering near 15^o is likely due to the invariant geometry of intra-molecular backbones [5]. It has been highlighted that the x-ray scattering associated with 2θ values between 20^o and 28^o are better indications of the inter-chain spacing. The positron annihilation lifetime spectroscopy is a powerful analytical tool that provides a more accurate quantification of the polymer free volume [12-16]. To calculate the

average cavity size of a polymer matrix, a correlation between the measured lifetime of ortho-positronium (o-Ps) and the size of the void volume is used.

3.1.2 Sorption in glassy polymers

Several models have been established to explain the sorption of gas molecules in glassy polymeric membranes. One of the most popular models frequently employed by membrane scientists is the dual-mode sorption theory. The dual-mode sorption model suggests the presence of two types of sorption sites in glassy polymers, namely Henry and Langmuir sites [17-18]. Henry sites are found in the densified regions of the polymeric membranes which accommodate mobile gas molecules via dilation of the polymeric matrix. Comparatively, the gas molecules in the Langmuir sites are less mobile and these sorption sites are formed due to the imperfect inter-chain packing during glass transition [7]. Langmuir sites are characteristics of glassy polymers.

Dual-mode sorption model is established based on equilibrium conditions and the gas concentration in given by equation (3-4) [17-18].

$$C = C_D + C_H = k_D p + \frac{C_H' bp}{1 + bp} \qquad (3\text{-}4)$$

C represents the total concentration of the gas penetrants. C_D and C_H represent the gas concentrations at the Henry sites and Langmuir sites respectively. k_D represents the Henry law constant. C_H' is the Langmuir capacity constant while b is a parameter which is associated with the affinity of the gas molecules with the Langmuir sites. C_H' probably

varies with polymer type and structure since the hole filling constant is dependent on the quantity of Langmuir sites available.

At the limits of low and high pressures, equation (3-4) simplifies to equations (3-5) and (3-6), respectively.

$$C = k_D p + C_H' bp \tag{3-5}$$

$$C = k_D p + C_H' \tag{3-6}$$

The solubility coefficient is given by the ratio of total penetrant concentration to pressure and is given by equation (3-7).

$$S = \frac{C}{p} = k_D + \frac{C_H' b}{1 + bp} \tag{3-7}$$

Both k_D and b can be represented by the Arrhenius type equations which are dependent on sorption enthalpies (i.e. ΔH_D and ΔH_H for Henry and Langmuir sites, respectively) and temperature (T). k_{D0} and b_0 are pre-exponential factors [19].

$$k_D = k_{D0} \exp\left(-\Delta H_D / RT\right) \tag{3-8}$$

$$b = b_0 \exp\left(-\Delta H_H / RT\right) \tag{3-9}$$

In addition to the dual-mode sorption model, another model developed from classical thermodynamics relates gas solubility to the Lennard-Jones temperature, ε/k where ε refers to the potential energy well depth parameter and k is the Boltzmann's constant. The model is represented by equation (3-10). M_i is related to the interactions between the polymer and the gaseous penetrants which therefore differ with the type of polymer. N_c is taken as 0.023 K^{-1} [20].

$$\ln S_A = M_i + N_c(\varepsilon_A / k) \tag{3-10}$$

There are other models which are based on non-equilibrium thermodynamics such as the non-equilibrium lattice fluid model and the tangent-hard-sphere-chain equation of state [21]. A detailed discussion of these models is beyond the scope of this work and can be obtained elsewhere [21].

3.1.3 Diffusion in glassy polymers

Similar to gas sorption, there are many models that explain the gas diffusivity in polymeric membranes. Depending on the model type and measurement methods, the diffusivity coefficients may vary and this has been documented in a work by Wang et al [17]. A quick review of the various types of diffusion coefficients and diffusion models is presented here. Paul and Koros proposed the partial immobilization model (also known as the dual mobility model) which accounts for the difference in the inherent gas diffusion at both the Langmuir and Henry sites [22-23]. D_D and D_H refer to the diffusion coefficients in the Henry and Langmuir sites, respectively. F represents the ratio of D_H to D_D and K is given as ($C'_H b/k_D$). p_2 is the pressure at the upstream boundary.

$$P = k_D\left(1 + \frac{FK}{1 + bp_2}\right)D_D \tag{3-11}$$

In the governing equation for the solution diffusion mechanism, P= SD, the diffusion coefficient is an average value i.e. $D = D_{avg}$. Considering this equation and the dual-mode sorption model represented by equation (3-7), the average diffusion coefficient, D_{avg} can be expressed as follows [17].

$$P = k_D\left(1+\frac{K}{1+bp_2}\right)D_{avg} \tag{3-12}$$

The apparent diffusion coefficient, D_{app} can be determined by the time lag approach. However, this approach is developed for obtaining the diffusion coefficient in rubbery polymers and hence is not exactly suitable for use with glassy polymers. This approach is based on the assumptions that Henry's law is applicable and the diffusion coefficient is independent of the gas concentration [17,21]. The relationship between the D_{app}, time lag (θ) and membrane thickness (l) is shown by equation (3-13). θ is obtained from the extrapolation of the steady state region of a plot of pressure versus time (at constant volume) as shown in Figure 3.3.

$$D_{app} = \frac{l^2}{6\theta} \tag{3-13}$$

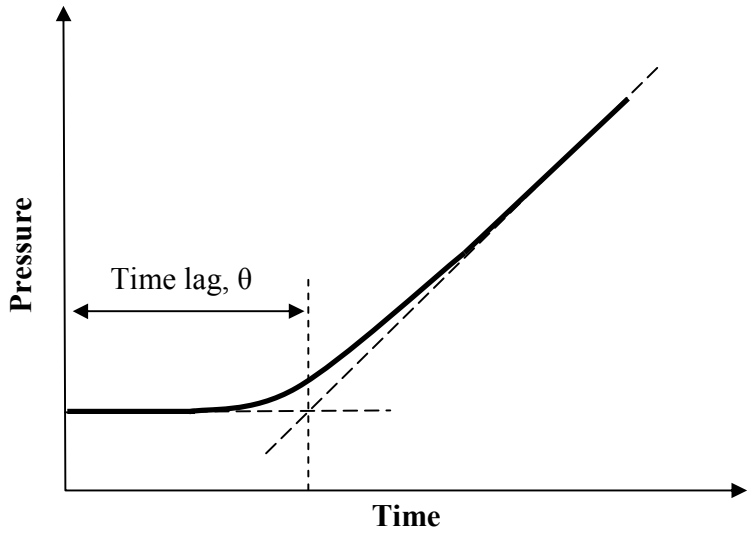

Figure 3.3 Time lag approach for determining apparent diffusivity, D_{app}

Cohen and Turnbull proposed the use of the free volume theory to determine the self-diffusion coefficient, D_f [7,21]. The model is shown by equation (3-14) where A^* and γ are constants, v^* is the minimum required volume of the void and v_f is the average free volume per molecule

$$D_f = A^* \exp\left(\frac{-\gamma v^*}{v_f}\right) \tag{3-14}$$

Fujita modified the free volume model by Cohen and Turnbull by introducing the polymer FFV. The modified model is represented by equation (3-15) where A_d and B_d are penetrant dependent parameters [24]. In general, for a faster diffusing gas, the value of A_d is larger than B_d.

$$D_f = A_d RT \exp\left(\frac{-B_d}{FFV}\right) \tag{3-15}$$

From a classical approach, the gas diffusion coefficient, D can be expressed in the form of an Arrhenius equation as shown by equation (3-16) Here, D_0 is the pre-exponential factor, R is the gas constant, T is the temperature in Kelvin and E_D is the activation energy for diffusion.

$$D = D_0 \exp\left(\frac{-E_D}{RT}\right) \tag{3-16}$$

Barrer and Van Amerongen proposed a correlation for the pre-exponential factor, D_0 and is shown by the equation (3-17). For glassy polymers, the numerical values for a and b are 0.64 and 11.5, respectively [25-26].

$$\ln D_0 = a\frac{E_D}{RT} - b \tag{3-17}$$

Based on Brandt's model, E_D is related to polymer dependent parameters c and f as well as the kinetic diameter (d_k) of the gas penetrant as represented by equation (3-18) [27]

$$E_D = cd_k^2 - f \qquad (3\text{-}18)$$

3.2 Plasticization by condensable gases and vapors

Penetrant-induced plasticization and conditioning are critical factors that influence the gas separation performance of polymer membranes. These phenomena cannot be neglected in hydrogen enrichment and natural gas separation where highly condensable gases such as CO_2 and H_2O are present [28-35]. Generally for H_2/CO_2 and CO_2/CH_4 separations using glassy polymeric membranes, plasticization and conditioning lead to the deterioration of the gas pair permselectivity due to the poorer molecular sieving effects. Since the effects of plasticization and conditioning significantly deteriorate the separation performance of polymer membranes, any effort toward its suppression or even elimination will reap beneficial impacts. In this section, the gist of plasticization and conditioning are presented to better understand their impacts on the gas separation efficiency of polymer membranes.

Basically, a number of definitions have been proposed to describe the plasticization phenomenon and its associated aspects [28-29]. Plasticization is a repertoire of pressure dependent phenomena that is caused by the dissolution of certain components within the polymer matrix. The dissolution of condensable gas species or heavy hydrocarbons swells up the polymer membrane. At relatively low CO_2 pressures, the gas permeability of a polyimide membrane decreases with increasing pressure. This behavior is attributed to

gradual saturation of sorption sites in the membrane structure (i.e. reduced solubility coefficient) which reduces the permeability due to the diminishing pathway available for the gas transport. Further increase in pressure typically results in an upward inflection in gas permeability which corresponds to the incipient point of plasticization. The pressure corresponding to the minimum gas permeability is commonly known as the "plasticization pressure" which is related to the threshold gas concentration to induce plasticization.

In fact, a high concentration of plasticizing gases within the polymeric matrix results in the disruption of chain packing and enhances the inter-segmental mobility. This results in higher free volume and gas diffusivity. The decline in the solubility coefficient is accompanied by a more rapid increase in the diffusion coefficient, thereby increasing the overall gas permeability. It has been found that for some polymeric membranes, the pressure-permeability relationship may not be sufficient to determine the onset of plasticization [37]. Therefore, another approach to determine the threshold pressure for plasticization is to examine the absolute heat of sorption as a function of pressure. The turning point at which the gradient of the absolute heat of sorption against pressure changes from a negative to a positive value marks the onset of plasticization [37].

Plasticization induced by condensable gas species leads to pressure, temperature, time and thickness dependence in the gas transport properties of glassy polymeric membranes [37-45]. The temperature dependence of CO_2-induced plasticization was investigated in a recent work by Duthie et al [45]. The variations in CO_2 permeability as a function of CO_2

fugacity at different operating temperatures reveal that the plasticization phenomenon is more pronounced at lower temperatures i.e. increasing temperature leads to higher plasticization fugacity. This is related to the lower solubility coefficients at higher temperatures. It is also expected to observe a non-constant CO_2 permeability for a certain period of time after the incipient point of plasticization. The extent of permeability increment and time frame is related to the polymer inherent properties like chemical structure and chain rigidity. For example, the relative increase in the gas permeability for a 6FDA-polyimide has been reported to be more than 40% after the lapse of several hours and it does not reach a steady-state value even within the experimentation time [43]. The thickness-dependence of CO_2-induced plasticization has been clearly illustrated using 6FDA-durene polyimide dense films in a study by Zhou et al [44]. An accelerated plasticization behavior is observed in ultra-thin films and this is attributed to the weak micro-mechanical properties and severe swelling effects caused by CO_2.

Another phenomenon that is closely associated with CO_2-induced plasticization is the effects of conditioning. Conditioning is related to the alterations in the properties of glassy polymers upon exposure to highly soluble gaseous penetrants [46]. It has been observed that the sorption of CO_2 into the polymer can severely and in most cases permanently alter the morphology and transport properties of the membrane even after complete desorption of the gas molecules [46]. The resultant conditioned membranes exhibit volume dilation and new steady-state gas transport properties. This irreversible volume expansion that is caused by the sorption of CO_2 molecules increases the capacity for further gas sorption to occur. It is believed that this is possibly accomplished through

the enlarged or newly created microvoids at the Langmuir sorption sites [46]. This volume expansion cannot be fully recovered to its original state due to the slow relaxation characteristics of glassy polymers. Therefore, CO_2 conditioning leads to simultaneous increment in gas diffusivity and solubility which is dependent on the extent of volume dilation. The conditioning responses of different polymers can be rather diverse and it has been proven that polyimides show significant volume dilation and increment in gas permeability [40].

3.3 Physical aging phenomenon

Glassy polymers are in a state of non-equilibrium and hence, the tendency for polymer chains to undergo gradual molecular rearrangements in order to attain equilibrium. The relaxation of polymer chains is known as physical aging. The aging phenomenon of polymeric membranes has been observed by many researchers and vast publications of aging-related studies can be found in the literature. One consequence of aging is the densification of the polymer matrix with a corresponding decrease in the available free volume. The loss of free volume is mainly due to the disappearance of Langmuir sites which are characteristics of glassy polymers. Two mechanisms were proposed to account for the collapse of free volume during the process of physical aging.

Alfrey postulated that the free volume present in polymeric membranes is not in the form of permanent cavities and diffusion of the free volume from the interior of the membrane to the surface causes some of the initially available free volume to be lost [47]. Figure 3.4

shows a schematic of the diffusion of free volume to the surface. The collapse of the free volume within the polymer matrix leads to a denser membrane and a subsequent decrease in the membrane thickness. Based on this mechanism, the rate of aging is sample dependent. In other words, the diffusion of free volume to the surface is more rapid for thin membranes, especially in the sub micron range. This is turn implies that the problem of aging is more pronounced in thin films.

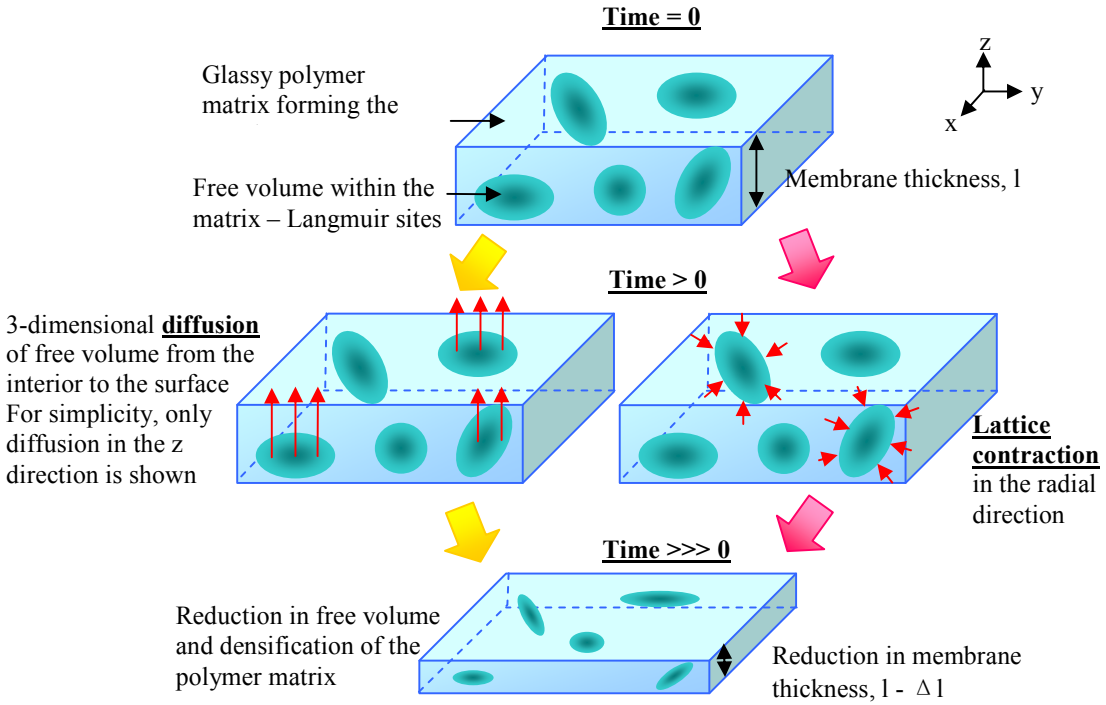

Figure 3.4 Diffusion of free volume and lattice contraction

However, the free volume diffusion model that is proposed by Alfrey may be inadequate for explaining the entire aging phenomenon. Therefore, Curro and co-workers and Hirai and Eyring suggested another mechanism to account for the decrease in the free volume during the physical aging of glassy materials [48-49]. In addition to the diffusion of free

volume to the surface, lattice contraction also plays a role in the reduction of the free volume in glassy materials. Lattice contraction is not sample dependent unlike the free volume diffusion. Figure 3.4 shows the effect of lattice contraction on the resultant membrane.

It has been shown that the aging rate is strongly dependent on the polymer type [50-51]. If the polymer has poor packing efficiency and high FFV values, the corresponding decline in the available free volume due to physical aging is higher than a polymer with low FFV. Kim and co-workers investigated the aging effects of thin 6FDA-based polyimide films [50-51]. They concluded that the higher the intrinsic free volume of the polyimide, the faster the aging rate. The aging response is also dependent on the gas type i.e. the gas with a larger kinetic diameter exhibits greater decline in the relative gas permeability with aging [50]. The corresponding densification of the polyimide film with aging was probed by ellipsometry where a reduction in the refractive index of the film was observed with aging time [51].

The relationship between the aging rate and film thickness has been extensively investigated [52-58]. In a study by Pfromm and Koros, the accelerated aging rates of thin polysulfone and a 6FDA-based polyimide films were reported [52]. The activation energy of permeation increases with aging time [52]. McCaig and Paul showed that for thick polyarylate films greater than 2.5 μm, the aging rate is independent of film thickness [53]. Huang and Paul studied the physical aging of thin polysulfone, Matrimid® and poly(2,6-dimethyl-1,4-phenylene oxide) films [54-56]. It was shown that the free volume diffusion

is not the only mechanism that accounts for the physical aging of thin polymer films. Various techniques were explored to accurately determine the thickness of the polymer films [54-56].

One critical problem of physical aging is the gas separation performance of these glassy polymeric membranes becomes time dependent. As the aging time increases, the decrease in free volume generally causes a decline in gas permeability and an increase in gas pair permselectivity [52-62]. However, some studies have revealed that other factors may influence the overall aging phenomenon. For instance, Lin and Chung reported that the physical aging of 6FDA-durene hollow fiber membrane is strongly affected by the spinning conditions, in particular the shear rates [59]. It has been concluded that two processes are simultaneously taking place during the aging of the hollow fiber, namely, relaxation of shear oriented chains and the decrease in cavities between polymer chains. The decrease in permeance is more drastic in the initial stage of physical aging. Kim et al. examined the effects of CO_2 exposure on physical aging and concluded that CO_2 exposure retards the drop in gas permeability [61]. For thin films which have not been exposed to CO_2, CO_2/CH_4 selectivity increases with aging time while for films which have been exposed to CO_2, selectivity decreases. Hence, this work shows that the nature of the gaseous penetrants influence the overall aging process. In order to yield time-independent gas separation performance using glassy polymeric membranes, it is necessary to determine methods which inhibit or at least retards the aging process.

3.4 Robeson upper bound relationships

It is always desirable to obtain gas separation membranes with both high permeability and permselectivity. However, there exists a tradeoff between permeability and permselectivity i.e. permeability increases at the expense of permselectivity and vice versa. Robeson gathered the permeability and permselectivity data for binary gas pairs that are available in the literature and discovered the existence of upper bound curves for the respective gas pairs [63]. An empirical relation shown by equation (3-19) is used to represent the upper bound where k and n are parameters. In a subsequent study by Freeman, the implications of the correlation proposed by Robeson are discussed and the equation is rearranged into the form shown in equation (3-20) [20]. β_{AB} and λ_{AB} are parameters. A comparison of these two equations shows that $k = \sqrt[\lambda_{AB}]{\beta_{AB}}$ and $n = -1/\lambda_{AB}$.

$$P_A = k\alpha_{AB}^{n} \tag{3-19}$$

$$\alpha_{AB} = \beta_{AB} / P_A^{\lambda_{AB}} \tag{3-20}$$

$$\ln \alpha_{AB} = \ln \beta_{AB} - \lambda_{AB} \ln P_A \tag{3-21}$$

A combination of equations (3-16), (3-17) and (3-18) from the diffusivity model and the governing equation for solution-diffusion i.e. P = SD gives the final form of the permeability-permselectivity relationship as shown by equation (3-22) [20]. A comparison of equations (3-21) and (3-22) reveals that the slope of the upper bound, λ_{AB} is only dependent on the kinetic diameters, d_A and d_B of the gas penetrants where A and B refers to the faster and slower moving gases, respectively. Hence, for a given gas pair, the slope of the upper bound is constant.

$$\ln \alpha_{AB} = -\left[\left(\frac{d_B}{d_A}\right)^2 - 1\right] \ln P_A + \left\{\ln\left(\frac{S_A}{S_B}\right) - \left[\left(\frac{d_B}{d_A}\right)^2 - 1\right]\left(b - f\left(\frac{1-a}{RT}\right)\right) - \ln S_A\right\} \quad (3\text{-}22)$$

$$\ln \alpha_{AB} = -\lambda_{A/B} \ln D_A + \left\{\ln\left(\frac{S_A}{S_B}\right) - \lambda_{A/B}\left(b - f\left(\frac{1-a}{RT}\right)\right)\right\} \quad (3\text{-}23)$$

Based on the theoretical interpretations of the Robeson upper bound, Freeman suggested some guidelines which bring about changes in the β_{AB} term. The development of polymeric membranes with better gas separation performance can be achieved by increasing the solubility selectivity and/or increasing chain stiffness and inter-chain spacing simultaneously. Equation (3-22) can be presented in the form of equation (3-23) and it can be seen that the diffusivity plays a more important role in determining the gas pair permselectivity since the solubility selectivity does not vary significantly from polymer to polymer.

Recently, Robeson revisited the permeability-permselectivity relationships and found that there are only minor changes to the position of the upper bound lines [64]. As predicted in the earlier work, the slope of the upper bound remains relatively unchanged since it is dependent only on the kinetic diameters of the gas pairs. With the discovery of new polymers with better gas separation indicators, most of the upper bound lines established in 2008 exhibit a parallel shift outwards from the original position in 1991 [64]. Robeson highlighted that a further increase in the permeability of the faster gas will not bring about an indefinite extension of the upper bound due to the transition of the gas transport mechanism from solution-diffusion to Knudsen diffusion. Robeson et al. used the database for analyzing the latest upper bound lines to propose a correlation between the

gas permeabilities [65]. The log-log plots of the gas permeabilities for a given gas pair display linear behavior over a wide range of gas permeabilities which suggests that solution diffusion is still the dominating gas transport mechanism [65]. In their work, a modified set of kinetic diameters which provides a better fit of the experimental data over the conventionally used values obtained from zeolites has been proposed [65].

3.5 References

[1] M. H. Cohen, H. L. Turnbull, Molecular Transport in Liquids and Glasses, J. Chem. Phys. 31 (1959) 1164.

[2] J. M. Prausnitz, R. N. Lichtenthaler, E. D. Azevedo, Molecular thermodynamics of fluid-phase equilibrium, Prentice-Hall, New York, 1986.

[3] W. J. Koros, M. W. Hellums, "Transport properties", Encyclopedia of Polymer Science, 2nd Edition, Ed. by J. I. Kroschwitz, Wiley-Interscience, New York, Supplement Volume 724 (1989).

[4] S. H. Jacobson, Molecular modeling studies of polymeric gas separation and barrier materials: structure and transport mechanisms, Polym. Adv. Technol., 5 (1994) 724.

[5] M. Herchel, D. Hofmann, P. Pullumbi, Molecular modeling of small-molecule permeation in polyimides and its correlation to free-volume distribution, Macromolecules, 37 (2004) 201.

[6] H. Fujita, Forschr. Hochpolym. Forsch. 3 (1961) 1.

[7] D. R. Paul, Y. P. Yampolskii, Polymeric gas separation membranes, CRC, Boca Raton, 1994.

[8] D. W. Van Krevelen, Properties of polymers - their correlation with chemical structure; their numerical estimation and prediction from additive group contributions, Elsevier, Amsterdam, 1990.

[9] A. Bondi, Physical properties of molecular crystals, liquids and glasses, Wiley, New York, 1968.

[10] J. Y. Park, D. R. Paul, Correlation and prediction of gas permeability in glassy polymer membrane materials via a modified free volume based group contribution method, J. Membr. Sci. 125 (1997) 23.

[11] R. F. Boehme, G. S. Cargill, X-ray scattering measurements demonstrating in-plane anisotropy in Kapton polyimide films, in K.L. Mittal (Ed.), Polyimides, Plenum Press, New York, 1984.

[12] D. M. Shrader, Y. C. Jean, Positron and positronium chemistry, Elsevier, Amsterdam, 1988.

[13] J. G. Victor, J. M. Torkelson, On measuring the distribution of local free volume in glassy polymers by photochromic and fluorescence techniques, Macromolecules 20 (1987) 2241.

[14] V. I. Bondar, B. D. Freeman, Y. P. Yampolski, Sorption of gases and vapors in an amorphous glassy perfluorodioxole copolymer, Macromolecules 32 (1999) 6163.

[15] K. Tanaka, T. Kawi, H. Kita, K. Okamoto, Y. Ito, Correlation between gas diffusion coefficient and positron annihilation lifetime in polymers with rigid polymer chains, Macromolecules 33 (2000) 5513.

[16] A. Nagel, K. Gu1nther-Schade, D. Fritsch, T. Strunskus, F. Faupel, Free volume and transport properties in highly selective polymer membranes, Macromolecules 35 (2002) 2071.

[17] R. Wang, C. Cao, T. S. Chung, A critical review on diffusivity and the characterization of diffusivity of 6FDA-6FpDA membranes for gas separation, J. Membr. Sci. 198 (2002) 259.

[18] T. S. Chung, C. Cao, R. Wang, Pressure and temperature dependence of the gas-transport properties of dense poly[2,6-toluene-2,2-bis(3,4dicarboxylphenyl) hexafluoropropane diimide] membranes, J. Polym. Sci. Part B Polym. Phys. 42 (2004) 354.

[19] R. E. Kesting, A. K. Fritzsche, Polymeric gas separation membranes, Wiley-Interscience, New York, 1993.

[20] B. D. Freeman, Basis of permeability/selectivity tradeoff relations in polymeric gas separation membranes, Macromolecules 32 (1999) 375.

[21] Y. Yampolskii, I. Pinnau, B. D. Freeman, Materials science of membranes for gas and vapor separation, England, John Wiley & Sons Ltd, 2006.

[22] D. R. Paul, W. J. Koros, Effect of partially immobilizing sorption on permeability and the diffusion time lag, J. Polym. Sci., Polym. Phys. Ed. 14 (1976) 675.

[23] W. J. Koros, Sorption and transport of gases in glassy polymers, Ph. D. dissertation, University of Texas, Austin, TX, 1977.

[24] K. Haraya, S.-T. Hwang, Permeation of oxygen, argon and nitrogen through polymer membranes, J. Membr. Sci. 71 (1992) 13.

[25] G. J. van Amerongen, The permeability of different rubbers to gases and its relation to diffusivity and solubility, J. Appl. Phys. 17 (1946) 972.

[26] R. M. Barrer, Permeability in relation to viscosity and structure of rubber, Trans. Faraday Soc. 38 (1942) 322.

[27] W. W. Brandt, Model Calculation of the Temperature Dependence of Small Molecule Diffusion in High Polymers, J. Phys. Chem. 63 (1959) 1080.

[28] E. S. Sanders, Penetrant-induced plasticization and gas permeation in glassy polymers, J. Membr. Sci. 37 (1988) 63.

[29] J. S. Chiou, J. W. Barlow, D. R. Paul, Plasticization of glassy polymers by CO_2, J. Appl. Polym. Sci. 30 (1985) 2633.

[30] R. G. Wissinger, M. E. Paulaitis, Glass transitions in polymer/CO_2 mixtures at elevated pressures, J. Polym. Sci. Part B Polym. Phys. 29 (1991) 631.

[31] Y. P. Handa, S. Lampron, M.L. O'Neill, On the plasticization of poly(2,6-dimethyl phenylene oxide) by CO_2, J. Polym. Sci. Part B Polym. Phys. 32 (1994) 2549.

[32] W. C. Wang, E. J. Kramer, W. G. Sachse, Effects of high pressure CO_2 on the glass transition temperature and mechanical properties of polystyrene, J. Polym. Sci. Part B Polym. Phys. 20 (1982) 1371.

[33] J. R. Fried, H. C. Liu, C. Zhang, Effect of sorbed carbon dioxide on the dynamic mechanical properties of glassy polymers, J. Polym. Sci: Polym Lett. 27 (1989) 385.

[34] T. S. Chow, Molecular interpretation of the glass transition temperature of polymer diluent systems, Macromolecules 13 (1980) 362.

[35] M. Wessling, Z. Borneman, Th. van den Boomgaard, C.A. Smolders, Carbon dioxide foaming of glassy polymers, J. Appl. Polym. Sci. 53 (1994) 1497.

[36] W. J. Koros, D. R. Paul, A. A. Rocha, Carbon dioxide sorption and transport in polycarbonate, J. Polym. Sci. Polym. Phys. Ed. 14 (1976) 687.

[37] T. S. Chung, C. Chun, R. Wang, Pressure and temperature dependences of gas transport properties of 6FDA-2, 6-DAT polyimide dense membranes, J. Polymer Science: Part B: Polym. Phys. 42, 354 (2004).

[38] H. Finken, in: Material Science of Synthetic Membranes, ACS Symposium Series No. 269, American Chemical Society, Washington, DC, 1984, 229.

[39] W. J. Schell, C. D. Houston, in: Industrial Gas Separations, ACS Symposium Series No. 223, American Chemical Society, Washington, DC, 1983, 125.

[40] M. R. Coleman, W. J. Koros, Conditioning of Fluorine-Containing Polyimides. 2. Effect of Conditioning Protocol at 8% Volume Dilation on Gas-Transport Properties, Macromolecules 32 (1999) 3106.

[41] S. Kanehashi, T. Nakagawa, K. Nagai, X. Duthie, S. Kentish, G. Stevens, Effects of carbon dioxide-induced plasticization on the gas transport properties of glassy polyimide membranes, J. Membr. Sci 298 (2007) 147.

[42] M. Wessling, I. Huisman, Th. van den Boomgaard, C.A. Smolders, Time-dependent permeation of carbon dioxide through a polyimide membrane above the plasticization pressure, J. Appl. Polym. Sci. 58 (1995) 1959.

[43] J. S. Chiou, D. R. Paul, Effects of carbon dioxide exposure on gas transport properties of glassy polymers, J. Membr. Sci. 32 (1987) 195.

[44] C. Zhou, T. S. Chung, R. Wang, Y. Liu, S. H. Goh, The accelerated CO_2 plasticization of ultra-thin polyimide films and the effect of surface chemical cross-linking on plasticization and physical aging, J. Membr. Sci. 225 (2003) 125.

[45] X. Duthie, S. Kentish, C. Powell, K. Nagai, G. Qiao, G. Stevens, Operating temperature effects on the plasticization of polyimide gas separation membranes, J. Membr. Sci. 294 (2007) 40.

[46] A.G. Wonders, D.R. Paul, Effects of CO_2 exposure history on sorption and transport in polycarbonate, J. Membr. Sci. 5 (1979) 63.

[47] T. Alfrey, G. Goldfinger, H. Mark, The apparent second-order transition point of polystyrene, J. Appl. Phys. 14 (1943) 700.

[48] L. G. Curro, R. R. Lagasse, R. Simba, Diffusion model for volume recovery in glasses, Macromolecules 15 (1982) 1621.

[49] N. Hirai, H. Eyring, Bulk viscosity of liquids, J. Appl. Phys. 29 (1958) 810.

[50] J. H. Kim, W. J. Koros, D. R. Paul, Physical aging of thin 6FDA-based polyimide membranes containing carboxyl acid groups. Part I. Transport properties, Polymer 47 (2006) 3049.

[51] J. H. Kim, W. J. Koros, D. R. Paul, Physical aging of thin 6FDA-based polyimide membranes containing carboxyl acid groups. Part II. Optical properties, Polymer 47 (2006) 3104.

[52] P. H. Pfromm, W. J. Koros, Accelerated physical aging of thin glassy polymer films: evidence from gas transport measurements, Polymer 36 (1995) 2379.

[53] M. S. McCaig, D. R. Paul, Effect of film thickness on the changes in gas permeability of a glassy polyarylate due to physical aging Part I. Experimental observations, Polymer 41 (2000) 629.

[54] Y. Huang, D. R. Paul, Physical aging of thin glassy polymer films monitored by gas permeability, Polymer 45 (2004) 8377.

[55] Y. Huang, D. R. Paul, Effect of temperature on physical aging of thin glassy polymer films, Macromolecules 38 (2005) 10148.

[56] Y. Huang, D. R. Paul, Physical aging of thin glassy polymer films monitored by optical properties, Macromolecules 39 (2006) 1554.

[57] B. W. Rowe, B. D. Freeman, D. R. Paul, Physical aging ultrathin glassy polymer films tracked by gas permeability, Polymer 50 (2009) 5565.

[58] C. Zhou, T.-S. Chung, R. Wang, S. H. Goh, A Governing equation for physical aging of thick and thin fluoropolyimide films, J. Appl. Polym. Sci. 92 (2004) 1758.

[59] W.-H. Lin, T.-S. Chung, The physical aging phenomenon of 6FDA-durene polyimide hollow fiber membranes, J. Polym. Sci: Part B: Polym. Phys. 38 (2000) 765.

[60] T.-S. Chung, E. R. Kafchinski, Aging phenomenon of 6FDA-polyimide/ polyacrylonitrile composite hollow fiber, J. Appl. Polym. Sci. 59 (1996) 77.

[61] J. H. Kim, W. J. Koros, D. R. Paul, Effects of CO_2 exposure and physical aging on the gas permeability of thin 6FDA-based polyimide membranes Part 1. Without crosslinking, J. Membr. Sci. 282 (2006) 21.

[62] T. H. Kim, Gas sorption and permeation in a series of aromatic polyimides, Ph.D. Thesis, The University of Texas at Austin, 1988.

[63] L. M. Robeson, Correlation of separation factor versus permeability for polymeric membranes, J. Membr. Sci. 62 (1991) 165.

[64] L. M. Robeson, The upper bound revisited, J. Membr. Sci. 320 (2008) 390.

[65] L. M. Robeson, B. D. Freeman, D. R. Paul, B. W. Rowe, An empirical correlation of gas permeability and permselectivity in polymers and its theoretical basis, J. Membr. Sci. 341 (2009) 178.

CHAPTER 4

METHODOLOGY

4.1 Materials

4.1.1 Polymers

The polyimides used in this study were synthesized via the chemical imidization approach. All the polyimides are based on 2,2'-bis(3,4-dicarboxyphenyl) hexafluoropropane dianhydride (6FDA) and the diamines used were 4,4'-oxydianiline (ODA), 1,5-naphthalenediamine (NDA) and 2,3,5,6-tetramethyl-1,4-phenylenediamine (TMPDA). 6FDA was purchased from Clariant (Germany), NDA from Acros Organics, and ODA and TMPDA from Sigma-Aldrich. The chemical structures of the monomers are illustrated in Figure 4.1. 6FDA, ODA and NDA were sublimated under vacuum prior to use. TMPDA was purified by recrystallization in methanol at 55 ^{o}C. N-methyl-2-pyrrolidone (NMP) from Merck was further purified via vacuum distillation at 70 ^{o}C before using the solvent for the polyimide synthesis.

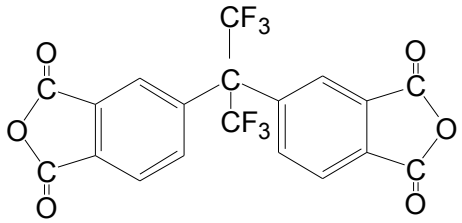

6FDA dianhydride

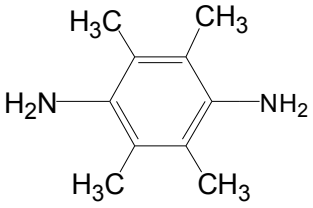

TMPDA diamine

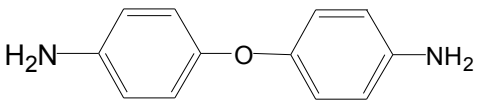

ODA diamine

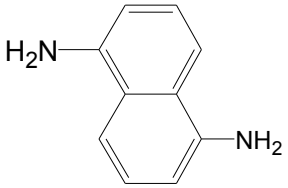

NDA diamine

Figure 4.1 Chemical structures of 6FDA, TMPDA, ODA and NDA monomers

For the synthesis of the polyimide, equimolar amounts of dianhydride and diamines were dissolved in NMP under nitrogen atmosphere to form a viscous solution of poly(amic acid) [1]. The solids content of the solution was 20 wt%. To synthesize the 6FDA-ODA/NDA copolyimides, the content of the respective diamines was varied between 25 to 75 mol % (i.e. the molar ratios of ODA:NDA are 25:75, 50:50 and 75:25). Subsequently, a mixture of triethylamine (or 3-picoline) and acetic anhydride with a molar ratio of 1:4 was added to form the polyimide. Triethylamine (or 3-picoline) and acetic anhydride were the reaction catalyst and dehydrating agent, respectively. The polyimide solution was precipitated in methanol and dried at 120 ^{o}C under vacuum prior to use. The general structure of a 6FDA-based polyimide is shown in Figure 4.2 (a) where the R group is representative of the diamine moiety

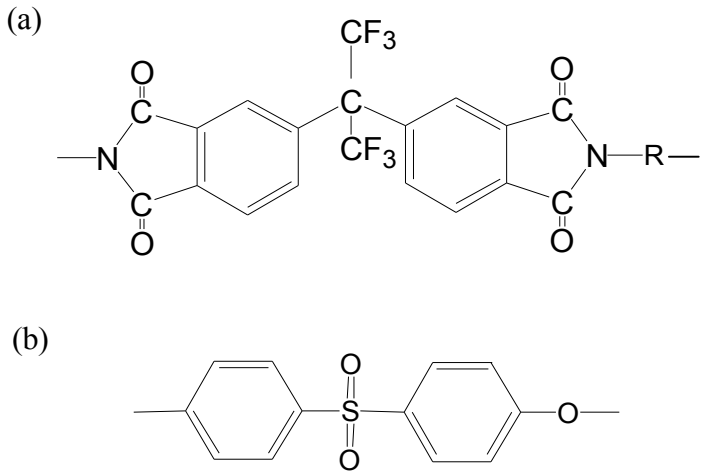

Figure 4.2 (a) General structure of a 6FDA-based polyimide and (b) chemical structure of polyethersulfone (PES)

Commercial Radel® A polyethersulfone (PES) was purchased from Solvay Advanced Polymers L.L.C., Georgia, USA. The PES pellets were dried at 120 ^{o}C under vacuum before use. Figure 4.2 (b) shows the chemical structure of PES.

4.1.2 Modification and crosslinking reagents

The aliphatic diamines, ethylenediamine (EDA), 1,3-diaminopropane (PDA) and 1,4-diaminobutane (BuDA) from Fluka were used as received. The chemical structures of the aliphatic diamines are depicted in Figures 4.3 (a) to (c). Three modification solutions were prepared for the post-treatment of polyimide dense membranes and each solution contains 1.65 M of the respective diamine in methanol [2]. For the chemical modification of 6FDA-NDA/PES dual-layer hollow fiber membranes, a 5 (w/w) % PDA in methanol solution was prepared and used.

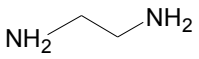

(a) ethylenediamine (EDA)

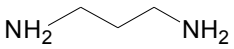

(b) 1,3-diaminopropane (PDA)

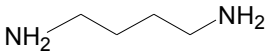

(c) 1,4-diaminobutane (BuDA)

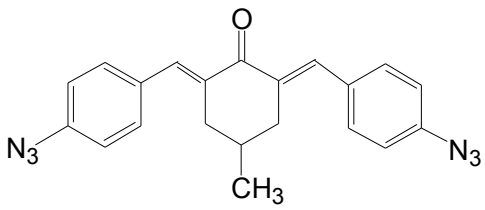

(d) 2,6-bis(4-azidobenzylidene)-4-methylcyclohexanone (azide)

Figure 4.3 Chemical structures of (a) EDA, (b) PDA, (c) BuDA and (d) azide

In the preparation of the pseudo interpenetrating polymer networks (pseudo-IPN), the azido-containing monomer, 2,6-bis(4-azidobenzylidene)-4-methylcyclohexanone (azide) from Sigma-Aldrich was used without further purification. The chemical structure of azide is depicted in Figure 4.3 (d).

4.2 Membrane fabrication and modification protocols

4.2.1 Polyimide dense films

For the casting of 6FDA-ODA and 6FDA-NDA homopolyimides, and 6FDA-ODA/NDA copolyimides, reagent grade dimethylformamide (DMF) from Fisher Chemicals was used as the solvent without further purification. A 2% (w/w) of the polymer solution was prepared by dissolving the polyimide in DMF. The solution was stirred overnight and subsequently filtered using 1.0 μm PTFE membrane before ring casting onto a Si wafer plate at 55 ^{o}C to allow slow evaporation of the solvent. After approximately one week, most of the solvent was removed and the nascent film was dried under vacuum following the heating protocol: (1) hold at 60 ^{o}C for 24 h, (2) increase the temperature to 250 ^{o}C at 12 ^{o}C/h, (3) hold at 250 ^{o}C overnight and (4) natural cooling. The thickness of the polyimide film is 50 ± 5 μm.

4.2.2 Polyimide/azide pseudo interpenetrating networks

To prepare the film casting solution, the azide monomer was first dissolved in the solvent and stirred for 1 hr. The solvents used for 6FDA-NDA/azide and 6FDA-TMPDA/azide were DMF and dichloromethane (DCM), respectively. Subsequently, the polyimide was added to the solution and stirred overnight. The polymer concentration in the solvent is 5 wt% while the azide loading in the polymer varied from 0 to 50 wt%. Table 4.1 shows the mass of the respective chemical species constituting the casting solutions. The solution

was filtered using 1.0 μm PTFE membrane before ring casting onto a Si wafer plate. The casting of 6FDA-NDA/azide and 6FDA-TMPDA/azide films was carried out at 55 ^{o}C and 25 ^{o}C, respectively. The casting temperature was selected based on the volatility of the solvent and to allow slow solvent evaporation for forming the polymer film. After approximately 5 days, most of the solvent has evaporated, leaving behind the nascent film. Further heat treatment of the 6FDA-based polyimide/azide films was conducted under vacuum as follows: (1) hold at 60 ^{o}C for 24 h, (2) increase to 250 ^{o}C at 12 ^{o}C/20 min, (3) hold at 250 ^{o}C for 24h, and (4) natural cooling. Depending on the loading of the azide monomer, the dense film thickness fall in the range of 50 ± 5 μm to 75 ± 5 μm.

Table 4.1 Mass compositions of polyimide/azide casting solutions

Polyimide/azide composition (wt%:wt%)	Mass of polyimide (g)	Mass of solvent* (g)	Mass of azide (g)
100:0	1.149	21.83	0
90:10			0.128
70:30			0.492
50:50			1.149

* The solvents for 6FDA-NDA and 6FDA-TMPDA are DMF and DCM, respectively.

4.2.3 Polyimide/polyethersulfone dual-layer hollow fiber membranes

4.2.3.1 Dope preparation

6FDA-NDA was selected as the material for the outer layer and a one polymer–two solvents ternary system was used for dope preparation. A binary solvent comprising of

NMP and tetrahydrofuran (THF) with the mass ratio of 5 to 3 was used [3]. The addition of volatile THF in the spinning dope potentially alters the precipitation path which changes the membrane morphology from porous to dense [4]. A good polymer concentration for fabricating hollow fibers with near defect-free outer selective layer is at or above the critical concentration [3]. Polymer solutions of different concentrations were prepared and the shear viscosity was obtained from a Rheometric Scientific ARES cone-and-plate rheometer using a shear rate of 10 s^{-1} at 25 ^{o}C. The relationship between shear viscosity and polymer concentration is shown in Figure 4.4. Based on the critical concentration for the 6FDA-NDA/NMP:THF (5:3) system, the outer layer dope composition was chosen as 27 wt% 6FDA-NDA and 73 wt% binary NMP:THF (5:3) solvent. By plotting the viscosity data on a semi-log plot (i.e. log (viscosity) vs. polymer concentration), a kink is observed at around 25 wt% which is close to the critical polymer concentration approximated from Figure 4.4. A phase diagram for the 6FDA-NDA/ NMP:THF (5:3)/ H_2O system is depicted in Figure 4.5. To obtain the phase diagram, polymer solutions with different solid contents were prepared using NMP:THF (5:3) as the solvent. Water was added as the non-solvent in the polymer solution until the occurrence of phase separation (as indicated by the gel formation). The resultant composition of the phase-separated polymer solution was determined. The inner layer dope consists of 30 wt% PES and 70 wt% NMP/H_2O (10:1). Water is added in the dope to increase the porosity of the inner layer and to eliminate the problem of a dense interface [3].

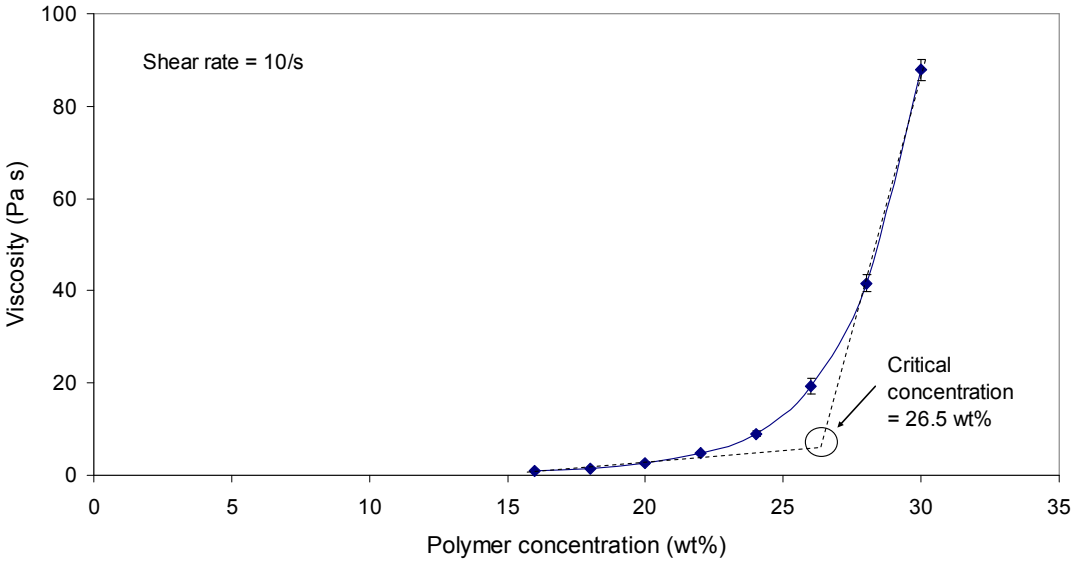

Figure 4.4 Plot of viscosity vs. concentration for the 6FDA-NDA/NMP:THF (5:3) system at 35 °C

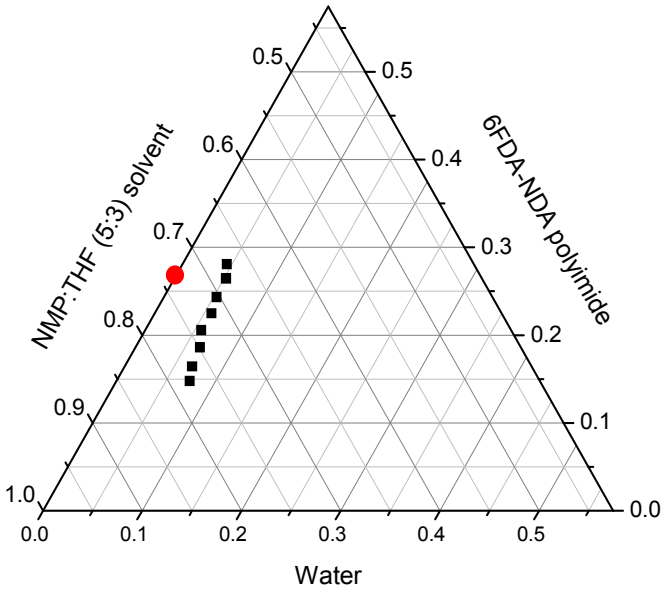

Figure 4.5 Phase diagram for 6FDA-NDA/(NMP:THF)/H_2O system at 25 °C

For the preparation of the dope solutions, the respective polymer was added gradually to the solvent under continuous agitation. The solution was stirred for 24 h at 25 ^{o}C to ensure complete dissolution. After which, the polymer dopes were left standing for another 24 h for degassing before introducing the solutions into the respective ISCO pumps. Due to the high viscosity of polymer solutions, in particular the outer layer dope, spinning was performed on the following day for degassing to take place.

4.2.3.2 Spinning conditions and solvent exchange

The 6FDA-NDA/PES dual layer hollow fiber membranes were fabricated by a dry-jet/wet spinning process [3]. The schematic of a lab-scale spinning line purchased from the Motianmo Technology Ltd. Company (Tianjin, China) is shown in Figure 4.6. The pressure supplied by the syringe pumps (ISCO Ltd) brings about the co-extrusion of the polymeric dopes through the triple orifice spinneret. A bore fluid was also extruded simultaneously through the bore of the spinneret. Figure 4.7 shows the dimensions of the dual-layer spinneret used in this study. The extruded nascent fibers enter the air gap region before contacting the coagulant. The fibers were collected by a take-up drum.

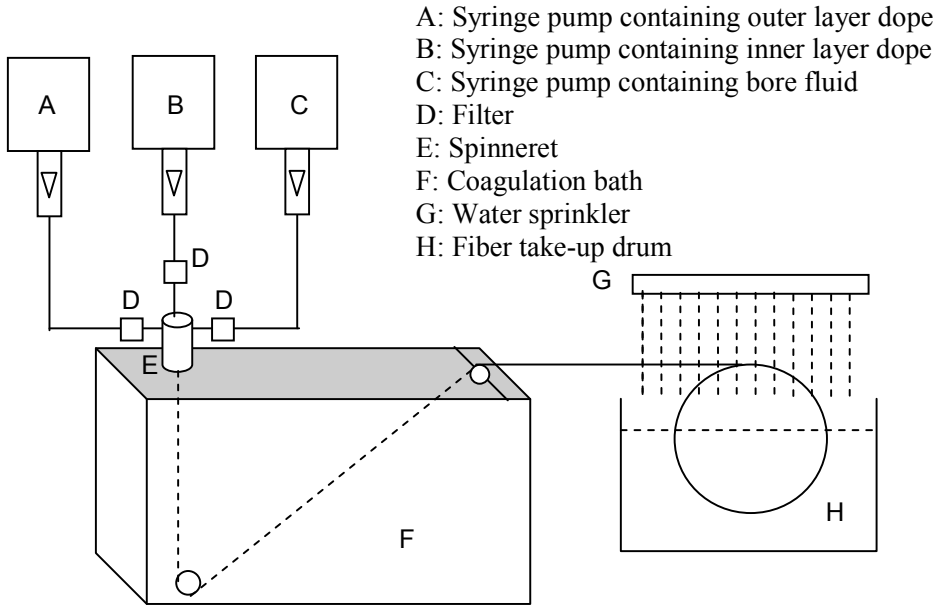

Figure 4.6 Schematic of hollow fiber spinning line

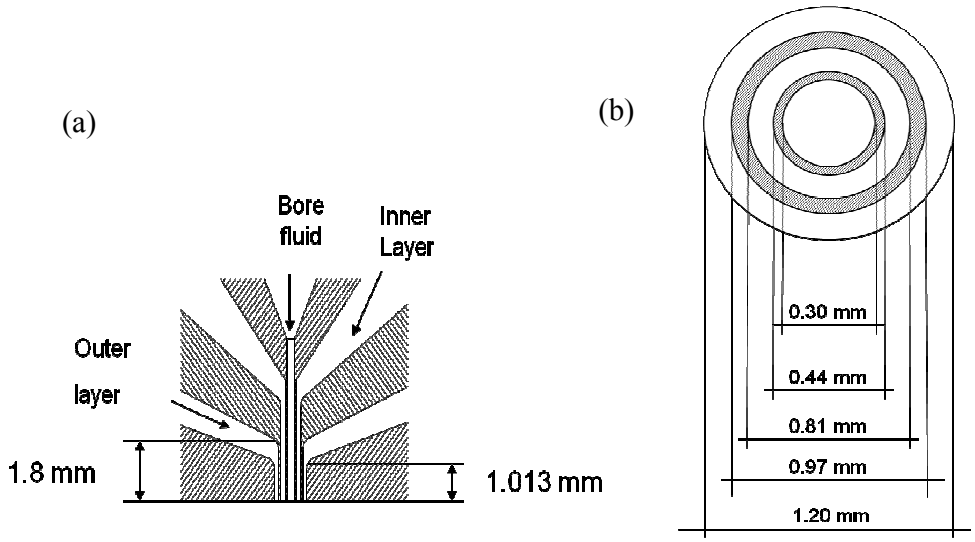

Figure 4.7 (a) Side view and (b) cross sectional view of a dual-layer hollow fiber spinneret

At a spinneret temperature of 25 ^{o}C, the outer surface morphology was porous as depicted in Figure 4.8. A spinneret temperature of 50 ^{o}C was needed to obtain a dense outer layer outer surface as shown in Figure 4.9. The higher spinneret temperature results in the partial vaporization of the more volatile THF solvent in the outer layer dope and creates a

polymer-rich phase, which is a pre-requisite to the formation of a dense structure. Table 4.2 summarizes the spinning parameters used in this study. In the preliminary stage of the work, various outer dope flow rates were investigated and the minimum flow rate required to produce fibers with almost defect free outer skin was selected. The inner dope flow rate was chosen based on the consideration that the ratio of the fiber outer diameter to twice the fiber thickness is preferably around 2. The as-spun fibers were immersed in water for two days to remove most of the solvents from the membranes. Solvent exchange was performed using a procedure which has been described previously i.e. (1) immersed in methanol 3 times, 30 min each time, (2) washed in n-hexane 3 times, 30 min each time and (3) air dry at 25 ^{o}C for 24 h.

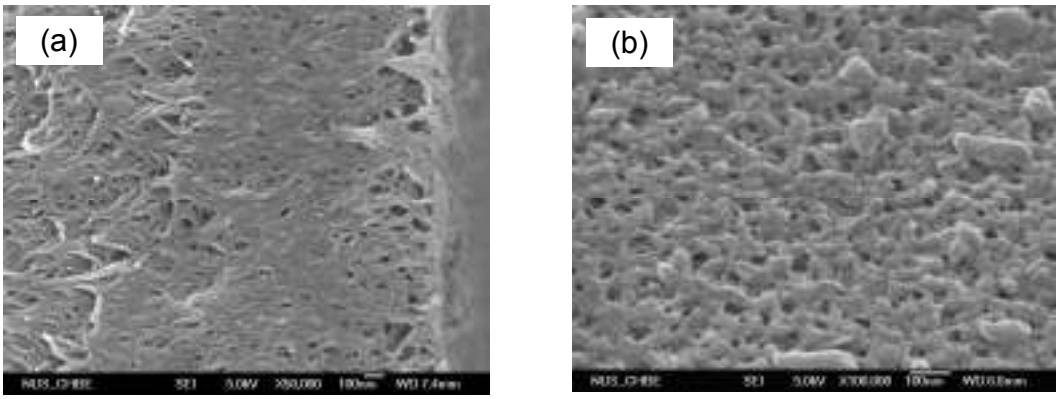

Figure 4.8 (a) Cross sectional view and (b) outer surface of 6FDA-NDA outer layer (air gap = 0.5 cm and spinneret temperature = 25 ^{o}C)

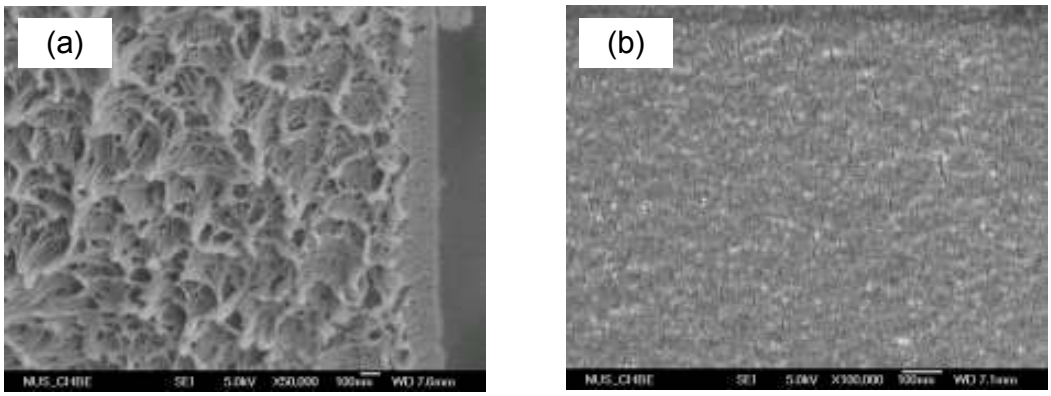

Figure 4.9 (a) Cross sectional view and (b) outer surface of 6FDA-NDA outer layer (air gap = 0.5 cm and spinneret temperature = 50 ^{o}C)

Table 4.2 Spinning conditions

Parameters	**A**	**B**	**C**
Outer-layer dope composition	27 wt% 6FDA-NDA, 73 wt% NMP/THF: 5:3 (w/w)		
Inner-layer dope composition	30 wt% PES, 70 wt% NMP/H_2O: 10:1 (w/w)		
Bore fluid composition	95/5 NMP/H_2O		
External coagulant	Water		
Outer layer dope flow rate (ml/min)	0.2		
Inner layer dope flow rate (ml/min)	0.8		
Bore fluid flow rate (ml/min)	0.3		
Coagulation bath temperature (^{o}C)	25		
Spinneret temperature (^{o}C)	50		
Take-up rate (cm/min)	Free fall		
Air gap (cm)	0.5	4	8

4.2.4 Diamine modification

For the diamine modification of dense polyimide films, the samples were immersed in the respective solutions (i.e. 1.65 M of diamine in methanol solution) for stipulated times of 15, 30, 60, 90 and 120 min at 25 ^{o}C. A fresh solution was used for each film. After which,

the modified films were washed with methanol for 5 min to remove residual unreacted diamines and dried at 70 ^{o}C under vacuum for 24 h.

For the hollow fiber membranes, a 5 (w/w)% of 1,3-diaminopropane (PDA) in methanol was used for post-treatment at 25 ^{o}C. Before modification, each fiber with approximate length of 25 cm was sealed with Araldite® quick settling epoxy at both ends. This prevents the diamine molecules to penetrate and react with the polyimide outer layer from the lumen side of the hollow fibers. The epoxy-sealed fibers were immersed in the PDA/methanol solution for stipulated times of 2 and 5 min. The PDA-modified fibers were washed in fresh methanol for 1 min and dried in air at 25 ^{o}C for 24 hr.

4.3 Membrane characterization

4.3.1 Fourier transform infrared spectroscopy (FTIR)

The chemical functionalities of the dense polymeric films were monitored by the attenuated total reflectance (ATR) mode using a Bio-Rad FTIR FTS 135 or a Shimadzu FTIR 8400 spectrometer. The number of scans for each sample was 32 and the scanning range was 650-2000 cm^{-1}. A ZnSe prism was used in conjunction with an ATR kit for the analysis of polymer films. As the azide monomer is in powder form, the sample was diluted with KBr (i.e. 1 mg of azide with 100 mg of KBr) and compressed into a pellet which was analyzed by the direct transmittance mode using the same scanning range.

4.3.2 X-ray photoelectron spectroscopy (XPS)

XPS measurements were carried out by an AXIS HSi spectrometer (Kratos Analytical Ltd., England) using a monochromatized Al KR X-ray source (1486.6 eV photons) under vacuum environment. All core-level spectra were obtained at a photoelectron take-off angle of 90° with respect to the sample surface.

4.3.3 Ultraviolet-visible light spectroscopy (UV-Vis)

After modifying the polyimide films, the spent diamine in methanol solutions were investigated in quartz cuvettes using a Shimadzu UV-1601 UV-Visible spectro-photometer in the wavelength ranging from 200 to 800 nm. UV-Vis analysis was conducted to track the presence of additional chemicals in the solution after reaction.

4.3.4 Gel permeation chromatography (GPC)

The molecular weights of the polyimides and the soluble portions of 6FDA-NDA/azide films were determined using gel permeation chromatography (GPC). For the synthesized polyimides, the concentration of the sample was 0.1 mg/ml of DMF. To test the soluble portions of the 6FDA-NDA/Azide films, the solution was diluted accordingly. The Waters GPC system comprises a Waters 2414 refractive index detector and a Waters 1515 isocratic HPLC pump. The system was allowed to reach stable equilibrium before

analysis and polystyrene standards (0.1 mg/ml DMF) were used for calibration. HPLC grade DMF was used as the mobile phase. The flow rate of the mobile phase was 1 ml/min and the injection volume was 50 μL. The testing temperature was set at 25 ^{o}C.

4.3.5 Gel content analysis

The gel content of the dense films was determined by immersing the samples into the original solvents at 25 ^{o}C (unless otherwise stated). The remaining insoluble portions of the membranes were dried under vacuum at 100 ^{o}C for 24h to remove the residual solvent before weighing. The gel content was calculated using equation (4-1)

$$\% \text{ Gel content} = M_1/M_0 \times 100\% \quad (4\text{-}1)$$

where M_1 and M_0 are the mass of the insoluble fraction and the original mass of the crosslinked films, respectively.

4.3.6 Density test

The density of the polymer film was determined using a Mettler Toledo balance coupled with a density kit. The mass of the sample in air and in ethanol was recorded. The measurements were conducted at 25 ^{o}C. The density can be calculated based on the buoyancy effect and the Archimedes' principle

$$\rho_{membrane} = \frac{w_0}{w_0 - w_1}\rho_{ethanol} \quad (4\text{-}2)$$

where w_0 and w_1 are the mass of the sample in air and ethanol, respectively and $\rho_{ethanol}$ is the density of ethanol.

4.3.7 Contact angle measurement

To examine the hydrophobic/hydrophilic nature of the membrane surface, the original 6FDA-ODA/NDA (50-50) film and the membranes modified with the respective diamines for an immersion time of 60 min were tested for their contact angles using a Ramé-Hart contact angle goniometer (model 100-22). The sample was fixed on a glass slide and a drop of deionised water was introduced on the sample surface by means of a Gilmont micro-syringe.

4.3.8 Thermal gravimetric analysis (TGA)

The thermal decomposition behaviors of the membranes were analyzed using a TGA 2050 Thermogravimetric Analyzer (TA Instruments). The mass of each sample is approximately 15 mg. The temperature was ramped from 50 ^{o}C to 800 ^{o}C at a heating rate of 20 ^{o}C/min under nitrogen purge. The temperature at 5 % weight loss is taken as the decomposition temperature of the material. Nitrogen was used as the purge gas and the flow rate was set at 100 ml/min.

4.3.9 Differential Scanning Calorimetry (DSC)

The glass transition temperatures (T_g) of the polymer films were characterized by differential scanning calorimetry (DSC) using a Mettler Toledo DSC 822 at heating and cooling rates of 20 ^{o}C/min. The mass of each sample is approximately 10 mg. The sample

is held at 50 ^{o}C for 2 min for stabilization, heated to 450 ^{o}C, held for another 2 min followed by cooling to 50 ^{o}C. The analysis was conducted under nitrogen purge at a flow rate of 30 ml/min. Two heating-and-cooling cycles were performed for each sample in order to remove the thermal history of the film. The T_g was obtained from the second heating curve and taken as the mid-point of the baseline shift region.

4.3.10 Dynamic mechanical analysis (DMA)

Dynamic mechanical analysis (DMA) measurements were carried with a TA Instruments DMA 2980 operating in a tension mode. The testing samples are 35 mm by 6 mm and the experiments were performed at a 1 Hz frequency and a heating rate of 3 ^{o}C min^{-1} from 30 to 480 ^{o}C.

4.3.11 Tensile measurement

The tensile properties of the 6FDA-ODA/NDA (50:50) pristine and PDA modified films before and after water sorption were determined using an Instron 5542 Universal Tensile tester. The analysis was carried out at 25 ^{o}C. The grip separation was set at 50 mm and a testing speed of 5 mm/min was used. The width of the thin film was 4.5 ± 0.5 mm and the membrane thickness was 0.050 ± 0.005 mm.

4.3.12 Nanoindentation

The moduli of the 6FDA-ODA and 6FDA-NDA films before and after PDA modification were measured by nanoindentation performed on a Hysitron Triboscope indenter system equipped with a Berkovich diamond tip. Loading and unloading rates of 100 μN/s were used. 5 points were examined on each specimen and the mean moduli of the membranes were obtained.

4.3.13 Wide angle x-ray diffraction (WAXRD)

The changes in intersegmental properties of the polymeric membranes were investigated using X-ray diffractor (XRD) Bruker, D8 series, GADDS (General Area Detector Diffraction system). The scanning range is from $2\theta = 2.5$ to 65.4^{o} Ni-filtered Cu X-ray source of wavelength 1.54 Å was used. Average *d*-spacing was determined based on the Bragg's law as shown in equation (4-3).

$$n\lambda = 2d \sin \theta \qquad (4\text{-}3)$$

where n is an integral number (1, 2, 3, . . .), λ denotes the X-ray wavelength, d represents the intersegmental spacing between two polymer chains and θ indicates the diffraction angle.

4.3.14 Positron annihilation lifetime spectroscopy (PALS)

The positron annihilation lifetimes of the host polyimides and the pseudo IPNs were obtained using positron annihilation lifetime spectroscopy (PALS). The experiments were conducted at the University of Missouri-Kansas City in Professor Y. C. Jean's research laboratory. The positron source of approximately 25 μCi of ^{22}Na was sealed by Kapton® films and then sandwiched between layers of polymeric membranes. The ^{22}Na source/polymer films assembly was wrapped in Al foil and clamped in between two sets of plastic scintillators and photomultipliers which are aligned facing to each other. The positrons emitted from the ^{22}Na source were absorbed by the polymer samples and were eventually annihilated. The lifetime of each positron terminates with the emission of two 0.511 MeV gamma rays. The generation of a 1.275 MeV gamma ray marks the incipient creation of the positron. The time difference between the detection of the start and end gamma rays were recorded using a fast-fast coincidence timing system. The resolution of the positron annihilation lifetime spectrometer was determined by measuring ^{60}Co and the full width at half maximum (FWHM) of the spectrum was 300 ps. All the lifetime spectra were binned into 1024 channels, with a channel width of 51 ps. The analyses were conducted at 25 ^{o}C and two million counts were collected in about 2 h for each PAL spectrum. A detailed description of the PALS can be obtained elsewhere [5].

4.3.15 Atomic force Microscopy

The surface topology of the 6FDA-ODA/NDA (50-50) membranes after diamine modification for 60 min was examined using a Nanoscope IIIa atomic force microscope (AFM) from Digital Instruments Inc. For each modified film, an area of 5 μm x 5 μm was scanned at a rate of approximately 1 Hz using the tapping mode of the AFM.

4.3.16 Field emission scanning electron microscopy (FESEM)

To observe the cross-sectional and surface morphology of hollow fiber membranes, the samples were immersed and fractured in liquid nitrogen. The fractured samples were coated using a JEOL JFC-1300 Auto Fine Coater fitted with Pt target (i.e. 20 mA and 30 s). The morphology of the dual-layer hollow fiber membrane was observed using field emission scanning electron microscopy (FESEM JEOL JSM-6700LV).

4.4 Molecular simulation

4.4.1 Molecular dimensions and nucleophilicity of diamines

Fukui function indices are reliable intramolecular site reactivity descriptors [6-7]. Hence, to determine the nucleophilicities of the aliphatic diamines used in this study, the Fukui function indices for electrophilic attacks were computed using the Materials Studio®

software by Accerlys. Geometry optimization of the respective diamines was done by the DMol3 module followed by the calculation of Fukui function for electrophilic attacks.

As the modification of the polyimide films using the diamines were carried out in methanol, the COSMO function was used whereby methanol was chosen as the solvent for the diamines. The resultant Fukui function indices based on the N atoms for the three aliphatic diamines were compared and the molecular models of the diamines were shown to provide visualization of the electron density distribution surrounding the active sites. The scale for the electron density used for all three diamines were standardized and the same isovalue was used. The isosurface generated (based on the isovalue) shows the surface whereby the electron density is uniform.

4.4.2 Polyimide free volume and mean square displacements

Materials Studio 4.3 from Accelrys was used for molecular dynamics simulation. Repeat units of 6FDA-ODA and 6FDA-NDA were constructed using the "Build" function. 6FDA-ODA, 6FDA-NDA, and 6FDA-ODA/NDA copolymers were constructed using the as-built repeat units. For constructing the polymer, 10 repeat units were used with amino group as the initiator and terminator. Isotactic polymer configuration with random torsion and head-to-tail orientation were assumed for simulating the polymer chains. For the copolyimides, equal reactivity ratios and probability of the repeat units were assumed during polymer construction. Energy minimization of the polyimide chains was performed prior to amorphous cell construction.

To simulate the dense polyimide membranes, the amorphous cell module was utilized for constructing a polymeric periodic cell based on compass forcefield calculations. The geometry of the configuration is allowed to be optimized following the construction of the amorphous cell. 10 polymer chains were used for construction. The amorphous cell was subjected to fine convergence with maximum interations of 10,000 before proceeding with molecular dynamics simulation by the Discover module. An equilibrium stage temperature of 298 K and equilibrium time of 5.0 ps were used. Isothermal-isobaric (NPT) ensemble was used for the simulation. A total of 100,000 steps with a step time of 1.0 fs and a dynamics time of 100 ps were employed.

The free volume and occupied volume of each amorphous polyimide were calculated using the Connolly task [52]. Connolly radii that correspond to the kinetic diameters of H_2 and CO_2 molecules were used. The simulated fractional free volumes (FFV) of the polyimides are dependent on the chosen Connolly radius since these are used as the probe particles. The mean square displacements of the polyimide chains constituting the amorphous cells were determined using the Analysis function of the amorphous cell module. To investigate the effects of diamine modification on the polymer chain rigidity, 6FDA-ODA and 6FDA-NDA homopolyimides were chosen for representative studies. For each polyimide, 2 chains with 10 repeat units were constructed and PDA linkages were constructed between consecutive imide rings on the respective polymer chains. The structures (with and without PDA crosslinking) were similarly subjected to minimization prior to molecular dynamics simulations. The mean square displacements of the polyimide chains with and without PDA crosslinking were compared.

4.5 Determination of gas transport properties

4.5.1 Constant volume-variable pressure gas permeation chamber

To test the gas permeation characteristics of both flat sheet and hollow fiber membranes, a constant volume-variable pressure gas permeation chamber was used. Figure 4.10 shows the schematic of the gas permeation testing apparatus which can be divided into 3 main segments: (1) feed and upstream, (2) gas permeation cell and (3) downstream. The first part comprises (i) a control valve to introduce the gas from the cylinder into the system, (ii) a pressure gauge to indicate the pressure of the feed tank/upstream, (iii) a gas reservoir with a capacity of 1000 cm^3 to maintain the upstream pressure during measurements. For testing flat membranes, the gas permeation cell consists of a metal porous support where the sample is placed and sealed with two o-rings to prevent gas leakage. The thickness of the dense membrane typically falls in the range of 50±5 μm. In the testing of hollow fiber membranes, the gas permeation cell is replaced by a ¼" Swagelok union tee which was used for making the hollow fiber membrane module. Typically, one membrane module houses two strands of fibers, each with a length of approximately 7 cm. The downstream segment is made up of a fixed volume assembly where the changes in the pressure are detected by a Baratron® pressure transducer by MKS Instruments Inc, USA. To calibrate the downstream volume, standard polycarbonate film was tested and the gas permeability data obtained from the literature was used to back-calculate the volume. The signals collected by the pressure transducers are sent to a data shuttle which is connected to a computer. The software for data logging

is Workbench PC for windows-v5.01.04. The temperature of the system is regulated by a temperature controller which is connected to a heating element and axial fans.

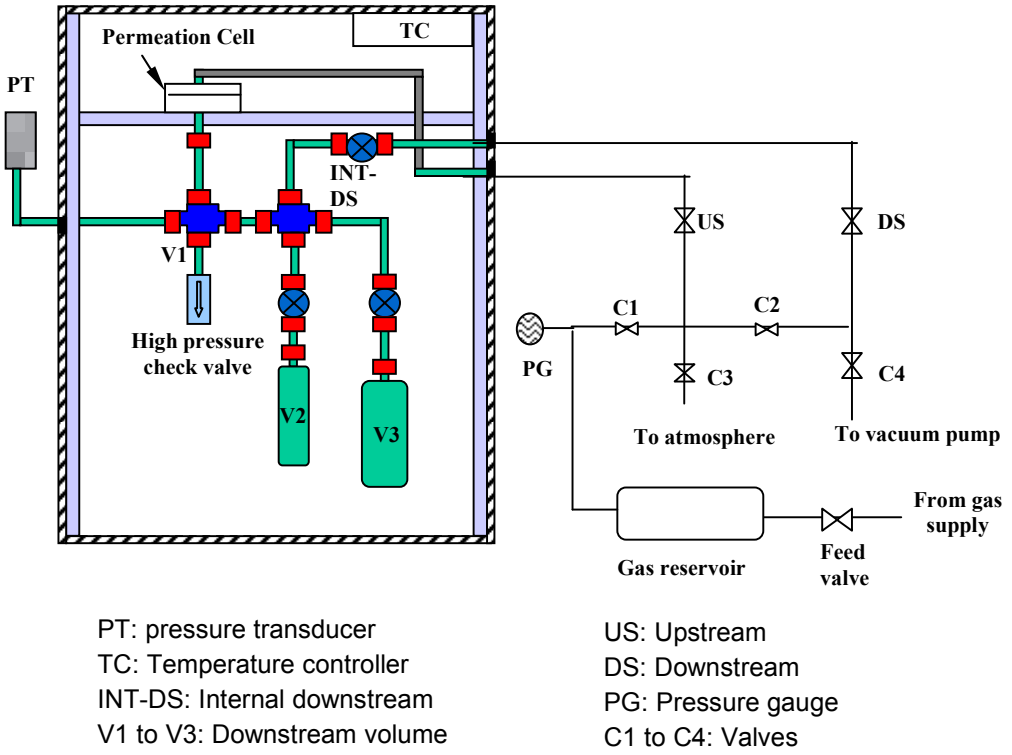

Figure 4.10 Constant volume-variable pressure gas permeation chamber for testing flat membranes (pure gas)

4.5.2. Pure gas permeation

The membrane of interest, be it dense film or hollow fiber was mounted and the entire system was subjected to vacuum for the removal of residual gases prior to testing. The gas transport properties of the dense films were tested in the order He, H_2, O_2, N_2, CH_4 and CO_2. H_2 permeation was conducted at 3.5 atm while CO_2 was tested at 3.5 and 10 atm. The remaining gases were tested at 10 atm. The operating temperature was 35 ^oC. To investigate the CO_2-induced plasticization behavior of the films, the testing pressure was

intermittently ramped from 2 to 30 atm. The rate of pressure increase (dp/dt) at steady state was used for the calculation of gas permeability according to equation (4-4)

$$P = \frac{273\times10^{10}}{760}\frac{VL}{AT\left(p_2\times 76/14.7\right)}\left(\frac{dp}{dt}\right) \tag{4-4}$$

where P is the gas permeability of a membrane in Barrer (1 Barrer = 1×10^{-10} cm^3 (STP)-cm/cm^2 s cmHg), V is the volume of the downstream chamber (cm^3), A refers to the effective membrane area (cm^2), l is the membrane thickness (cm), T is the operating temperature (K) and the upstream pressure is given by p_2 (psia).

The ideal permselectivity of a membrane for gas A to gas B, α_{AB} was evaluated as follows.

$$\alpha_{AB} = \frac{P_A}{P_B} \tag{4-5}$$

where P_A and P_B are the gas permeabilities for gases A and B, respectively.

For the pristine hollow fibers, the gases were tested in the order H_2, O_2, N_2, CH_4 and CO_2. For the diamine modified fibers, only the transport properties of H_2 and CO_2 were tested. The pure gas tests were conducted at a temperature of 35 ^oC and a transmembrane pressure of 20 psia (1.36 atm). This is equivalent to an upstream pressure of 5.3 psig (0.36 atm). The pressure was selected based on the consideration that most hollow fibers fabricated using 6FDA-based polyimides are easily plasticized by CO_2 even at low upstream pressures of 20-50 psia (1.36 to 3.40 atm) [8-9]. For consistency, all the other gases were tested at 20 psia. To investigate the CO_2-induced plasticization behavior of the

fibers, the testing transmembrane pressure was intermittently ramped from 20 psia to 200 psia (1.36 to 13.6 atm).

The rate of pressure increase (dp/dt) at steady state was used for the calculating the gas permeance. Equations (4-6) and (4-7) were used to determine the gas permeance of the hollow fiber membranes and ideal gas pair permselectivity, respectively.

$$\frac{P}{l} = \frac{273 \times 10^{10}}{760} \frac{V}{AT\left(p_2 \times 76 / 14.7\right)} \left(\frac{dp}{dt}\right) \tag{4-6}$$

where P/l is the gas permeance in GPU (1 GPU = 1×10^{-6} cm^3 (STP)/cm^2 s cmHg), l is the thickness of the membrane selective layer (cm), V is the volume of the downstream chamber (cm^3), A refers to the effective membrane area (cm^2), T is the operating temperature (K) and the upstream pressure is given by p_2 (psia).

$$\alpha = \frac{\left(P/l\right)_A}{\left(P/l\right)_B} \tag{4-7}$$

where $(P/l)_A$ and $(P/l)_B$ are the permeances for gas A and B, respectively.

4.5.3 Mixed gas permeation

Binary H_2/CO_2 and CO_2/CH_4 gas permeation tests were conducted for selected samples with promising ideal gas pair permselectivity. To test the mixed gas separation performance of the membranes, slight modifications to the constant volume-variable pressure gas permeation testing system described in Section 4.5.2 were made (see Figure 4.11) [10]. In the mixed gas testing facility, the membrane is tested in cross-flow

configuration. An additional valve (C5) at the upstream segment is included to adjust the stage cut by changing the retentate flow rate. At the downstream portion, the valve C6 is added for introducing the accumulated permeate gas to an Agilent 7890 gas chromatographer (GC) for the analysis of the gas composition.

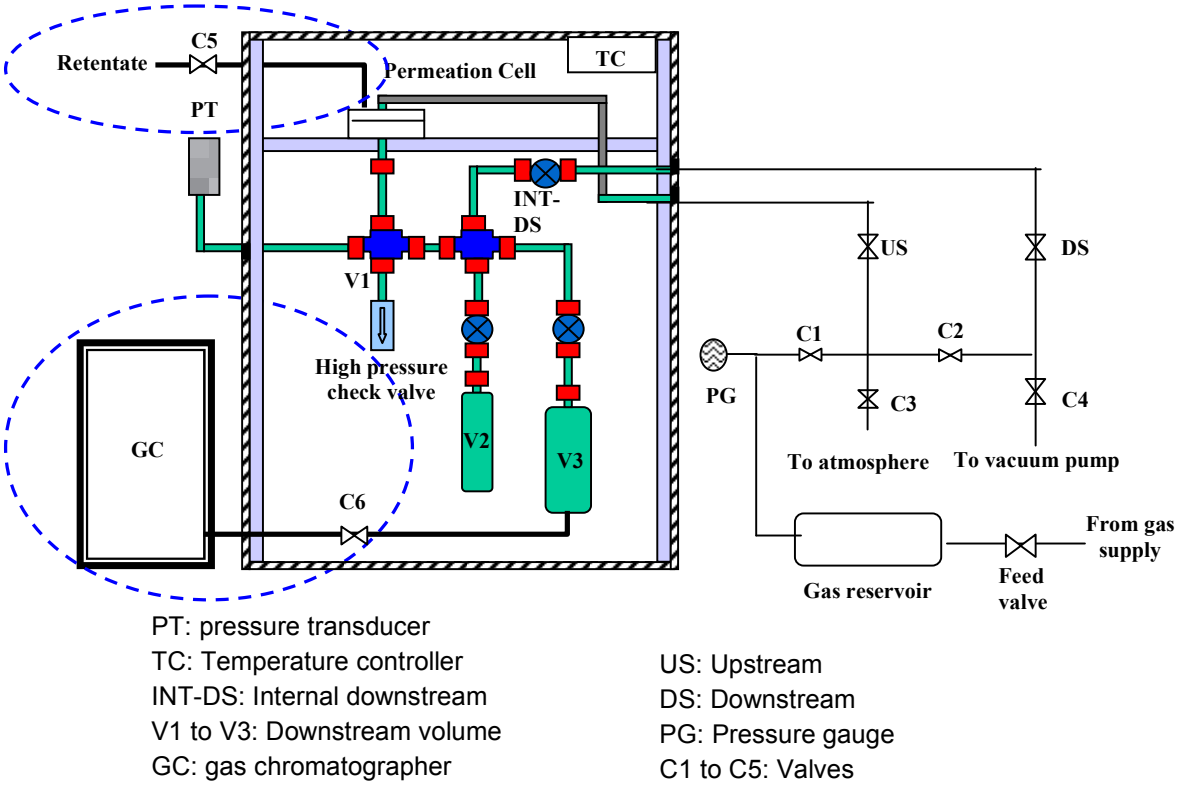

Figure 4.11 Constant volume-variable pressure gas permeation chamber for testing flat membranes (mixed gas)

The GC consists of a valve switching system that is connected to the 2-column assembly, injection port and vacuum pump. A thermal conductivity detector (TCD) is used. In the 2-column assembly, the first is a HP-PLOTQ column while the second is a molecular sieve 5A column, both purchased from Agilent Technologies, Singapore. As the gas permeation testing is conducted at sub-atmospheric pressures, the leakage of air into the system is somewhat inevitable. For CO_2/CH_4 gas pair, the PLOTQ column alone is sufficient to

separate air, CH_4 and CO_2. However, for the H_2/CO_2 gas pair, the PLOTQ column cannot separate air from H_2 and hence the need of the molecular sieve column to achieve this. Helium was used as the carrier gas for all the GC testing. Due to the relative difference in the thermal conductivity between helium and the tested gases, the characteristics peaks in the chromatogram for all the gases other than H_2, are positive. The compositions of the feed gas were (1) 50% H_2 and 50% CO_2 and (2) 90% CO_2 and 10% CH_4.

For flat membranes, binary H_2/CO_2 permeation tests were performed at 35 ^oC and 7 atm. The CO_2/CH_4 mixed gas tests were conducted at 10, 20 and 30 atm and the temperature was 35 ^oC. The gas permeability was determined using equations (4-8) and (4-9) as follows:

$$P_A = \frac{273\times10^{10}}{760}\frac{y_A VL}{AT\left(76/14.7\right)\left(x_A p_2\right)}\left(\frac{dp}{dt}\right) \tag{4-8}$$

$$P_B = \frac{273\times10^{10}}{760}\frac{y_B VL}{AT\left(76/14.7\right)\left(x_B p_2\right)}\left(\frac{dp}{dt}\right) \tag{4-9}$$

where P_A and P_B are the permeabilities (Barrer) of gases A and B, respectively. p_2 is the upstream feed gas pressure (psia) and p_1 represents the downstream permeate gas pressure (psia). x and y refers to the gas molar fraction in the feed and the permeate accordingly (%). Subsequently, the mixed gas selectivity can be simplified into the calculating equation as described in equation (2) due to the negligible downstream pressure.

For hollow fiber membranes, the H_2/CO_2 mixed gas tests were conducted at a transmembrane pressure of 200 psia (13.6 atm) and a temperature of 35, 45 or 55 ^oC. Equations (4-10) and (4-11) were used to compute H_2 and CO_2 permeances, respectively.

$$\left(\frac{P}{l}\right)_{H_2} = \frac{273\times10^{10}}{760}\frac{y_{H_2}V}{AT\left(76/14.7\right)\left(x_{H_2}p_2\right)}\left(\frac{dp}{dt}\right) \quad (4\text{-}10)$$

$$\left(\frac{P}{l}\right)_{CO_2} = \frac{273\times10^{10}}{760}\frac{y_{CO_2}V}{AT\left(76/14.7\right)\left(x_{CO_2}p_2\right)}\left(\frac{dp}{dt}\right) \quad (4\text{-}11)$$

where $(P/l)_{H2}$ and $(P/l)_{CO2}$ are the H_2 and CO_2 permeances, respectively. p_2 is the upstream feed gas pressure (psia) and p_1 represents the downstream permeate gas pressure (psia). x and y refers to the gas molar fraction in the feed and the permeate accordingly (%). Subsequently, the mixed gas selectivity can be simplified into the calculating equation as described in equation (2) due to the negligible downstream pressure.

4.5.4 Measurements of gas sorption

Carbon dioxide sorption tests for the dense films were conducted using a Cahn D200 microbalance sorption cell at 35 ^{o}C over a pressure range of 0 to 250 psia (0 to 17.0 atm) [11]. A schematic of the microbalance sorption cell is depicted in Figure 4.12. For each run, films with thickness of 50±5 μm, diameter of 1 cm and total mass of approximately 80-100 mg were placed on the sample pan. The system was evacuated for 24 h prior to testing. The gas at a specific pressure was fed into the system. The mass of gas sorbed by the membranes at equilibrium was recorded. Subsequent sorption experiments were done by further increment of the gas pressure. The equilibrium sorption value obtained was corrected by the buoyancy force.

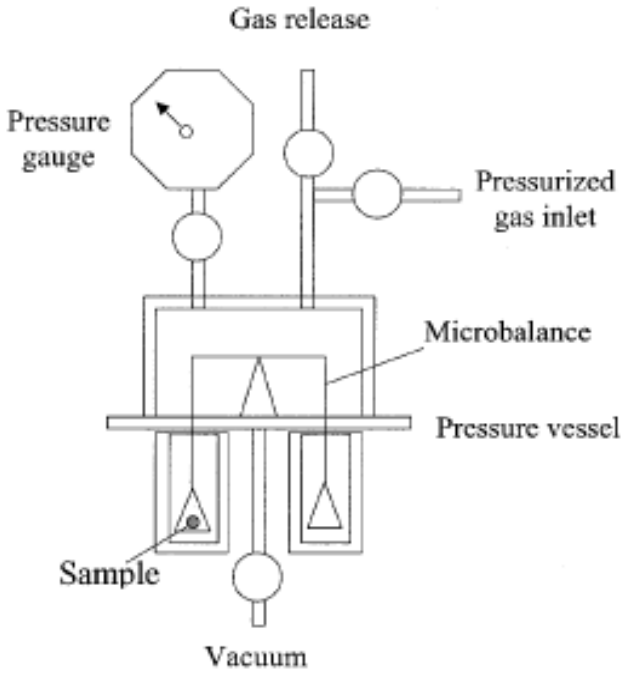

Figure 4.12 Microbalance sorption cell

4.6 References

[1] C. Cao, R. Wang, T. S. Chung, Y. Liu, Formation of high-performance 6FDA-2,6-DAT asymmetric composite hollow fiber membranes for CO_2/CH_4 separation, J. Membr. Sci. 209 (2002) 309.

[2] T. S. Chung, L. Shao, P. S. Tin, Surface modification of polyimide membranes by diamines for H_2 and CO_2 separation, Macromol. Rapid Commun. 27 (2006) 998.

[3] D. F. Li, T. S. Chung, R. Wang, Y. Liu, Fabrication of fluoropolyimide/ polyethersulfone dual-layer asymmetric hollow fiber membranes for gas separation, J. Membr. Sci. 198 (2002) 211.

[4] D. T. Clausi, W. J. Koros, Formation of defect-free polyimide hollow fiber membranes for gas separations, J. Membr. Sci. 167 (2000) 79-89.

[5] Y.C. Jean, J. P. Yuan, J. Liu, Q. Deng, H. Yang, Correlations between gas permeation and free-volume hole properties probed by positron annihilation spectroscopy, J. Polym. Sci. Part B Polym. Phys. 33 (1995) 2365.

[6] W. Yang, W. J. Mortier, The use of global and local molecular parameters for the analysis of the gas-phase basicity of amines, J. Am. Chem. Soc. 108 (1986) 5708.

[7] P. Kolandaivel, G. Praveena, P. Selvarengan, Study of atomic and condensed atomic indices for reactive sites of molecules, J. Chem. Sci. 117 (2005) 591.

[8] J. Ren, R. Wang, T. S. Chung, D. F. Li, Y. Liu, The effects of chemical modifications on morphology and performance of 6FDA-ODA/NDA hollow fiber membranes for CO_2/CH_4 separation, J. Membr. Sci. 222 (2003) 133.

[9] Y. Liu, T. S. Chung, R. Wang, D. F. Li, M. L. Chng, Chemical cross-linking modification of polyimide/poly(ether sulfone) dual-layer hollow fiber membranes for gas separation, Ind. Eng. Chem. Res. 42 (2003) 1190.

[10] L. Shao, T.-S. Chung, S. H. Goh, K. P. Pramoda, Polyimide modification by a linear aliphatic diamine to enhance transport performance and plasticization resistance, J. Membr. Sci. 256 (2005) 46

[11] S.-X. Cheng, T.-S. Chung, R. Wang, R. H. Vora, Gas-sorption properties of 6FDA–durene/1,4-phenylenediamine (pPDA) and 6FDA–durene/1,3-phenylene diamine (mPDA) copolyimides, J. Appl. Polym. Sci. 90 (2003) 2187

CHAPTER 5

EFFECT OF DIAMINE PROPERTIES AND MODIFICATION DURATION ON THE H_2/CO_2 SEPARATION PERFORMANCE OF DIAMINE-MODIFIED POLYIMIDE MEMBRANES

This chapter is published as a journal paper

Bee Ting Low, Youchang Xiao, Tai Shung Chung, Ye Liu, Simultaneous occurrence of chemical grafting, crosslinking and etching on the surface of polyimide membranes and their impact on H_2/CO_2 separation, *Macromolecules* 41 (2008) 1297-1309.

5.1 Introduction

The gradual emergence of a hydrogen-based economy for a future sustainable environment, together with the demand for hydrogen as a chemical feedstock from the industries, navigates the continuous push and emphasis on hydrogen separation with outstanding efficiency [1-4]. Membrane technology competes with other conventional separation techniques including absorption, pressure swing adsorption and cryogenic distillation in hydrogen purification [1-2]. Nevertheless, due to the inherent advantages of membrane technology, there is no doubt to its major role in hydrogen separation [1-7].

Currently, hydrogen enrichment using membranes makes up a significant portion of the overall membrane market for gas/vapor related separations and is expected to increase over the next few decades [4]. In year 2000, the separation of nitrogen from air contributed almost 50% of the total membrane market (US$155 million) while CO_2/CH_4 and H_2 separations amount to US$30 million and US$25 million, respectively [4]. As a forecast, the membrane market for hydrogen separation is expected to manifest a six-fold increment to US$150 million in year 2020 [4]. The future prospects of membrane technology in hydrogen separation are evident [6].

The separation of hydrogen from methane, nitrogen and argon in ammonia purge-gas streams has long been commercialized and the challenge awaiting membrane researchers is the separation of H_2 from plasticizing gases such as CO_2 [4]. To date, steam reforming of methane serves as the economically favored route for the industrial production of

hydrogen as compared to alternative methods including partial oxidation of methane and auto-thermal reforming [1-2] To improve H_2 purity (decrease CO concentration), a water gas shift reactor (WGSR) is required downstream which operates under high or low temperature modes [1-2]. The main composition of the product stream from the WGSR is 75 mol% H_2 and 19 mol% CO_2 [1-2].

Membranes which are hydrogen-rejective allow CO_2 to permeate preferentially. Freeman and co-workers identified that the ether oxygen in ethylene oxide units among other functional groups provide a good balance between high CO_2 permeability and CO_2/H_2 permselectivity [8-10]. Lin et al. reported highly permeable, CO_2-selective membranes comprising of a copolymer network of poly(ethylene glycol) diacrylate and poly(ethylene glycol) methyl ether acrylate whose performance heightens with CO_2 plasticization [11]. Excellent gas separation performance can be realized, especially under low temperature conditions. Lin et al. reported a mixed-gas CO_2/H_2 selectivity of 31 at an operating temperature of -20 ^{o}C [11]. Other polymeric membranes which allow the preferential transport of more condensable gases (e.g. CO_2) have been reported by Merkel and Toy [12-13].

For hydrogen selective membranes, palladium membranes are capable of producing H_2 of high purity but the flux is rather inferior [1]. The transport of H_2 across Pd membranes occurs in seven consecutive steps; (i) movement of H_2 molecules to the membrane surface facing the feed, (ii) dissociation of H_2 into H^+ and electrons, (iii) adsorption of H^+ in the membrane, (iv) diffusion of H^+ across the membrane, (v) desorption of H^+ from the

membrane, (vi) reassociation of H^+ and electrons to form H_2, and (vii) diffusion of H_2 from the permeate side of the membrane [1]. Thin Pd membranes are necessary for higher flux. Therefore, attempts have been made by Athayde et al. [14] and Mercea et al. [15] to fabricate "sandwich membrane" whereby the metals are deposited on one or both sides of a polymeric support. However, due to the brittleness of Pd membranes and the considerable cost of precious Pd metal, they are not commercially attractive [1-2]. In addition, it is difficult or almost impossible to fabricate defect-free Pd hollow fiber membranes, which possess a larger surface to volume ratio due its poor processability.

A novel approach which attempts to combine the high selectivity of Pd with the good processability of polymers in the form of metal-polymeric nanocomposite membranes has been introduced. However, the improvement in the gas separation performance of metal-polymeric nanocomposite membranes remains uncertain. Fritsch and Peinemann incorporated 15 wt% Pd within a poly(amide-imide) matrix and a slight enhancement in H_2/CO_2 selectivity is achieved at the expense of H_2 permeability [16]. Compton et al. fabricated hybrid Pd-polyimide membranes (5 wt% Pd loading) and there is no enhancement in H_2/CO_2 permselectivity and the H_2 permeability is lower than the neat polyimide films [17]. The decrease in H_2 permeability is due to the presence of Pd nanoclusters which increases the tortuosity and hence siginifcantly decreases H_2 diffusivity [16-17]. The different effects of Pd on H_2/CO_2 selectivity may be due to the variation in Pd loading in the polymeric nanocomposite membranes [16-17]. A high Pd loading is necessary to enhance the solubility selectivity significantly in order to compensate the decrease in diffusivity selectivity.

Polymeric membranes which are selective for H_2 can be employed for refinery streams at low temperatures and tail stream from PSA units [1]. Despite the processability of polymeric materials along with significantly lower cost, H_2-selective polymeric membranes are far from commercialization. Most polymers exhibit low intrinsic H_2/CO_2 selectivity in the range 0.5 – 5 [7]. The high diffusivity of H_2 coupled with the high solubility of CO_2 makes the separation of this gas pair via the solution diffusion mechanism through polymeric membranes intricate. Among the various classes of polymers, polyimides are widely studied for use in gas separation due to their inherent advantages [18-20]. Studies involving the modification of polyimide membranes and carbonization of polyimide precursors for gas separation have been investigated extensively. However, the use of carbonized polyimide membranes for H_2/CO_2 separation has not been reported [21-23]. Polyimides, especially those containing (2,2'-bis(3,4-dicarboxyphenyl) hexafluoropropane dianhydride) (6FDA) moiety are good materials for gas separation membranes because the $-C(CF_3)_2$ group is expected to account for both high gas permeability and gas pair permselectivity [24-27]. In addition to the favorable gas transport properties, fluorine-containing polyimides also possess excellent thermal and mechanical characteristics [28-30]. However, 6FDA-based polyimides too suffer from poor intrinsic H_2/CO_2 selectivity and the gas separation performance may deteriorate in the presence of plasticizing gases. Therefore, in order to enhance the physicochemical properties of the 6FDA-based polyimides and to maintain the performance of the polymeric membrane even in harsh chemical environment, one promising approach is the modification of polyimides by chemical methods.

Chung and co-workers have developed a simple diamino modification technique applied to polyimides. This solid state modification is carried out as a post-treatment step following membrane fabrication and is performed at room temperature. This method has been applied to both dense and hollow fiber membranes. Liu et al. discussed the mechanism for the crosslinking process and proposed that polymer swelling by methanol is a pre-requisite to reaction [24]. During the chemical modification, the amine group reacts favorably with the imide ring, resulting in the cleavage of the ring and the resultant formation of two amide groups [24-26,30-37]. Amine containing compounds of various configurations have been explored by Chung's group, including aromatics (e.g. p-xylenediamine) [24-26,30], linear aliphatics (e.g. ethylenediamine) [31], cyclics (e.g. 1,3-cyclohexanebis(methylamine)) [33], network structure with plentiful supply of NH_2 groups (e.g. polyamidoamine dendrimers) [34-37], etc. Most of the works related to diamino crosslinking of the polyimides are focused on carbon dioxide removal from natural gas [24-26,30-37].

The robustness of this chemical modification approach motivates one to engage the same method for H_2/CO_2 separation. In a recent work reported by Chung et al., 6FDA-durene membranes were crosslinked using aliphatic diamines [7]. Surprisingly, the ideal H_2/CO_2 permselecitivity of 1,3-diaminopropane crosslinked film increases by 100 times after an immersion duration of 10 min [7]. All the crosslinked films exhibit gas separation performance above the trade off line [7].

In view of the present state of art for H_2/CO_2 separation using membranes, the objective of this work is to investigate the diamino modification of a copolyimide, 6FDA-ODA/NDA on the gas separation performance for H_2/CO_2 gas pair. This polymer was chosen based on the consideration of its lower material cost as compared to 6FDA-durene [26]. In addition, there are limited studies reported in the literature which employed 6FDA-ODA/NDA copolyimide as the working polymer and this polymer has not been used for H_2/CO_2 separation.

In this study, three aliphatic diamines, namely ethylenediamine, 1,3-diaminopropane and 1,4-diaminobutane are used. The effects of different immersion times on the gas transport parameters are investigated. In addition, the occurrence of polymeric backbone scission during the chemical modification, which has not been formally reported in previous works, is proposed here. A comparison between the gas separation performance of diamine modified 6FDA-ODA/NDA and 6FDA-durene dense membranes is presented. Lastly, the effectiveness of the modification approach which is dependent on the nature of the polyimides and the diamines will be discussed.

5.2 Results and discussion

5.2.1 Characterization of the modified films

The dense membranes before and after chemical modification were studied using ATR-FTIR. With reference to Figure 5.1, the pure 6FDA-ODA/NDA film exhibits a

characteristic doublet near 1717 cm^{-1} and 1783 cm^{-1} which is attributed to the carbonyl group of the imide ring, the former resulting from the asymmetric stretch of C=O and the latter is brought about by the symmetric stretch of the carbonyl group. The characteristic peak at 1359 cm^{-1} is due to the C-N stretch of the imide group while the peak at 1096 cm^{-1} is indicative of the transverse stretch of C–N–C in the imide group. The peak at 718 cm^{-1} is due to the out-of-plane bending of C–N–C in the imide group.

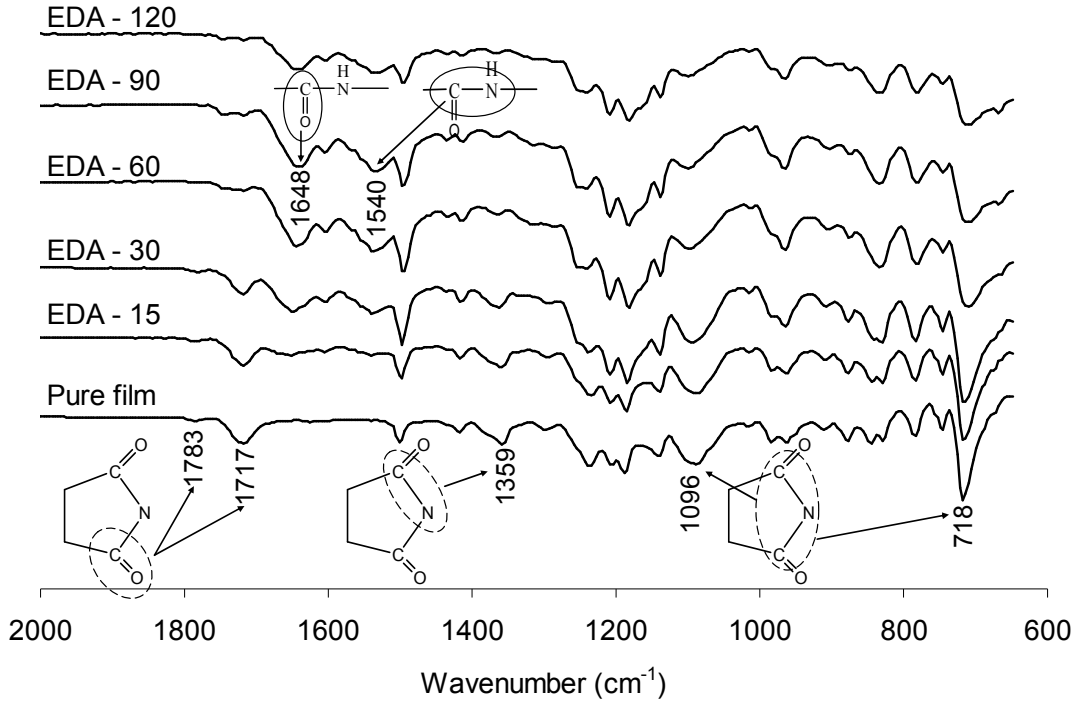

Figure 5.1 FTIR spectra of EDA modified films at different immersion times

Upon modifying the pure polymeric film with EDA, distinct peaks representative of the amide groups are clearly visible. Referring to Figure 5.1, the characteristic peaks at 1648 cm^{-1} and 1540 cm^{-1} are attributed to C=O stretch and C-N stretch of the amide group, respectively. This supports the reaction mechanism proposed by Liu et al [24]. As the immersion time is increased, the characteristic peaks of the amide groups become more

prominent while the peaks representative of the imide groups become less intense. The trends observed for PDA and BuDA modified membranes for different immersion times are similar to EDA modified films (data not shown).

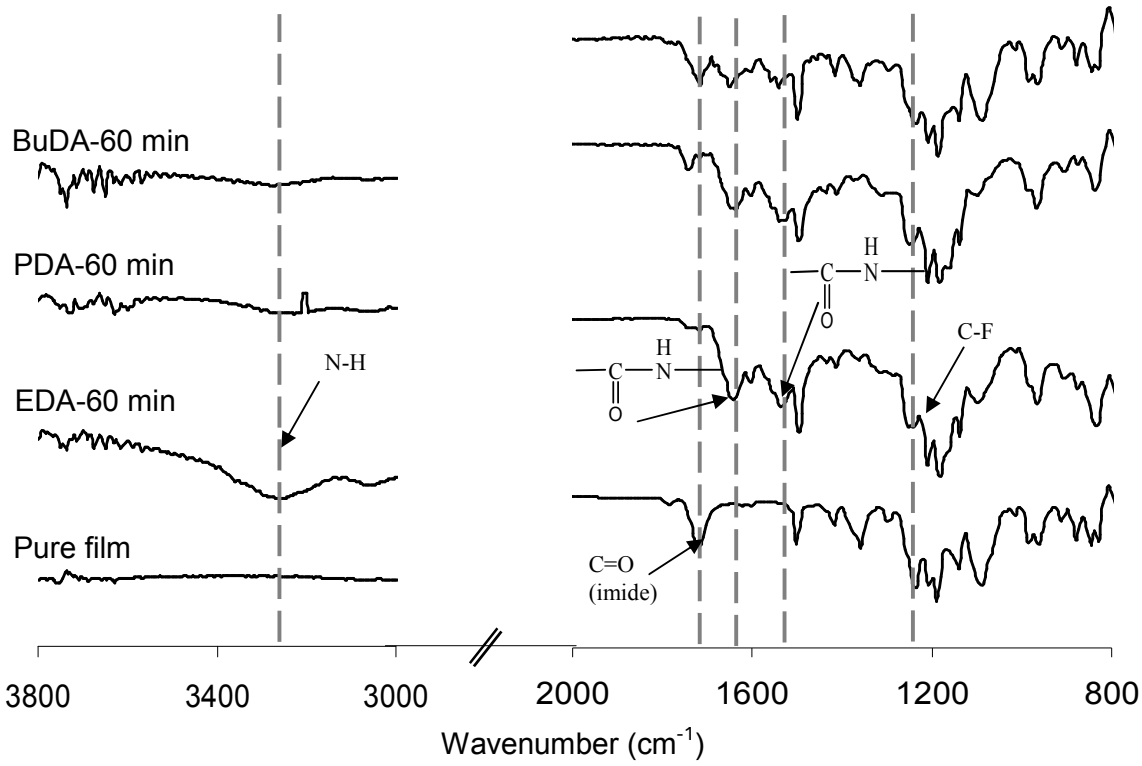

Figure 5.2 FTIR spectra of diamine modified films with immersion time of 60 min

The different diamines react with the polyimide membrane to varying extent. Figure 5.2 shows the FTIR spectra of the unmodified film together with EDA, PDA and BuDA modified films for immersion duration of 60 min. The characteristic peak representing C-F at 1242 cm^{-1} is used as the reference peak since the $C(CF_3)_2$ group is unaffected by the modification. Apparently, for the EDA modified film, the amide peaks at 1648 cm^{-1} and 1540 cm^{-1} are relatively sharper, reflecting the higher concentration of amide groups present. For PDA and BuDA modified films, the characteristic peaks of the amide group

are less intense which implies a smaller degree of conversion from imide to amide groups. The peak representative of the C=O group in the imide ring at 1717 cm^{-1} is almost imperceptible for the EDA modified film but remains visible for BuDA modified film. This shows that EDA modification results in the greatest proportion of amide groups in the amide-imide polymeric network which is due to its highest reactivity.

The diamines in methanol solutions may react with the dense polyimide film in various ways. The initiation step involves the reaction of one of the amine groups constituting the diamine molecule with an imide group. Subsequently, if the other amine group from the same molecule remains free, the diamine is attached to the polymer chain via chemical grafting as shown in Figure 5.3 (a). On the other hand, crosslinking of two polyimide chains via the reaction of each amine group with neighboring imide groups may occur (Figure 5.3 (b)). The reaction between the amine group and the imide ring breaks the ring structure, creating two amide groups. Recall that amide groups are electrophilic by nature and hence are susceptible to nucelophilic attacks. In fact, amide groups readily exchange with amine groups [38]. Since the diamine is in excess, there exists the possibility of reaction between another diamine molecule and the amide group in the main chain, causing scission of the polymeric skeleton (Figure 5.3(c)).

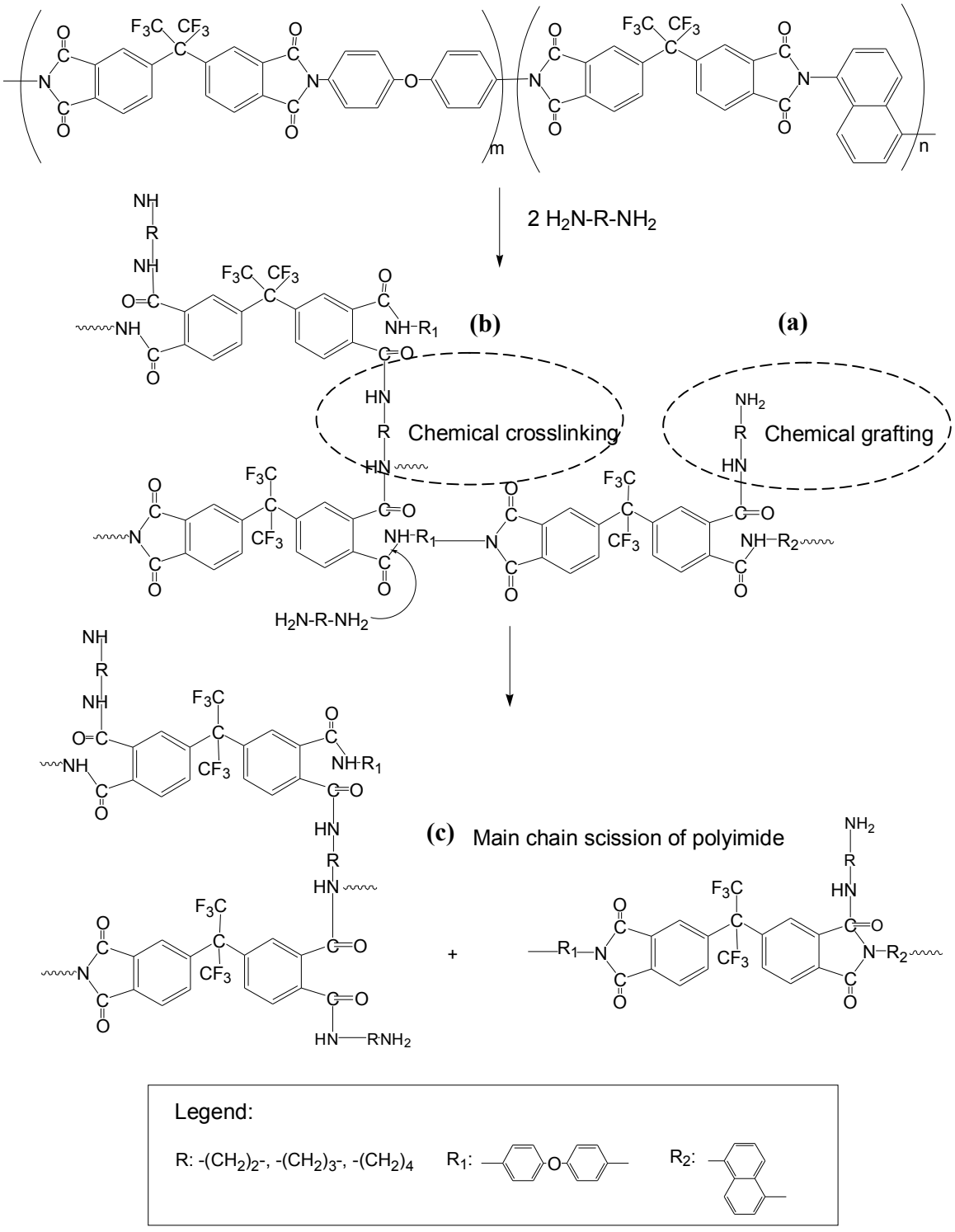

Figure 5.3 Reaction mechanisms between diamines and polyimide

The degrees of chemical grafting and crosslinking by different modification reagents differ. With reference to Figure 5.2, a broad peak at 3250 cm^{-1} that is representative of the N-H bond in amine group is observed only for the EDA modified film which implies the presence of a considerable number of free amine groups. Hence, this suggests that although the high reactivity of EDA results in the significant conversion of imide to amide groups, majority of the conversion is due to grafting instead of crosslinking. The presence of free amine groups on the surface of EDA modified membrane also alters the hydrophobic/hydrophilic nature of the membrane. The contact angle of the original polyimide film is 93^{o} which indicates that the surface is slightly hydrophobic. However, the contact angle of EDA modified film for immersion time of 60 min is 83^{o}. Hence, the modification of the polyimide membrane with EDA increases the hydrophilicity of the surface. The contact angles of PDA and BuDA modified film are 92^{o} and 88^{o}, respectively which are comparable to that of the original polyimide membrane.

A good indication of the extent of chemical crosslinking by the respective modification reagents is provided by the gel content of the modified films. The gel content of EDA, PDA and BuDA modified membranes (immersion time of 60 min) are 15 %, 30 % and 9 %, respectively. PDA modified membrane gave the highest gel content which shows that it the most effective crosslinking agent for this type of 6FDA-polyimide. The results from the gel content analysis reinforce the suggestion that the bulk of the amide groups formed by EDA modification is due to chemical grafting. If majority of the conversion is due to chemical crosslinking, the gel content of EDA modified films should be the highest which is not so. The gel content of BuDA modified film is smaller than EDA modified film.

This is due to the larger molecular dimensions of BuDA molecule which inhibits its penetration into the polymeric matrix. Hence, majority of the chemical modification by BuDA occurs at the surface.

A closer look at the resultant diamine/methanol solutions after reaction supports the existence of polymeric main chain scission. For long immersion times, the resultant solutions (EDA and PDA) turn slightly orange (this is the color of the polyimide). Hence, the resultant solutions after modification were analyzed using UV-Vis spectroscopy. Figures 5.4 (a) to (c) show the UV-Vis spectra of the various modification solutions. The peak intensity and peak area increases with increasing modification time. The trend is obvious for EDA and PDA in methanol solution. However, for BuDA in methanol solutions, the change in the spectra with immersion time is negligible. No peaks are detected in the UV-Vis spectra of the diamine/methanol solutions before modification. This shows that neither the diamines nor methanol absorb radiation in the UV-Vis range. Therefore, the existence of peaks in the spectra of the resultant diamine/methanol solutions after long immersion times is attributed to the presence of polyimide fragments which absorbs in the UV-Vis range.

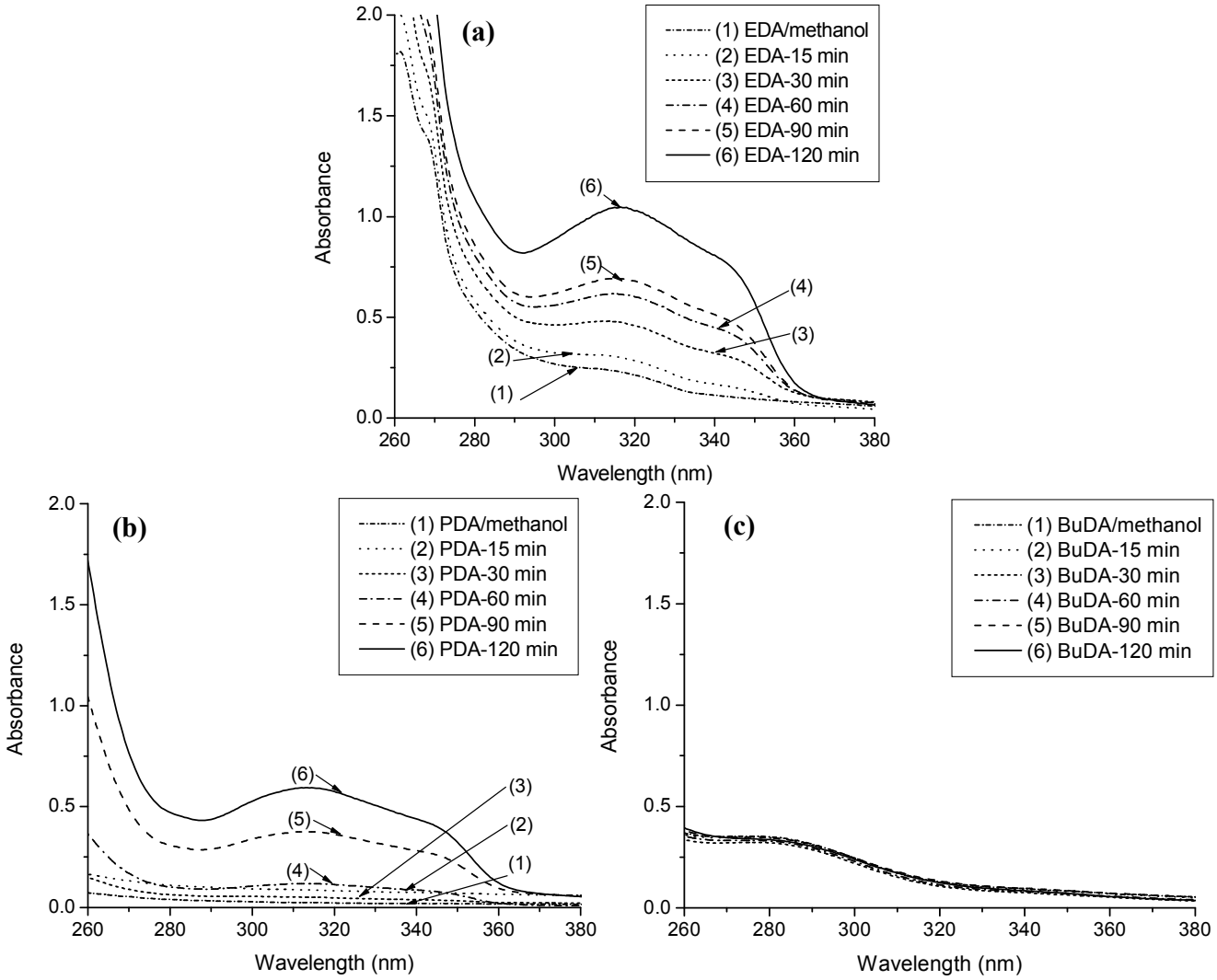

Figure 5.4 UV-Vis spectra of (a) EDA, (b) PDA and (c) BuDA in methanol solutions after modification

To investigate the topology of the modified films, AFM analysis was performed. Figures 5.5 (a) to (c) show the 3-dimensional plots of the surfaces of the diamine modified polyimide films. EDA modified film represented by Figure 5.5 (a) shows a highly rugged terrain while BuDA modified film represented by Figure 5.5 (c) shows an almost smooth surface. This visual evidence further supports the proposed chain scission mechanism which occurs during the chemical modification process. The mean roughness of the EDA, PDA and BuDA modified films are 6.777, 0.831 and 0.783 nm respectively. The degree

of chemical etching by EDA is much more severe than PDA and BuDA, thereby giving rise to a rougher surface. The increased roughness of EDA modified film also intensifies the surface hydrophilicity. The mean roughness of PDA and BuDA modified films are comparable.

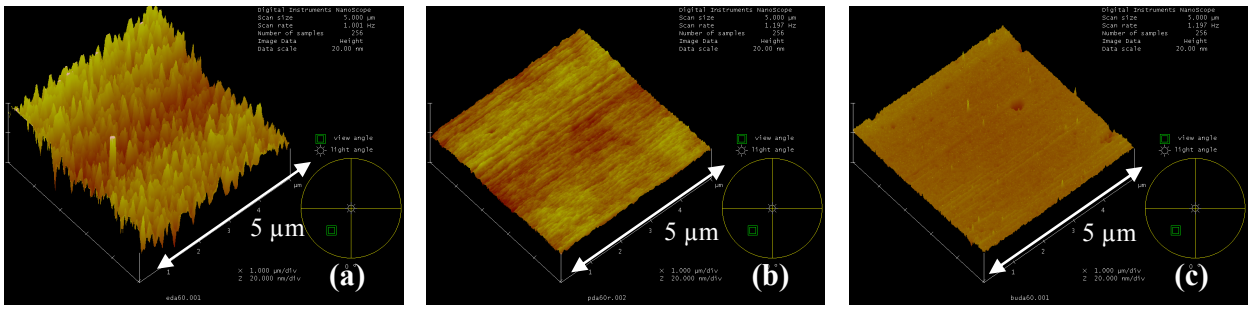

Figure 5.5 AFM images of 6FDA-ODA/NDA dense films modified using (a) EDA, (b) PDA and (c) BuDA for an immersion time of 60 min

The differences in the UV-Vis peak intensities and mean roughness of the membranes using the three diamines can be explained using the nucleophilicities and molecular dimensions of the respective diamines. Molecular simulation using Accelrys Materials Studio® software gives the Fukui function for electrophilic attacks at the active sites (N atoms) of the diamines in methanol [39-40]. Figure 5.6 shows the simulated PDA molecule while Table 5.1 summarizes the results computed by the software. The pK_a values of the diamines are also included in Table 5.1 [41]. A larger pK_a value typically implies greater basicity of the compound which indicates greater reactivity. The pK_a values increase in the order of EDA < PDA < BuDA i.e. BuDA is the most reactive. (Please note that there is a mistake in the pKa trend reported in the published paper, Low et al. Macromolecules 41 (2008) 1297.) Conversely, the computed Fukui function indices increase in the order of BuDA < PDA < EDA i.e. EDA is the most reactive. Hence, the

computed Fukui indices seem to be in contrary to the theoretical pKa values. One possible explanation for this observed deviation is the pKa values are applicable for aqueous medium and largely considers the reactivity of the end amino groups. However, the molecular simulation of the diamines take into account the entire molecule and the Fukui index is computed based on the overall electron density surrounding the diamine. Therefore, the Fukui index is perhaps a better indicator of the diamine nucleophilicity. In the following discussion, EDA is taken to be the most nucleophilic among the studied diamines. EDA has the smallest molecular length of 5.32 Å and hence, it is able to penetrate deeper into the dense polymeric matrix. Both the high nucleophilicity and small molecular dimension of EDA facilitates the reaction, causing more severe main chain scission. The polymeric fragments formed as a result of the chain scission diffuse into the solution, thereby increasing the peak area and intensity. Hence, the peaks obtained from the UV-Vis analysis are the most prominent for EDA/methanol solutions. The greater penetration and reactivity of EDA also account for the considerably larger mean roughness for the EDA modified film.

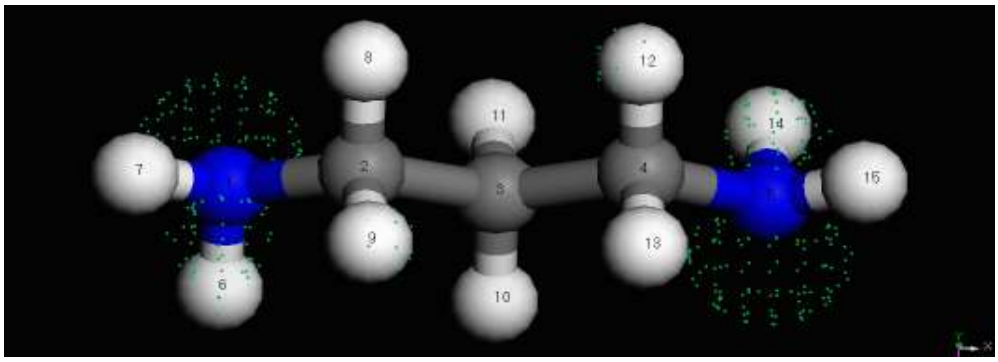

Figure 5.6 Molecular simulation showing the electron density surrounding the nucleophilic sites of a PDA molecule

Table 5.1 Fukui indices, dimensions and pKa values of the aliphatic diamines

Diamine	Length (Å)	Fukui index (based on N atom)		pKa
		Mulliken	Hirshfeld	
EDA	5.32	0.196	0.216	9.92
PDA	6.58	0.184	0.197	10.55
BuDA	7.83	0.180	0.191	10.82

Thermal gravimetric analyses of the polymeric films before and after modification were conducted (results not shown). All the modified films exhibit dual transitions while the unmodified film shows a single transition. The original copolyimide is stable up to 500 ^{o}C whereas the modified films exhibit the onset of degradation at approximately 150-200 ^{o}C. With increasing immersion time, the weight loss of the polymeric films was greater for the same temperature increment. Hence, chemical modification decreases the thermal stability of the polyimide films. In addition, as majority of the H_2/CO_2 mixtures that require separation normally contains H_2O as a contaminant, the thermal stability of the neat polyimide film and the 90 min PDA crosslinked membrane before and after water sorption were determined. The results obtained showed that there is negligible change in the thermal stability of the films after water sorption. Hence, the thermal stability of the modified membranes can be maintained even in the presence of water.

The thermal stability of the chemically modified polyimide films with amino compounds and the reversible reaction between the imide rings and amine groups have been studied in detail by Shao et al. and Powell et al [31,33,42]. Shao et al. proposed the elimination of the diamine molecules upon the reversible formation of the amide groups back to the imide rings after thermal annealing [42]. Powell et al. explored the phenomenon further and suggested that in addition to the elimination of the diamines, main chain scission of

the polymeric backbone also occurs [42]. Gel permeation chromatography was carried out for the unmodified film and the modified film after thermal treatment and a decline in the molecular weight of the latter was reported [42]. The combined ideas from Shao et al. and Powell et al. suggest that main chain scission and release of diamines occur during the thermal treatment of the modified membranes.

However, in our study, we showed that main chain scission occurred during the chemical modification process. This implies that the decrease in polymer molecular weight after thermal treatment may not be fully attributed to main chain scission arising from the heat treatment. Polymeric backbone breakage which occurs during chemical modification too brings about a decline in the molecular weight after the elimination of the diamines. Not all the polymeric fragments formed as a result of chain scission end up in solution after modification since the polymeric chains that form the membrane are twined and tangled to each other. Those fragments in the solution probably have shorter chain lengths and are nearer to the membrane surface, thereby facilitating their diffusion into the solution. Therefore, we propose a modified scheme which suggests that main chain scission occurs with long immersion time and further backbone breakage and the release of diamines occur during thermal treatment.

The mechanical properties of the neat 6FDA-ODA/NDA films and the membranes modified with PDA for 90 min were analyzed. With reference to Table 5.2, the elongation at break of the PDA modified membrane decreases by ~ 15 % as compared to the pure polyimide film. This decrease is possibly due to the existence of weak points within the

membrane resulting from the effect of chemical etching (main chain breakage) caused by the reactive diamines. Similarly, the unmodified and modified membranes were immersed in water before undergoing the mechanical analysis. The results are shown in Table 5.2 and a quick comparison reveals that the extensions at break for the membranes with or without water sorption are comparable. This shows that the mechanical integrity of the diamine modified membranes can be maintained even when employed for aggressive feed streams that contains water as the contaminant.

Table 5.2 Mechanical properties of the films with and without water sorption

Sample	Max tensile stress (MPa)	Extension at break (%)	Tensile stress at break (MPa)	Modulus (GPa)
Without water sorption				
6FDA-ODA/NDA pure film	10.91 ± 0.28	5.73 ± 0.05	10.84 ± 0.28	2.92 ± 0.12
PDA crosslinked for 90 min	11.61 ± 0.05	4.85 ± 1.50	11.56 ± 0.05	3.02 ± 0.06
With water sorption				
6FDA-ODA/NDA pure film	9.03 ± 1.15	5.74 ± 0.88	8.89 ± 1.13	3.11 ± 0.10
PDA crosslinked for 90 min	9.01 ± 0.46	5.07 ± 0.17	8.89 ± 0.62	2.84 ± 0.10

To study the changes in the interstitial space of the polyimide films after chemical modification, XRD analysis was performed. The d-spaces of the unmodified and modified 6FDA-ODA/NDA dense membranes remain in the range 5.77 ± 0.15Å, regardless of the diamines used. This observation is consistent with the work by Ren et al. where 6FDA-ODA/NDA hollow fibers were modified with p-xylylenediamine and negligible change in d-space was observed [26]. In another work by Cao et al., 6FDA-2,6-DAT (2,6-diamino toluene) hollow fibers were crosslinked by aromatic diamines and no

change in d-space was observed after modification [30]. The d-space of the pure 6FDA-2,6-DAT membrane is 5.69 Å [30]. Previous works by Chung and co-workers employing 6FDA-durene as the working polymer for diamines modification showed decline in d-space with increasing immersion time. For instance, the modification of 6FDA-durene with PDA for an immersion time of 10 min changes the d-space from 6.40 Å to 5.86 Å [7].

Considering these three 6FDA-based polyimides, a generalization for the effect of diamino modification on the d-space of these polyimide membranes can be drawn. Referring to Figure 5.7, for polyimide membranes with a smaller d-space (proportional to free volume) to begin with, diamino modification does not bring about chain tightening effects, regardless of the type of diamines used. Since the d-spaces of 6FDA-ODA/NDA and 6FDA-2,6-DAT are comparable and are relatively smaller than 6FDA-durene, both do not exhibit significant changes in d-space after chemical modification. On the other hand, as the original 6FDA-durene has a larger d-space, the diamino modification results in noticeable decline in d-space. Another interesting phenomenon is the similarity in the average d-space of 6FDA-durene after considerable extent of modification with the d-spaces of 6FDA-ODA/NDA and 6FDA-2,6-DAT membranes.

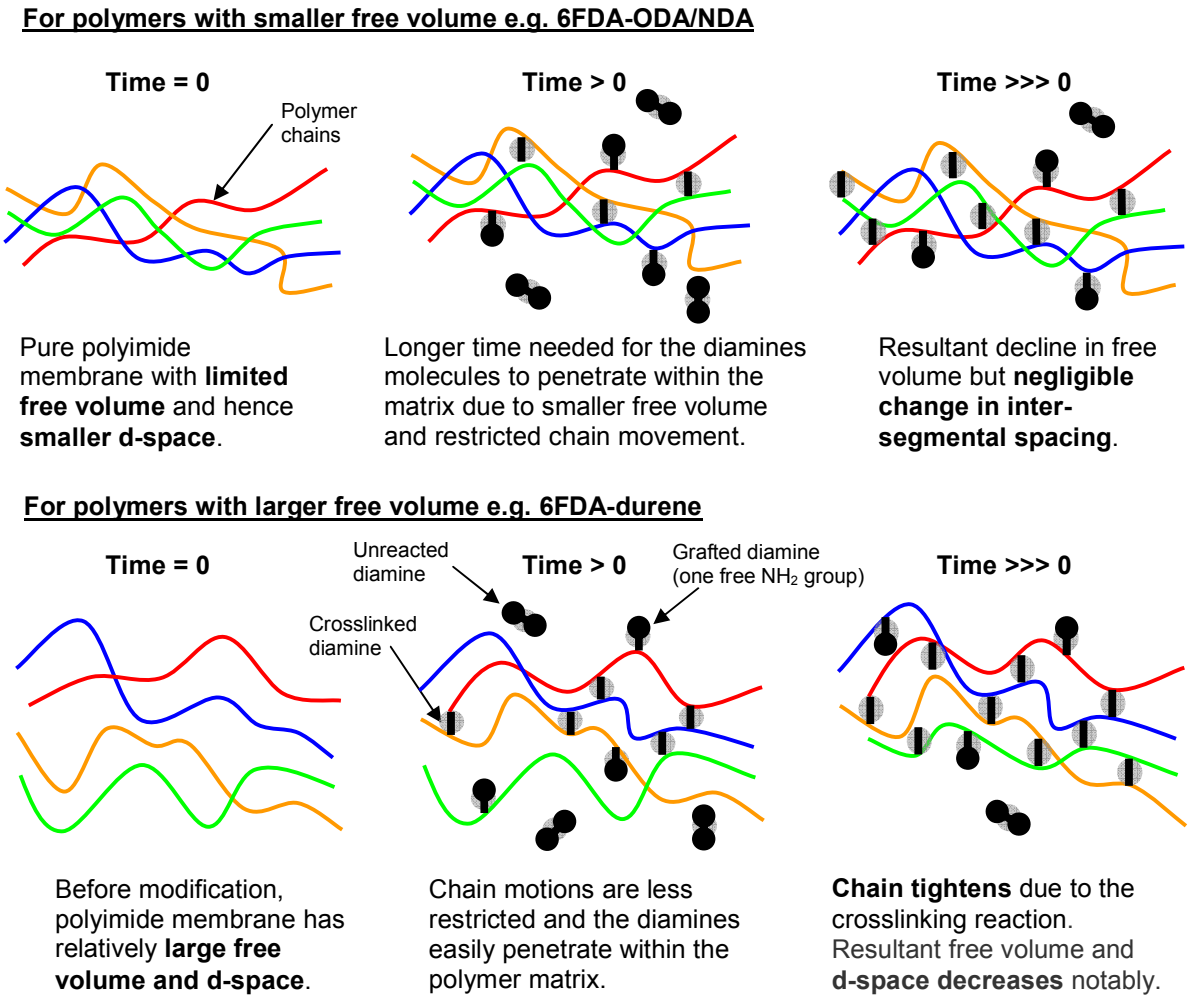

Figure 5.7 Effects of modification on inter-segmental spacing of polyimide films

5.2.2 Gas separation properties of modified copolyimide films

The permeability (P) of a gas through a polymeric membrane is dependent on the diffusivity (D) and solubility (S) of the gas as shown in equation (5-1). Both the gas diffusivity and solubility are in turn dependent on the available free volume present within the polymeric matrix.

$$P = SD \qquad (5\text{-}1)$$

The ideal permselectivity of a membrane for a particular gas pair depends on the interplay between the diffusivity selectivity and the solubility selectivity

$$\alpha_{H2/CO2} = \left(\frac{D_{H2}}{D_{CO2}}\right)\left(\frac{S_{H2}}{S_{CO2}}\right) \quad (5\text{-}2)$$

where D_{H2} and D_{CO2} represent the diffusivity of H_2 and CO_2, respectively; S_{H2} and S_{CO2} are the solubility of H_2 and CO_2, respectively.

Generally, the chemical modification of polyimide membranes with diamines results in three scenarios. Firstly, the crosslinking reaction may tighten the polymeric chains (decrease d-space), thereby resulting in lower free volume. On the other hand, diamine molecules grafted or crosslinked to the polymer chains introduces additional organic moiety to the polymeric matrix which too reduces the available free volume and hence acts as a hindrance for the transport of gas molecules. Lastly, the amide groups formed as a result of the reaction between the imide and amine groups and the unreacted free amine groups affects polymer-polymer and polymer-penetrant interactions.

The gas permeabilities of H_2 and CO_2 through the 6FDA-ODA/NDA films modified using EDA, PDA and BuDA as a function of immersion duration are shown in Table 5.3. The decrease in gas permeability with increasing immersion time is due to the reduction of free volume resulting from the presence of additional diamines moieties since XRD analysis indicates negligible change in d-space after modification. The difference in the reactivity and diffusivity of the diamines within the membrane accounts for the difference in the relative declines in the gas permeabilities. As previously mentioned, EDA being the smallest and most nucleophilic diamine is able to modify (includes both grafting and

crosslinking) the polyimide membrane by the largest extent within a short immersion time. For an immersion duration of 15 min, H_2 permeability decreases by approximately 25% for EDA modified film which is larger than the corresponding decrease for PDA modified film (~10%). For BuDA modified film, H_2 permeability increases by about 5%. This increment is due to the effect of methanol swelling. As BuDA is a larger molecule with lower nucleophilicity, it takes time for the diamine to penetrate and react with the imide group. Hence, at a short modification time of 15 min, the limited degree of crosslinking does not offset the effects of methanol swelling for small gases like H_2.

Table 5.3 Gas permeation properties of pristine and diamine modified 6FDA-ODA/NDA membranes at 35 ^{o}C and 3.5 atm

Samples	Permeability (Barrer)		Selectivity
	H_2	CO_2	H_2/CO_2
6FDA-ODA/NDA pure film	69.78	29.01	2.3
EDA modified for			
15 min	51.50	9.47	5.4
30 min	36.84	2.08	17.7
60 min	26.72	0.98	27.1
90 min	22.70	0.76	29.7
120 min	16.55	0.71	23.4
PDA modified for			
15 min	60.14	9.06	6.6
30 min	36.55	1.58	23.2
60 min	23.34	0.60	39.2
90 min	16.48	0.26	64.1
120 min	13.90	0.23	60.0
BuDA modified for			
15 min	70.74	14.18	5.0
30 min	63.04	13.33	4.7
60 min	55.11	6.24	8.8
90 min	45.82	3.98	11.5
120 min	38.55	1.84	20.9

Barrer = 1×10^{-10} cm^3 (STP)-cm/cm^2 s cmHg = 7.5005 x 10^{-18} $m^2s^{-1}Pa^{-1}$

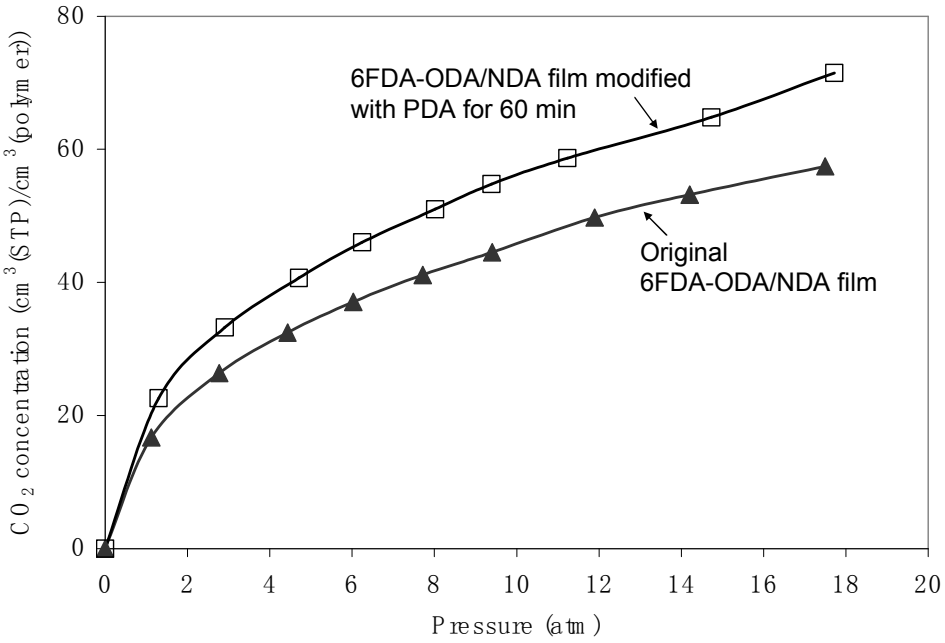

Figure 5.8 CO_2 sorption isotherms of unmodified and modified dense films

The diamino modification of polyimide membranes alters both the diffusivity selectivity and the solubility selectivity. Sorption tests were conducted for the original polyimide membrane and the membrane modified with PDA for immersion duration of 60 min. Figure 5.8 shows the CO_2 sorption isotherms for the unmodified and modified polyimide films. CO_2 sorption increases after PDA modification. The increase in gas sorption may be due to the increase in available sorption sites within the polymer matrix or enhanced polymer-penetrant interactions. Since the diamino modification decreases the available free volume, the increase in gas sorption is hence attributed to the increase in polymer-penetrant interactions. Therefore, PDA modification decreases the solubility selectivity for H_2/CO_2. This in turn implies that the enhancement in diffusivity selectivity after diamino modification more than compensate for the decline in solubility selectivity. Hence, the H_2/CO_2 permselectivity increases after modification.

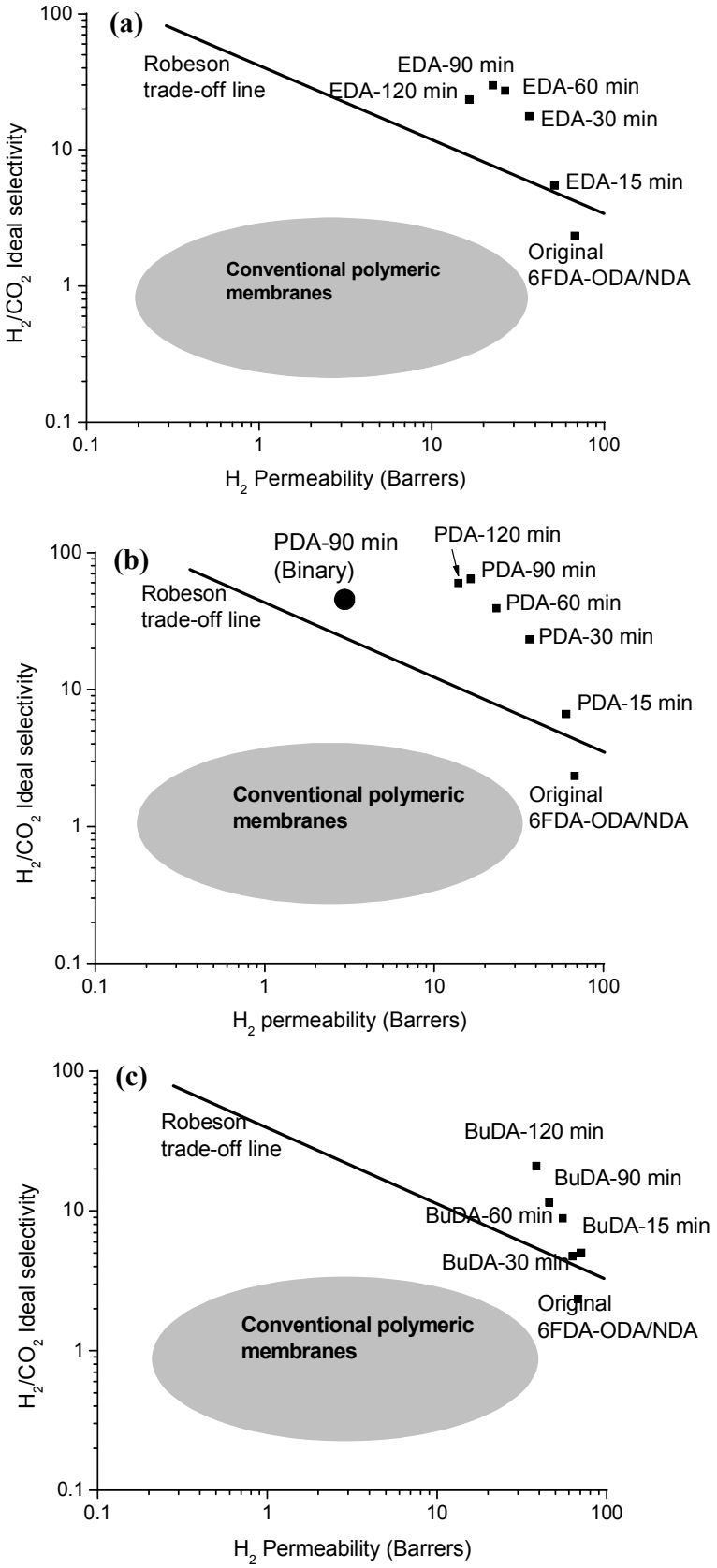

Figure 5.9 H_2/CO_2 separation performance of (a) EDA, (b) PDA and (c) BuDA modified 6FDA-ODA/NDA films compared to the trade-off line

Figure 5.9 shows the gas separation performance of the diamino modified 6FDA-ODA/NDA dense films in comparison to the Robeson trade off line [43]. However, one important point to ponder is that the Robeson upper bound is only valid for homogeneous membranes [43]. Robeson et al. suggested that for laminated films like the diamines modified membranes in this work, the gas separation performance of the modified layer may be in close proximity to the upper limit [43]. Mohr and co-workers investigated the surface fluorination of poly(4-methy-1-pentene) and highlighted the use of a series resistance model to estimate the gas transport properties of the fluorinated layer [44]. This series resistance model can be extended to the diamine modified membranes in our study. Based on a simplified resistance model as depicted in Figure 9.10, the relationships between the modified layer thickness (L_1) and the permeability of the modified layer (P_1) are shown by equations (5-3) to (5-5).

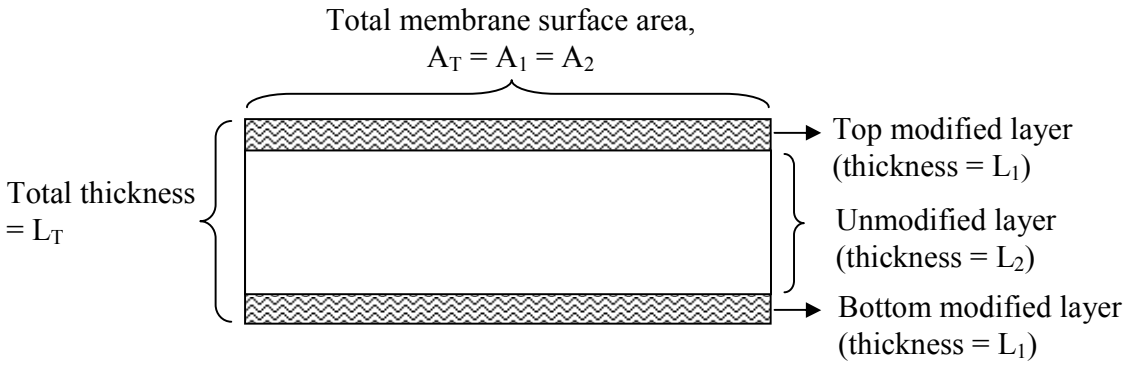

Figure 5.10 Schematic of a diamine modified polyimide film (simplified)

The assumptions made in the development of the simplified model includes (1) homogeneous modified layer, (2) negligible modification of the circular piece of membrane from the radial direction and (3) equal thickness of the top and bottom modified layers.

$$\frac{L_T}{P_T A_T} = \frac{2L_1}{P_1 A_1} + \frac{L_2}{P_2 A_2} \tag{5-3}$$

$$\frac{L_T}{P_T} = \frac{2L_1}{P_1} + \frac{(L_T - 2L_1)}{P_2} \tag{5-4}$$

$$P_1 = \Big/ \left[\frac{L_T}{P_T} - \frac{(L_T - 2L_1)}{P_2} \right] \tag{5-5}$$

P refers to the permeability, L refers to the thickness and A represents the surface area. The subscripts 1 and 2 refer to the modified and unmodified layers, respectively while T represents the total or overall property.

Equation (5-5) cannot be solved explicitly due to the dependence of P_1 and L_1. Therefore, an approximate thickness of the modified layer is required before a rough value of P_1 can be determined. From the dissolution of the one-sided PDA modified (90 min) membranes, the thickness of the dissolved portions can be determined, given the density of the neat polyimide film as 1.4 g./cm^3 (determined from the buoyancy method) and the diameter of the modified film as 1.5 cm. The rough thickness of the dissolved portion subtracted from the initial thickness of the membrane provides an estimate of the thickness of the modified layer. The mean approximate thickness of the modified layer is 4.87±0.67 μm. With this rough value of L_1, the permeabilities of H_2 and CO_2 through the diamine modified layer (determined from equation (5-5)) are 3.37 and 0.043 Barrer, respectively and the corresponding ideal H_2/CO_2 selectivity is 78. When this point is plotted against the Robeson plot, its position still falls above the upper bound as shown in Figure 5.11.

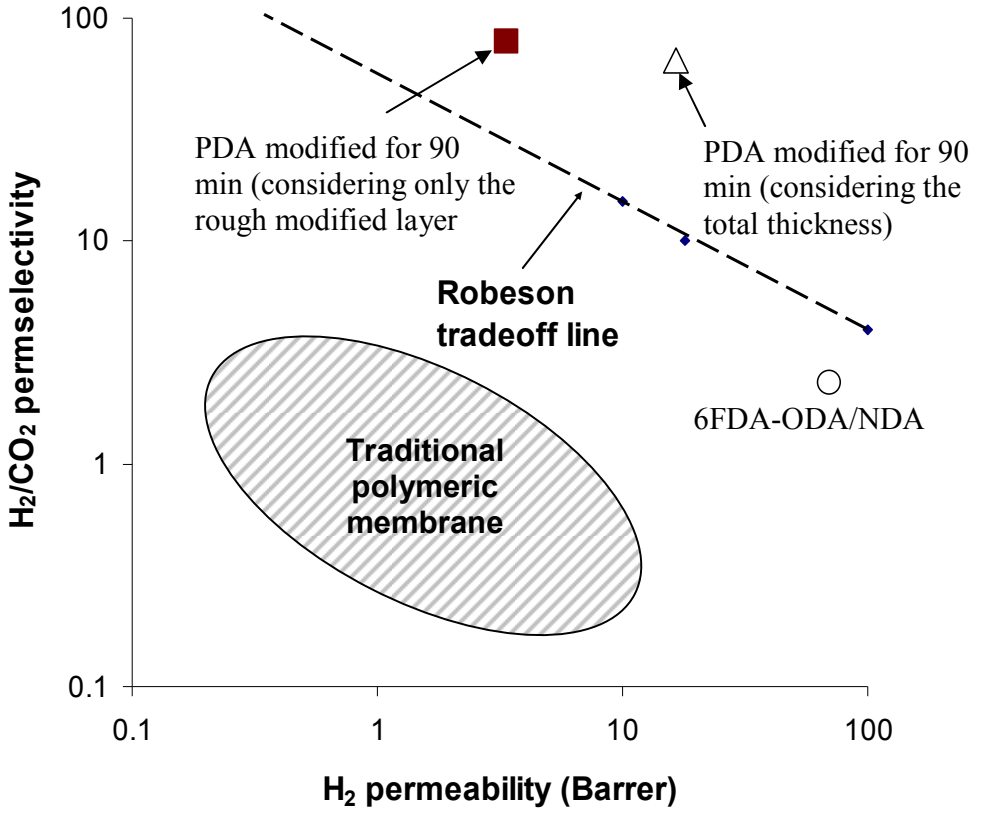

Figure 5.11 Gas separation performance of the 90 min PDA crosslinked membrane

The rough thickness of the modified layer obtained as such may be an underestimate or overestimate of the true value. The immersion of the modified membrane in DMF not only dissolves the unmodified polymeric matrix but also the portions that are grafted by the diamines and the regions which have smaller degree of crosslinking. The grafting of diamines also changes the gas separation performance of the membrane and therefore should be considered in the determination of the modified layer thickness. Hence, the approximate thickness which we have determined may be an underestimate of the true value of the modified layer. If this is the case, the actual position indicating the gas

separation performance of the modified layer alone, probably falls further away from the upper bound. Hence, this provides preliminary justification for the claim that the PDA modified 6FDA-ODA/NDA membranes exhibit better performance than conventional polymers.

On the other hand, the counter-argument is that the diamine modified layer is certainly not homogeneous as assumed in the simplified resistance model. The outermost surface is modified to a larger extent and the degree of modification decreases with increasing membrane depth from the axial direction. This implies the existence of a stratified structure within the diamine modified layer. The highly modified outermost layer may be the determining factor for the enhancement in H_2/CO_2 permselectivity while the remaining modified portions may only exert a marginal effect on the overall gas separation performance. In this case, the rough thickness may be overestimated. Therefore, further studies are required to provide a closer estimate for the true value of the modified layer which significantly contributes to the enhancement in H_2/CO_2 permselectivity. Although the gas separation performance of the modified membranes reported in this work cannot be compared directly with the Robeson trade off line, the results obtained nevertheless suggest the potential use of the diamines modified membranes for H_2 purification.

The ideal H_2/CO_2 permselectivity of 6FDA-ODA/NDA films modified using EDA, PDA and BuDA are shown in Table 5.3. A comparison of the gas separation performance of the three diamines modified films shows that PDA modification brings about greater

enhancement in H_2/CO_2 permselectivity as compared to EDA and BuDA modification. For instance, immersing the dense films in the EDA, PDA and BuDA in methanol solutions for 90 min increases the H_2/CO_2 selectivity by 13, 27 and 5 times, respectively. The polymer intrinsic H_2/CO_2 selectivity is 2.3 and after modifying the original film with PDA for 90 min, an ideal H_2/CO_2 selectivity of 64 was achieved in the present work. The corresponding H_2 permeability was 17 Barrer. In view of the promising result obtained from the pure gas tests, the dense membrane modified with PDA for immersion time of 90 min was used for mixed gas tests. The H_2/CO_2 selectivity obtained from mixed gas tests was 45 and the H_2 permeability was 3 Barrer. The decrease in H_2/CO_2 selectivity and H_2 permeability in mixed gas tests were due to the effects of competitive sorption between the two gases. Nevertheless, the gas separation performance of the PDA modified 6FDA-ODA/NDA dense film (immersion time of 90 min) in a binary system is still encouraging despite the presence of undesirable competitive sorption between H_2 and CO_2.

In order to enhance H_2/CO_2 selectivity, the diamine used for modification has to be able to reduce polymeric chain mobility. The effectiveness of the modification reaction is thus dependent on the nucleophilicities and molecular dimensions of the diamines. BuDA is the least nucleophilic and it has the largest molecular dimensions. Hence, it is harder for BuDA molecules to penetrate within the polymeric matrix which is a pre-requisite for the reaction to take place. Hence, majority of the modification occurs at the surface and an overall smaller percentage of the polymeric matrix is affected. Furthermore, as the length of BuDA molecule is longer, the molecule backbone is more flexible. Hence, the chains

are still mobile to certain extent even after chemical crosslinking. On the other hand, EDA too does not inhibit chain-to-chain movement effectively due to the presence of significant chemical grafting and severe chemical etching. Therefore, both BuDA and EDA are not effective crosslinking reagents for the enhancement of H_2/CO_2 permselectivity of these polyimide dense films.

For the effective modification of polyimide membranes with diamino compounds, the balance between the interplay of chemical crosslinking and chemical etching must be established. Moreover, the diamine needs to have the potential to crosslink neighboring polyimide chains since pure grafting of diamine on the polyimide does not restrict inter-chain movements which are necessary for significant improvement in H_2/CO_2 permselectivity. PDA has the appropriate molecular dimension and reactivity. Therefore, PDA is the most effective reagent for the diamino modification of polyimide membranes to enhance H_2/CO_2 selectivity.

Generally, diamine modification of 6FDA-ODA/NDA films using EDA, PDA and BuDA increases H_2/CO_2 selectivity with increasing immersion duration. However, for EDA and PDA modified films, the H_2/CO_2 selectivity exhibits a peak at an immersion time of 90 min and beyond which, the gas pair selectivity starts to decline (Table 5.3). This trend can be explained from the molecular aspect of the effects of modification on chain packing and rigidity. Recall that the diamino modification of polyimide membranes causes the imide rings to open, forming two amide groups. The destruction of the ring structure in the polymeric main chain decreases the polymeric backbone rigidity [33].

At short immersion time, the inter-chain movements are restricted after crosslinking while the backbone rigidity is maintained since majority of the imide rings are intact, providing the mechanical integrity of the polymeric chains forming the network. However, with long modification time, most of the imide rings have opened, forming the amide groups. As such, although the chain to chain movement is inhibited effectively, the backbone rigidity is greatly reduced. Hence, for long modification duration, the mobility of the polymeric chains increases and this accounts for the decrease in H_2/CO_2 selectivity.

Table 5.4 compares the H_2/CO_2 gas separation performance of 6FDA-durene and 6FDA-ODA/NDA. For 6FDA-durene membranes, relatively shorter immersion times were required and modification with PDA for 10 min gave H_2/CO_2 selectivity of 101 which is 100 times greater than the intrinsic selectivity. However, the H_2 permeability decreases by 60 times. This tradeoff between permeability and selectivity is often a problem encountered by membrane scientists. In the present work, longer immersion times are required before substantial crosslinking effects are experienced. This is because of the smaller free volume of 6FDA-ODA/NDA and the lesser swelling effect by methanol. For 6FDA-ODA/NDA, the highest H_2/CO_2 selectivity achieved was 64 (30 times increment) but the decrease in H_2 permeability is not as drastic as 6FDA-durene. For PDA modified 6FDA-ODA/NDA membranes (immersion time of 90 min), H_2 permeability only decreases by 4 times. The selectivity of 6FDA-ODA/NDA membranes modified with PDA peaks at 90 min and fails to increase with further modification. This is due to the effects of chemical etching from prolonged immersion times. Nonetheless, 6FDA-ODA/NDA modified membrane provides a better compromise between good H_2/CO_2

selectivity and H_2 permeability and also lower material cost as compared to 6FDA-durene.

Table 5.4 H_2/CO_2 separation performance of PDA modified 6FDA-durene and 6FDA-ODA/NDA dense membranes at 35°C and 3.5 atm

6FDA-durene (Chung et al.) [7]*			6FDA-ODA/NDA (current work)		
Modification time (min)	**P_{H_2} (Barrer)**	**α_{H_2/CO_2}**	**Modification time (min)**	**P_{H_2} (Barrer)**	**α_{H_2/CO_2}**
0	600	1	0	68	2.3
1	200	4	30	37	23
5	15	38.5	60	23	39
10	10	101	90	17	64

* Permeability and ideal permselectivity values are approximated from plots

5.3 Conclusions

6FDA-ODA/NDA polyimide dense films were modified successfully, forming a poly(amide-imide) network which was verified by ATR-FTIR analysis. UV-Vis analysis of the resultant modification solutions together with AFM analysis of the topology of the modified films supported the occurrence of chemical etching during the modification process. ATR-FTIR and gel content analysis verified the presence of considerable chemical grafting for EDA modification. Among the three aliphatic diamines, EDA is the most nucleophilic and has the smallest molecular dimensions. Hence, main chain scissions for EDA modified films were more severe. TGA analysis showed a reduction in the thermal stability of the membranes after diamino modification. Based on the XRD results, there was no significant change in the d-spacing. One observation is the diamino modification of polyimide membranes results in chain tightening effects only for polyimides with larger free volume. In general, the diamino modification of 6FDA-

ODA/NDA membranes increases the ideal H_2/CO_2 permselectivity. PDA was identified as the most effective modification reagent for enhancing the H_2/CO_2 permselectivity of 6FDA-ODA/NDA films. An ideal H_2/CO_2 permselectivity of 64 which is 30 times larger than the polymer intrinsic permselectivity was obtained with PDA modification for 90 min and mixed gas tests returned a selectivity of 45. In conclusion, H_2/CO_2 separation performance can be tailored via the appropriate selections of diamine and immersion duration.

5.4 References

[1] N. W. Ockwig, T. M. Nenoff, Membranes for hydrogen separation, Chem. Rev. 107 (2007) 4078.

[2] J. A. Ritter, A. D. Ebner, State-of-the-art adsorption and membrane separation processes for hydrogen production in the chemical and petrochemical industries, Sep. Sci. Technol. 42 (2007) 1123.

[3] J. D. Perry, K. Nagai, W. J. Koros, Polymer membranes for hydrogen separations, MRS Bulletin 31 (2006) 745.

[4] R. Baker, Future directions of membrane gas-separation technology, Membrane Technology 138 (2001) 5.

[5] T. C. Merkel, B. D. Freeman, R. J. Spontak, Z. He, I. Pinnau, P. Meakin, A. J. Hill, Ultrapermeable, reverse-selective nanocomposite membranes, Science 296 (2002) 519.

[6] R. W. Baker, Future Directions of Membrane Gas Separation Technology, Ind. Eng. Chem. Res. 41 (2002) 1393.

[7] T. S. Chung, L. Shao, P. S. Tin, Surface modification of polyimide membranes by diamines for H_2 and CO_2 separation, Macromol. Rapid Commun. 27 (2006) 998.

[8] H. Lin, B. D. Freeman, Materials selection guidelines for membranes that remove CO_2 from gas mixtures, J. Mol. Struct. 739 (2005) 57.

[9] H. Lin, E. Van Wager., J. S. Swinnea, B. D. Freeman, J. S. Pas, A. J. Hill, S. Kalakkunnath, D. S. Kalika, Transport and structural characteristics of crosslinked poly(ethylene oxide) rubbers, J. Membr. Sci. 276 (2006) 145.

[10] R. D. Raharjo, H. Lin, D. F. Sanders, B. D. Freeman, S. Kalakkunnath, D. S. Kalika, Relation between network structure and gas transport in crosslinked poly(propylene glycol diacrylate), J. Membr. Sci. 283 (2006) 253.

[11] H. Lin, E. Van Wager, B. D. Freeman, L. G. Toy, R. P. Gupta, Plasticization-enhanced hydrogen purification using polymeric membranes, Science 311 (2006) 639.

[12] T. C. Merkel, L. G. Toy, Comparison of hydrogen sulfide transport properties in fluorinated and nonfluorinated polymers, Macromolecules 39 (2006) 7591.

[13] L. G. Toy, K. Nagai, B. D. Freeman, I. Pinnau, Z. He, T. Masuda, M. Teraguchi, Y. P. Yampolskii, Pure-gas and vapor permeation and sorption properties of poly [1-phenyl-2-[p-(trimethylsilyl)phenyl]acetylene] (PTMSDPA), Macromolecules 33 (2000) 2516.

[14] A. L. Athayde, R. W. Baker, P. Nguyen, Metal composite membranes for hydrogen separation, J. Membr. Sci. 94 (1994) 299.

[15] P. Mercea, L. Muresan, V. Mecea, Permeation of gases through metallized polymer membranes, J. Membr. Sci. 24 (1985) 297.

[16] D. Fritsch, K.-V. Peinemann, Novel highly permselective 6F-poly(amide-imide)s as membrane host for nano-sized catalysts, J. Membr. Sci. 99 (1995) 29.

[17] J. Compton, D. Thompson, D. Kranbuehl, S. Ohl, O. Gain, L. David, E. Espuche, Hybrid films of polyimide containing in situ generated silver or palladium nanoparticles: Effect of the particle precursor and of the processing conditions on the morphology and the gas permeability, Polymer 47 (2006) 5303.

[18] Y. Dai, M. D. Guiver, G. P. Robertson, Y. S. Kang, Effect of hexafluoro-2-propanol substituents in polymers on gas permeability and fractional free volume, Macromolecules 38 (2005) 9670.

[19] M. D. Guiver, G. P. Robertson, Y. Dai, F. Bilodeau, Y. S. Kang, K. J. Lee, J. Y. Jho, J. O. Won, Structural characterization and gas-transport properties of brominated matrimid polyimide, J. Polym. Sci. Part A Polym. Chem. 40 (2002) 4193.

[20] D. Ayala, A. E. Lozano, J. de Abajo, C. Garćia-Perez, J. G. de la Campaa, K.-V. Peinemann, B. D. Freeman, R. Prabhakar, Gas separation properties of aromatic polyimides, J. Membr. Sci. 215 (2003) 61.

[21] Y. K. Kim, J. M. Lee, H. B. Park, Y. M. Lee, The gas separation properties of carbon molecular sieve membranes derived from polyimides having carboxylic acid groups, J. Membr. Sci. 235 (2004) 139.

[22] Y. L. Kim, H. B. Park, Y. M. Lee, Preparation and characterization of carbon molecular sieve membranes derived from BTDA–ODA polyimide and their gas separation properties, J. Membr. Sci. 255 (2005) 265.

[23] Y. Xiao, Y. Dai, T. S. Chung, M. D. Guiver, Effects of brominating Matrimid polyimide on the physical and gas transport properties of derived carbon membranes, Macromolecules 38 (2005) 10042

[24] Y. Liu, R. Wang, T. S. Chung, Chemical crosslinking modification of polyimide membranes for gas separation, J. Membr. Sci. 189 (2001) 231.

[25] Y. Liu, T. S. Chung, R. Wang, D. F. Li, M. L. Chng, Chemical cross-linking modification of polyimide/poly(ether sulfone) dual-layer hollow fiber membranes for gas separation, Ind. Eng. Chem. Res. 42 (2003) 1190.

[26] J. Ren, R. Wang, T. S. Chung, D. F. Li, Y. Liu, The effects of chemical modifications on morphology and performance of 6FDA-ODA/NDA hollow fiber membranes for CO_2/CH_4 separation, J. Membr. Sci. 222 (2003) 133.

[27] M. R. Coleman, W. J. Koros, The transport properties of polyimide isomers containing hexafluoroisopropylidene in the diamine residue, J. Polym. Sci.: Part B: Polym. Phy. 32 (1994) 1915.

[28] S. A. Stern, Y. Mi, H. Yamamoto, A. K. St. Clair, Structure/permeability relationships of polyimide membranes. Applications to the separation of gas mixture, J. Polym. Sci., Part B: Polym. Phy. 27 (1989) 1887.

[29] M. R. Coleman, W. J. Koros, Conditioning of fluorine-containing polyimides. 2. Effect of conditioning protocol at 8% volume dilation on gas-transport properties, Macromolecules 32 (1999) 3106.

[30] C. Cao, T. S. Chung, Y. Liu, R. Wang, K. P. Pramoda, Chemical cross-linking modification of 6FDA-2,6-DAT hollow fiber membranes for natural gas separation, J. Membr. Sci. 216 (2003) 257.

[31] L. Shao, T. S. Chung, S. H. Goh, K. P. Pramoda, Polyimide modification by a linear aliphatic diamine to enhance transport performance and plasticization resistance, J. Membr. Sci. 256 (2005) 46.

[32] Y. Liu, M. L. Chng, T. S. Chung, R. Wang, Effects of amidation on gas permeation properties of polyimide membranes, J. Membr. Sci. 214 (2003) 83.

[33] L. Shao, T. S. Chung, S. H. Goh, K. P. Pramoda, The effects of 1,3-cyclohexanebis(methylamine) modification on gas transport and plasticization resistance of polyimide membranes, J. Membr. Sci. 267 (2005) 78.

[34] Y. Xiao, T. S. Chung, M. L. Chng, Surface characterization, modification chemistry and separation performance of polyimide and polyamidoamine dendrimer composite films, Langmuir 20 (2004) 8230.

[35] Y. Xiao, L. Shao, T. S. Chung, D. A. Schiraldi, Effects of thermal treatments and dendrimers chemical structures on the properties of highly surface cross-linked polyimide films, Ind. Eng. Chem. Res. 44 (2005) 3059.

[36] T. S. Chung, M. L. Chng, K. P. Pramoda, Y. Xiao, PAMAM dendrimer-induced cross-linking modification of polyimide membranes, Langmuir 20 (2004) 2966.

[37] L. Shao, T. S. Chung, S. H. Goh, K. P. Pramoda, Transport properties of cross-linked polyimide membranes induced by different generations of diaminobutane (DAB) dendrimers, J. Membr. Sci. 238 (2004) 153.

[38] G. O. Shonaike, G. P. Simon, (Ed) *Polymer blends and alloys*; Marcel Dekker: New York, 1999.

[39] W. Yang, W. J. Mortier, The use of global and local molecular parameters for the analysis of the gas-phase basicity of amines, J. Am. Chem. Soc. 108 (1986) 5708.

[40] P. Kolandaivel, G. Praveena, P. Selvarengan, Study of atomic and condensed atomic indices for reactive sites of molecules, J. Chem. Sci. 117 (2005) 591.

[41] D. R. Lide, (Ed.) *CRC handbook of physics and chemistry*; CRC Press: Cleveland, Ohio, 2006.

[42] C. E. Powell, X. J. Duthie, S. E. Kentish, G. G. Qiao, G. W. Stevens, Reversible diamines cross-linking of polyimide membranes, J. Membr. Sci. 291 (2007) 199.

[43] L. M. Robeson, Correlation of separation factor versus permeability for polymeric membranes, J. Membr. Sci. 62 (1991) 165.

[44] J. M. Mohr, D. R. Paul, T. E. Mlsna, R. J. Lagow, Surface fluorination of composite membranes. Part I. Transport properties, J. Membr. Sci. 55 (1991) 131.

CHAPTER 6

INFLUENCE OF POLYIMIMDE INTRINSIC FREE VOLUME AND CHAIN RIGIDITY ON THE EFFECTIVENESS OF DIAMINE MODIFICATION

This chapter is published as a journal paper

Bee Ting Low, Youchang Xiao, Tai Shung Chung, Amplifying the molecular sieving capability of polyimide membranes via coupling of diamine networking and molecular architecture, *Polymer* 50 (2009) 3250-3258.

6.1 Introduction

The hypothetical hydrogen economy is envisioned as the optimal solution for global sustainability, in terms of controlling greenhouse gas emission and reducing worldwide dependence on oil [1-2]. Nevertheless, significant barriers to the extensive use of hydrogen as fuel are inevitably present. In midst of the wide array of challenges pertaining to the future success of the hydrogen economy, hydrogen purification and storage emerged as the overriding concerns [1]. Currently, large scale hydrogen generation is obtained via steam reforming of methane followed by the water-gas shift reaction [1-4]. The product stream leaving this unit operation contains carbon dioxide as the key contaminant. Hydrogen purification to eliminate CO_2 is therefore of paramount importance. Conventional separation processes (e.g. pressure swing adsorption and cryogenic distillation) for hydrogen enrichment are highly capital and energy intensive [1-2]. Conversely, membrane based separation is more energy efficient and environmentally friendly [1-6]. The future promises of the hydrogen economy have stimulated the interest of many researchers to develop high performance membranes for H_2/CO_2 separation.

Polymers are attractive materials for fabricating gas separation membranes because of their processability and affordable costs. Generally, glassy polymers are H_2-selective while rubbery polymers are CO_2-selective [3-4, 7-11]. Each membrane type has its pros and cons, and the ultimate choice of the membrane is largely dependent on the operating conditions and applications. Glassy aromatic polyimides display superior

physicochemical properties desirable for making gas separation membranes and there are numerous active studies on novel polyimides which are specifically engineered to enhance gas transport properties [12-25]. A comprehensive literature survey on engineered polyimides reported in the past two decades is conducted [24-41]. The H_2/CO_2 separation performances of the polyimide membranes are plotted against the Robeson trade off line as depicted in Figure 6.1 [42-43]. Recently, Robeson revisited the upper bounds for various gas pairs including H_2/CO_2 [43]. The minor shift and skew observed in the present H_2/CO_2 upper bound are attributed to the discovery of highly permeable polymers e.g. poly(trimethylsilylpropyne) [43].

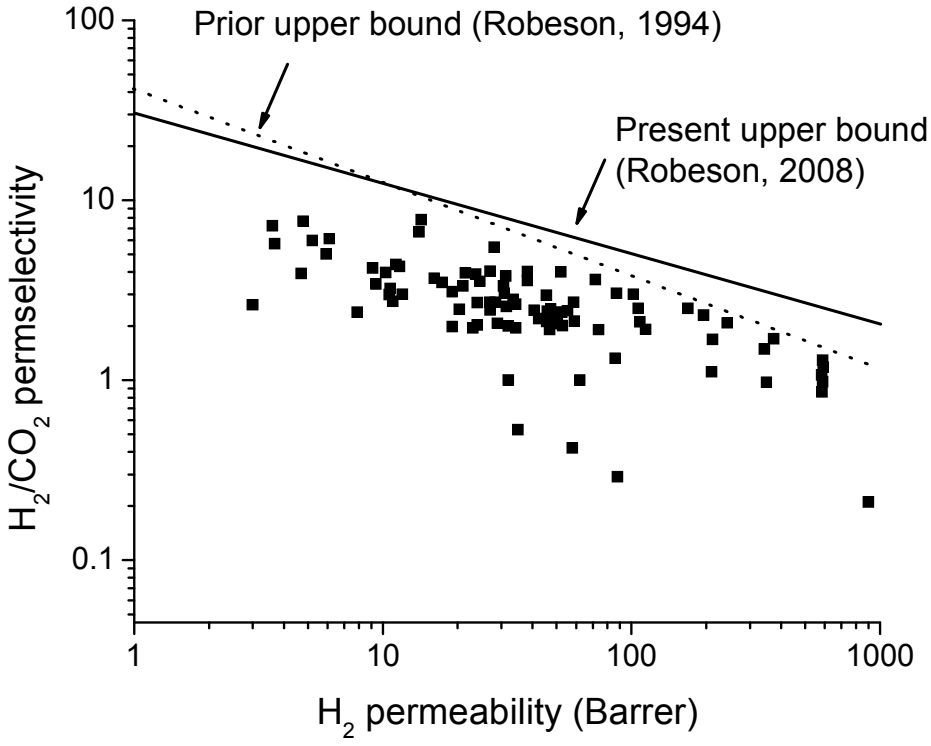

Figure 6.1 Robeson plot of molecularly designed polyimide membranes

Despite the continuous efforts by membrane scientists to explore novel polyimides via the permutations of different diamines and dianhydrides, the H_2/CO_2 separation performances of these materials remain nevertheless inferior. The H_2/CO_2 selectivity of polyimide membranes generally falls in the range of 0.2 – 7.8 [24-41]. Generally, the marginal increment in H_2/CO_2 selectivity obtained from the molecular design of polyimides does not compensate for the marked decline in H_2 permeability. For instance, Liu et al. investigated the gas transport properties of 4,4'-(hexafluoroisopropylidene) diphthalic anhydride (6FDA)-durene/ sulfone-containing diamine (3,3'-DDS) copolyimides and found that increasing 3,3'-DDS content from 25 to 75 mol% improves H_2/CO_2 selectivity from 2.3 to 5.5 but a drastic drop in the corresponding H_2 permeability from 85 to 5 is observed [25]. Similar conclusions can be inferred from other related works, whereby the gain in H_2/CO_2 selectivity at the expense of H_2 permeability is simply not justifiable [24,28-30].

In a nutshell, the molecular architecture of polyimides is ineffective for H_2/CO_2 separation and polyimide membranes display intrinsic H_2/CO_2 permselectivity that are not attractive for commercial applications. Based on the solution-diffusion mechanism for gas transport across dense polymeric membranes, the gas pair (A/B) permselectivity is governed by the diffusivity (D_A/D_B) and solubility (S_A/S_B) selectivities. For the H_2/CO_2 pair, D_{H2}/D_{CO2} is generally greater than unity since H_2 has smaller molecular dimension. On the contrary, S_{H2}/S_{CO2} is smaller than one due to the higher critical temperature and condensability of CO_2. The physical properties of H_2 and CO_2 are listed in Table 6.1 [30]. Another factor that possibly contributes to the high CO_2 solubility in polyimide

membranes is the favorable interactions between quadrupolar CO_2 molecules with the electrophilic imide groups that constitute the polymer. The undesirable coupling of these parameters results in poor intrinsic H_2/CO_2 permselectivity of numerous polyimide membranes.

Table 6.1 Physical properties of H_2 and CO_2

Property	**H_2**	**CO_2**
Kinetic diameter, d_k (Å)	2.98	3.30
Collision diameter, σ_c (Å)	2.92	4.00
Effective diameter, σ_{eff} (Å)	2.90	3.63
Critical temperature, T_c (K)	33.3	304.2
Molecule polarity	Non-polar	Quadrupolar

Since molecular design of novel polymers fails to generate significant breakthroughs for high performance H_2-selective polymeric membranes, alternative approaches including chemical modification, polymer blending, carbonization and organic-inorganic hybrids have been investigated [3, 44-51]. Among these options, the diamine modification of polyimide membranes has been demonstrated to effectively enhance the intrinsic H_2/CO_2 separation performance [3, 44-51]. In a pioneering work by Chung et al., it was found that the modification of 6FDA-durene with aliphatic diamines notably enhances H_2/CO_2 selectivity [3]. For instance, the chemical modification of 6FDA-durene with 1,3-diaminopropane for 5 min brings about a 100 fold increment in H_2/CO_2 selectivity [3]. The applicability of this modification approach on polyimide membranes has been verified in subsequent studies by Shao et al., Low et al. and Aberg et al [44-46]. The improvement in H_2/CO_2 permselectivity is attributed to the fact that the enhancement in D_{H2}/D_{CO2} (i.e. better size sieving effects) more than compensates for the decrease in

S_{H2}/S_{CO2} (i.e. greater CO_2 sorption) after diamine modification [45]. It can be concluded from these works that the effectiveness of diamine modification in enhancing H_2/CO_2 selectivity greatly depends on the (1) electrophilicity and d-space of the polyimides, (2) nucleophilicity and molecular dimensions of the diamines and (3) modification duration [44-46].

A fundamental goal of our current research is to expand the H_2/CO_2 separation performance envelope defined by the permeability-permselectivity trade-off relationship. This study was undertaken to determine the feasibility of integrating molecular design with diamine modification for maximizing the molecular sieving potential of aromatic polyimide membranes. We envisage that this technique can be utilized to fine tune and optimize the enhancement in H_2/CO_2 separation factor achievable via diamine modification. In our previous work, copoly (4,4'-diphenyleneoxide/1,5-naphthalene-2,2'-bis(3,4-dicarboxylphenyl) hexafluoropropane diimide (6FDA-ODA/NDA) films with equimolar composition of ODA to NDA (50:50) were modified with a series of aliphatic diamines with different spacer lengths [45]. It was determined that 1,3-diaminopropane is the most effective modification reagent for this polyimide [45]. The nucleophilicity and molecular dimensions of the diamines were identified as important parameters which influences the effectiveness of the modification [45].The present study aims to elucidate and evaluate the effects of polyimide free volume and rigidity on the effectiveness of diamine modification. To better understand the role of polymer free volume and rigidity in the modification process, a series of 6FDA-ODA/NDA homo- and co- polyimides are employed for systematic investigation. Polyimides based on the same monomers are

utilized to avoid complex interferences between the different functional groups and conformational properties on the gas separation performance. A critical assessment of the pristine and diamine modified co-polyimide membranes for H_2/CO_2 separation via experimental and simulation approaches is presented.

6.2 Results and Discussion

6.2.1 Characterization

The dense membranes before and after PDA modification were studied using ATR-FTIR. The characteristic peak representing C-F at 1242 cm^{-1} is used as the reference peak since the $C(CF_3)_2$ group is unaffected by the modification. With reference to Figure 6.2 (a), the pristine homo- and co- polyimides films exhibit a characteristic doublet at 1725 cm^{-1} and 1794 cm^{-1}, representative of the C=O group constituting the imide ring. The characteristic peak at 1362 cm^{-1} is attributed to the C-N stretch of the imide group while the peak at 1096 cm^{-1} is indicative of the transverse stretch of C–N–C in the imide group. The peak at 718 cm^{-1} is due to the out-of-plane bending of C–N–C in the imide group. The NDA moiety consists of naphthalene group which is clearly distinguishable from the ODA moiety. The weak peak at 1548 cm^{-1} and the doublet at 1605 cm^{-1} and 1629 cm^{-1} results from the C=C stretch of the naphthalene structure [52]. The strong peaks at 783 cm^{-1} and 1420 cm^{-1} are due to the disubstituted naphthalene structure and the out-of-plane vibrations of the three adjacent H atoms, respectively [52]. The various peaks in the region 1400-1000 cm^{-1} (including the strong peak at 1166 cm^{-1}) are representative of

naphthalenes [52]. The characteristic peaks of ODA moiety includes 830 cm^{-1} and 1019 cm^{-1}, indicative of the out-of-plane deformation vibration of neighboring H atoms and 1,4-disubstituted benzenes, respectively [52].

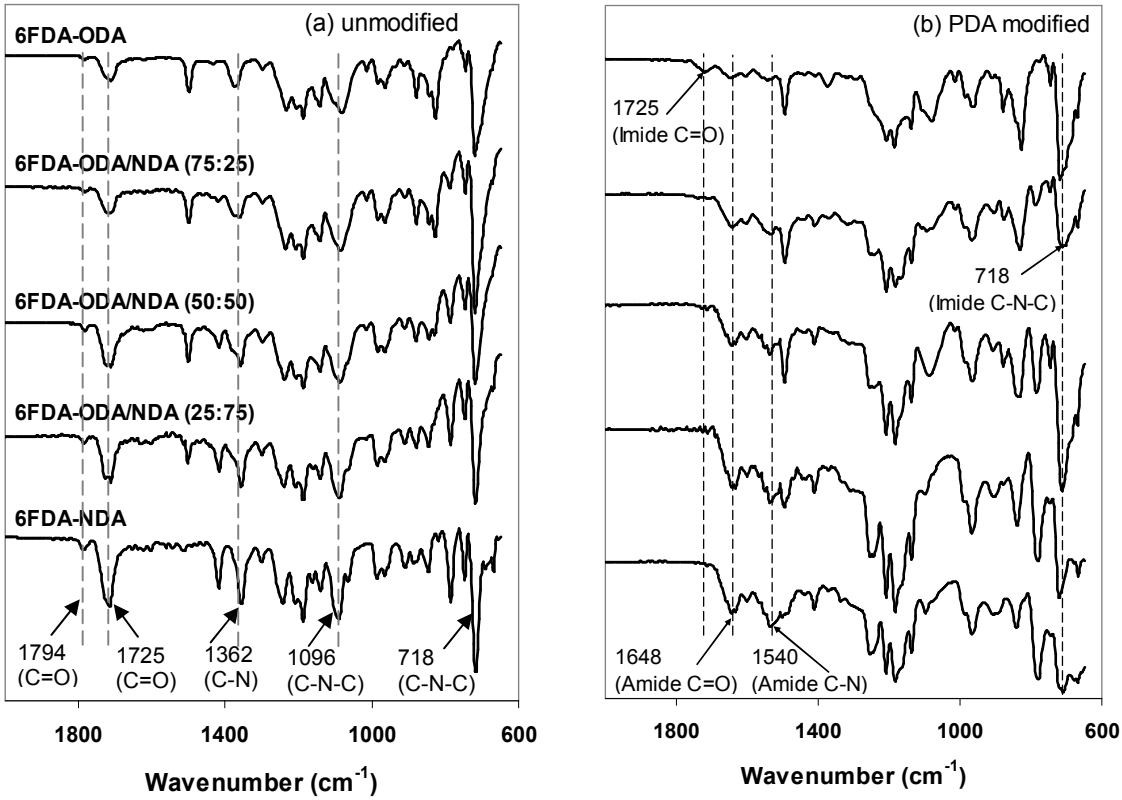

Figure 6.2 FTIR spectra of (a) unmodified and (b) PDA-modified 6FDA-ODA/NDA dense membranes

Upon modifying the polymeric films with PDA, distinct peaks representative of the amide groups are clearly visible. Referring to Figure 6.2 (b), the characteristic peaks at 1648 cm^{-1} and 1540 cm^{-1} are attributed to C=O stretch and C-N stretch of the amide group, respectively. One observation is that the peaks representative of the amide groups are more prominent as the molar composition of NDA increases. The peaks representative of the imide groups are still present in 6FDA-ODA after PDA modification. These provide

evidence that there is greater conversion from imide to amide groups for 6FDA-NDA homopolymer and copolymer with greater percentage of NDA moiety.

The elemental composition of the polyimide film surface was analyzed using XPS. The results are shown in Table 6.2. The N_{1s}/F_{1s} ratios of the synthesized polyimides are in the range 0.32 to 0.35. The theoretical N_{1s}/F_{1s} ratio for 6FDA-based polyimide is 0.33. After PDA modification, the N_{1s}/F_{1s} ratio increases with the molar composition of NDA which implies that a greater degree of amidation occurred for polyimides with higher NDA content. The higher nitrogen content after diamine modification is attributed to the following: (1) chemical grafting, (2) crosslinking and (3) presence of trace amounts of residual PDA molecules. This shows that the different diamine compositions of polyimide membranes affect the extent of modification.

Table 6.2 Elemental composition of polyimide membrane surface before and after PDA modification determined by XPS

Polymer	No modification			90 min PDA modification		
	N_{1s}	F_{1s}	N_{1s}/F_{1s}	N_{1s}	F_{1s}	N_{1s}/F_{1s}
6FDA-ODA	3.68	11.09	0.33	7.06	7.98	0.88
6FDA-ODA/NDA (75/25)	3.70	11.45	0.32	8.31	8.94	0.93
6FDA-ODA/NDA (50/50)	2.78	8.80	0.32	8.00	7.77	1.03
6FDA-ODA/NDA (25/75)	3.79	11.76	0.32	8.64	7.75	1.12
6FDA-NDA	4.42	12.78	0.35	9.20	7.91	1.16

The PDA modified films were analyzed for the gel content and the results are presented in Table 6.3. The gel content of the PDA modified film is an indication of the extent of crosslinking. The gel content increases as the molar composition of NDA in the polyimide increases. Thus, 6FDA-NDA exhibits the greatest degree of crosslinking.

Table 6.3 Gel content of PDA modified polyimide films

Polymer	Gel content (wt %)
6FDA-ODA	10 ± 2
6FDA-ODA/NDA (75:25)	14 ± 2
6FDA-ODA/NDA (50:50)	26 ± 4
6FDA-ODA/NDA (25:75)	43 ± 4
6FDA-NDA	55 ± 3

An attempt to estimate the penetration depth of the PDA molecules from the film surface to the polymer bulk was performed. In our previous work, the estimation was achieved by means of the gel content analysis and a simplified resistance model proposed by Mohr et al [45,53]. Figure 6.3 shows a schematic of the simplified resistance model. The resistance model is established based on the following assumptions: (1) homogenous modified layer, (2) negligible modification from the radial direction and (3) equal thickness of the top and bottom modified layers [45].

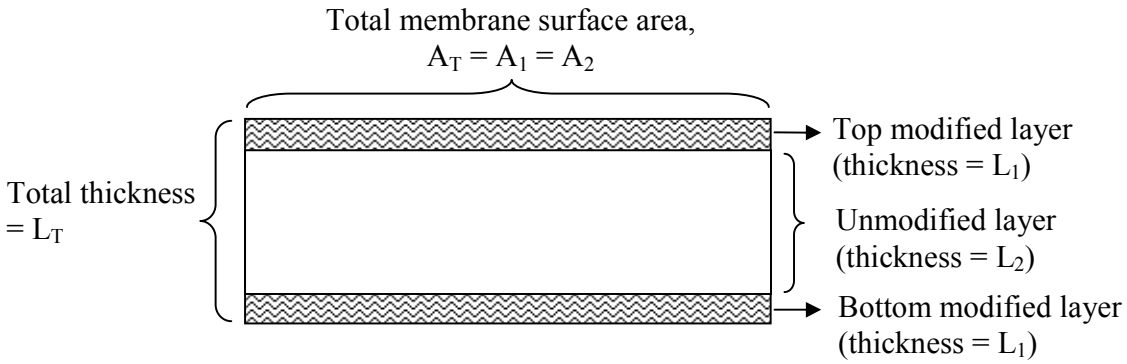

Figure 6.3 Simplified resistance model for the PDA modified film [45]

Here, the same approach was employed and the penetration depth of the PDA molecules is taken as the thickness of the top (or bottom) modified layer [45]. The estimated penetration depths are presented in Table 6.4. The penetration depth of the diamine molecules increases with the molar composition of NDA i.e. polyimide free volume.

Table 6.4 Extent of PDA penetration during the modification of polyimide films

Sample	Estimated penetration depth (μm)
6FDA-ODA	1.2 ± 0.4
6FDA-ODA/NDA (75:25)	3.5 ± 0.3
6FDA-ODA/NDA (50:50)	4.8 ± 0.8
6FDA-ODA/NDA (25:75)	11.4 ± 0.4
6FDA-NDA	14.7 ± 0.2

To determine the inter-chain spacing of the polyimide films, XRD analysis was conducted and the spectra obtained for the unmodified and modified films are shown in Figure 6.4 (a) and (b), respectively. The average d-space for 6FDA-NDA (5.73 Å) is the highest while the d-space for 6FDA-ODA (5.23 Å) is the smallest. Increasing the molar composition of NDA in the copolyimide results in larger chain-to-chain spacing since the introduction of the rigid NDA moiety disrupts the packing of the polymer chains. Hence, the free volume of the polymer increases with NDA content. For 6FDA-ODA polymer, there is a peak at $2\theta = 21.4^{o}$ which is indicative of the semi-crystalline nature of 6FDA-ODA [26]. No significant difference in the average d-space of the polyimide membranes before and after PDA modification was observed from XRD analysis.

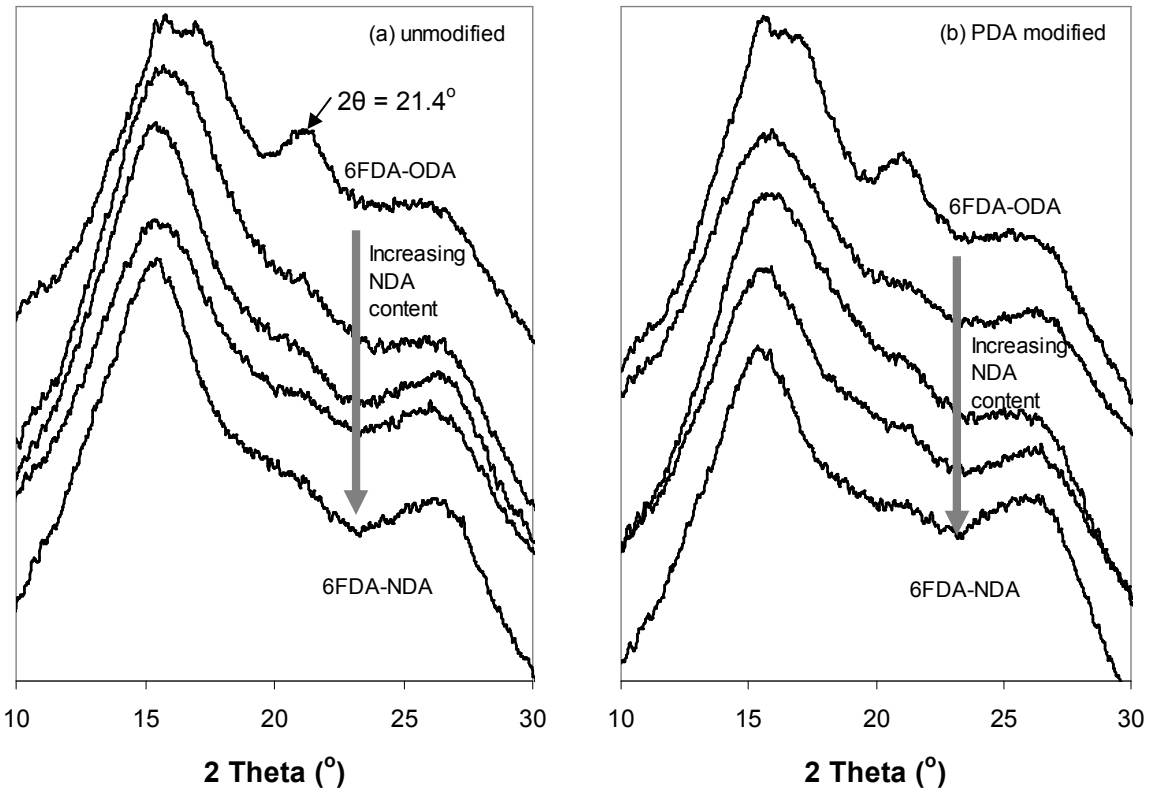

Figure 6.4 WAXD spectra of (a) unmodified and (b) PDA-modified 6FDA-ODA/NDA films

The moduli of 6FDA-ODA and 6FDA-NDA films before and after PDA modification were tested using nanoindentation and the results are summarized in Table 6.5. The modulus of 6FDA-NDA is approximately 50% greater than 6FDA-ODA. This outcome was within our expectation since the modulus of a material is related to its stiffness. The building blocks of 6FDA-NDA consist of highly rigid naphthalene structure while 6FDA-ODA comprises of flexible phenyl-O-phenyl linkages. For 6FDA-NDA, PDA modification for 90 min results in a 20% increment in modulus while for 6FDA-ODA, the changes in modulus after modification is negligible.

Table 6.5 Mechanical properties of pristine and PDA-modified homopolyimides

Polymer	6FDA-ODA		6FDA-NDA	
	Pristine	PDA modified	Pristine	PDA modified
Modulus (GPa)	3.34 ± 0.16	3.53 ± 0.12	5.13 ± 0.25	6.19 ± 0.23

6.2.2 Molecular simulation

To mimic the packing of polyimide chains in dense membranes, amorphous cells packed with the respective polymers were simulated. The amorphous cell for 6FDA-NDA is depicted in Figure 6.5. The Connolly algorithm was employed to determine the occupied and free volume within the amorphous cells [53]. Using these values, the fractional free volume (FFV) of the polyimide can be obtained from molecular simulation. The fractional free volume (FFV) of the 6FDA-based homo- and co- polyimides are summarized in Table 6.6. Referring to Table 6.6, increasing the NDA composition increases the FFV of the polymer. The packing density of the rigid 6FDA-NDA homopolyimide is the lowest, resulting in relatively more open and accessible cavities within the polymeric matrix. The reverse is true for the 6FDA-ODA polyimide. Two Connolly radii, each corresponding to the kinetic diameters of H_2 and CO_2 respectively, were used for estimating the polymer FFV. It has been highlighted in a work by Park and Paul that the polymer FFV is dependent on the nature of the gas penetrants and the universal applicability of the conventional group contribution approach for calculating the FFV is questioned [55]. Our simulated FFV results similarly suggest the dependence of the polymer free volume on the size of gas penetrants.

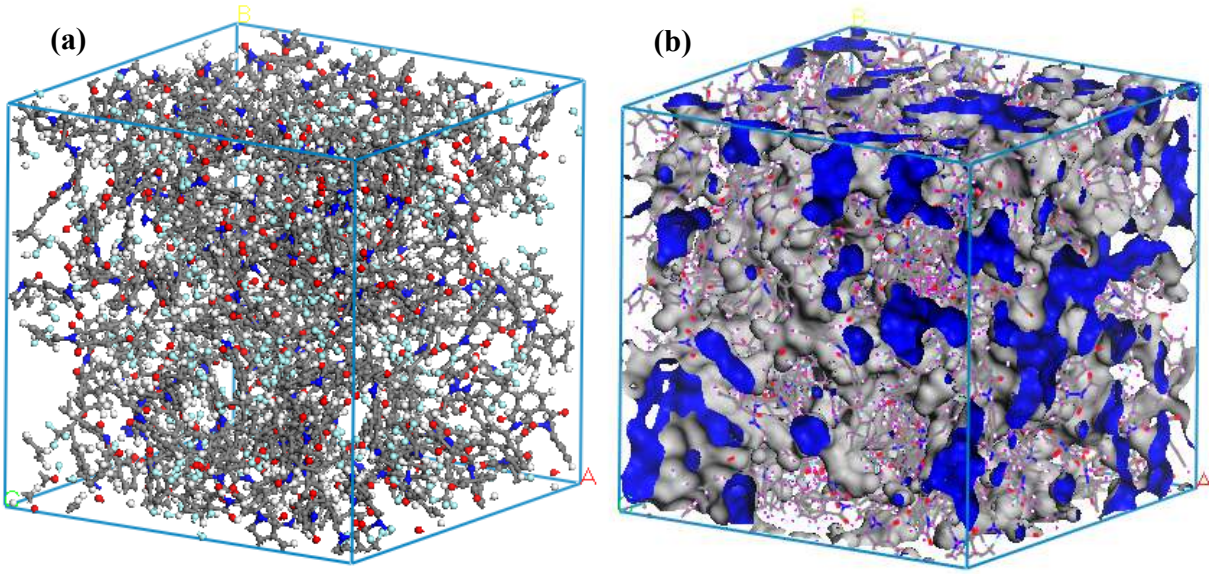

Figure 6.5 (a) Simulated amorphous cell containing 6FDA-NDA homopolyimide chains and (b) Occupied and free volume of the amorphous cell (grey: Van der Waals surface; blue: Connolly surface with probe radius of 1.49 Å)

Table 6.6 Simulated FFV of copolyimides

Properties	Molar ratio of ODA to NDA				
	100:0	**75:25**	**50:50**	**25:75**	**0:100**
FFV (H_2)[a]	0.1820	0.2069	0.2078	0.2169	0.2241
FFV (CO_2)[b]	0.1618	0.1870	0.1889	0.1977	0.2063

[a] Simulated FFV based on a Connolly radius of 1.49 Å.
[b] Simulated FFV based on a Connolly radius of 1.65 Å.

To investigate the underlying motion of the molecules, the mean square displacements (MSD) of the polymeric chains within the amorphous cell were obtained from molecular dynamics simulation. The polymeric chains in a solid matrix are in continuous motion and the MSD of a polymer is an important dynamic property that reflects the mobility of polymer chains. By using the MSD instead of the displacement of the polymeric chain, a scalar quantity is utilized instead of a vector, which better illustrates the overall mobility of the macromolecules. With reference to Figure 6.6, 6FDA-ODA exhibits the greatest

MSD while 6FDA-NDA shows the smallest MSD. Increasing the NDA composition increases the chain rigidity which in turn decreases the MSD of the polyimide chains.

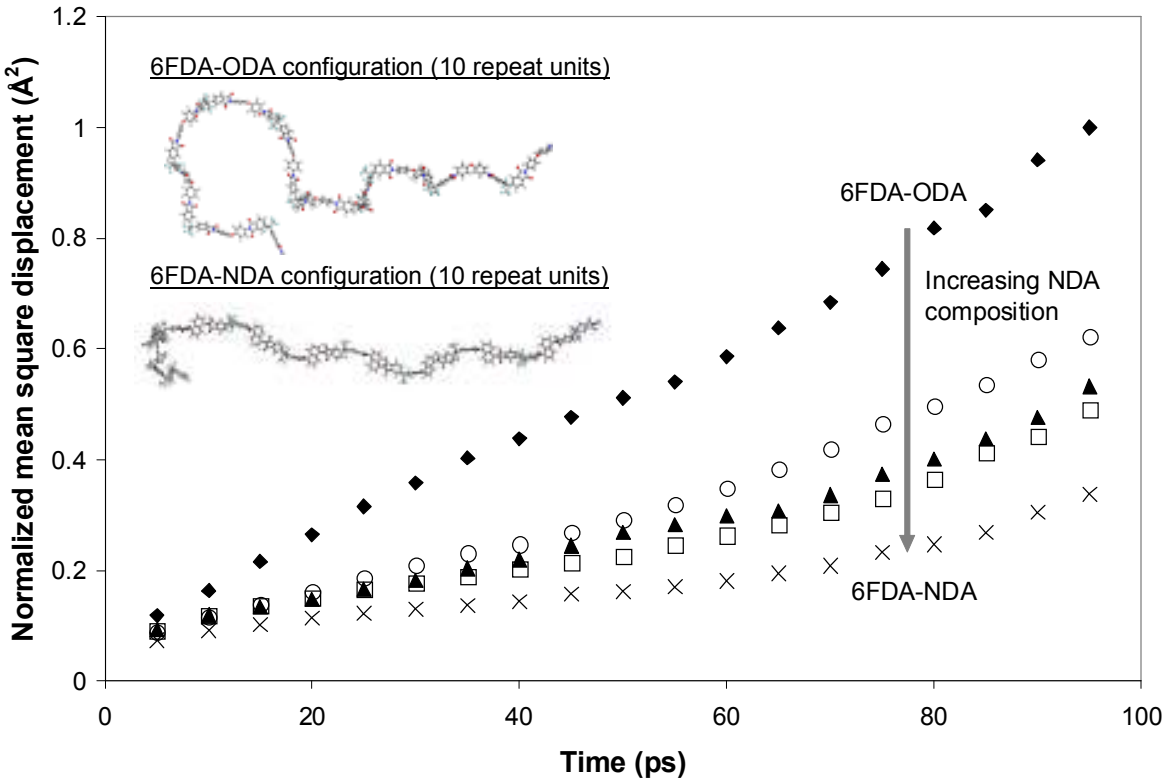

Figure 6.6. Simulated mean square displacements of 6FDA-ODA/NDA copolyimide series

6.2.3 Gas transport properties

The H_2 and CO_2 permeability coefficients for the 6FDA-ODA/NDA polyimides are shown in Table 6.7. The intrinsic gas permeability of this copolyimide series is coherent with the FFV of the polymers. A higher molar composition of NDA results in a greater FFV value and the corresponding gas permeability is higher. 6FDA-ODA exhibits the lowest gas permeability which is attributed both to its lower FFV and semi-crystalline

structure. With reference to Table 6.7, it is obvious that the molecular design of this copolyimide series does not lead to significant changes in H_2/CO_2 selectivity. This conclusion is similar to those derived from previous works on polyimide designs [24-41]. Among these polyimides, 6FDA-NDA with the largest free volume results in the lowest intrinsic H_2/CO_2 selectivity while 6FDA-ODA with the lowest free volume results in marginally higher H_2/CO_2 selectivity.

Table 6.7. H_2 and CO_2 transport properties of pristine and PDA-modified copolyimide films

Polymer	No modification			PDA-modified for 90 min		
	Permeability (Barrer)		H_2/CO_2 selectivity	Permeability (Barrer)		H_2/CO_2 selectivity
	H_2	CO_2		H_2	CO_2	
6FDA-ODA	27	11	2.5	23	2.8	8.2
6FDA-ODA/NDA (75/25)	49	21	2.3	22	0.73	30
6FDA-ODA/NDA (50/50)	68	29	2.3	16	0.26	62
6FDA-ODA/NDA (25/75)	74	34	2.2	9.1	0.098	93
6FDA-NDA	78	43	1.8	12	0.10	120

Barrer = 1×10^{-10} cm^3 (STP)-cm/cm^2 s cmHg = 7.5005 x 10^{-18} $m^2s^{-1}Pa^{-1}$

Upon modifying the copolyimide membranes with PDA/methanol solution, significant changes in the H_2/CO_2 selectivity are observed. With reference to Table 6.7, 6FDA-NDA exhibits the greatest enhancement in H_2/CO_2 selectivity from an intrinsic value of 1.8 to an impressive separation factor of 120. The results obtained from our present work once again support the viability of the diamine modification for improving H_2/CO_2 selectivity of polyimide membranes. It can be seen clearly from the results that increasing NDA composition leads to greater improvement in H_2/CO_2 selectivity when the same diamine modification conditions (1.65 M PDA in methanol, modification duration of 90 min) were employed. 6FDA-ODA shows the least increment in H_2/CO_2 selectivity from 2.5 to 8.2. It

is interesting to see that the ideal H_2/CO_2 selectivity trend is reversed after diamine modification. Polyimide with a higher intrinsic free volume leads to a greater decline in gas permeability after modification.

During the diamine modification process, the swelling of the polymer matrix by methanol occurs simultaneously with the chemical reactions taking place. This methanol swelling effect facilitates the transport of PDA molecules which in turn influences the extent of diamine modification. To investigate the different degrees of methanol swelling for the different polyimide films, the gas transport properties of the films after immersion in methanol are tested and presented in Table 6.8. The % increment in gas permeability after methanol swelling is higher for the polyimide with a greater NDA content. This implies that the degree of methanol swelling is greater for polyimides with higher NDA content. Methanol swelling is dependent on the intrinsic free volume and chain rigidity i.e. polymers with high free volume and chain flexibility are more easily swelled. From the results shown in Table 6.8, it is evident that the polymer free volume is the dominating factor for methanol swelling. The incorporation of NDA moiety in the polyimide leads to significant increment in free volume and amplifies the effects of methanol swelling. The presence of NDA moiety that increases the polymer chain rigidity fails to suppress the extent of methanol swelling. It can be inferred that the polymer free volume influences the degree of methanol swelling more than the polymer chain rigidity. Polyimide with a higher free volume enhances methanol swelling which in turn facilitates the diffusion and reaction of diamine molecules within the polymeric matrix, giving rise to larger extent of modification. The greater degree of diamine-modified network with increasing NDA

composition is proven by the higher N/F ratio from XPS analysis, the higher gel content and the prominent amide peaks shown by FTIR characterization. The space filling effects of the diamines within the polymeric matrix decrease the available pathways for gas transport and enhance the diffusivity selectivity of H_2/CO_2 gas pair [45].

Table 6.8 H_2 and CO_2 transport properties of methanol-swelled polyimide films

Sample	H_2 permeability (Barrer)		% increase	CO_2 permeability (Barrer)		% increase
	Pristine	Methanol immersion		Pristine	Methanol immersion	
6FDA-ODA	27	34	26	11	14	27
6FDA-ODA/NDA (75:25)	49	64	31	21	31	48
6FDA-ODA/NDA (50:50)	68	98	44	29	51	76
6FDA-ODA/NDA (25:75)	74	152	105	34	95	179
6FDA-NDA	78	244	213	43	182	323

Another possible factor that influences the effectiveness of diamine modification for enhancing the H_2/CO_2 selectivity of polyimide membranes is the polymer rigidity. Polymer rigidity is related to the chain stiffness and side group bulkiness. Generally, increasing the rigidity of the polymer chains leads to better H_2/CO_2 selectivity. The copolyimides employed in our work differ in the diamine moiety and the polymer rigidity is dependent on the chain stiffness rather than the side group bulkiness. The naphthalene structure in NDA moiety gives rise to higher chain stiffness while the -O- connector linking the phenyl rings in ODA moiety results in greater flexibility. The MSD of the polyimide (Figure 6.6) can be used to reflect the polymer rigidity i.e. rigid polymer

exhibits lower MSD. Hence, based on the molecular simulation results, it can be inferred that increasing the molar composition of NDA increases the rigidity of the polyimides.

When the polyimides are chemically modified with PDA, there are two intervening factors affecting the rigidity of the diamine-modified polymer. The first factor is due to the breakage of the imide rings which lowers chain stiffness. The attachment of the PDA moiety on the polyimide chain via the reaction of one NH_2 group with the imide ring is similar to the presence of a bulky side appendage on the polymer chain. This increases the rigidity of the modified polymer. To explore the effects of PDA modification on the polymer rigidity, molecular simulation was performed using 6FDA-NDA and 6FDA-ODA as the model polyimides. The mean square displacements of the polyimide chains before and after PDA crosslinking were determined. With reference to Figure 6.7, the MSD of 6FDA-NDA chains decreases after PDA crosslinking. Hence, the rigidity of 6FDA-NDA increases after PDA crosslinking. The 20% increment in elastic modulus of 6FDA-NDA film after PDA modification (Table 6.5) similarly reflects the greater chain stiffness of the resultant polyimide matrix. This result is within our expectation since diamine crosslinking typically inhibits polymeric chain movements.

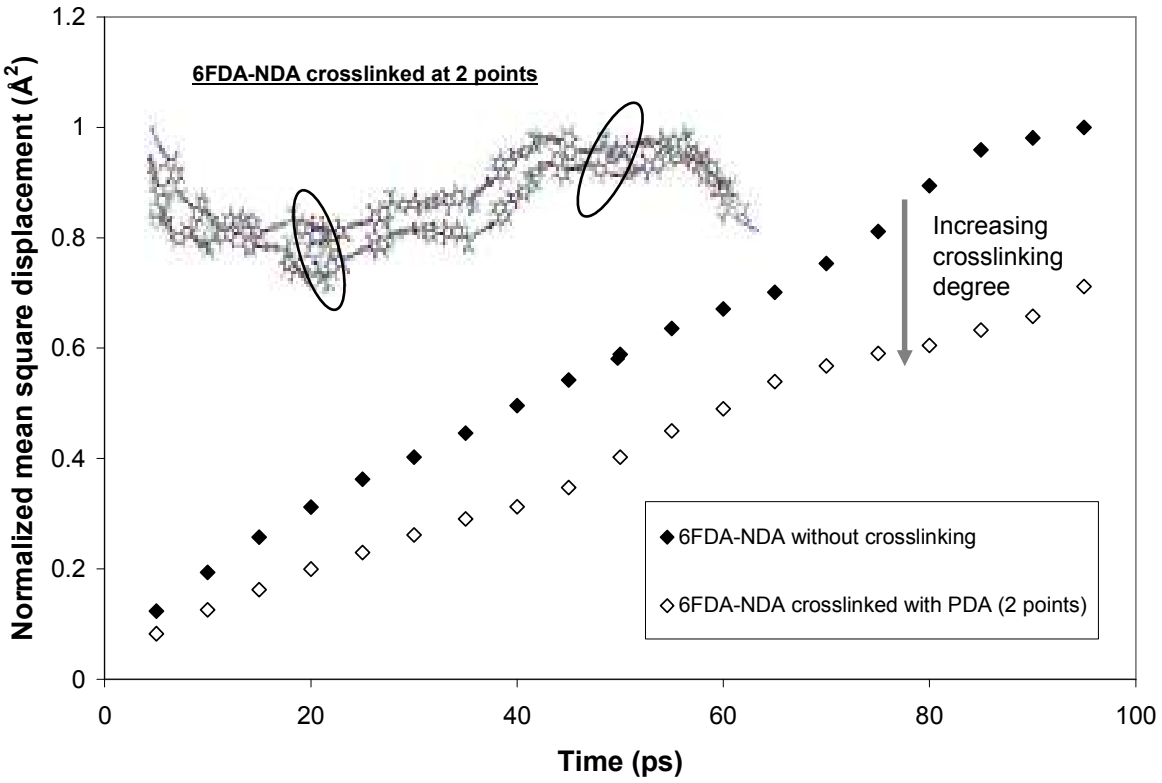

Figure 6.7 Effect of PDA crosslinking on the mean square displacements of 6FDA-NDA polyimide chains

A surprisingly reverse trend in MSD was observed when 6FDA-ODA was subjected to PDA crosslinking. With reference to Figure 6.8, PDA crosslinking decreases the MSD of 6FDA-ODA. This phenomenon can be adequately explained by taking a closer look at the chemical structures of the homopolyimides. For 6FDA-NDA, both the imide ring and naphthalene groups contribute to the polymer rigidity. After PDA modification, the rigid naphthalene structures maintain the backbone rigidity while the attachment of a PDA moiety constitutes a bulky side group to the polymer chain. Hence, the overall rigidity of 6FDA-NDA increases after PDA crosslinking. For 6FDA-ODA, the imide ring dominates the overall chain rigidity since the –O- linkage between two phenyl rings is relatively

flexible. Therefore, the destruction of the imide ring upon PDA modification reduces the chain stiffness of 6FDA-ODA. The increase in polymer rigidity via the integration of PDA moiety does not compensate for the decrease in chain stiffness rooted from the cleavage of the imide rings. One point to highlight here is that despite the increase in the MSD of the 6FDA-ODA chains upon the incorporation of PDA, a slight improvement in H_2/CO_2 selectivity is nevertheless observed. The enhancement in H_2/CO_2 permselectivity after the PDA modification is attributed to an increase in chain rigidity, a decrease in free volume and a possible shift in the free volume distribution towards the smaller cavity sizes. The decrease in the free volume and the shift in free volume distribution are due to the space filling effects of the diamines [56-57]. Therefore, although PDA crosslinking of 6FDA-ODA leads to an increment in MSD (i.e. lowers chain rigidity) which should reduce H_2/CO_2 selectivity, the increment in the gas pair selectivity brought about by the reduction in free volume and the shift in the free volume distribution more than compensate for the decline. Hence, an overall marginal improvement in H_2/CO_2 selectivity was observed for 6FDA-ODA films. This suggests that the effectiveness of dimaine modification is dependent on the intrinsic polymer rigidity. Diamine modification of polyimide with greater intrinsic rigidity leads to effective inhibition of chain movements which is favorable for improving H_2/CO_2 permselectivity.

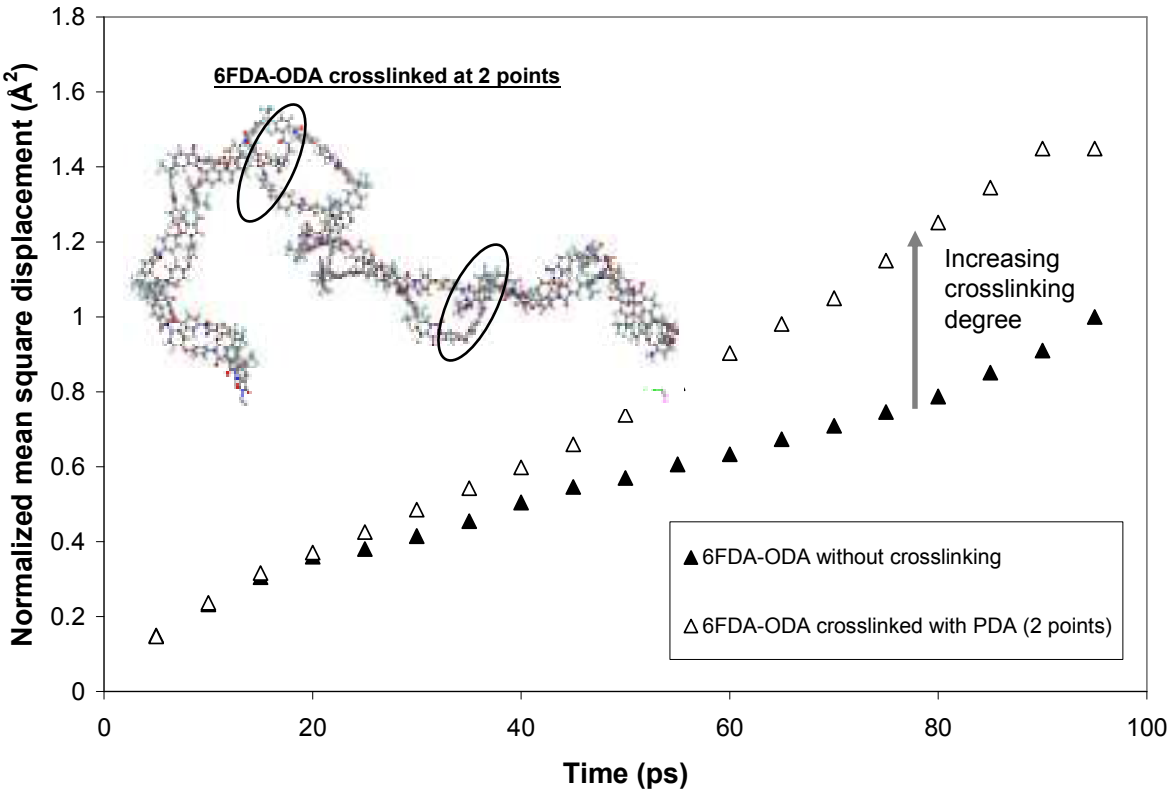

Figure 6.8 Effect of PDA crosslinking on the mean square displacements of 6FDA-ODA polyimide chains

Although the diamine modification of polyimide films is a good approach for enhancing the intrinsic H_2/CO_2 separation performance, it is important to note that the resultant films are not homogenous. This implies that the H_2/CO_2 transport properties are dependent on the film thickness. Therefore, we have chosen the 6FDA-ODA/NDA (50:50) polyimide for a representative study and films of different thicknesses were prepared and subjected to the same modification condition (i.e. 1.65 M PDA, 90 min). With reference to Table 6.9, as the film thickness increases, a notably increase in gas permeability is observed while the corresponding gas pair selectivity decreases. This phenomenon can be adequately explained by the simplified resistance model (Figure 6.3) for the PDA

modified films [45]. This model has been employed in Section 6.3.1 for estimating the penetration depth of the PDA molecules from the surface to the depth of the polyimide films.

Table 6.9 H_2 and CO_2 transport properties of PDA modified 6FDA-ODA/NDA (50:50) films with different thickness

Film thickness (μm)	H_2 permeability (Barrer)	CO_2 permeability (Barrer)	P_{H2}/P_{CO2}
30	9.1	0.14	65
50	16	0.26	62
70	27	0.49	55
100	33	0.83	40

Based on the model, the H_2 and CO_2 permeabilities are represented by equations (6-1) and (6-2), respectively. The ideal H_2/CO_2 selectivity is given by equation (6-3).

$$\frac{L_{T,H2}}{P_{T,H2}A_T}=\left(\frac{2L_1}{P_1A_1}+\frac{L_2}{P_2A_2}\right)_{H2} \Rightarrow \frac{L_{T,H2}}{P_{T,H2}}=\left(\frac{2L_1}{P_1}+\frac{L_2}{P_2}\right)_{H2} \tag{6-1}$$

$$\frac{L_{T,CO2}}{P_{T,CO2}A_T}=\left(\frac{2L_1}{P_1A_1}+\frac{L_2}{P_2A_2}\right)_{CO2} \Rightarrow \frac{L_{T,CO2}}{P_{T,CO2}}=\left(\frac{2L_1}{P_1}+\frac{L_2}{P_2}\right)_{CO2} \tag{6-2}$$

$$\frac{P_{T,H2}}{P_{T,CO2}}=\frac{\left(\frac{2L_1}{P_1}+\frac{L_2}{P_2}\right)_{CO2}}{\left(\frac{2L_1}{P_1}+\frac{L_2}{P_2}\right)_{H2}} \tag{6-3}$$

P_T is the overall permeability and P_1 and P_2 refer to the permeabilities of the modified and unmodified layers. A refers to the membrane surface area as shown in Figure 6.3.

Next, consider the system of membranes with different film thicknesses. Since the modification condition is the same, it is reasonable to assume that the thickness and

permeability of the modified layer are similar i.e. P_1 and L_1 are constant. Another assumption is that the bulk of the membrane exhibits the same extent of methanol swelling regardless of the film thickness i.e. P_2 is constant. Hence, L_2 increases with increasing film thickness. Referring to equations (6-1) and (6-2), a larger L_2 leads to higher $P_{T,H2}$ and $P_{T,CO2}$. This accounts for the higher gas permeabilities as the film thickness increases from 30 μm to 100 μm. Similarly, the model can be used to explain the decline in H_2/CO_2 selectivity as the film thickness increases. A closer look at equation (6-3) reveals that $\left(\frac{L_1}{P_1}\right)_{CO2} >>> \left(\frac{L_1}{P_1}\right)_{H2}$. This implies that any increase in L_2 contributes more to the denominator term in equation (6-3). Therefore, a smaller $\frac{P_{T,H2}}{P_{T,CO2}}$ is obtained when the film thickness increases.

It is evident that both the polymer free volume and rigidity influence the effectiveness of the diamine modification which in turn determines that enhancement in H_2/CO_2 selectivity that can be achieved. One point to highlight here is that chain rigidity reflects the frustration in the packing of polymers which implies that the polymer free volume and rigidity are inter-dependent parameters. Based on the results obtained in this study, a polyimide with a higher free volume and rigidity (6FDA-NDA) would yield the greatest enhancement in H_2/CO_2 selectivity. This is attributed to the fact that polymer with a larger free volume allows for greater extent of diamine penetration and reaction while higher rigidity enables the polymer to maintain or increase its chain stiffness. Both factors are favorable for improving the H_2/CO_2 selectivity of the polyimide membranes.

6.3 Conclusions

The coupling of polyimide molecular design and diamine modification represents an excellent approach for optimizing the enhancement in H_2/CO_2 permselectivity of polyimide membranes. We have identified two important parameters that influence the effectiveness of PDA modification in improving H_2/CO_2 selectivity i.e. polymer free volume and rigidity. Polymer free volume affects the degree of methanol swelling which in turn determines the extent of diamine penetration and reaction. Therefore, a polyimide with a higher free volume generates a denser diamine-modified network which is necessary for improving H_2/CO_2 selectivity. The H_2/CO_2 separation performance of the diamine modified membranes is not merely dependent on the quantity but also the quality of the resultant chemical bridges. Polymer rigidity affects the ability of the polymer to maintain its chain stiffness upon the destruction of the imide rings during the diamine treatment. Hence, a polyimide with greater rigidity leads to a modified polymer network with restricted chain movements, thereby improving the H_2/CO_2. Polyimides with high free volume and rigidity are ideal candidates for diamine modification and the enhancement in H_2/CO_2 selectivity that can be reaped is expected to supersede other polyimides.

6.4 References

[1] N. W. Ockwig, T. M. Nenoff, Membranes for hydrogen separation, Chem. Rev. 107 (2007) 4078.

[2] L. Shao, B. T. Low, T. S. Chung, A. R. Greenberg, Polymeric membranes for the hydrogen economy: Contemporary approaches and prospects for the future, J. Membr. Sci. 327 (2009) 18.

[3] T. S. Chung, L. Shao, P. S. Tin, Surface modification of polyimide membranes by diamines for H_2 and CO_2 separation, Macromol. Rapid Commun. 27 (2006) 998.

[4] H. Lin, E. Van Wager, B. D. Freeman, L. G. Toy, R. P. Gupta, Plasticization-enhanced hydrogen purification using polymeric membranes, Science 311 (2006) 639.

[5] J. D. Perry, K. Nagai, W. J. Koros, Polymer membranes for hydrogen separations, MRS Bulletin 31 (2006) 745.

[6] R. Baker, Future directions of membrane gas-separation technology, Membrane Technology 138 (2001) 5.

[7] J. Qiu, J. M. Zheng, K. V. Peinemann, Gas transport properties of poly(trimethylsilylpropyne) and ethylcellulose filled with different molecular weight trimethylsilylsaccharides: Impact on fractional free volume and chain mobility, Macromolecules 40 (2007) 3213.

[8] H. Lin, B. D. Freeman, Materials selection guidelines for membranes that remove CO_2 from gas mixtures, J. Mol. Struct. 739 (2005) 57.

[9] A. Car, C. Stropnik, W. Yave, K.V. Peinemann, PEG modified poly(amide-b-ethyleneoxide) membranes for CO2 separation, J. Membr. Sci. 307 (2008) 88.

[10] T. C. Merkel, B. D. Freeman, R. J. Spontak, Z. He, I. Pinnau, P. Meakin, A. J. Hill, Ultrapermeable, reverse-selective nanocomposite membranes, Science 296 (2002) 519.

[11] N. P. Patel, M. A. Hunt, S. Lin-Gibson, S. Bencherif, R. J. Spontak, Tunable CO_2 transport through mixed polyether membranes, J. Membr. Sci. 251 (2005) 51.

[12] T. S. Chung, M. L. Chng, K. P. Pramoda, Y. Xiao, PAMAM dendrimer-induced cross-linking modification of polyimide membranes, Langmuir 20 (2004) 2966.

[13] T. H. Kim, W. J. Koros, G. R. Husk, K. C. O'Brien, Relationship between gas separation properties and chemical structure in a series of aromatic polyimides, J. Membr. Sci. 37 (1988) 45.

[14] Y. J. Fub, C. C. Hua, H. Z. Qui, K. R. Lee, J. Y. Lai, Effects of residual solvent on gas separation properties of polyimide membranes, Sep. Purif. Technol. 62 (2008) 175.

[15] Y. C. Wang, S. H. Huang, C. C. Hu, C. L. Li, K. R. Lee, D. J. Liaw, J. Y. Lai, Sorption and transport properties of gases in aromatic polyimide membranes, J. Membr. Sci. 248 (2005) 15.

[16] D. Ayala, A. E. Lozano, J. de Abajo, C. Garćia-Perez, J. G. de la Campaa, K.-V. Peinemann, B. D. Freeman, R. Prabhakar, Gas separation properties of aromatic polyimides, J. Membr. Sci. 215 (2003) 61.

[17] Y. Dai, M. D. Guiver, G. P. Robertson, Y. S. Kang, Effect of hexafluoro-2-propanol substituents in polymers on gas permeability and fractional free volume, Macromolecules 38 (2005) 9670.

[18] M. D. Guiver, G. P. Robertson, Y. Dai, F. Bilodeau, Y. S. Kang, K. J. Lee, J. Y. Jho, J. O. Won, Structural characterization and gas-transport properties of brominated matrimid polyimide, J. Polym. Sci. Part A Polym. Chem. 40 (2002) 4193.

[19] S. A. Stern, Polymers for gas separations: the next decade, J. Membr. Sci. 94 (1994) 1.

[20] S.A. Stern, Y. Mi, H. Yamamoto, A. K. St. Clair, Structure/permeability relationships of polyimide membranes. Applications to the separation of gas mixture, J. Polym. Sci., Part B: Polym. Phy. 27 (1989) 1887.

[21] M. R. Coleman, W. J. Koros, Conditioning of fluorine-containing polyimides. 2. Effect of conditioning protocol at 8% volume dilation on gas-transport properties, Macromolecules 32 (1999) 3106.

[22] C. Cao, T. S. Chung, Y. Liu, R. Wang, K. P. Pramoda, Chemical cross-linking modification of 6FDA-2,6-DAT hollow fiber membranes for natural gas separation, J. Membr. Sci. 216 (2003) 257.

[23] M. R. Coleman, W. J. Koros, The transport properties of polyimide isomers containing hexafluoroisopropylidene in the diamine residue, J. Polym. Sci.: Part B: Polym. Phy. 32 (1994) 1915.

[24] W. H. Lin, R. H. Vora, T. S. Chung, Gas transport properties of 6FDA-durene/1,4-phenylenediamine (pPDA) copolyimides, J. Polym. Sci. Part B Polym. Phy. 38 (2000) 2703.

[25] S. L. Liu, R. Wang, T. S. Chung, M. L. Chng, Y. Liu, R. H. Vora, Effect of diamine composition on the gas transport properties in 6FDA-durene/3,3'-diaminodiphenyl sulfone copolyimides, J. Membr. Sci. 202 (2002) 165.

[26] M. R. Coleman, W. J. Koros, Isomeric polyimides based on fluorinated dianhydrides and diamines for gas separation applications, J. Membr. Sci. 50 (1990) 285.

[27] K. Tanaka, H. Kita, K. Okamoto, A. Nakamura, Y. Kusuki, Gas permeability and permselectivity in polyimides based on 3,3',4,4'-biphenyltetracarboxylic dianhydride, J. Membr. Sci. 47 (1989) 203.

[28] J. Fang, H. Kita, K. I. Okamoto, Gas permeation properties of hyperbranched polyimide membranes, J. Membr. Sci. 182 (2001) 245.

[29] M. Al-Masri, H. R. Kricheldorf, D. Fritsch, New polyimides for gas separation. 1. polyimides derived from substituted terphenylenes and 4,4‘-(Hexafluoroiso propylidene) diphthalic anhydride, Macromolecules 32 (1999) 7853.

[30] S. L. Liu, R. Wang, Y. Liu, M. L. Chng, T. S. Chung, The physical and gas permeation properties of 6FDA-durene/2,6-diaminotoluene copolyimides, Polymer 42 (2001) 8847.

[31] C. Staudt-Bickel, W. J. Koros, Improvement of CO_2/CH_4 separation characteristics of polyimides by chemical crosslinking, J. Membr. Sci. 155 (1999) 145.

[32] S. Shishatskiy, C. Nistor, M. Popa, S. P. Nunes, K. V. Peinemann, Polyimide asymmetric membranes for hydrogen separation: Influence of formation conditions on gas transport properties, Adv. Engrg. Mat. 8 (2006) 390.

[33] W. H. Lin, T. S. Chung, Gas permeability, diffusivity, solubility, and aging characteristics of 6FDA-durene polyimide membranes, J. Membr. Sci. 186 (2001) 183.

[34] J. W. Xu, M. L. Chng, T. S. Chung, C. B. He, R. Wang, Permeability of polyimides derived from non-coplanar diamines and 4,4′-(hexafluoro isopropylidene)diphthalic anhydride, Polymer 44 (2003) 4715.

[35] H. Yamamoto, Y. Mi, S. A. Stern, A. K. St. Clair, Structure/permeability relationships of polyimide membranes. II, J. Polym. Sci: Part B: Polym. Phys. 28 (1990) 2291.

[36] S. A. Stern, R. Vaidyanathan, J. R. Pratt, Structure/permeability relationships of siliconcontaining polyimides, J. Membr. Sci. 49 (1990) 1.

[37] J. Hao, K. Tanaka, H. Kita, K. I. Okamoto, Synthesis and properties of polyimides from thianthrene-2,3,7,8-tetracarboxylic dianhydride-5,5,10,10-tetraoxide, J. Polym. Sci. Part A Polym. Chem. 36 (1998) 485.

[38] K. J. Kim, S. H. Park, W. W. So, D. J. Ahn, S. J. Moon, CO_2 separation performances of composite membranes of 6FDA-based polyimides with a polar group, J. Membr. Sci. 211 (2003) 41.

[39] K. Tanaka, H. Kita, M. Okano, K. I. Okamoto, Permeability and permselectivity of gases in fluorinated and non-fluorinated polyimides, Polymer 33 (1992) 585.

[40] Z. Wang, T. Chen, J. Xu, Gas transport properties of novel cardo poly(aryl ether ketone)s with pendant alkyl groups, Macromolecules 33 (2000) 5672.

[41] Z. K. Xu, M. Böhning, J. Springer, F. P. Glatz, R. Mülhaupt, Gas transport properties of soluble poly(phenylene sulfone imide)s, J. Polym. Sci. Part B Polym. Phys. 35 (1997) 1855.

[42] L. M. Robeson, W.F. Burgoyne, M. Langsam, A. C. Savoca, C. F. Tien, High performance polymers for membrane separation, Polymer 35 (1994) 4970.

[43] L. M. Robeson, The upper bound revisited, J. Membr. Sci. 320 (2008) 390.

[44] L. Shao, L. Liu, S. X. Cheng, Y. D. Huang, J. Ma, Comparison of diamino crosslinking in different polyimide solutions and membranes by precipitation observation and gas transport, J. Membr. Sci. 312 (2008) 174.

[45] B. T. Low, Y. Xiao, T. S. Chung, Y. Liu, Simultaneous occurrence of chemical grafting, crosslinking and etching on the surface of polyimide membranes and their impact on H_2/CO_2 separation, Macromolecules 41 (2008) 1297.

[46] C. M. Aberg, A. E. Ozcam, J. M. Majikes, M. A. Seyam, R. J. Spontak, Extended chemical crosslinking of a thermoplastic polyimide: macroscopic and microscopic property development, Macromol. Rapid Commun. 29 (2008) 1461.

[47] S. S. Hosseini, M. M. Teoh, T. S. Chung, Hydrogen separation and purification in membranes of miscible polymer blends with interpenetration networks, Polymer 49 (2008) 1594.

[48] H. B. Park, C. H. Jung, Y. M. Lee, A. J. Hill, S. J. Pas, S. T. Mudie, E. Van Wagner, B. D. Freeman, D. J. Cookson, Polymers with cavities tuned for fast selective transport of small molecules and ions, Science 318 (2007) 254.

[49] Y. K. Kim, J. M. Lee, H. B. Park, Y. M. Lee, The gas separation properties of carbon molecular sieve membranes derived from polyimides having carboxylic acid groups, J. Membr. Sci. 235 (2004) 139.

[50] Y. L. Kim, H. B. Park, Y. M. Lee, Preparation and characterization of carbon molecular sieve membranes derived from BTDA–ODA polyimide and their gas separation properties, J. Membr. Sci. 255 (2005) 265.

[51] M. D. Guiver, N. L. Thi, G.P. Robertson, Composite gas separation membranes, US Patent No. 20,020,062,737 (2002).

[52] Socrates, G. Infrared and Raman characteristic group frequencies: Tables and charts, 3rd ed.; Wiley: New York, 2000; p 163 -166.

[53] User guide, Visualizer tools section, Calculating Atom Volume and Surfaces, Version 4.3; Acceryls Materials Studio 2008.

[54] J. M. Mohr, D. R. Paul, T. E. Mlsna, R. J. Lagow, Surface fluorination of composite membranes. Part I. Transport properties, J. Membr. Sci. 55 (1991) 131.

[55] J. Y. Park, D. R. Paul, Correlation and prediction of gas permeability in glassy polymer membrane materials via a modified free volume based group contribution method, J. Membr. Sci. 125 (1997) 23.

[56] Y. Xiao, T. S. Chung, M. L. Chng, Surface characterization, modification chemistry and separation performance of polyimide and PAMAM dendrimer composites, Langmuir 20 (2004) 8230.

[57] Y. Liu T. S. Chung, M. L. Chng, R. Wang, Effects of amidation on gas permeation properties of polyimide membranes, J. Membr. Sci. 214 (2003) 83.

CHAPTER 7

DIAMINE MODIFICATION OF POLYIMIDE/POLYETHERSULFONE DUAL LAYER HOLLOW FIBER MEMBRANES FOR HYDROGEN ENRICHMENT

This chapter contains unpublished work

7.1 Introduction

Hydrogen is a major feedstock for producing numerous commodity chemicals and is a zero-pollutant green fuel that may dominate the future energy infrastructure [1-2]. The steam reforming of methane coupled with the water-gas shift reaction in refinery industries is the major route for hydrogen production [1-2]. The hydrogen-rich product stream contains carbon dioxide as the main contaminant, and water and carbon monoxide in trace amounts. In view of the paramount significance of hydrogen enrichment, it is anticipated that this separation process will constitute a sizable portion of the future membrane market that is likely to be concentrated in petrochemical and energy applications [3].

To date, polymers remain the most viable commercial choice among the diversity of membrane materials [1,4-8]. However, due to the undesirable combination of high H_2 diffusivity and CO_2 solubility, it is a challenging task to separate H_2 and CO_2 using polymeric membranes. Generally, glassy polymers are H_2-selective while rubbery polymers are selective for CO_2. For glassy polymeric membranes, another problem associated with hydrogen purification is the CO_2-induced plasticization which deteriorates the molecular sieving ability of the polymer. The design of novel materials and the advancement of fabrication techniques are critical for overcoming the bottlenecks and to develop useful membranes for H_2/CO_2 separation

Recently, significant progresses on polymeric materials for hydrogen purification have been made. Dense flat polymeric membranes have been developed with characteristics selective for either condensable gases (i.e. CO_2 and H_2O) or hydrogen. Organic materials containing poly(ethylene oxide) units in the form of cross-linked networks or block co-polymers are ideal for fabricating CO_2-selective membranes [9-12]. For H_2-selective polymeric membranes, the diamine modification of polyimides emerges as a promising strategy for achieving good H_2/CO_2 permselectivity [1,13-17]. In a pioneering work by Chung et al, the modification of 6FDA-durene dense membrane with 1,3-diaminopropane for 5 min increases the intrinsic H_2/CO_2 permselectivity from 1 to 100 [13]. The feasibility of this approach on polyimide dense films has been verified in subsequent works by Shao et al, Low et al. and Aberg et al with in-depth science and analyses [14-17].

Although the chemistry of the diamine modification technique has been established and key parameters for optimizing the reactions have been identified, all prior studies on the diamine modification of polyimides for H_2/CO_2 separation focus only on dense flat films. Since most polymers display inferior H_2/CO_2 separation characteristics, the fabrication of asymmetric membranes using these materials has yet received high priority and attention by most membrane scientists. Therefore, hydrogen enrichment by means of asymmetric polymeric membranes is rarely reported. However, the asymmetric configuration is of greater commercial significance. Industrial gas separation membranes are typically in the form of spiral wound or hollow fiber modules [3]. The latter module assembly is more attractive because of the larger surface to volume ratio (i.e. higher packing density) [18-

20]. In contrast to the casting of dense films, the fabrication of hollow fibers is undoubtedly more complex but know-how on the spinning process to design hollow fiber membranes for separating other gas pairs is readily available in the literature [21-26].

Extensive studies on the fabrication of single layer hollow fiber membranes using polyimides based on 4,4'-(hexafluoroisopropylidene) diphthalic anhydride (6FDA) have been conducted. For instance, Cao et al. and Ren et al. prepared 6FDA-polyimide mono-layer hollow fibers and the subsequent modification of the membranes with p-xylylene diamine improves the CO_2/CH_4 selectivity [27-28]. Liu and co-workers crosslinked 6FDA-durene/mPDA(50:50)/ polyethersulfone dual layer hollow fibers with p-xylylene diamine and the CO_2/CH_4 selectivity elevated from 44 to 101 after a modification duration of 5 min and the approach effectively suppresses the CO_2-induced plasticization [29]. Therefore, it would be interesting to apply the previous knowledge as well as to create new science and understanding on the fabrication of polyimide hollow fiber membranes especially for H_2/CO_2 separation. The feasibility of post-treating these hollow fiber membranes with aliphatic diamines (e.g. 1,3-diaminopropane (PDA)) for hydrogen purification is worth investigating.

In this study, the dual-layer hollow fiber membrane configuration has been chosen to reduce the material cost of using high performance fluorinated polyimides [21,30-31]. In addition, since the diamine modification is performed as a post-treatment step, utilizing an inner support layer that remains chemically invariant towards the diamines prevents substructure resistance arising from the densification of the porous support. In a

fundamental study by Low et al., it is highlighted that the PDA modification of poly(1,5-naphthalene-2,2'-bis(3,4-phthalic)hexafluoro propane)diimide (6FDA-NDA), a polyimide with high intrinsic free volume and chain rigidity, brings about significant improvement in the H_2/CO_2 permselectivity [16]. Therefore, we have selected 6FDA-NDA polyimide as the material for the outer selective layer. Since polyethersulfone is a relatively low-cost commercial polymer and does not react chemically with diamines, it is chosen as the inner layer material. We aim to fabricate functional dual-layer hollow fibers with the following characteristics: (1) an ultra-thin dense selective skin, (2) delamination-free and (3) porous interface and substructure with minimal transport resistance [30-32].

The objectives of this work are to develop dual-layer hollow fiber membranes for H_2/CO_2 separation and to study the effect of aliphatic diamine treatment for this application. Prior works on the fabrication and/or modification of polyimide/PES dual layer hollow fibers are typically for O_2/N_2 and CO_2/CH_4 separations. This study marks our first attempt in the exploration of hollow fiber membranes which are tailored for H_2/CO_2 separation. An investigation on the effect of air gap on the intrinsic gas separation properties of the as-spun fibers, especially for the H_2/CO_2 pair, will be conducted. A comprehensive analysis of the peculiar trends observed for the permselectivity of different gas pairs is conducted and hypotheses developed from the molecular aspects are proposed. The pristine hollow fibers with suitable H_2/CO_2 transport properties are treated with 1,3-diaminopropane (PDA) which has appropriate nucleophilicity and molecular dimensions for effective modification [13-15]. A comparison of the H_2/CO_2 separation performance displayed by the pristine and PDA-modified hollow fiber membranes is presented and the anti-CO_2

plasticization characteristics of the membranes after PDA modification are evaluated. The challenges encountered in this work and the recommendations to optimize the diamine modification of polyimide/PES hollow fibers are highlighted.

7.2 Results and Discussion

7.2.1 Morphology of the dual-layer hollow fiber membranes

The bulk and surface morphologies of the dual-layer hollow fiber membranes spun using Condition A are depicted in Figure 7.1. The cross-sectional images show that the dual layer hollow fiber is delamination-free and exhibits a high degree of concentricity. The outer diameter (OD) is 890 μm and the wall thickness (Δh) is 210 μm i.e. the OD/2Δh factor is 2.1. Therefore, the fiber may meet the requirements for withstanding the high pressure operations associated with membrane gas separation. The bulk of the PES support layer is a cellular structure with finger-like macrovoids. Both the outer and inner surfaces of the inner layer are highly porous. This implies that the PES support layer may not create additional gas transport resistance. Referring to Figure 7.2, the structure of the 6FDA-NDA outer layer is asymmetric with a dense skin layer of about 120 nm or less at the outer edge. The fibers spun at a higher air gap exhibit a thicker dense skin layer. In contrast to the inner layer, the polyimide outer layer is macrovoid-free which is related to its thickness. There is a critical thickness where the structure of a membrane transforms from a macrovoid to a sponge-like morphology [30,33]. The outer surface of the 6FDA-NDA layer is apparently dense while the inner surface is porous. The relatively thin and

dense skin at the outer layer, and the porous interface and bulk morphologies of the hollow fibers are desirable for achieving selective gas transport.

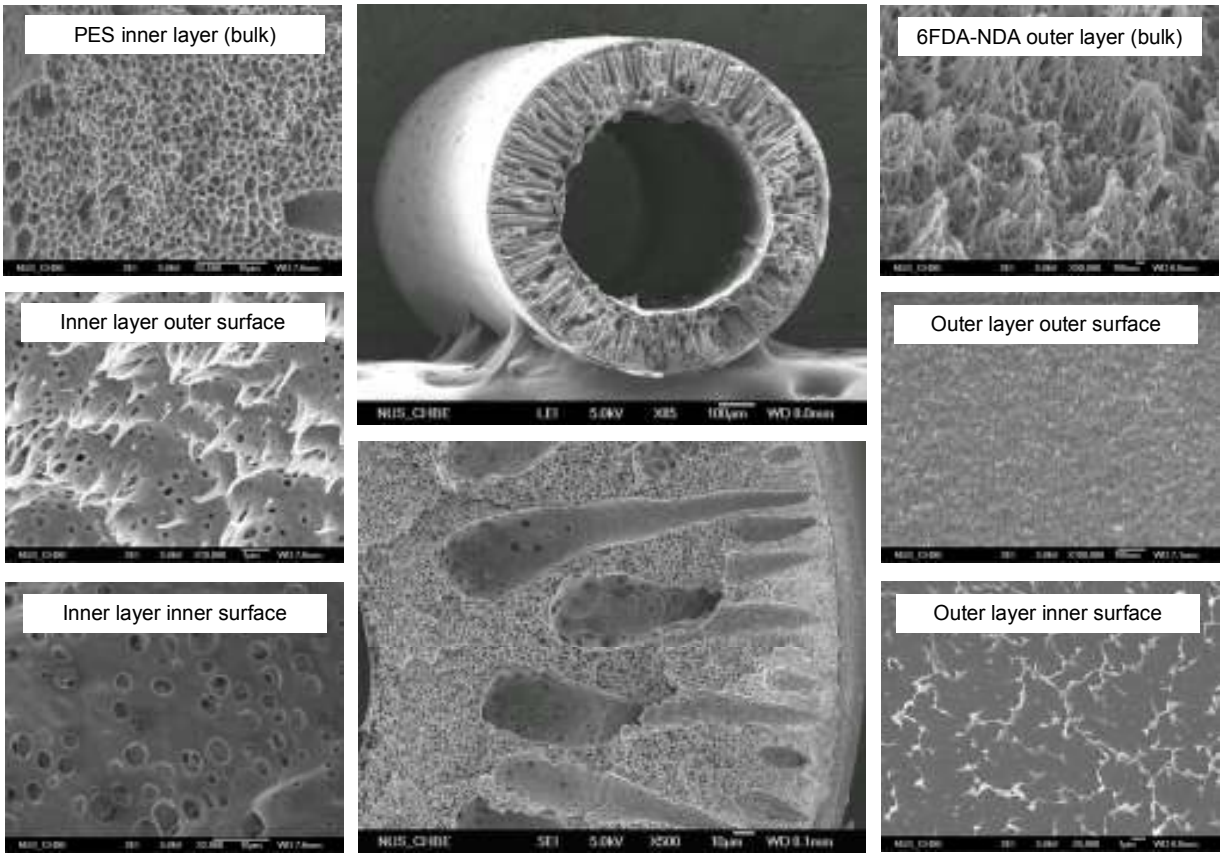

Figure 7.1 Bulk and surface morphologies of 6FDA-NDA/PES dual layer hollow fiber spun using Condition A

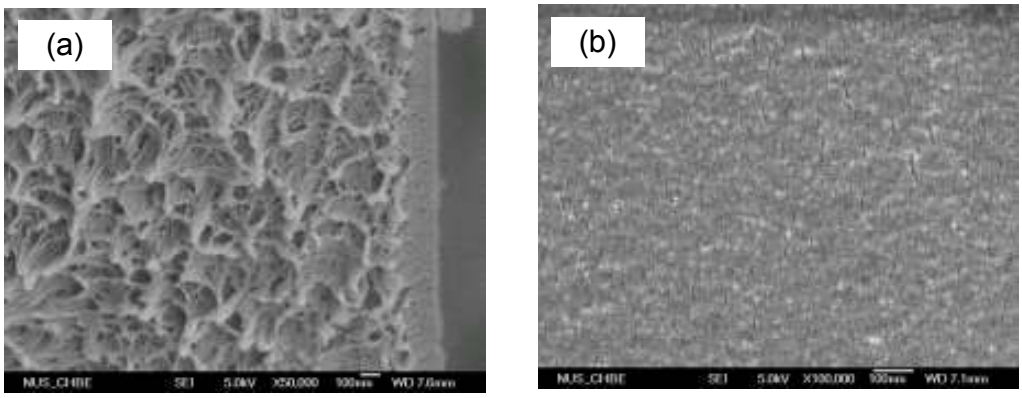

Figure 7.2 (a) Cross sectional view and (b) outer surface of 6FDA-NDA outer layer (air gap = 0.5 cm and spinneret temperature = 50 ^{o}C)

7.2.2 Influence of air gap on gas transport properties

The gas transport properties of the pristine fibers are summarized in Figures 7.3 (a) to (c). For all the tested gases, the permeance decreases as the air gap increases. For each spinning condition, the permeance follows the order: $(P/l)_{H2} > (P/l)_{CO2} > (P/l)_{O2} > (P/l)_{N2} > (P/l)_{CH4}$. This trend is in accordance to the kinetic diameters of the gases where d_{H2} (2.89 Å) < d_{CO2} (3.30 Å) < d_{O2} (3.46 Å) < d_{N2} (3.64 Å) < d_{CH4} (3.80 Å). Interestingly, the permselectivity for the various gas pairs displays different trends as the air gap changes. The H_2/CO_2 permselectivity decreases as the air gap increases. For O_2/N_2 pair, as the air gap is varied from 0.5 to 4 cm, a higher O_2/N_2 permselectivity is obtained but further increase in the air gap to 8 cm results in a lower selectivity. The CO_2/CH_4 selectivity increases with increasing air gap. For 6FDA-NDA dense film, the intrinsic H_2/CO_2, O_2/N_2 and CO_2/CH_4 selectivities are 1.8, 5.2 and 37.4, respectively at 35 ^oC and 10 atm.

Two hypotheses are proposed to account for the effects of different air gaps on the gas permeance and gas pair permselectivity. Using the spinneret and fiber dimensions, the elongational draw ratios corresponding to the air gaps of 0.5, 4 and 8 cm are 2.2, 3.9 and 4.8, respectively [30-31]. This implies that spinning at a higher air gap induces a greater elongational stress on the extruded nascent fibers before precipitation in the external coagulant bath. Although the outer surface of the fibers is relatively dense and solution-diffusion is the dominating mechanism for gas transport, Knudsen diffusion via the larger pores are mutually present. The larger elongational stress may reduce the population of Knudsen pores in the apparently dense outer skin.

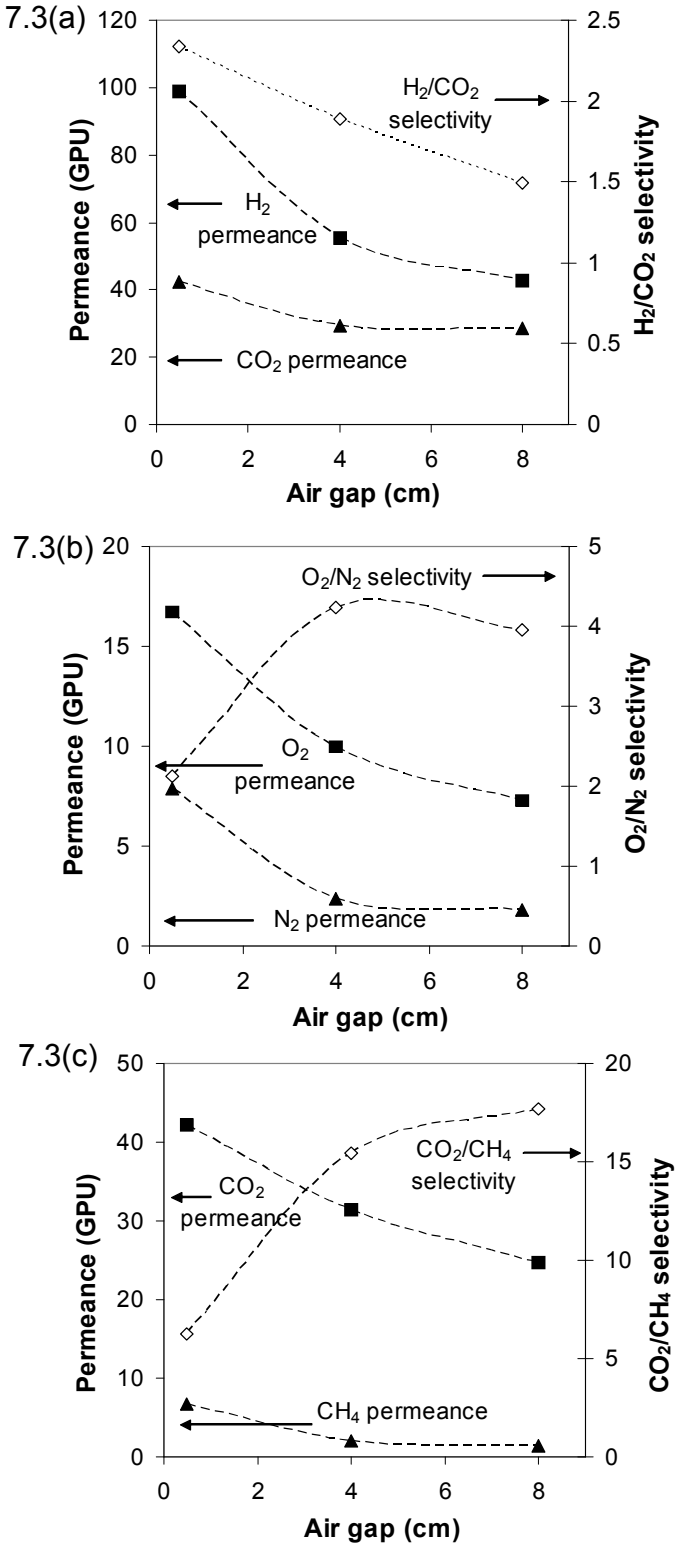

Figure 7.3 Effect of air gap on the gas transport properties for (a) H_2/CO_2, (b) O_2/N_2 and CO_2/CH_4

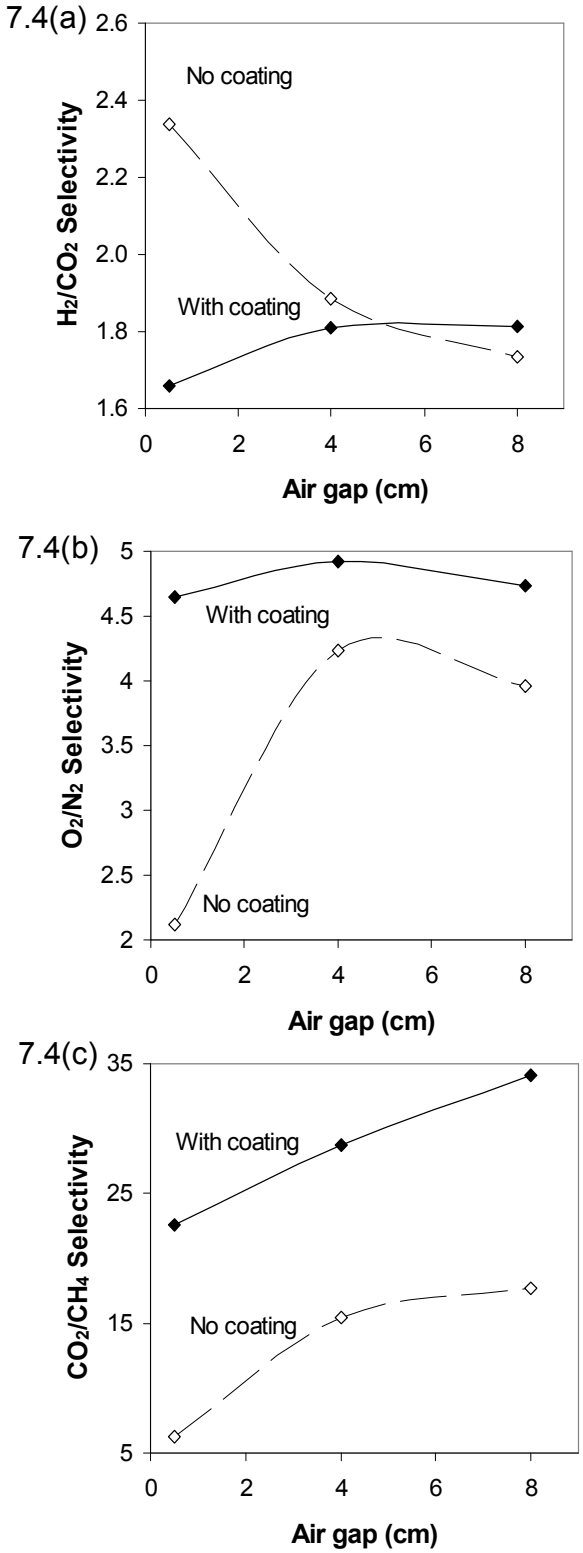

Figure 7.4 Effect of silicone rubber coating on (a) H_2/CO_2, (b) O_2/N_2 and CO_2/CH_4 selectivity

To validate this claim, the gas transport properties of silicone rubber-coated hollow fiber membranes were quantified. Referring to Table 7.1, the gas permeances of the hollow fibers after silicone rubber coating decrease due to the effective sealing of Knudsen pores on the membrane surface. Next, let us examine the effect of silicone rubber coating on the gas pair selectivity of the membranes as shown in Figure 7.4 (a) to (c). For the H_2/CO_2 pair, the selectivity increases with increasing air gap after silicone rubber coating. This is in contrast to the decreasing H_2/CO_2 selectivity trend observed before coating. The Knudsen H_2/CO_2 selectivity is 4.7 while the solution-diffusion selectivity is 1.8. Therefore, the higher H_2/CO_2 selectivity observed for the pristine membranes at a lower air gap is attributed to the Knudsen diffusion. After sealing the Knudsen pores with silicone rubber, solution-diffusion becomes the dominating gas transport mechanism. In fact, at a higher air gap, the H_2/CO_2 selectivity of the fibers before and after coating converges to the polymer intrinsic separation factor of 1.8. For O_2/N_2 and CO_2/CH_4, the observed trends in gas pair selectivity before and after coating are similar. The Knudsen selectivity for O_2/N_2 and CO_2/CH_4 are 0.94 and 0.60, respectively which are significantly small compared to the solution-diffusion selectivity of 5.2 and 37.4, respectively. Considering the negligible Knudsen selectivity, the overall selectivity of the fibers with and without coating is largely attributed to the solution-diffusion.

In an earlier work by Wang and Chung, it has been reported that increasing the shear stress experienced by the hollow fiber membranes during spinning changes the surface porosity of the membranes [34]. As the shear stress increases, the population of Knudsen pores exhibits an up-and-down trend. The initial increase is attributed to the

disappearance of pores large enough for Poiseuille flow and the subsequent formation of Knudsen pores. The later decline in the quantity of Knudsen pores is due to the chain tightening effects at higher shear stress. The results presented here suggest that the changes in the elongational stress may introduce similar transformation in the surface porosity of the membranes.

Table 7.1 Effect of silicone rubber coating on the gas permeance

Gas	Air gap = 0.5 cm		Air gap = 4 cm		Air gap = 8 cm	
	$(P/l)_{no\ coat}$	$(P/l)_{coated}$	$(P/l)_{no\ coat}$	$(P/l)_{coated}$	$(P/l)_{no\ coat}$	$(P/l)_{coated}$
H_2	98.7	60.3	55.5	42.2	42.7	35.9
O_2	16.7	9.5	10.0	5.5	7.3	5.1
N_2	7.9	2.0	2.4	1.1	1.8	1.1
CH_4	6.7	1.6	2.0	0.8	1.4	0.6
CO_2	42.2	36.4	29.4	23.3	24.6	8.8

* $(P/l)_{no\ coat}$ and $(P/l)_{coated}$ refers to the gas permeance in GPU before and after silicone rubber coating, respectively.

Another hypothesis to explain the observed phenomenon is the difference in the molecular orientation of polymer chains for fibers spun at different air gaps. In a work by Cao et al., it has been suggested that the elongational stress results in the stretching of polymer chains and enhances the chain packing near the outer skin of the hollow membranes [35]. A higher air gap results in a larger elongational stress which tightens the membrane structure and results in lower gas permeance. The change in the molecular orientation of polymer chains enhances the polymer packing efficiency and potentially alters the free volume distribution of the dense selective skin. Figure 7.5 depicts the possible shift and sharpening in the free volume distributions as the air gap changes. This proposed hypothesis considers primarily the diffusion of gas penetrants based on their kinetic diameters. Referring to Figure 7.5, the shaded region below the free volume

distribution curve, and between the cavity sizes corresponding to the kinetic diameters of gas X and gas Y is an indication of the X/Y selectivity. A larger area implies that there are more effective free volumes which are accessible to the gas with a smaller kinetic diameter (i.e. gas X). In the following discussion, the term A_{eff} is used to represent this area.

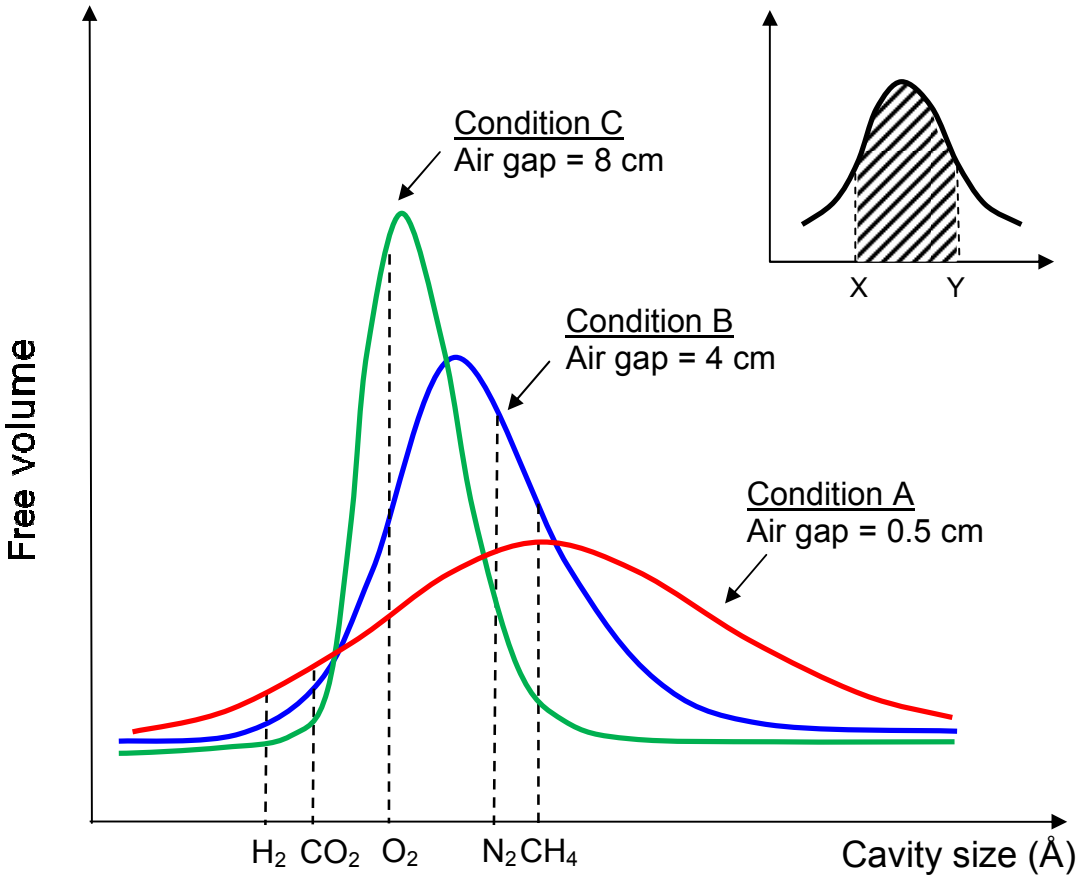

Figure 7.5 Predicted shift and sharpening of the free volume distribution at varying air gaps

For the H_2/CO_2 pair, the cavity sizes that correspond to the kinetic diameters of H_2 and CO_2 are at the extreme left of the distribution curve. Thus, majority of H_2 and CO_2 molecules are able to pass through the dense skin layer of hollow fiber membranes which

accounts for the poor H_2/CO_2 selectivity. As the air gap increases, A_{eff} decreases slightly and this is in accordance to the marginal decrease in H_2/CO_2 selectivity at a higher air gap. For the O_2/N_2 pair, A_{eff} increases as the air gap changes from 0.5 to 4 cm and a further increase in air gap to 8 cm brings about a smaller A_{eff}. The O_2/N_2 selectivity exhibits a similar up-and-down trend with increasing air gap. Lastly, for the CO_2/CH_4 gas pair, a larger air gap results in a greater A_{eff} which agrees with the better CO_2/CH_4 selectivity of the hollow fiber membranes spun at a higher air gap. Therefore, the optimal air gap or elongational draw ratio for maximizing the gas pair selectivity is dependent on the kinetic diameters of the gaseous penetrants.

The influence of elongational draw ratio on the O_2/N_2 transport properties of Torlon® single-layer hollow fibers has been reported by Peng and Chung [24]. In their work, the O_2/N_2 permselectivity displays an up-and-down trend with increasing draw ratio. Conversely, the O_2 permeance exhibits a down-and-up behavior. The initial increase in O_2/N_2 permselectivity and decrease in O_2 permeance is attributed to the effect of better molecular orientation which creates more monodisperse free volume distributions. Beyond an optimal draw ratio of about 10, reverse trends are observed and this may be due to the creation of minor defects from the overstretching of polymer chains. Compared to our present work, a similar up-and-down relationship between O_2/N_2 selectivity and draw ratio (or air gap) is observed but the O_2 permeance decreases as the draw ratio increases from 2.2 to 4.8. In fact, this decrease in permeance is observed for all the tested gases. This is because the draw ratios investigated in this work are significantly lower and perhaps still far from the stretching limit which is reflected by the optimal draw ratio. As

a result, an increase in draw ratio before reaching the stretching limit not only gives rise to more monodisperse free volume (i.e. sharpening of the free volume distribution) but also fine tunes the interstitial space (i.e. shift in the free volume distribution).

7.2.3 Effect of 1,3-diaminopropane modification on H_2/CO_2 transport properties

The second objective of this study is to modify 6FDA-NDA/PES dual layer hollow fibers with 1,3-diaminopropane (PDA) for achieving better H_2/CO_2 separation performance. Using the pure gas transport properties of the pristine membranes as a basis, the hollow fibers fabricated by Condition A have higher H_2 permeance and H_2/CO_2 selectivity, and was selected for the diamine modification. The changes in the pure gas permeance and ideal H_2/CO_2 permselectivity of the pristine and PDA-modified fibers are summarized in Table 7.2. A short modification duration of 2 min leads to a 90 % decline in the H_2 permeance while the H_2/CO_2 selectivity increases by a factor of 2.5. As the modification duration increases to 5 min, the H_2/CO_2 selectivity increases from 6.3 to 36 while the H_2 permeance decreases from 7.5 to 1.8 GPU.

Table 7.2 Effect of PDA modification duration on H_2 and CO_2 gas transport properties

PDA modification time (min)	0	2	5
H_2 permeance (GPU)	104	7.5	1.8
CO_2 permeance (GPU)	43.0	1.2	0.05
Ideal selectivity	2.4	6.3	36

* Pure gas permeation tests conducted at 35 ^{o}C and 20 psia unless otherwise stated

1GPU = 1×10^{-6} cm^3 (STP)/cm^2 s cmHg

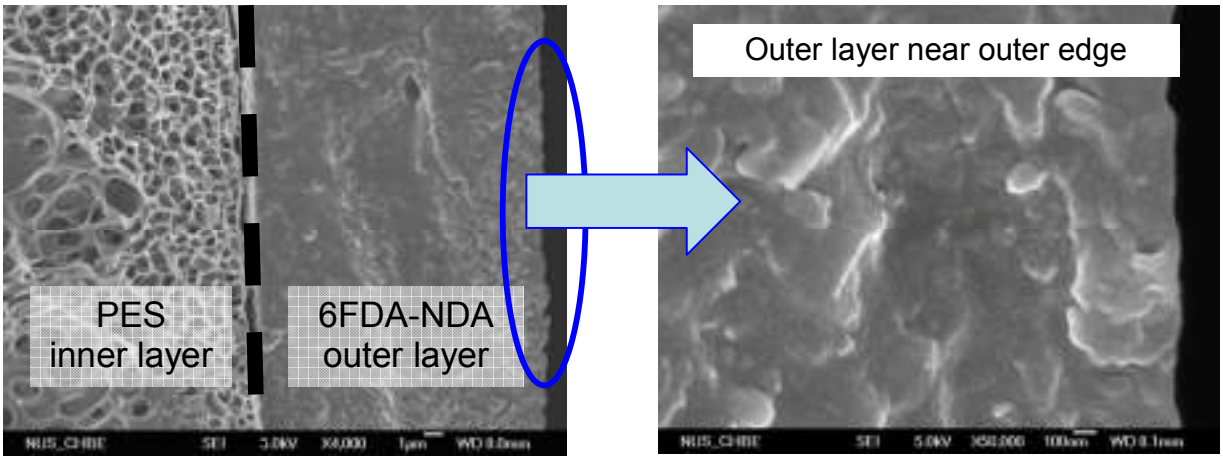

Figure 7.6 Cross sectional views of hollow fiber spun using Condition A after PDA modification for 2 min

The cross sectional morphology of the hollow fiber after PDA modification for 2 min is shown in Figure 7.6. In contrast to the asymmetric structure of the 6FDA-NDA outer layer of the pristine fiber as shown in Figure 7.2 (a), the outer layer of the PDA modified fiber is much dense. A previous work on the p-xylylenediamine modification of 6FDA-ODA/NDA single layer hollow fiber membranes by Ren et al. shows that the modification only occurs at the surface i.e. densification of the thin layer near the outer surface while maintaining the asymmetric structure [28]. In our study, the diamine modification results in the densification of the entire polyimide outer layer. This explains for the drastic drop in the gas permeance even with relatively short modification duration. The difference in the morphology of the diamine modified fibers in this present study and in the work by Ren et al. may be attributed to the following. Firstly, the molecular dimension of PDA is smaller than p-xylylenediamine and thus has a greater degree of penetration across the polyimide layer. Another reason for this is the different swelling effects of the fibers in methanol. In a previous work by Low et al., it has been shown that 6FDA-NDA with high free volume is more easily swelled in a methanol environment

[16]. In addition, the thickness of the polyimide layer may result in the different extent of methanol swelling. In our work, the 6FDA-NDA outer layer with a thickness of 10 μm probably shows more severe methanol swelling as compared to the 6FDA-ODA/NDA single layer hollow fibers.

During the PDA modification process in a methanol environment, diffusion and reaction fonts exist across the membrane as shown in a simplified schematic in Figure 7.7. In fact, several pairs of diffusion and reaction fronts occur simultaneously at an instant of the modification process. A pre-requisite to the diffusion and reaction of diamines within the polyimide matrix is methanol swelling. The swelling of the polymeric matrix enhances the diamine diffusion. At the initial stage of the modification process, the diffusion of diamines occurs rapidly and the PDA molecules penetrate deeper before reacting with the imide groups i.e. the diffusion front moves faster than the reaction front. Thus, the diamine modification occurs even in the bulk of the polyimide outer layer. As the modification time increases, a considerable portion of the polymeric matrix has been modified and this reduces the availability of free space for diamine diffusion. The extent of diamine penetration decreases and the rate at which the diffusion and reaction fronts move becomes comparable. This allows further modification to occur near the outer surface. Therefore, for a short modification duration of 2 min, a small extent of modification occurs throughout the polyimide outer layer. This accounts for the large drop in gas permeance and the marginal increase in H_2/CO_2 permselectivity. For a longer modification time of 5 min, the diffusion of the diamines is hindered and a greater degree of modification can take place near the surface. This explains for the larger increase in

H_2/CO_2 selectivity from 6.3 to 36. A similar concept has been proposed by Mohr et al. to explain the reaction profiles in surface fluorinated poly(4-methyl-1-pentene) (PMP) membranes [36]. The reaction profile for the diamine-modified polyimide film is analogous to that of the surface fluorinated PMP membranes, where an intermediate reaction profile between the two limiting cases of diffusion-controlled and reaction-dominated scenarios is applicable. The resultant membrane comprises a gradient of chemically modified polymer layers after the surface treatment.

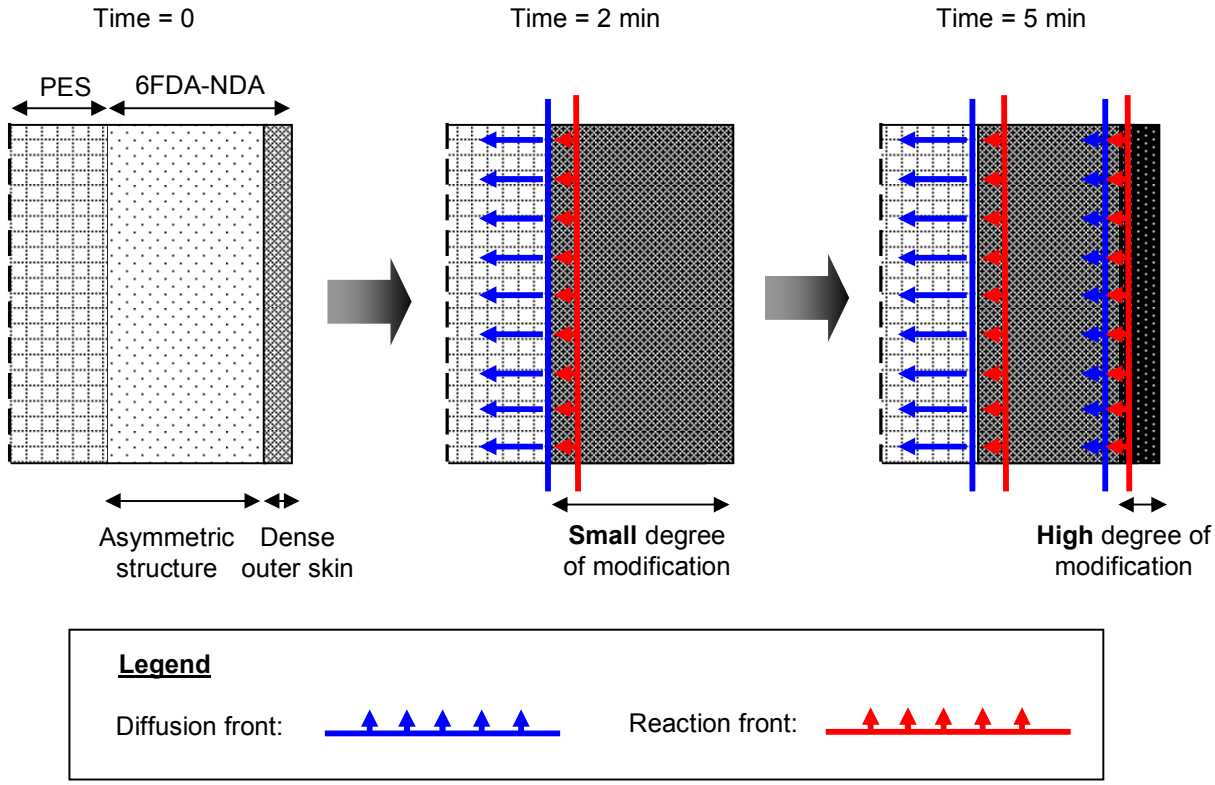

Figure 7.7 Diamine diffusion and reaction fronts for the PDA modification of hollow fibers in methanol

In contrast to the H_2/CO_2 transport properties of the PDA-modified dense film reported in the work by Low et al., the PDA-modified hollow fibers show more drastic decline in gas flux but the corresponding increment in H_2/CO_2 selectivity is relatively more inferior.

Low et al. reported an impressive increase in H_2/CO_2 selectivity from 1.8 to 120 while the gas permeability decreased from 78 to 12 Barrer after modifying 6FDA-NDA dense film with 1.65 M PDA for 90 min. An extended series resistance model can be used to account for the less than optimal improvement in H_2/CO_2 selectivity after the diamine modification of asymmetric hollow fiber membranes. Figure 7.8 shows the extended resistance model for the PDA modified 6FDA-NDA/PES dual layer hollow fiber and the expected influence of the number of partially modified layers (n) on the apparent H_2/CO_2 selectivity.

The ideal membrane configuration after diamine modification is a fully modified and thin selective layer on the pristine structure (i.e. n=0 in Figure 7.8). In this case, an optimal enhancement in H_2/CO_2 selectivity can be reaped from the diamine modification. However, due to the nature of the modification process, a gradient of reaction occurs on the 6FDA-NDA layer and in fact, the modification proceeds across the entire membrane cross-section i.e. n tends to infinity. As the number of partially modified layers increases, the apparent H_2/CO_2 selectivity decreases. These partially modified layers create additional sub-structure resistance which bring about a large decline in gas flux but do not contribute to the enhancement in H_2/CO_2 selectivity. For simplicity, in the extended resistance model proposed here, a membrane consisting of distinct modified layers with varying degrees of modification is considered. However, in reality, the resultant membrane consists of a gradient and stratified structure without a clear boundary of demarcation. This has been highlighted in the work by Mohr et al. where the permeation

term for the fluorine-modified polymer in the resistance model is replaced by an integral term that takes into account the variation of permeability with membrane thickness [36].

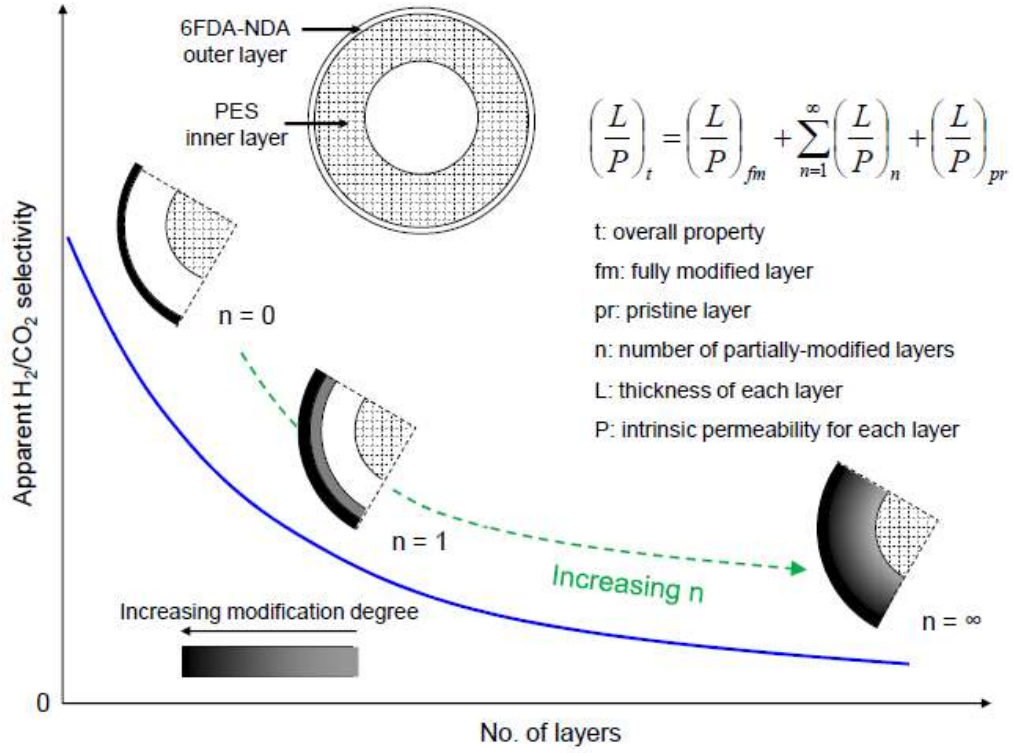

Figure 7.8 Extended resistance model for the PDA modified 6FDA-NDA/PES dual-layer hollow fiber

The CO_2-induced plasticization behaviors of the pristine and PDA-modified hollow fibers are investigated. The impact of CO_2-induced plasticization is greater for thin polymeric membranes and it has been reported that polyimide hollow fibers usually show signs of plasticization at low pressure of 20 psia. Surprisingly, the pristine 6FDA-NDA/PES hollow fiber used in our study does not display severe plasticization effects. In fact, the pure CO_2 permeance remains relatively constant as the upstream pressure is increased from 20 to 200 psi. This may be attributed to the rigid naphthalene structure of 6FDA-NDA polymer. The CO_2-plasticization behaviors of the PDA-modified fibers are shown

in Figure 7.9 (a). It is evident that the diamine modification improves the anti-swelling property of the membrane and suppresses CO_2-induced plasticization. The anti-plasticization effect improves as the modification duration increases. This implies that a higher H_2/CO_2 selectivity may be obtained at elevated pressures as depicted in Figure 7.9 (b).

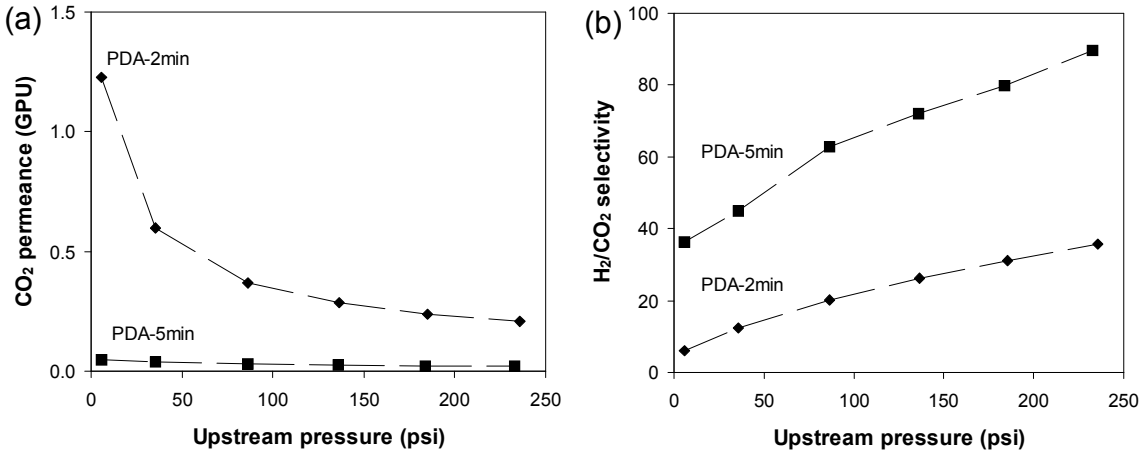

Figure 7.9 Effect of CO_2 pressure on the (a) CO_2 permeance and (b) H_2/CO_2 selectivity of PDA-modified 6FDA-NDA/PES fibers (H_2 tested at 20 psia)

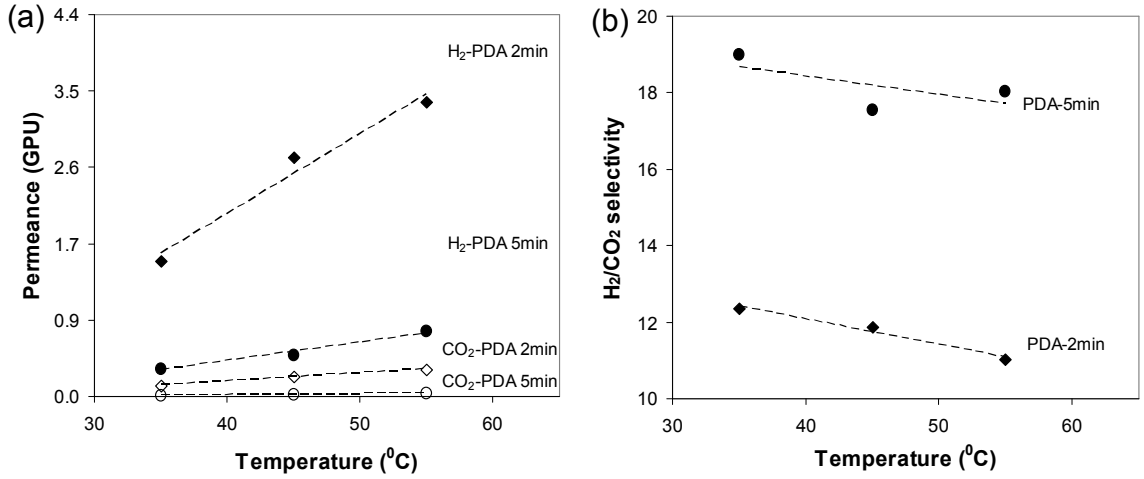

Figure 7.10 Effect of temperature on (a) gas permeance and (b) permselectivity (H_2/CO_2 50:50 binary gas tests conducted at a transmembrane pressure of 200 psia)

Binary gas tests were performed for the PDA-modified 6FDA-NDA/PES dual layer hollow fibers at different temperatures and the results are depicted in Figures 7.10 (a) and (b). Referring to Figure 7.10 (a), both the H_2 and CO_2 permeance increases with temperature. The greater permeance is attributed to the enhanced gas diffusivity at increased temperature. The H_2/CO_2 selectivity decreases slightly with increasing temperature. A lower CO_2 solubility is expected at higher temperatures but the increase in CO_2 diffusivity more than compensates for the decline. Based on the temperature dependence of the gas permeances, the activation energy for gas permeation can be obtained from the Arrhenius equation as follows:

$$\left(\frac{P}{l}\right)=\left(\frac{P}{l}\right)_0 \exp\left(\frac{-E_P}{RT}\right) \tag{7-1}$$

P_0 is the pre-exponential factor, Ep is the activation energy in $Jmol^{-1}$, R is the ideal gas constant i.e. 8.314 $Jmol^{-1}K^{-1}$ and T is the absolute temperature in K.

The activation energy for H_2 increases from 32.9 to 35.7 $kJmol^{-1}$ as the PDA modification duration increases from 2 to 5 min. The higher activation energy is due to the increased chain rigidity after prolonged PDA modification. The CO_2 activation energy remains relatively constant regardless of the modification duration (i.e. 37.8 and 37.9 $kJmol^{-1}$ for 2 and 5 min modification, respectively). Quantitatively, a negative $\Delta E_{p(A/B)}$ between gas A and B indicates a decrease in permselectivity with increasing temperature. For the PDA modified hollow fibers, the $E_{p,H2}$ is smaller than the $E_{p,CO2}$ which is in accordance to the lower selectivity at higher temperatures. The PDA-modified fibers exhibit enhanced gas permeance with negligible loss in selectivity at higher temperatures.

7.3 Conclusions

It has been demonstrated in this present work that the elongational stress induced by the air gap during spinning alters the surface porosity and free volume distribution of the apparently dense outer skin of the hollow fiber membranes. The PDA modification of 6FDA-NDA/PES dual layer hollow fiber membranes is capable of increasing the H_2/CO_2 separation performance. A higher H_2 permeance is obtained at a higher temperature while maintaining the H_2/CO_2 selectivity. However, the PDA-modified fiber exhibits low gas permeance and the increase in H_2/CO_2 permselectivity is lesser than the optimal that can be reaped. This is attributed to penetration and reaction of diamine molecules across the bulk of the polyimide outer layer which densifies the entire structure.

In order to harvest the full benefits of the diamine modification approach for polyimide hollow fibers, the problem of sub-structure resistance needs to be overcome and will be explored in our future work. This involves the hindering of the diffusion front which may be achievable by lowering the concentration of the diamine modification solution or by eliminating the use of methanol which swells up the membrane. Besides varying the post-treatment protocol, the optimization of the spinning conditions may be investigated. Since the PDA modification densifies the entire outer layer, fabricating dual-layer hollow fibers with much thinner outer layer wall thickness may be beneficial.

7.4 References

[1] L. Shao, B. T. Low, T. S. Chung, A. R. Greenberg, Polymeric membranes for the hydrogen economy: Contemporary approaches and prospects for the future, J. Membr. Sci. 327 (2009) 18.

[2] N. W. Ockwig, T. M. Nenoff, Membranes for hydrogen separation, Chem. Rev. 107 (2007) 4078.

[3] R. W. Baker, Future directions of membrane gas separation technology, Ind. Eng. Chem. Res. 41 (2002) 1393.

[4] H. B. Park, C. H. Jung, Y. M. Lee, A. J. Hill, S. J. Pas, S. T. Mudie, E. Van Wagner, B. D. Freeman, D. J. Cookson, Polymers with cavities tuned for fast selective transport of small molecules and ions, Science 318 (2007) 254.

[5] Y. K. Kim, H. B. Park, Y. M. Lee, Preparation and characterization of carbon molecular sieve membranes derived from BTDA–ODA polyimide and their gas separation properties, J. Membr. Sci. 255 (2005) 265.

[6] Y. C. Wang, S. H. Huang, C. C. Hu, C. L. Li, K. R. Lee, D. J. Liaw, J. Y. Lai, Sorption and transport properties of gases in aromatic polyimide membranes, J. Membr. Sci. 248 (2005) 15.

[7] Y. Dai, M. D. Guiver, G. P. Robertson, Y. S. Kang, Effect of hexafluoro-2-propanol substituents in polymers on gas permeability and fractional free volume, Macromolecules 38 (2005) 9670.

[8] M. R. Coleman, W. J. Koros, Conditioning of fluorine-containing polyimides. 2. Effect of conditioning protocol at 8% volume dilation on gas-transport properties, Macromolecules 32 (1999) 3106.

[9] H. Lin, E. Van Wager, B. D. Freeman, L. G. Toy, R. P. Gupta, Plasticization-enhanced hydrogen purification using polymeric membranes, Science 311 (2006) 639.

[10] A. Car, C. Stropnik, W. Yave, K.-V. Peinemann, Tailor-made Polymeric Membranes based on Segmented Block Copolymers for CO_2 Separation, Adv. Funct. Mater. 18 (2008) 2815.

[11] N. P. Patel, R. J. Spontak, Mesoblends of polyether block copolymers with poly(ethylene glycol), Macromolecules 37 (2004) 1394.

[12] H. Lin, B. D. Freeman, Materials selection guidelines for membranes that remove CO_2 from gas mixtures, J. Mol. Struct. 739 (2005) 57.

[13] T. S. Chung, L. Shao, P. S. Tin, Surface modification of polyimide membranes by diamines for H_2 and CO_2 separation, Macromol. Rapid Commun. 27 (2006) 998.

[14] L. Shao, L. Liu, S. X. Cheng, Y. D. Huang, J. Ma, Comparison of diamino crosslinking in different polyimide solutions and membranes by precipitation observation and gas transport, J. Membr. Sci. 312 (2008) 174.

[15] B. T. Low, Y. Xiao, T. S. Chung, Y. Liu, Simultaneous occurrence of chemical grafting, crosslinking and etching on the surface of polyimide membranes and their impact on H_2/CO_2 separation, Macromolecules 41 (2008) 1297.

[16] B. T. Low, Y. Xiao, T. S. Chung, Amplifying the molecular sieving capability of polyimide membranes via coupling of diamine networking and molecular architecture, Polymer 50 (2009) 3250.

[17] C. M. Aberg, A. E. Ozcam, J. M. Majikes, M. A. Seyam, R. J. Spontak, Extended chemical crosslinking of a thermoplastic polyimide: macroscopic and microscopic property development, Macromol. Rapid Commun. 29 (2008) 1461.

[18] V. Abetz, T. Brinkmann, M. Dijkstra, K. Ebert, D. Fritsch, K. Ohlrogge, D. Paul, K. V. Peinemann, S. P. Nunes, N. Scharnagl, M. Schossig, Developments in membrane research: from material via process design to industrial application, Adv. Eng. Mater. 8 (2006) 328.

[19] J. Lemanski, G. Lipscomb, Effect of shell-side flows on hollow-fiber membrane device performance, AIChE J. 41 (1995) 2322.

[20] D. F. Li, R. Wang, T. S. Chung, Fabrication of lab-scale hollow fiber membrane modules with high packing density, Sep. Purif. Technol. 40 (2004) 15.

[21] D. F. Li, T. S. Chung, R. Wang, Y. Liu, Fabrication of fluoropolyimide/ polyethersulfone dual-layer asymmetric hollow fiber membranes for gas separation, J. Membr. Sci. 198 (2002) 211.

[22] C. C. Pereira, R. Nobrega, K. V. Peinemann, C. P. Borges, Hollow fiber membranes obtained by simultaneous spinning of two polymer solutions: a morphological study, J. Membr. Sci. 226 (2003) 35.

[23] H. A. Tsai, C. Y. Kuo, J. H. Lin, D. M. Wang, A. Deratani, C. Pochat-Bohatier, K. R. Lee, J. Y. Lai, Morphology control of polysulfone hollow fiber membranes via water vapor induced phase separation, J. Membr. Sci. 278 (2006) 390.

[24] N. Peng, T. S. Chung, J. Membr. Sci. The effects of spinneret dimension and hollow fiber dimension on gas separation performance of ultra-thin defect-free Torlon® hollow fiber membranes, 310 (2008) 455.

[25] D. T. Clausi, W. J. Koros, J. Membr. Sci. Formation of defect-free polyimide hollow fiber membranes for gas separations, 167 (2000) 79.

[26] M. Khayet, M. C. García-Payo, F. A. Qusay, K. C. Khulbe, C. Y. Feng, T. Matsuura, Effects of gas gap type on structural morphology and performance of hollow fibers, J. Membr. Sci. 311 (2008) 259.

[27] C. Cao, T. S. Chung, Y. Liu, R. Wang, K. P. Pramoda, Chemical cross-linking modification of 6FDA-2,6-DAT hollow fiber membranes for natural gas separation, J. Membr. Sci. 216 (2003) 257.

[28] J. Ren, R. Wang, T. S. Chung, D. F. Li, Y. Liu, The effects of chemical modifications on morphology and performance of 6FDA-ODA/NDA hollow fiber membranes for CO_2/CH_4 separation, J. Membr. Sci. 222 (2003) 133.

[29] Y. Liu, T. S. Chung, R. Wang, D. F. Li, M. L. Chng, Chemical Cross-Linking Modification of Polyimide/Poly(ether sulfone) Dual-Layer Hollow-Fiber Membranes for Gas Separation, Ind. Eng. Chem. Res. 42 (2003) 1190.

[30] D. Li, T. S. Chung, R. Wang, Morphological aspects and structure control of dual-layer asymmetric hollow fiber membranes formed by a simultaneous co-extrusion approach, J. Membr. Sci. 243 (2004) 155.

[31] N. Widjojo, S. D. Zhang, T. S. Chung, Y. Liu, Enhanced gas separation performance of dual-layer hollow fiber membranes via substructure resistance reduction using mixed matrix materials, J. Membr. Sci. 306 (2007) 147.

[32] I. Pinnau, W. J. Koros, Relationship between substructure resistance and gas separation properties of defect-free integrally skinned asymmetric membranes, Ind. Eng. Chem. Res. 30 (1991) 1837.

[33] N. Vogrin, C. Stropnik, V. Musil, M. Brumen, The wet phase separation: the effect of cast solution thickness on the appearance of macrovoids in the membrane forming ternary cellulose acetate/acetone/water system, J. Membr. Sci. 207 (2002) 139.

[34] R. Wang, T. S. Chung, Determination of pore sizes and surface porosity and the effect of shear stress within a spinneret on asymmetric hollow fiber membranes, J. Membr. Sci. 188 (2001) 29.

[35] C. Cao, T. S. Chung, S. B. Chen, Z. Dong, The study of elongation and shear rates in spinning process and its effect on gas separation performance of poly(ether sulfone) (PES) hollow fiber membranes, Chem. Eng. Sci. 59 (2004) 1053.

[36] J. M. Mohr, D. R. Paul, T. E. Mlsna, R. J. Lagow, Surface fluorination of composite membranes Part1. Transport properties, J. Membr. Sci. 55 (1991) 131.

CHAPTER 8

MEMBRANES COMPRISING OF PSEUDO-INTERPENETRATING POLYMER NETWORKS FOR CO_2/CH_4 SEPARATION

This chapter is published as a journal paper

Bee Ting Low, Tai Shung Chung, Hongmin Chen, Yan Ching Jean, Kumari Pallathadka Pramoda, Tuning the free volume cavities of polyimide membranes via the construction of pseudo-interpenetrating networks for enhanced gas separation performance, *Macromolecules* 42 (2009) 7042–7054.

8.1 Introduction

The implementation and establishment of the membrane technology for gas separation are dependent on the constructive integration of membrane material advancement, membrane configuration and module design, and process optimization [1-4]. Indeed, the development of high performance membrane materials is the vital aspect among these considerations [1,5]. Polymers are attractive candidates for membrane fabrication due to the ease of processability, good physiochemical properties and low production costs [6-9]. In order to satisfy the demands from diverse applications, the properties of polymers can be tailored by various approaches. The molecular architecture of polymers by the permutations of numerous monomers represents one of the conventional approaches by membrane scientists to accomplish this goal [8-9]. Glassy polyimides have been extensively studied as promising materials for gas separation membranes and the molecular tailoring method has been particularly effective for enhancing the CO_2/CH_4 separation performance of polyimide membranes [10-13]. The integration of soft rubbery segments with hard glassy segments in the form of block copolymers has been explored and these materials display recommendable CO_2/N_2 and CO_2/H_2 separation properties [14-15]. The molecular design technique creates novel polymers with robust separation performance and excellent intrinsic properties but is less attractive from the economical aspect as the approach is time consuming and incurs substantial costs.

The modification of existing polymers is an alternative route for functionalizing either the selective layer or the bulk of the membrane. This is realizable by various techniques

including chemical modification, thermal annealing, ion-beam irradiation and plasma treatment [16-26]. Hayes proposed a diamine modification approach as a post-treatment for polyimide membranes [16]. This technique was comprehensively examined by Chung and co-workers for enhancing the CO_2/CH_4 and H_2/CO_2 separation performance of polyimide membranes [17-19]. The simplicity and applicability to asymmetric hollow fiber membranes are the merits of this approach but the reversible nature of the reaction at high temperatures constitutes a major limitation [18,20]. Wind et al. employed diol crosslinking at elevated temperatures for polyimides containing carboxylic acid groups to improve CO_2/CH_4 selectivity and to suppress CO_2-induced plasticization of the dense membrane [21-22]. The diol crosslinking technique has been implemented on hollow fiber membranes by Omole et al. In their study, the diol-grafted polyimide is used for fabricating the hollow fibers via phase inversion and the subsequent thermal annealing of the membrane leads to the formation of diol cross-links [23]. However, the diol crosslinking approach is only applicable for polyimides containing carboxylic acid groups. Bromination, sulfonation and metal-ions exchange are other means to chemically modify polymers [24-25]. Despite the potential use of ion-beam irradiation and plasma treatment in altering the gas transport properties, the high cost and difficulty in obtaining uniform modification may limit the industrial application of this technique. Polymer modification is simple and may produce significant changes in the properties of the resultant organic matter. However, the long term performance and stability of the membranes may become questionable when subjected to aggressive feeds and harsh operating conditions.

Polymer blending is a viable approach which may synergistically combine the merits of different materials [27-31]. Generally, polymer blends display varying degrees of miscibility and homogenous blends are preferred for membrane fabrication since the uniformity is a pre-requisite for stable and reliable membrane performance [27-31]. The resultant polymer blends may exhibit exceptional properties that supersede the respective native polymers. Maeda and Paul explored the use of poly(phenylene oxide)/polysulfone blends in gas separation and for specific blend compositions, the resultant CO_2/CH_4 selectivity exceeds that of the pure component polymers [28]. Bos et al. developed Matrimid®/P84 blend membranes with anti-CO_2 plasticization characteristics and good CO_2/CH_4 separation performance [30]. The advantages of polymer blending are simplicity, reproducibility and relatively short development time since it utilizes the existing polymer database. Nevertheless, one severe deficiency of polymer blending is the issue of component miscibility. In fact, there is limited availability of polymer pairs which are compatible with each other and most blends exhibit phase separation at certain compositions.

Interpenetrating polymer network (IPN) is a refinement of linear polymer blends where two different polymer networks physically intermingle with each other in the same spatial region without chemical bonds between them [32-38]. In distinction to linear polymer blend systems where coarse phase separation frequently occurs, the physical interconnections present in an IPN greatly enhances the degree of polymer compatibility. A network polymer that encompasses a linear polymer gives rise to a pseudo- or semi-IPN [32]. A pseudo-IPN is produced either by (1) the polymerization of the precursors of

a branched polymer in the presence of a pre-formed linear polymer or (2) the formation of a straight-chain polymer within a pre-existing network. One shortcoming of the aforementioned methods for producing pseudo-IPNs is the extractability of the linear component from the composite material [32]. Therefore, attempts were made to immoblize the linear component within the semi-IPN via chemical bonds with the networked polymer [32,34]. This results in interconnected pseudo-IPNs and it has been shown that such intra-linkages greatly influence the structural properties of the resultant materials. IPNs are novel and versatile composite materials for many applications, including their prospective use as a barrier material for gas separation. The interconnections between the constituent polymers in an IPN possibly reduce the undesirable swelling effects of polymers by highly condensable gases. This favorable characteristic of IPNs may be exploited in natural gas purification which involves plasticizing components like CO_2 and H_2O. Despite the merits of IPN materials and their potential use in membrane gas separation, the studies devoted to this research area are rather limited [39-44].

In this study, a synthetic strategy for the construction of pseudo-IPNs by the polymerization of multi-functional azido-containing monomers within pre-formed linear polyimide frameworks is explored. Considering the ability of 2,6-bis(4-azidobenzylidene)-4-methylcyclohexanone (azide) to react spontaneously in the presence of heat or UV light and its rigid conjugated structure, it was chosen as the monomer for creating the network polymer [40]. Here, the network polymer formed by the azide monomer is termed poly(azide). Polyimide has not been extensively investigated as a

component for forming IPN materials. In view of its superior intrinsic properties, it is worthwhile to explore its application in this area. Hence, fluorinated polyimides, poly(1,5-naphthalene-2,2'-bis(3,4-phthalic) hexafluoropropane) diimide (6FDA-NDA) and poly(2,3,5,6-phenylene-2,2'-bis(3,4-carboxylphenyl) hexafluoropropane) diimide (6FDA-TMPDA), with high free volume and rigidity were selected as the host polymers for creating the pseudo-IPNs. The high free volume provides the opportunity to manipulate the cavity distribution of the resultant composite material upon the formation of the branched poly(azide). The anticipated change in the free volume distribution is likely to impact the gas transport properties of the membranes. Aromatic polyimides with limited chain mobility provide the ideal rigid frameworks for the polymerization of azide. A firm molecular scaffold is essential to minimize the likelihood of generating a phase separated semi-IPN. This is attributed to the fact that when the azide monomers react to form a polymer network, there is a tendency for the branched macromolecule to push apart the existing linear polymer chains. Hence, the susceptibility of the linear pre-polymers to the molecular force results in the formation of undesirable phase separated domains [33].

6FDA-based polyimide/azide membranes with varying compositions are fabricated and characterized. The chemical reactions occurring during the thermal treatment are investigated in order to elucidate and validate the pseudo-IPNs formation. Depending on the functionalities of the host polymer, chemical crosslinks may be formed between the linear and the branched polymer, resulting in an interconnected pseudo-IPN. The homogeneity and thermal properties of the semi-IPN membranes are analyzed, and the

changes in the free volume and free volume distribution in relation to the gas transport properties of the composite films are discussed. The CO_2/CH_4 separation performance and CO_2–induced plasticization behavior of these semi-IPN membranes are highlighted.

8.2 Results and Discussion

8.2.1 Chemical reactions of 2,6-bis(4-azidobenzylidene)-4-methylcyclohexanone

In this study, the chosen azido-containing monomer for creating the network polymer is of complicated chemical nature due to the presence of various reactive functional groups. This section aims to elucidate the relative reactivity of different functional groups. The azido group, N_3 is a linear 1,3-dipolar structure which easily forms nitrene in the presence of heat or ultra-violet radiation. Nitrenes are highly reactive, short-lived nitrogen intermediates. The nitrogen atom has four non-bonded electrons which accounts for the electrophilicity of nitrene. Nitrenes are capable of insertion into C-H bonds and addition to unsaturated C-C bonds (i.e. alkenes, alkynes and arenes) [45]. Figure 8.1 shows the formation of nitrene and the possible reactions of the different functional groups with the nitrene radical.

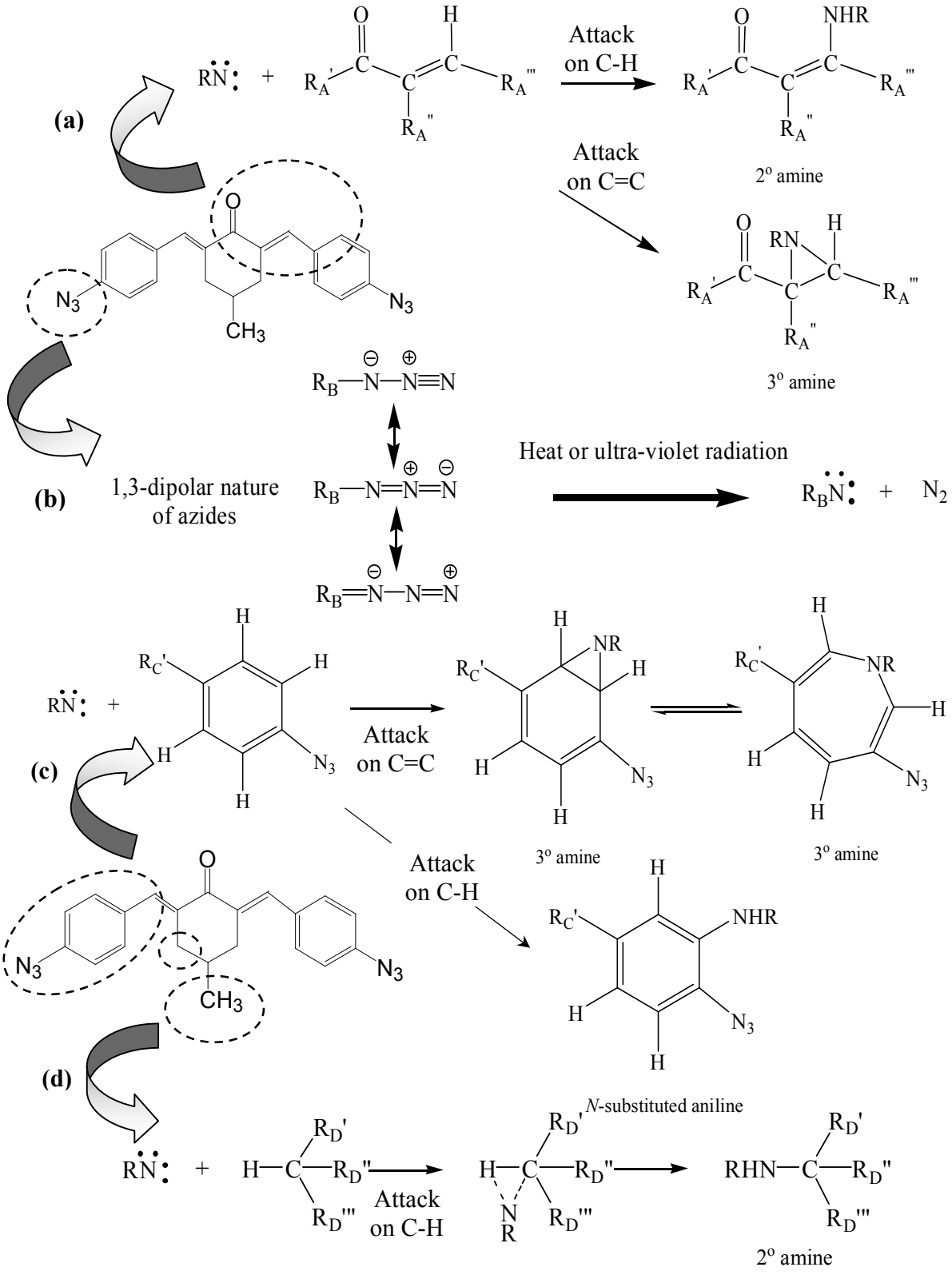

Figure 8.1 (a) Reactions of nitrene with alkene C=C and C-H bonds, (b) generation of nitrene from azide, (c) reactions of nitrene with benzene C=C and C-H bonds and (d) reaction of nitrene with alkyl C-H bonds

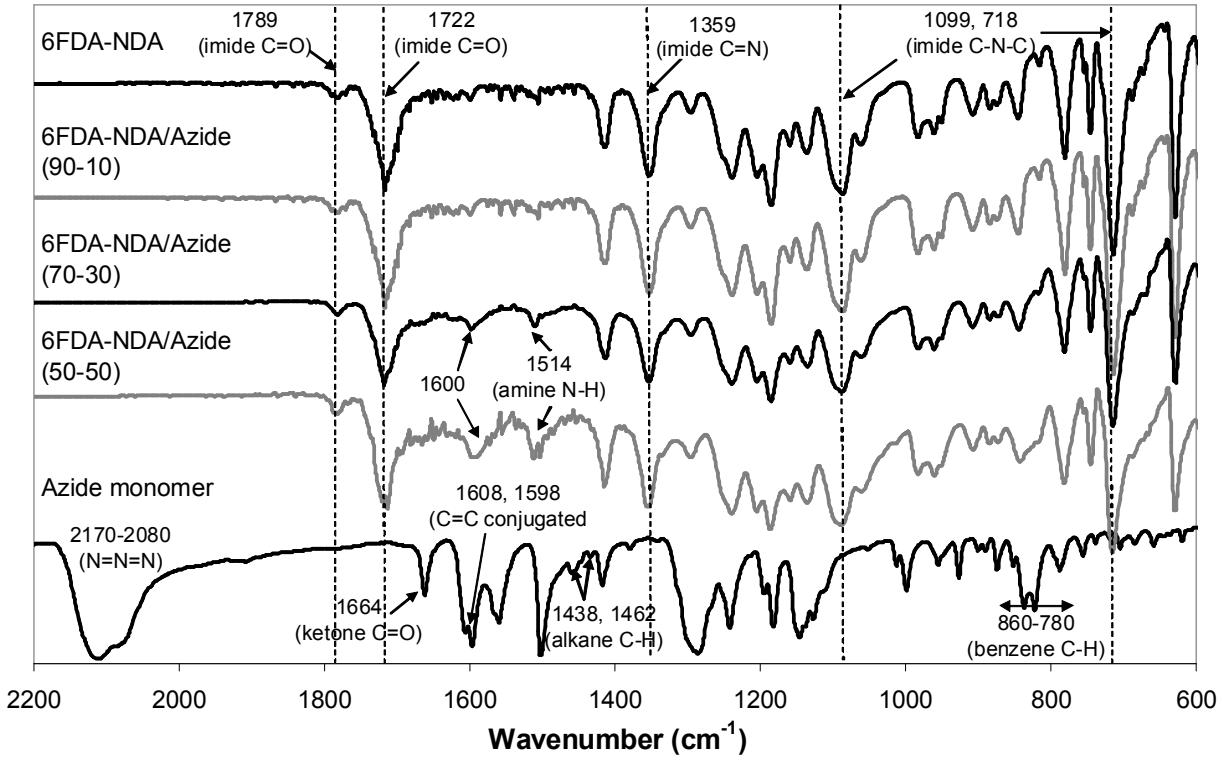

Figure 8.2 FTIR spectra of 6FDA-NDA, 6FDA-NDA/azide films and azide monomer

FTIR analyses were performed to verify the reactions induced by the azide monomer. Figure 8.2 depicts the FTIR spectra for the azide monomer and 6FDA-NDA/azide films. Referring to the spectrum for azide, the strong band in the region 2170-2080 cm^{-1} is due to the asymmetric stretching vibration of the N=N=N group [46]. The prominent peak at 1664 cm^{-1} is attributed to C=O stretching vibration of the α,β-,α',β'-di-unsaturated ketone (i.e. >C=C-CO-C=C<) [46]. The C=C stretching vibration of this conjugated system gives rise to a doublet at 1608 and 1598 cm^{-1}. The series of bands in the region 860-780 cm^{-1} result from the C-H out-of-plane vibrations of 1,4-disubstituted benzenes [46]. The peaks at 1438 cm^{-1} and 1462 cm^{-1} reflect the alkane C-H deformation vibrations [46]. The pristine 6FDA-NDA film exhibits two peaks at 1719 cm^{-1} and 1789 cm^{-1} which are

attributed to the carbonyl group of the imide ring [19]. The characteristic peak at 1356 cm^{-1} is due to the C-N stretch of the imide group while the peak at 1095 cm^{-1} is indicative of the transverse stretch of C–N–C in the imide group [19]. The peak at 716 cm^{-1} is due to the out-of-plane bending of C–N–C in the imide group [19].

With the incorporation of azide to the polyimide host, the characteristic peak of the N=N=N group is not observed. This provides evidence for the formation of nitrene (Figure 8.1 (b)) and its subsequent reaction i.e. polymerization of azide. With reference to Figure 8.2, the addition of azide results in the appearance of two strong peaks at 1600 and 1514 cm^{-1}. The transformation of the original doublet at 1608 and 1598 cm^{-1} of the azide monomer to the single peak at 1600 cm^{-1} for the 6FDA-NDA/azide films indicates some changes in the chemical functionalities. The peak at 1600 cm^{-1} may be attributed to the presence of α,β-unsaturated ketones with a β-amino group (Figure 8.1 (a), reaction with C-H bond) [46]. This implies that the C-H bond at the β-position of the unsaturated ketone is susceptible to electrophilic attacks by nitrenes. The intra-molecular hydrogen bonding between the amino and ketone group accounts for the slight broadening of this peak. The peak at 1514 cm^{-1} is representative of the N-H deformation vibration of secondary amines [46]. Generally, the selectivity of C-H insertion follows the reactivity pattern of tertiary > secondary > primary C-H bonds [45]. The alkane C-H deformation vibration of the azide monomer is not observed in the composite polymeric films which support the C-H insertion of nitrenes (Figures 8.1 (a) and (d)). Conversely, the series of bands reflecting the C-H out-of-plane vibrations of the di-substituted benzenes are present with some slight changes in the peak intensity and position. This is due to the co-

existence of 1,4-disubstituted phenylene rings of the poly(azide) and the naphthalene structure of the polyimide. Due to the stability of the benzene ring which comprises the highly conjugated π electrons, the C-H bonds of the phenyl group are not easily attacked by the nitrene radicals (Figure 8.1 (c)). The homolytic bond dissociation energies for CH_3-H and C_6H_5-H are 435 kJ/mol and 460 kJ/mol, respectively [47]. This implies that the reaction between nitrene and alkyl C-H bond is more feasible from the thermodynamics aspect. The characteristic peak of tertiary amine is not observed which indicates that the cycloaddition of nitrenes to the phenyl ring and the C=C bonds has not occurred (Figure 8.1 (c)). The unfavorable addition of nitrene to the C=C bonds has been reported by Kelman et al. and Shao et al. where azido-containing compounds were used to crosslink rubbery poly(1-(trimethylsilyl)-1-propyne) (PTMSP) and poly(4-methyl-2-pentyne) (PMP), respectively [48-49]. Similar results are obtained from the FTIR spectra of 6FDA-TMPDA/azide films.

Based on the reaction chemistry of nitrenes and the chemical functionalities of the host polyimides, the following conclusions can be made. The azide monomer with multi-reactive sites reacts with its own species to form a network polymer. The nitrene radicals react with the C-H bonds of the (1) α,β-unsaturated ketone, (2) - CH_3 substituent group and (3) cyclohexanone structure. There is no reaction with the alkene and benzene C=C double bonds due to the presence of steric hindrance and the high stability of the conjugated system. The higher bond dissociation energy of the aromatic C-H bond makes its less vulnerable to nitrene attack. For the two host polyimides which are considered in our study here, the main difference is the presence of –CH_3 groups in the diamine

moieties. 6FDA-NDA does not contain any functional groups that potentially react with azide while 6FDA-TMPDA with the methyl substituent groups may reacts with azide. Hence, depending on the chemical nature of the host polymer, the combination of polyimide and poly(azide) may results in a pseudo-IPN or an interconnected pseudo-IPN.

8.2.2 Validation of the formation of a pseudo-IPN and interconnected pseudo-IPN

The gel content of 6FDA-NDA/azide and 6FDA-TMPDA/azide films annealed at different temperatures is shown in Figures 8.3 (a) and (b), respectively. The existence of the insoluble gel in the film reflects the formation of crosslinked networks. Comparing the gel content of the membranes with polyimide/azide composition of 90/10, 6FDA-NDA/azide films dissolve completely in the solvent regardless of the annealing temperature. Conversely, for the 6FDA-TMPDA/azide film annealed at 100 ^{o}C, the gel content is approximately 60 wt% and beyond an annealing temperature of 150 ^{o}C, the film contains more than 90 wt% of insoluble mass. The low extractability of 6FDA-TMPDA/azide films implies that these two components react with each other to form an inter-connected pseudo-IPN. The high gel content of 6FDA-TMPDA/azide (70/30) film was further verified by using a stronger solvent (i.e. NMP) for extraction at 180 ^{o}C. Referring to Figure 8.3 (b), the extractability of the film in NMP is higher than in DMF. Nevertheless, a high gel content of > 90 % is obtained for the film that is annealed at 250 ^{o}C. Based on the discussion in Section 8.3.1, the nitrene radicals react with the methyl C-H bonds of 6FDA-TMPDA to form chemical cross-links. Considering the variation in the

gel content of 6FDA-TMPDA/azide films annealed at different temperatures, it can be inferred that the incipient reaction of azide falls between 80-100 ^{o}C.

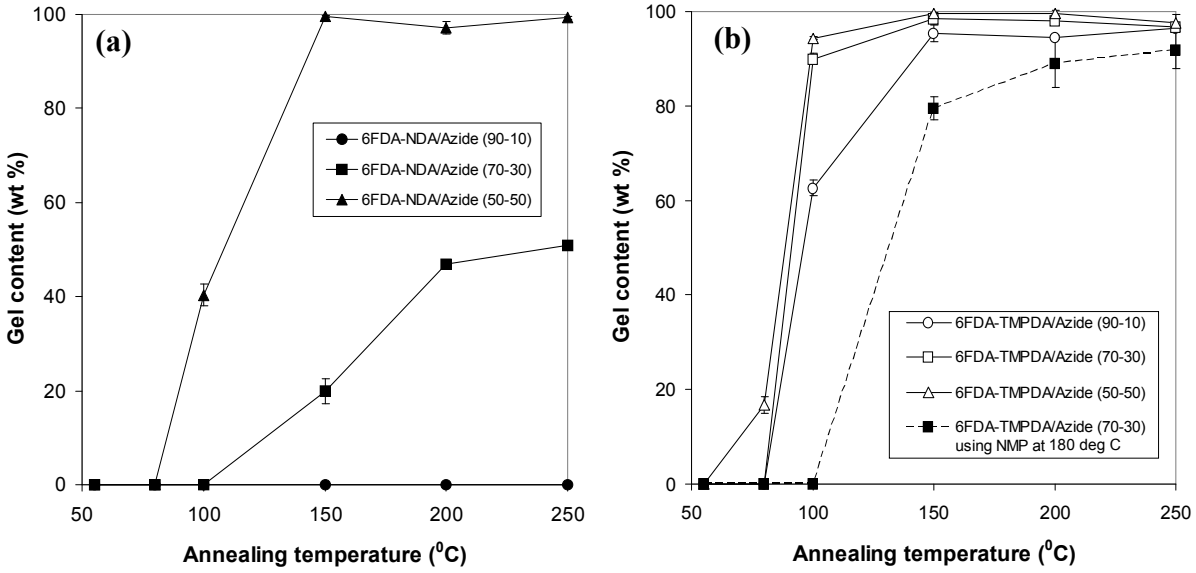

Figure 8.3 Gel content of (a) 6FDA-NDA/azide and (b) 6FDA-TMPDA/azide films using DMF and DCM as solvents, respectively (unless otherwise stated)

When 6FDA-NDA is used as the host polyimide, the azide monomer solely reacts with its species to form a polymer network which physically interlocks the linear polyimide chains. At a low azide concentration of 10 wt%, the degree of interpenetration between 6FDA-NDA and the poly(azide) is limited. Thus, the resultant films dissolve completely in the solvent. Referring to Figure 8.3 (a), at higher azide concentrations, the gel content of the films increases and for the 6FDA-NDA/azide films annealed beyond a temperature of 150 ^{o}C, the gel content is > 90 wt%. Hence, the extent of interpenetration between 6FDA-NDA and the in-situ formed branched polymer improves significantly which makes it is difficult for the solvent molecules to extract the linear polymer chains.

Since a significant portion of the 6FDA-NDA/azide films (90/10 and 70/30) is soluble in DMF (i.e. the solvent for 6FDA-NDA), it would be interesting to analyze the molecular weights of the soluble components. It is believed that most of the soluble mass should be contributed by the linear host polyimide which has better extractability in the solvent. The chromatograms obtained from the GPC analyses are depicted in Figure 8.4. For 6FDA-NDA, the shoulder peak at an elution time of approximately 24 min represents the population of the polyimide with lower molecular weights. With the addition of azide, the intensity of this shoulder peak decreases considerably. Moreover, it can be seen that the molecular weight distributions of the soluble components progressively shift towards a lower elution time (i.e. higher molecular weight) as the composition of azide increases.

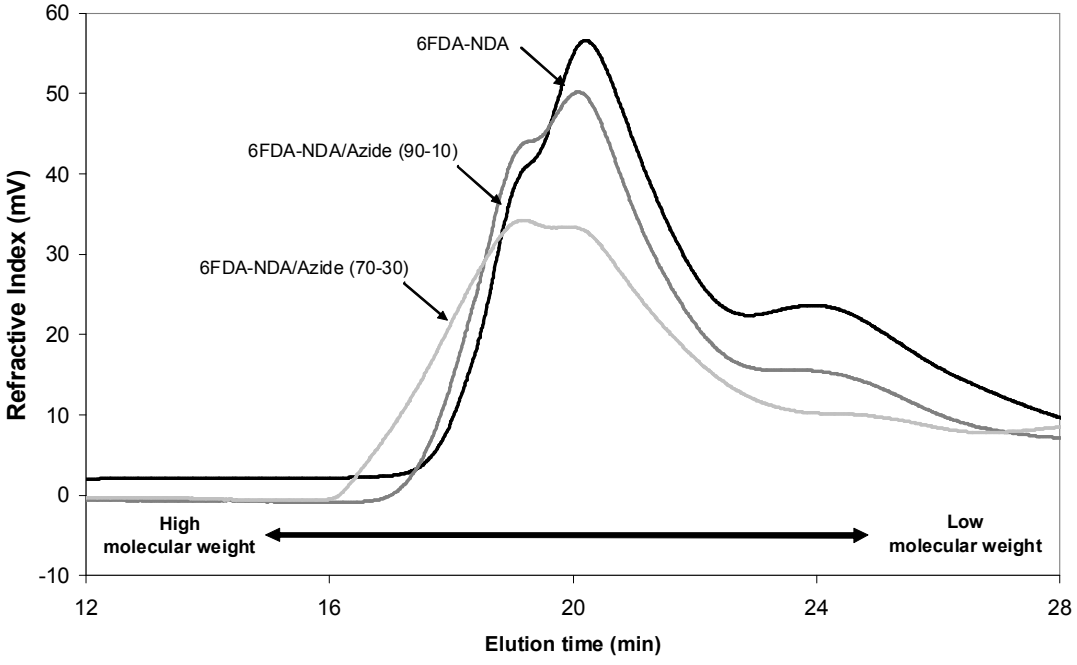

Figure 8.4 GPC analysis of the soluble portions of 6FDA-NDA/azide films

The shift in the molecular weights distribution may be attributed to the entanglement of the linear polyimide with the poly(azide) in the solvent. At low concentrations of azide, the monomers are sparsely dispersed in the polyimide host and the resultant membrane contains tiny domains of low molecular weights poly(azide) embedded in the polyimide matrix. The small domains of poly(azide) are easily extracted together with the polyimide in the solvent and they probably remain entangled in the solution. However, as the concentration of azide increases, the size of the poly(azide) domains becomes larger. Hence, the size of the extractable poly(azide) in entanglement with the polyimide similarly increases. The insoluble portions comprise of extensive networks that physically interlock the linear chains effectively and block the access of the solvent molecules. The conclusions drawn from the FTIR, gel content and GPC analyses are 6FDA-NDA/azide forms a pseudo-IPN (Figure 8.5 (a)) while 6FDA-TMPDA/azide results in an interconnected pseudo-IPN (Figure 8.5 (b)).

8.2.3 Physical properties of the pseudo IPNs

The homogeneity of a material is an important requirement for its use in all applications. For polymers that constitute two or more components, the miscibility of the components determines the overall homogeneity. The transparency of the polymer film provides a preliminary indication of the degree of miscibility i.e. transparent films signify uniformity while opaque films indicate possible phase separation between the components. The 6FDA-NDA/azide films are completely transparent even for a high azide composition of 50 wt%. However, for 6FDA-TMPDA/azide films, at an azide content of 50 wt%, the as-

cast film is opaque and heterogeneous. This suggests the likely occurrence of phase separation between the 6FDA-TMPDA and poly(azide) phases. The variation in the degree of miscibility may be attributed to the (1) difference in the solvent used, (2) film casting temperature, (3) solvent evaporation rate, and (4) chemical structure and functionalities of the host polyimides. The polymeric membranes, with the exception of 6FDA-TMPDA/azide (50:50) film which is inherently brittle, have good mechanical properties. The non-uniformity and brittleness of the 6FDA-TMPDA/azide (50:50) film limits its application and further characterization of this membrane is unnecessary.

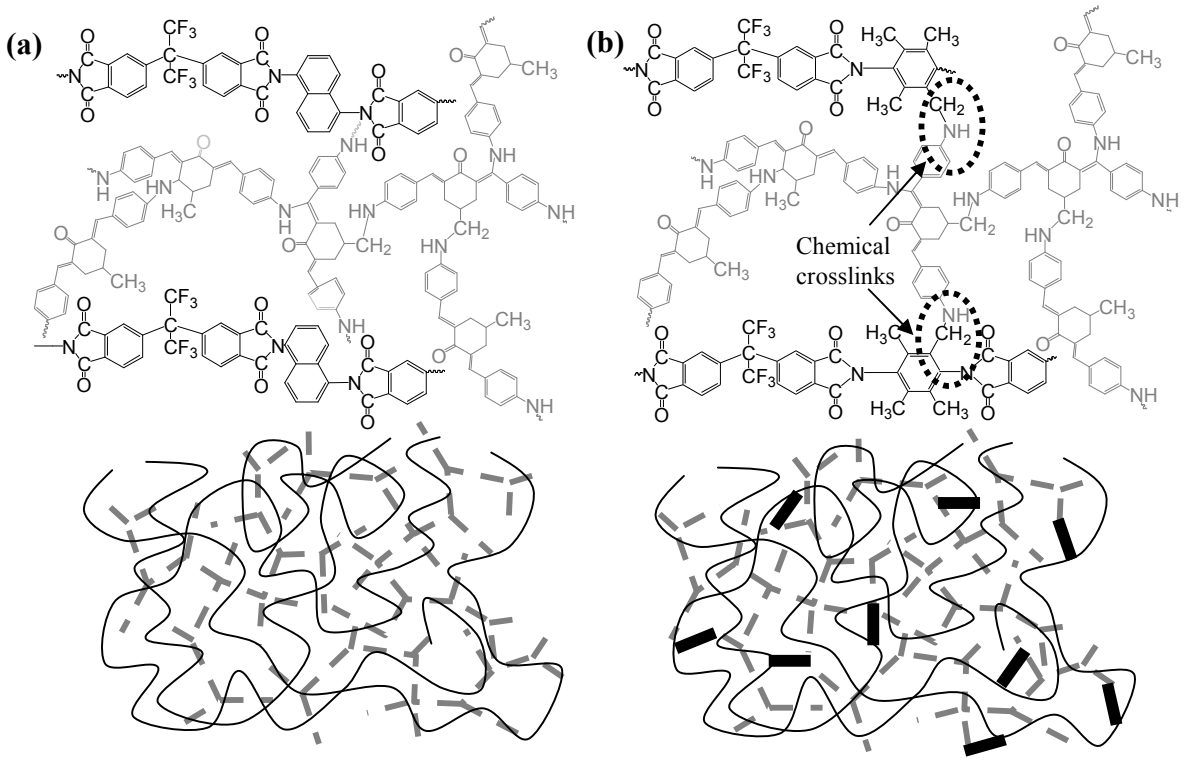

Figure 8.5 Schematics of (a) 6FDA-NDA/azide pseudo-IPN and (b) 6FDA-TMPDA/azide interconnected pseudo-IPN
IPN: (__) host polyimide; (grey bar) poly(azide) network; (black bar) chemical cross-links

The glass transition temperatures of the composite polymeric films were investigated and the results are shown in Figures 8.6 (a) and (b). The presence of a single glass transition temperature is taken as a proof of the blend homogeneity for the pseudo-IPNs. For 6FDA-NDA, the incorporation of azide brings about a significant decline in the glass transition temperatures (T_g). An attempt was made to cast a pure azide solution and it was found that it has poor film forming properties. Upon solvent evaporation, only small pieces of the poly(azide) samples remain. In order to approximate the T_g of poly(azide), DSC was conducted for this sample. The poly(azide) shows a glass transition temperature of 282.6 ^oC. Therefore, the lower T_g of poly(azide) compared to 6FDA-NDA accounts for the decrease in T_g after the addition of Azide. The pristine 6FDA-NDA polyimide exhibits a sharp transformation in the exothermic heat flow at the glass transition temperature while the change for the 6FDA-NDA/azide films occurs over a broad temperature range. The broadening of the glass transition indicates the co-existence of multiple nano-domains with varying compositions (i.e. nano-hetereogeneities) [33]. Each of these nano-domains has its own T_g and the resultant distribution of T_gs accounts for the observed broadening at the transition. For 6FDA-TMPDA/azide films, the decrease in T_g is less drastic. The chemical crosslinks formed between the poly(azide) and 6FDA-TMPDA restrict the chain movement of the host polyimide and increase its T_g. This partially counteracts the effect of lowering T_g attributed by the poly(azide) phases. A similar broadening of the glass transition for 6FDA-NDA/azide films is observed for 6FDA-TMPDA/azide. DMA was conducted for the pseudo-IPNs and the results are shown in Figures 8.7 (a) and (b). The tan δ displays a single local maximum as a function of temperature which further proves the homogeneity of the material.

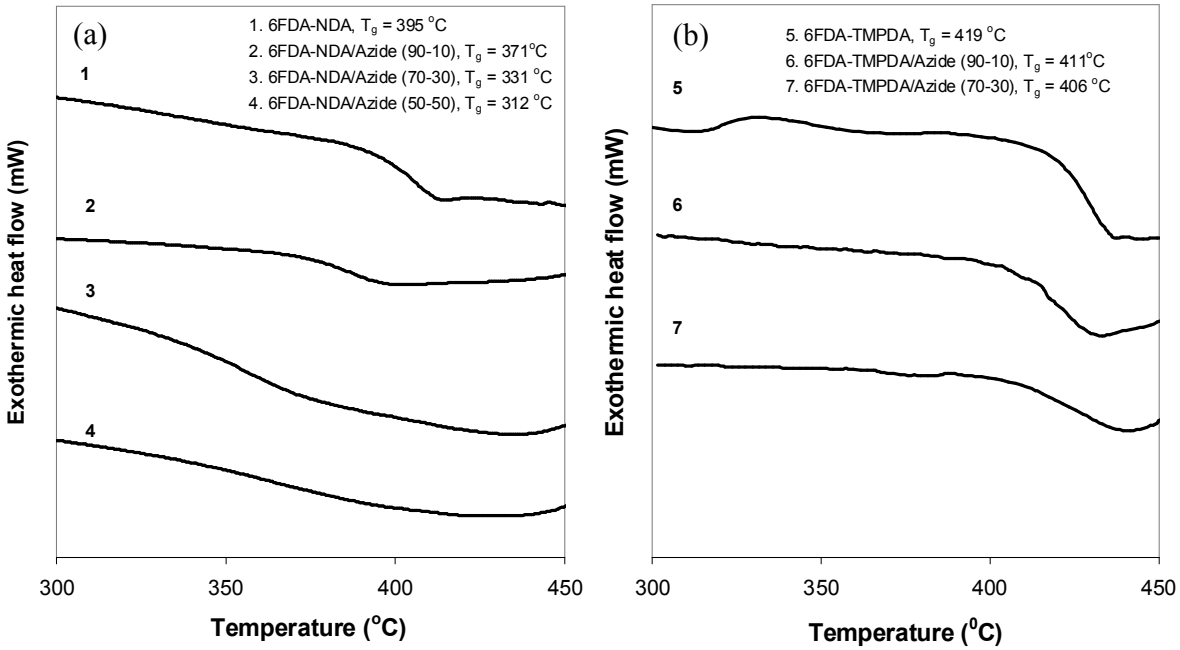

Figure 8.6. DSC analysis of (a) 6FDA-NDA/azide and (b) 6FDA-TMPDA/azide films

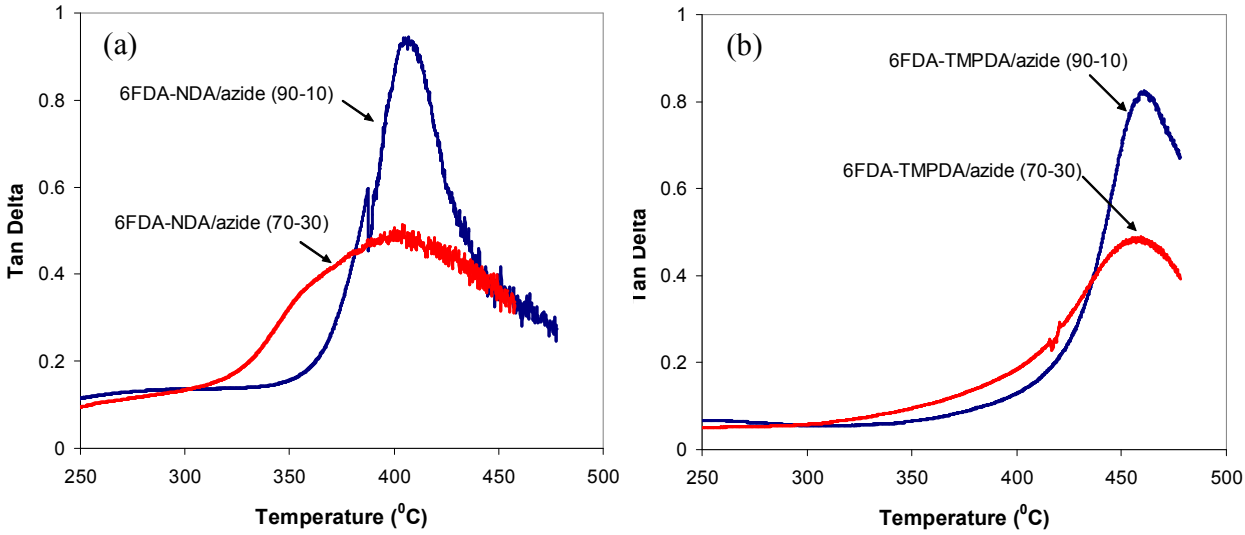

Figure 8.7 DMA of (a) 6FDA-NDA/azide and (b) 6FDA-TMPDA/azide films

The thermal degradation properties of the pseudo-IPNs were analyzed and the temperatures at 5 % weight loss are summarized in Table 8.1. The incorporation and polymerization of azide within the polyimide frameworks decrease the thermal stability

of the membranes. This is attributed to the lower degradation temperature of the poly(azide) domains. Comparing the decomposition temperatures of the pseudo-IPNs (i.e. 380-470 ^{o}C depending on the composition of azide) with other polymers, the thermal properties of the composite materials are not inferior and are sufficient for use in most polymeric membrane-based separations. The derivative weight loss for all the pseudo-IPNs shows two major degradation peaks, one in the range of 300-500 ^{o}C and the other between 500-700 ^{o}C. The former is a due to the decomposition of the azide domains while the latter is attributed to the degradation of the polyimide domains. There is no indication of reaction reversibility for both the pseudo-IPNs at elevated temperatures.

Table 8.1 Thermal decomposition properties of 6FDA-polyimide/azide pseudo IPNs

Sample	Temperature at 5% weight loss (^{o}C)
6FDA-NDA	516.5
6FDA-NDA/Azide (90-10)	468.4
6FDA-NDA/Azide (70-30)	418.0
6FDA-NDA/Azide (50-50)	381.3
6FDA-TMPDA	504.6
6FDA-TMPDA/Azide (90-10)	432.3
6FDA-TMPDA/Azide (70-30)	394.1
6FDA-TMPDA/Azide (50-50)	-
Poly(azide)	359.8

The chain packing of the pseudo-IPNs and the free volume distribution were investigated. Figures 8.8 (a) and (b) shows the results obtained from the XRD analyses of the 6FDA-NDA/azide and 6FDA-TMPDA/azide films. For the 6FDA-NDA/azide films, the addition of azide leads to a marginal decrease in the average d-space from 5.7 to 5.5 Å. Moreover, the intensities of the shoulder peaks at $2\theta = 20$ and 26^{o} (corresponding d-spaces of 4.4 and

3.4 Å) with respect to the prominent amorphous peak show gradual increases at higher Azide contents. Similarly, for 6FDA-TMPDA/azide films, the d-space changes from 6.0 to 5.7 Å with the incorporation of azide. The addition of azide alters the chain packing of the original host polyimides and densifies the polymer matrix.

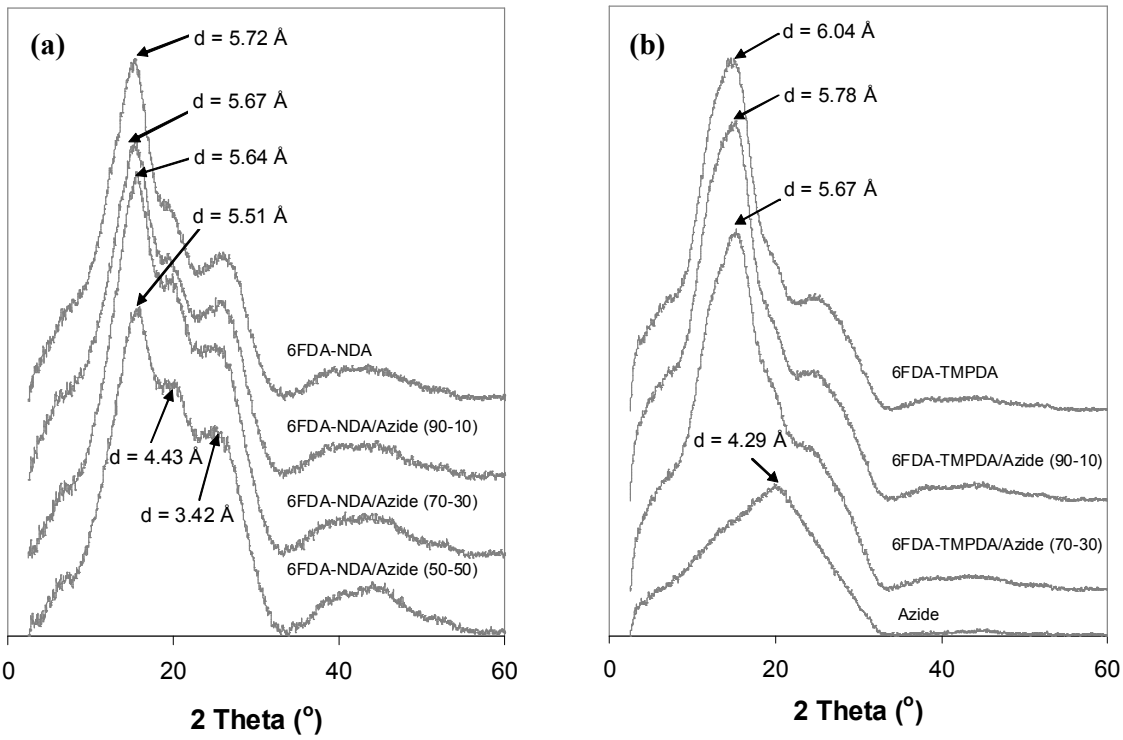

Figure 8.8 XRD analysis of (a) 6FDA-NDA/azide and (b) 6FDA-TMPDA/azide films

The free volumes and free volume distributions of the peudo-IPNs were probed using PALS. The raw data obtained were resolved into three finite lifetime components using the PATFIT program which assumes a Gaussian distribution for the logarithm of the lifetime for each component [50]. The first component is due to the annihilation of para-positronium (p-Ps) ($\tau_1 \approx 0.125$ ns), the second is contributed by the free positrons ($\tau_2 \approx$ 0.4 ns) and the last component is attributed to the annihilation of localized ortho-

positronium (o-Ps) in the polymer free volume (τ_3 > 0.5 ns) [51]. Thus, τ_3 is a useful parameter for determining the average cavity size in the polymer and the corresponding intensity, I_3 reflects the quantity of cavities present. The mean free-volume radius (r_3 in Å) can be computed using a semi-empirical equation based on a spherical infinite potential well model as shown by equation (8-1) [51].

$$\tau_3^{-1} = 2\left[1 - \frac{r_3}{r_3 + \Delta r} + \frac{1}{2\pi}\sin\left(\frac{2\pi(r_3)}{r_3 + \Delta r}\right)\right] \tag{8-1}$$

where Δr is an empirical constant (1.656 Å) obtained by fitting well-defined cavities with known dimensions (e.g. zeolites). Since the cavities are assumed to be spherical, the mean free volume of a cavity and the relative fractional free volume are given by equations (8-2) and (8-3), respectively [51].

$$v_{f3} = \frac{4}{3}\pi(r_3)^3 \tag{8-2}$$

$$FFV = C_m I_3 v_{f3} \tau_3 \tag{8-3}$$

where C_m is a material-dependent constant (0.001-0.003 for polymers). The positronium lifetimes and intensities, and the calculated free volume radius and FFV are summarized in Table 8.2.

Generally, the addition of azide to the host polyimides decreases the τ_3 and I_3 values. This means that the formation of a poly(azide) network within the linear polyimide framework leads to smaller cavity sizes and reduces the quantity of free volume. A comparison between the pristine 6FDA-NDA film and the pseudo-IPN with 10 wt% azide shows that the τ_3 decreases from 2.94 to 2.57 ns while the corresponding r_3 changes from 3.60 to 3.33 Å. Further increase in the azide content does not adjust the τ_3 and r_3 values. I_3 which

indicates the quantity of free volume, decreases from 5.36 to 1.55 % as the azide content in the film increases from 0 to 50 wt %. The corresponding FFV changes from 1.88 to 0.43%. These demonstrate that a small amount of azide is sufficient to fulfill the purpose of altering the free volume cavity size while an overdose of azide merely leads to diminishing free volume with no variation on the mean cavity size. For the 6FDA-TMPDA/azide films, raising the azide content from 0 to 30 wt% steadily decreases the τ_3 and I_3 values. In other words, both the size and quantity of the free volumes diminish gradually in the presence of more poly(azide) domains.

Table 8.2 Positronium lifetimes, intensities, mean free-volume radii and fractional free volume for 6FDA-NDA/azide and 6FDA-TMPDA/azide films

Sample	τ_3 (ns)	I_3 (%)	r_3(Å)	v_{f3}(Å^3)	FFV(%)
6FDA-NDA	2.94 ± 0.02	5.36 ± 0.06	3.60 ± 0.01	195.16 ± 1.67	1.88 ± 0.04
6FDA-NDA/Azide (90-10)	2.57 ± 0.03	2.66 ± 0.05	3.33 ± 0.02	154.97 ± 2.36	0.74 ± 0.02
6FDA-NDA/Azide (70-30)	2.59 ± 0.05	1.97 ± 0.05	3.35 ± 0.03	157.05 ± 3.70	0.56 ± 0.03
6FDA-NDA/Azide (50-50)	2.58 ± 0.04	1.55 ± 0.04	3.34 ± 0.02	155.40 ± 3.40	0.43 ± 0.02
6FDA-TMPDA	2.70 ± 0.02	6.13 ± 0.06	3.42 ± 0.01	168.13 ± 1.56	1.86 ± 0.03
6FDA-TMPDA/Azide (90-10)	2.60 ± 0.03	4.43 ± 0.06	3.36 ± 0.01	158.29 ± 2.02	1.26 ± 0.03
6FDA-TMPDA/Azide (70-30)	2.47 ± 0.03	3.87 ± 0.06	3.26 ± 0.02	144.57 ± 2.13	1.01 ± 0.03
6FDA-TMPDA/Azide (50-50)	-	-	-	-	-

To have a clearer picture of the free volume distribution of the pseudo-IPNs, MELT analysis was utilized and the results are illustrated in Figures 8.9 (a) and (b) [52]. The peak between 2 ns and 3.5 ns is attributed to the o-Ps annihilation in the amorphous region of the polymeric films [53]. Referring to Figure 8.9(a), the incorporation of 10 wt% azide to 6FDA-NDA shifts the peak to the left and a narrower distribution is observed. For 30 and 50 wt % Azide, the positions of the peaks remain essentially the

same but the peak intensities decrease. This is in agreement with the trend of constant τ_3 and decreasing I_3 concluded from the PATFIT results. For 6FDA-TMPDA/azide films, the incorporation of 10 wt% azide similarly shifts the peak to the right and a further increment to 30 wt% azide gives rise to a sharper distribution. Therefore, an effective tuning of the free volume cavities of the host polyimides can be achieved via the addition of appropriate amounts of azide monomers.

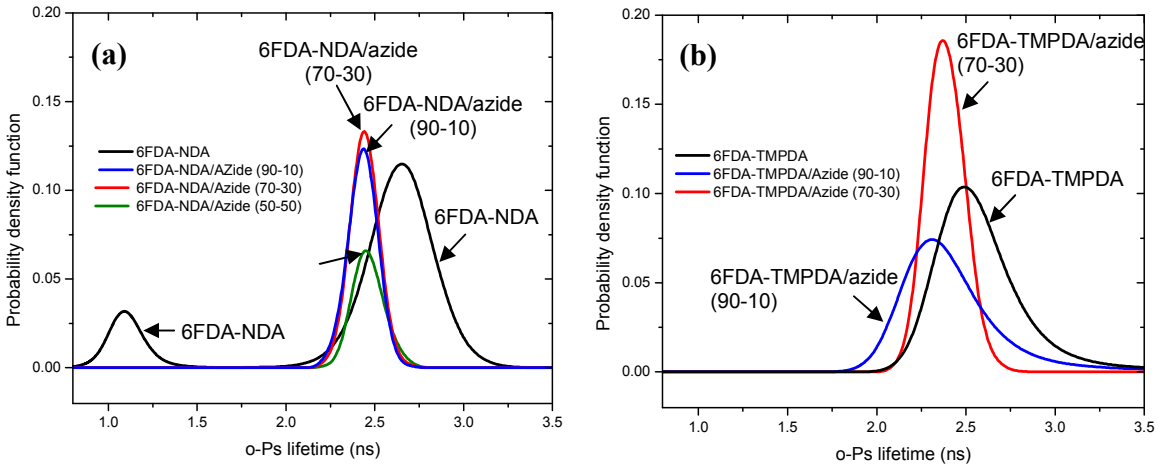

Figure 8.9 PALS analysis of the (a) 6FDA-NDA/azide and (b) 6FDA-TMPDA/azide films

8.2.4 Gas transport properties and potential application in membrane gas separation

The changes in the size and quantity of the cavities, and the free volume distribution of the pseudo-IPNs may be beneficial for the separation of small molecules by polymeric membranes. Therefore, the polyimide/poly(azide) composite films were analyzed for their gas transport properties. The pure gas permeability and ideal gas pair permselectivity of the pseudo-IPNs are shown in Tables 8.3 and 8.4, respectively. From Table 8.3, it can be seen that the gas permeability for both series of pseudo-IPNs decrease in the following

order: $P_{He} > P_{H2} > P_{CO2} > P_{O2} > P_{N2} > P_{CH4}$. This trend is in accordance to the kinetic diameters of the gases where d_{He} (2.60 Å) < d_{H2} (2.89 Å) < d_{CO2} (3.30 Å) < d_{O2} (3.46 Å) < d_{N2} (3.64 Å) < d_{CH4} (3.80 Å). The gas transport properties of the polymeric membranes can be correlated to the free volume and free volume distribution. PALS analyses have shown that the addition of azide decreases the size and quantity of free volume. This consequently reduces the available pathways within the polymeric matrix for gas transport to take place and thus the gas permeability decreases with increasing azide loadings as shown in Table 8.3. For both series of pseudo-IPNs, the increase in azide content decreases the relative FFV. The natural logarithm of the gas permeability is inversely proportional to the FFV which is in agreement with the exponential relationship between gas permeability and FFV proposed by Alentiev and Yampolski [54].

Table 8.3 Pure gas permeability of 6FDA-NDA/azide and 6FDA-TMPDA/azide films tested at 35 ^{o}C and 10 atm (unless otherwise stated)

Sample	Gas permeability (Barrer)						
	He	$H_{2\ (3.5\ atm)}$	O_2	N_2	CH_4	$CO_{2\ (3.5\ atm)}$	CO_2
6FDA-NDA	80.2	77.6	8.99	1.74	1.02	42.6	38.0
6FDA-NDA/Azide (90-10)	43.9	38.6	3.27	0.54	0.26	14.7	12.9
6FDA-NDA/Azide (70-30)	30.2	26.0	1.80	0.28	0.14	7.75	6.61
6FDA-NDA/Azide (50-50)	24.4	21.1	1.38	0.20	0.11	5.87	4.99
6FDA-TMPDA	261	358	69.9	19.4	15.5	362	315
6FDA-TMPDA/Azide (90-10)	153	186	29.3	7.12	5.29	155	133
6FDA-TMPDA/Azide (70-30)	79.4	86.1	9.65	1.97	1.22	44.1	38.6
6FDA-TMPDA/Azide (50-50)	-	-	-	-	-	-	-

Barrer = 1 x 10^{-10} cm^3 (STP)-cm/cm^2 s cmHg = 7.5005 x 10^{-18} m^2 s^{-1} Pa^{-1}

Table 8.4. Ideal gas pair permselectivity of 6FDA-NDA/azide and 6FDA-TMPDA/azide films

Sample	Permselectivity			
	O_2/N_2	CO_2/CH_4	H_2/CO_2	H_2/N_2
6FDA-NDA	5.18	37.4	1.82	44.6
6FDA-NDA/Azide (90-10)	6.06	49.5	2.63	71.6
6FDA-NDA/Azide (70-30)	6.43	47.2	3.35	92.9
6FDA-NDA/Azide (50-50)	6.90	45.4	3.60	105
6FDA-TMPDA	3.60	20.3	1.00	18.5
6FDA-TMPDA/Azide (90-10)	4.12	25.1	1.20	26.1
6FDA-TMPDA/Azide (70-30)	4.90	31.6	1.95	43.7
6FDA-TMPDA/Azide (50-50)	-	-	-	-

One point to highlight here is the gas permeability of the polymeric membrane is dependent on both the mean cavity size (i.e. r_3) and the quantity of free volume (i.e. I_3). PALS analyses utilize positron with a dimension of 1.6 Å to probe the free volume [53]. This means that cavity sizes larger than 1.6 Å are considered in the free volume analysis. However, the cavities with hole size in between 1.6 Å and the kinetic diameter of the gas are inaccessible to the gas molecules and do not contribute to the overall gas transport. From Table 8.2, the r_3 and relative FFV for 6FDA-NDA is greater than 6FDA-TMPDA but the gas permeability of the latter is more than three times higher than the former. One reason to account for this discrepancy is the inaccessible free volume of 6FDA-NDA possibly makes up a major portion of the total free volume probed by the positrons. Due to the complexity of the o-Ps formation within the polymer membranes, the I_3 value may be influenced by other parameters in addition to the quantity of free volume. In fact, the o-Ps pick-off annihilation intensity depends on the probability of o-Ps formation which is related to the chemical environment in which the o-Ps pickoff occurs. Both 6FDA-NDA and 6FDA-TMPDA consist of electrophilic imide rings but due to the different diamine moiety that constitutes each polyimide, the degree of electrophilicity varies. The

difference in the electron density affects the probability of forming a positronium i.e. bonding of a trapped positron to a free electron. With these intervening parameters in play, a direct comparison of the relative FFV obtained from PALS analysis for the two host polyimides may not be appropriate. For the pseudo-IPNs, the presence of the poly(azide) similarly changes the chemical environment. Nevertheless, for each series of pseudo-IPNs, the chemical species present are the same i.e. the host polyimide and the poly(azide). Hence, a comparison of the free volume data within each series of pseudo-IPNs is justifiable.

The incorporation of 10 wt% azide to 6FDA-NDA considerably enhances the CO_2/CH_4 selectivity from 37 to 50 which is attributed to the effective tuning of cavity sizes i.e. r_3 changes from 3.6 to 3.3 Å and the free volume distribution becomes narrower. The sharpening of the free volume distribution eliminates the larger cavities where CH_4 transport takes place more favorably. From Table 8.4, it is clear that further increase in the azide concentration brings about a slight decrease in the CO_2/CH_4 selectivity. The additional azide does not alter the mean cavity size but decreases the quantity of free volume for CO_2 transport i.e. smaller I_3. The decrease in the available free volume impacts CO_2 transport more than CH_4. The addition of azide from 0 to 50 wt% modifies the size and quantity of the free volume effectively, resulting in an increase in H_2/N_2 selectivity from 45 to 105. The improvement in H_2/CO_2 selectivity is not impressive as the transport of CO_2 is not effectively hindered. For O_2/N_2, only a slight increase in selectivity is obtained because of the close kinetic diameters of O_2 and N_2.

For 6FDA-TMPDA/azide interconnected pseudo-IPNs, the increase in the azide content from 0 to 30 wt% leads to a steady increase in the CO_2/CH_4 selectivity as the mean cavity size decreases from 3.4 to 3.3 Å. At a low azide content of 10 wt%, the free volume distribution shifts towards the region of lower cavity sizes while a further increment to 30 wt % azide significantly sharpens the free volume distribution as shown in Figure 8.9 (b). Moreover, the formation of chemical cross-links between the 6FDA-TMPDA and poly(azide) phases enhances the chain rigidity of the polymer chains, thereby enhancing the CO_2/CH_4 selectivity. The trends for the remaining gas pairs are similar to 6FDA-NDA/azide films. As depicted in Figure 8.10, the CO_2/CH_4 separation performances of the polyimides and the pseudo IPNs display typical trade-off relationship between permeability and permselectivity.

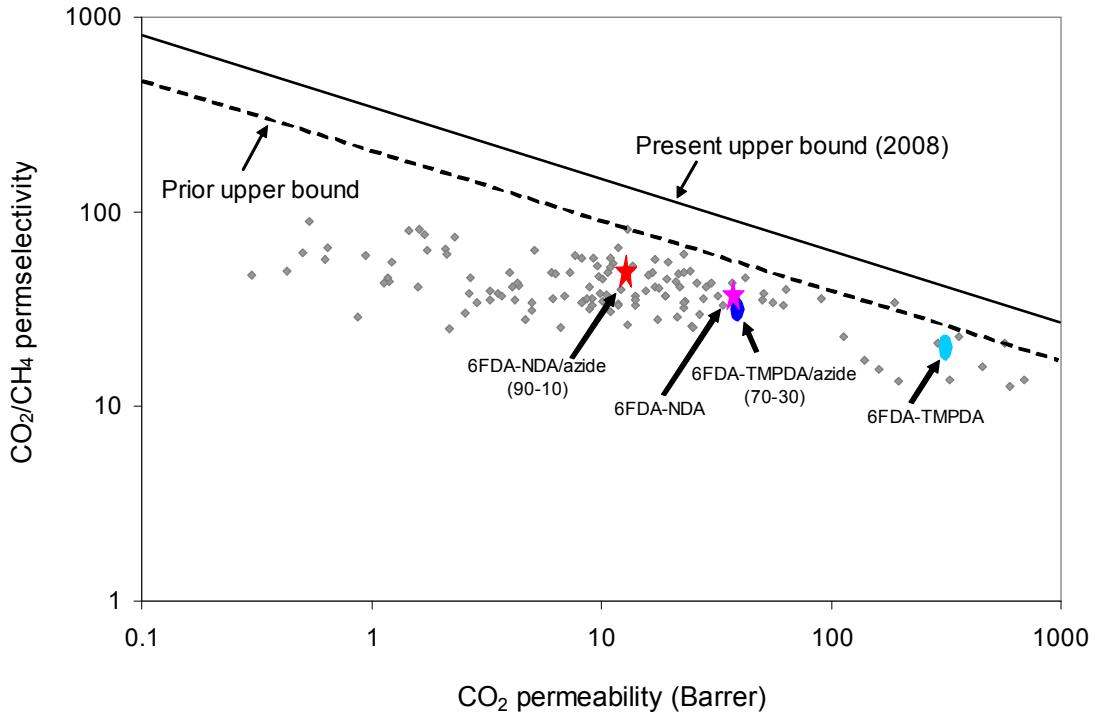

Figure 8.10 Comparison between the CO_2/CH_4 separation performance of the polyimide/azide membranes with the Robeson's upper bound

Binary CO_2/CH_4 tests were conducted for the pristine polyimide films and the pseudo-IPN membranes with good ideal permselectivity. A comparison of the gas separation performance of the membranes at different pressures is shown in Table 8.5. The results obtained from the mixed gas tests are in agreement with the pure gas permeation tests i.e. the addition of azide improves the CO_2/CH_4 permselectivity. Due to the competitive sorption effects rooted from the co-existence of two gas species in the feed stream, the gas permeability obtained from mixed gas tests is lower. As shown in Table 8.5, 6FDA-TMPDA suffers from severe CO_2-induced plasticization which accounts for the increase in CO_2 permeability and the significant loss of CO_2/CH_4 selectivity at elevated pressures. Conversely, 6FDA-NDA exhibits mild plasticization response where the CO_2 permeability stays relatively constant while the selectivity decreases. The incorporation of azide effectively eliminates the undesirable effects of CO_2-induced plasticization. The CO_2 permeability and CO_2/CH_4 selectivity of 6FDA-TMPDA/azide (70-30) and 6FDA-NDA/azide (90-10) decrease as the pressure increases. This is attributed to the saturation of CO_2 sorption sites at higher pressures.

Table 8.5 CO_2/CH_4 separation performance obtained from binary gas tests at 35 ^oC.

Sample	Binary CO_2/CH_4 (90:10) at 10 atm		Binary CO_2/CH_4 (90:10) at 20 atm		Binary CO_2/CH_4 (90:10) at 30 atm	
	P_{CO2} (Barrer)	$\alpha_{CO2/CH4}$	P_{CO2} (Barrer)	$\alpha_{CO2/CH4}$	P_{CO2} (Barrer)	$\alpha_{CO2/CH4}$
6FDA-NDA	25.8	45.9	25.8	41.8	26.0	32.2
6FDA-NDA/azide (90-10)	18.2	56.5	16.2	47.1	12.0	37.1
6FDA-TMPDA	246	24.8	254	18.1	276	9.3
6FDA-TMPDA/azide (70-30)	37.1	32.1	31.7	26.8	28.9	25.4

Barrer = 1 x 10^{-10} cm^3 (STP)-cm/cm^2 s cmHg = 7.5005 x 10^{-18} m^2 s^{-1} Pa^{-1}

A potential application of the polyimide/poly(azide) pseudo-IPNs is membrane-based natural gas sweetening. Membrane technology is attractive for the industrial purification of natural gas but one major limitation of using polymeric membranes is the tendency for the polymers to swell in the presence of plasticizing components i.e. CO_2, H_2S and H_2O. Plasticization results in pressure, temperature and time dependency of the membranes separation performance. Thus, polymeric membranes with anti-plasticization properties are desirable for reliable separation performance in the long run. In view of these concerns, the CO_2-plasticization behaviors of the pristine polyimides and the respective pseudo-IPN with the most promising CO_2/CH_4 selectivity were investigated.

The CO_2-plasticization curves are depicted in Figures 8.11 (a) and (b). 6FDA-NDA with the highly rigid naphthalene structures shows no sign of CO_2-induced plasticization up to a testing pressure of 30 atm and 6FDA-NDA/azide (90-10) showed similar decline in CO_2 permeability with increasing pressure. 6FDA-TMPDA is more easily swelled by the condensable CO_2 and the onset of CO_2-induced plasticization is at 15 atm. The addition of azide to 6FDA-TMPDA effectively suppresses this undesirable effect i.e. absence of CO_2-induced plasticization up to 30 atm. The formation of denser interconnected pseudo-IPNs restricts the chain movement and enhances the anti-plasticization property of the material.

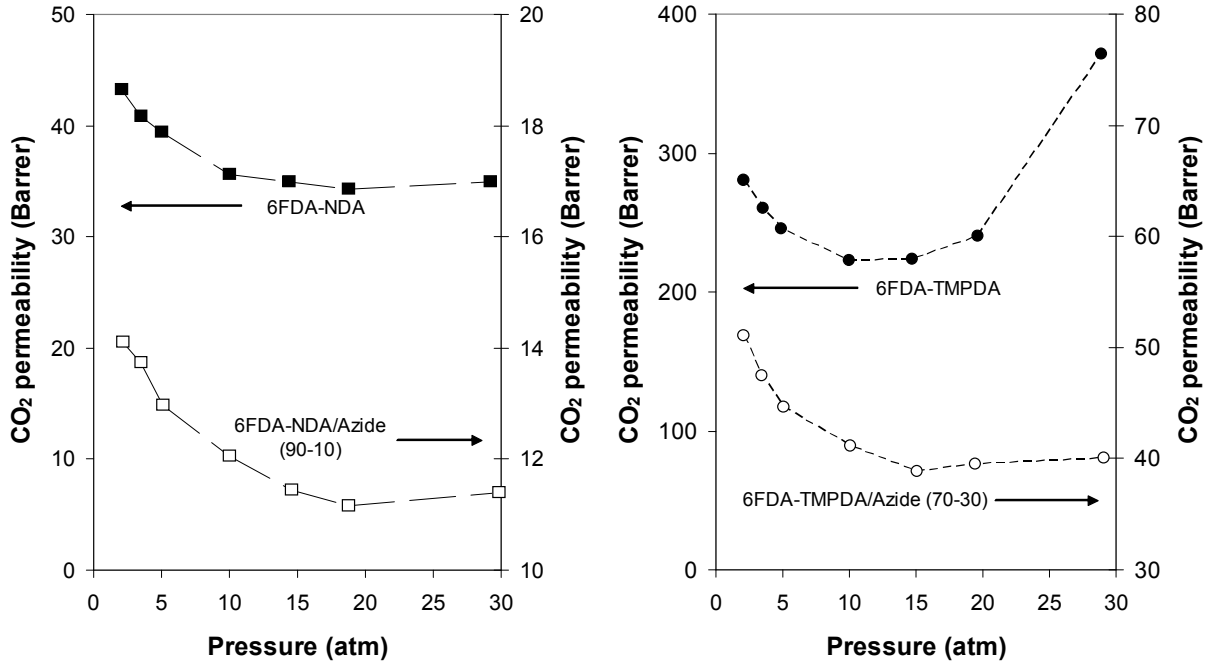

Figure 8.11 CO_2 plasticization behavior of (a) 6FDA-NDA and 6FDA-NDA/azide (90-10) and (b) 6FDA-TMPDA and 6FDA-TMPDA/azide (70-30) films

8.3 Conclusions

The in-situ polymerization of azide within rigid polyimide frameworks creates homogeneous pseudo-IPNs with enhanced gas transport properties. The tendency of the nitrenes to react with C-H bonds is a potentially useful way of functionalizing unactivated C-H bonds that are present in numerous polymers. The incorporation and polymerization of azide within the host polyimide effectively manipulates the cavity size and free volume distribution. The exploration of this synthetic approach on dense flat membranes provides the fundamental understanding of the pseudo-IPNs formation and their physiochemical properties. As a continuation of this study, the future work should be devoted to investigating (1) the feasibility of this approach on asymmetric membranes, (2) the

possibility of using other azido-containing monomers for tuning the free volume distribution, and (3) the potential use of this material for other applications.

The applicability of this approach to asymmetric membranes is undeniably challenging due to the complexity of the pseudo-IPN formation coupled with the phase inversion process. The formation of the pseudo-IPN prior to phase inversion may be required if the extractability of the azido-containing monomer by the external coagulant poses a problem. For the spinning of hollow fibers, the pre-heating of the polymer dope in the syringe pump or within the spinneret leads to partial formation of the pseudo-IPN. This reduces the extractability of the azido-monomers from the extruded fibers during precipitation. To fabricate flat asymmetric membranes, the partial evaporation of the as-cast film at elevated temperatures before immersing into the coagulant bath may be a feasible approach. Another possible solution is the use of appropriate coagulant which is a poor solvent for the azido-monomers. The molecular dimensions of the azido-containing monomer greatly influence the cavity size of the resultant pseudo-IPNs. The azide monomer employed in our study has relatively large molecular dimensions and thus there is a limit on the tuning of the free volume distribution. The choice of other azido-containing monomers with smaller dimensions may create pseudo-IPNs that are beneficial for H_2/CO_2 separation. It may also be possible to create pseudo-IPNs with multi-modal free volume distribution via utilizing appropriate combinations of monomers with different molecular dimensions. Pseudo-IPNs with multi-modal free volume distribution may achieve simultaneous increase in both permeability and permselectivity. Due to the nature of the nitrene reactions, amine derivatives are formed which possibly

alters the hydrophilicity of the material. Therefore, the polyimide/poly(azide) pseudo IPNs may be useful in pervaporation (e.g. alcohol dehydration) and vapor permeation applications.

8.4 References

[1] Y. Xiao, B. T. Low, S. S. Hosseini, T. S. Chung, D. R. Paul, The strategies of molecular architecture and modification of polyimide-based membranes for CO_2 removal from natural gas-A review, Prog. Polym. Sci. 34 (2009) 561.

[1] J. Lemanski, G. Lipscomb, Effect of shell-side flows on hollow-fiber membrane device performance, AIChE J. 41 (1995) 2322.

[2] B. D. Bhide, S. A. Stern, Membrane processes for the removal of acid gases from natural gas. II. Effects of operating conditions, economic parameters, and membrane properties, J. Membr. Sci. 81 (1993) 239

[3] V. Abetz, T. Brinkmann, M. Dijkstra, K. Ebert, D. Fritsch, K. Ohlrogge, D. Paul, K. V. Peinemann, S. P. Nunes, N. Scharnagl, M. Schossig, Developments in membrane research: from material via process design to industrial application, Adv. Eng. Mater. 8 (2006) 328.

[4] R. W. Baker, Future directions of membrane gas separation technology, Ind. Eng. Chem. Res. 41 (2002) 1393.

[5] S. A. Stern, Polymers for gas separations: the next decade, J. Membr. Sci. 94 (1994) 1.

[6] H. Lin, E. Van Wager, B. D. Freeman, L. G. Toy, R. P. Gupta, Plasticization-enhanced hydrogen purification using polymeric membranes, Science 311 (2006) 639.

[7] A. J. Kelkar, D. R. Paul , Water vapor transport in a series of polyarylates, J. Membr. Sci. 181 (2001) 199.

[8] H. B. Park, C. H. Jung, Y. M. Lee, A. J. Hill, S. J. Pas, S. T. Mudie, E. Van Wagner, B. D. Freeman, D. J. Cookson, Polymers with cavities tuned for fast selective transport of small molecules and ions, Science 318 (2007) 254.

[9] C. E. Sroog, Polyimides, Prog. Polym. Sci. 16 (1991) 561.

[10] M. L. Cecopieri-Gómez, J. Palacios-Alquisira, J. M. Domínguez, On the limits of gas separation in CO_2/CH_4, N_2/CH_4 and CO_2/N_2 binary mixtures using polyimide membranes, J. Membr. Sci. 293 (2007) 53.

[11] M. R. Coleman, W. J. Koros, Isomeric polyimides based on fluorinated dianhydrides and diamines for gas separation applications, J. Membr. Sci. 50 (1990) 285.

[12] Y. C. Wang, S. H. Huang, C. C. Hu, C. L. Li, K. R. Lee, D. J. Liaw, J. Y. Lai, Sorption and transport properties of gases in aromatic polyimide membranes, J. Membr. Sci. 248 (2005) 15.

[13] A. Car, C. Stropnik, W. Yave, K.-V. Peinemann, Tailor-made Polymeric Membranes based on Segmented Block Copolymers for CO_2 Separation, Adv. Funct. Mater. 18 (2008) 2815.

[14] N. P. Patel, R. J. Spontak, Mesoblends of polyether block copolymers with poly(ethylene glycol), Macromolecules 37 (2004) 1394.

[15] R.A. Hayes, Amine-modified polyimide membranes, US Patent No. 4,981,497 (1991).

[16] Y. Xiao, T. S. Chung, M. L. Chng, Surface characterization, modification chemistry and separation performance of polyimide and PAMAM dendrimer composites, Langmuir 20 (2004) 8230.

[17] L. Shao, L. Liu, S. X. Cheng, Y. D. Huang, J. Ma, Comparison of diamino crosslinking in different polyimide solutions and membranes by precipitation observation and gas transport, J. Membr. Sci. 312 (2008) 174.

[18] B. T. Low, Y. Xiao, T. S. Chung, Y. Liu, Simultaneous occurrence of chemical grafting, crosslinking and etching on the surface of polyimide membranes and their impact on H_2/CO_2 separation, Macromolecules 41 (2008) 1297.

[19] C. E. Powell, X. J. Duthie, S. E. Kentish, Reversible diamine cross-linking of polyimide membranes, J. Membr. Sci. 291 (2007) 199.

[20] J. D. Wind, D. R. Paul , W. J. Koros, Natural gas permeation in polyimide membranes, J. Membr. Sci. 228 (2004) 227.

[21] J. D. Wind, C. Staudt-Bickel, D. R. Paul, W. J. Koros, Solid-state covalent cross-linking of polyimide membranes for carbon dioxide plasticization reduction, Macromolecules 36 (2003) 1882.

[22] I. C. Omole, S. J. Miller, W. J. Koros, Increased molecular weight of a cross-linkable polyimide for spinning plasticization resistant hollow fiber membranes, Macromolecules 41 (2008) 6367.

[23] B. Kruczek, T. Matsuura, Effect of metal substitution of high molecular weight sulfonated polyphenylene oxide membranes on their gas separation performance, J. Membr. Sci. 167 (2000) 203.

[24] M. D. Guiver, G. P. Robertson, Y. Dai, F. Bilodeau, Y. S. Kang, K. J. Lee, Structural characterization and gas-transport properties of brominated Matrimid polyimide, J. Polym. Sci. Part A: Polym. Chem. 40 (2003) 4193.

[25] J. B. Ilconich, X. Xu, M. Coleman, P. J. Simpson, Impact of ion beam irradiation on microstructure and gas permeance of polysulfone asymmetric membranes, J. Membr. Sci. 214 (2003) 143.

[26] R.-C. Ruaan, T.-H. Wu, S.-H. Chen, J.-Y. Lai, Oxygen/nitrogen separation by polybutadiene/polycarbonate composite membranes modified by ethylenediamine plasma, J. Membr. Sci. 138 (1998) 213.

[27] Y. Maeda, D. R. Paul, Selective gas transport in miscible PPO-PS blends, Polymer 26 (1985) 2055.

[28] N. Muruganandam, D. R. Paul, Evaluation of substituted polycarbonates and a blend with polystyrene as gas separation membranes, J. Membr. Sci. 34 (1987) 185.

[29] A. Bos, I. Punt, H. Strathmann, M. Wessling, Suppression of gas separation membrane plasticization by homogeneous polymer blending, AIChE J. 47 (2001) 1088.

[30] S. S. Hosseini, M. M. Teoh, T. S. Chung, Hydrogen separation and purification in membranes of miscible polymer blends with interpenetration networks, Polymer 49 (2008) 1594.

[31] I. Gitsov, C. Zhu, Novel functionally grafted pseudo semi-interpenetrating networks constructed by reactive linear-dendritic copolymers, J. Am. Chem. Soc. 125 (2003) 11228.

[32] J. M. Meseguer Dueñas, D. Torres Escuriola, G. Gallego Ferrer, M. Monleón Pradas, J. L. Gómez Ribelles, P. Pissis, A. Kyritsis, Miscibility of poly(butyl acrylate)−poly(butyl methacrylate) sequential interpenetrating polymer networks, Macromolecules 2001, 34, 5525.

[33] S. B. Pandit, S. S. Kulkarni, V. M. Nadkarni, Interconnected interpenetrating polymer networks of polyurethane and polystyrene. 2. Structure-property relationships, Macromolecules 27 (1994) 4595.

[34] T. Tamai, A. Imagawa, Q. Tran-Cong, Semi-interpenetrating polymer networks prepared by in situ photo-crosslinking of miscible polymer blends, Macromolecules 27 (1994) 7486.

[35] C. Leger, Q. T. Nguyen, J. Neel, C. Streicher, Level and kinetics of PVP extraction from blends, interpenetrating polymer blends and semiinterpenetrating polymer networks, Macromolecules 28 (1995) 143.

[36] M. Wang, K. P. Pramoda, S. H. Goh, Mechanical behavior of pseudo-semi-interpenetrating polymer networks based on double-C60-end-capped poly(ethylene oxide) and poly(methyl methacrylate), Chem. Mater. 16 (2004) 3452.

[37] A. Izuka, H. H. Winter, T. Hashimoto, Self-similar relaxation behavior at the gel point of a blend of a cross-linking poly(ε-caprolactone) diol with a poly(styrene-co-acrylonitrile), Macromolecules 30 (1997) 6158.

[38] J. Kurdi, A. Kumar, Formation and thermal stability of BMI-based interpenetrating polymers for gas separation membranes, J. Membr. Sci. 280 (2006) 234.

[39] M. L. Chng, Y. Xiao, T.-S. Chung, M. Torrida, S. Tamai, Enhanced propylene/propane separation by carbonaceous membrane derived from poly(aryletherketone)/2,6-bis(4-azidobenzylidene)-4-methyl-cyclohexanone interpenetrating network, Carbon 47 (2009) 1857.

[40] A. Bos, I. G. M. Punt, M. Wessling, H. Strathmann, Suppression of CO_2-plasticization by semiinterpenetrating polymer network formation, J. Polym. Sci. Part B Polym. Phys. 36 (1998) 1547.

[41] D. S. Lee, W. K. Kang, J. H. An, S. C. Kim, Gas transport in polyurethane-polystyrene interpenetrating polymer network membranes. II. Effect of crosslinked state and annealing, J. Membr. Sci. 75 (1992) 15.

[42] J. Kurdi, A. Kumar, Structuring and characterization of a novel highly microporous PEI/BMI semi-interpenetrating polymer network, Polymer 46 (2005) 6910.

[43] S. Saimani, A. Kumar, Semi-IPN asymmetric membranes based on polyether imide (ULTEM) and polyethylene glycol diacrylate for gaseous separation, J. Appl. Polym. Sci. 110 (2008) 3606.

[44] C. J. Moody, G. H. Whitham, Reactive intermediates. New York, Oxford University Press, 1992.

[45] G. Socrates, Infrared and Raman characteristic group frequencies: tables and charts 3rd edition, New York, Wiley; 2000.

[46] R. T. Morison, R. N. Boyd, Organic Chemistry, 6th edition, 1992, Prentice Hall, USA.

[47] S. D. Kelman, B. W. Rowe, C. W. Bielawski, S. J. Pas, A. J. Hill, D. R. Paul, B. D. Freeman, Crosslinking poly[1-(trimethylsilyl)-1-propyne] and its effect on physical stability, J. Membr. Sci. 320 (2008) 123.

[48] L. Shao, J. Samseth, M.-B. Hägg, Crosslinking and stabilization of nanoparticle filled PMP nanocomposite membranes for gas separations, J. Membr. Sci. 326 (2009) 285.

[49] P. Kirkegaard, M. Eldrup, O. E. Mogensen, N. J. Pedersen, Program system for analysing positron lifetime spectra and angular correlation curves, Comput. Phys. Commun. 23 (1981) 307.

[50] S. J. Lue, D.-T. Lee, J.-Y. Chen, C.-H. Chiu, C.-C. Hu, Diffusivity enhancement of water vapor in poly(vinyl alcohol)–fumed silica nano-composite membranes: Correlation with polymer crystallinity and free-volume properties, J. Membr. Sci. 325 (2008) 831.

[51] A. Shukla, L. Hoffmann, A. A. Manuel, M. Peter, Melt 4.0 a program for positron lifetime analysis, Mater. Sci. Forum 255 (1997) 233.

[52] M.-L. Cheng, Y.-M. Sun, H. Chen, Y. C. Jean, Change of structure and free volume properties of semi-crystalline poly(3-hydroxybutyrate-co-3-hydroxyvalerate) during thermal treatments by positron annihilation lifetime, Polymer 50 (2009) 1957.

[53] A. Y. Alentiev, Y. P. Yampolskii, Meares equation and the role of cohesion energy density in diffusion in polymers, J. Membr. Sci 206 (2002) 291.

CHAPTER 9

CONCLUSIONS AND RECOMMENDATIONS

9.1 Conclusions

9.1.1 A review of the research objectives of this work

The potential of using membrane technology for hydrogen and natural gas purifications is evident. Polymers are the preferred materials for fabricating gas separation membranes due to the ease of processability, and relatively lower material and fabrication costs. For H_2/CO_2 separation, because of the undesirable coupling of high H_2 diffusivity with CO_2 solubility, majority of the polymeric membranes display poor intrinsic H_2/CO_2 permselectivity. Hence, the search is on for polymeric membranes with better H_2/CO_2 separation performance. For the purification of natural gas, polymers with recommendable CO_2/CH_4 separation performance are available and the next step is to enhance the anti-plasticization property of the material.

In this work, the diamine modification of polyimide membranes with aliphatic diamines to enhance the H_2/CO_2 separation performance has been investigated. The chemistry and key factors that influence the effectiveness of the modification approach are examined systematically. This technique is demonstrated on asymmetric hollow fiber membranes which are of greater commercial importance. A novel pseudo-interpenetrating polymer network comprising of a polyimide and an azido-containing monomer is used for CO_2/CH_4 separation and the anti-plasticization properties of the membrane are characterized.

9.1.2 Diamine modification of polyimide dense membranes for H_2/CO_2 separation

Diamine modification is an effective approach for enhancing the intrinsic H_2/CO_2 selectivity of polyimide membranes. The properties of diamines and polyimides affect the degree of crosslinking and hence the increment in H_2/CO_2 selectivity that can be reaped. A series of aliphatic diamines with different spacer lengths has been investigated and 1,3-diaminopropane (PDA) is found to be the most appropriate modification reagent for copoly(4,4'-diphenyleneoxide/1,5-naphthalene-2,2'-bis(3,4-dicarboxylphenyl) hexafluoro propane diimide (6FDA-ODA/ NDA (50:50)) dense membranes. An increment in the ideal H_2/CO_2 selectivity from 2.3 to 64 is obtained after an immersion duration of 90 min. Chemical grafting, crosslinking and chain scission occur simultaneously during the diamine modification. The extent of each reaction type is dependent on the nucleophilicity and molecular dimensions of the diamines. The appropriate selections of diamine and modification duration are required to crosslink the polymer chains substantially for achieving the better gas separation performance.

The combination of polyimide molecular design and diamine modification represents an excellent approach for optimizing the enhancement in H_2/CO_2 permselectivity of polyimide membranes. Two important parameters (i.e. polymer free volume and rigidity) that influence the effectiveness of PDA modification in improving the H_2/CO_2 selectivity have been identified. Polymer free volume affects the degree of methanol swelling which in turn determines the extent of diamine penetration and reaction. Therefore, a polyimide with a higher free volume generates a denser diamine-modified network which is

necessary for improving H_2/CO_2 selectivity. The polymer rigidity affects the ability of the polymer to maintain its chain stiffness upon the destruction of the imide rings during the diamine treatment. Hence, a polyimide with greater rigidity leads to a modified polymer network with restricted chain movements, thereby improving the H_2/CO_2 selectivity. 6FDA-NDA has the highest free volume and rigidity, thus exhibiting remarkable improvement in ideal H_2/CO_2 selectivity from 1.8 to 120 after modification. Conversely, 6FDA-ODA which is deficient in terms of free volume and rigidity, demonstrates marginal increment in H_2/CO_2 selectivity from 2.6 to 8.3.

9.1.3. Modification of 6FDA-NDA/PES dual layer hollow fiber membranes with 1,3-diaminopropane

The fundamental investigations on the modification of polyimide dense membranes with aliphatic diamines lay the foundation for scaling up the technique to asymmetric hollow fiber membranes which are of greater commercial importance. Dual-layer 6FDA-NDA/ polyethersulfone (PES) hollow fiber membranes are fabricated via the dry jet/wet spinning and are subsequently post-treated with 1,3-diaminopropane (PDA). Interestingly, the optimal air gap for maximizing the gas pair selectivity varies for the different gas pairs and two hypotheses are proposed to explain the observed phenomenon. A higher air gap reduces the population of Knudsen pores in the apparently dense outer skin layer and induces greater elongational stresses on the polymer chains. The latter enhances polymer chain alignment and packing which possibly results in the shift and sharpening of the free volume distribution.

The fibers spun at a lower air gap exhibit higher H_2 permeance and H_2/CO_2 selectivity, and are selected for PDA modification. Due to the influence of methanol swelling and the high initial diffusion rates of the diamines, the chemical post-treatment densifies the entire polyimide outer layer. This creates additional resistance to gas transport which hinders the enhancement in H_2/CO_2 permselectivity that can be reaped. The PDA modified 6FDA-NDA/PES hollow fibers exhibit good anti-swelling properties against CO_2, and an increment in H_2 permeance can be obtained at higher temperatures with negligible decrease in the H_2/CO_2 permselectivity.

9.1.4 Pseudo-interpenetrating polymer network for CO_2/CH_4 separation

The formation of homogenous pseudo-interpenetrating polymer networks (IPN) to alter the free volume distribution of polyimide membranes is explored. The pseudo-IPNs consist of a polymer network formed by azido-containing monomers and fluorinated polyimides. The changes in the gas permeability and gas pair permselectivity of the semi-IPNs are adequately mapped to the variation in the free volume distributions characterized by the positron annihilation lifetime spectroscopy. Depending on the functionalities of the host polyimides, chemical cross-links are formed between the azide network and the pre-formed linear polyimide. The pseudo-IPNs display improved CO_2/CH_4 separation performance and better chemical resistance. The chemical bridges in conjunction with the interpenetrating network restrict the mobility of the polymer chains and suppress CO_2-induced plasticization.

9.2 Recommendations

9.2.1 Motivation

In the preceding studies, the chemical modification approaches to improve the H_2/CO_2 and CO_2/CH_4 separation performance of glassy polymeric membranes have been explored. The rationale for using the diamine modification approach and the formation of the pseudo-interpenetrating network is to increase the H_2/CO_2 and CO_2/CH_4 diffusivity selectivity via the reduction in free volume and the restriction of polymer chain mobility. For the separation of CO_2/CH_4 using glassy polymers, altering the CO_2 solubility via interactions with different chemical functional groups may be beneficial. Previous studies have shown that organic-inorganic hybrid membranes may yield promising gas separation performance but the poor adhesion between the phases poses a significant challenge. It may be possible to circumvent this issue by utilizing sub-nano fillers to form molecular level mixed matrix membranes and to anchor the filler to the polymer via chemical reactions. It would be interesting to examine the use of rubbery polymers to fabricate reverse-selective membranes for CO_2. In addition to the future membrane research from the material aspect, the operational issues need to be taken into account. The pure and mixed gas permeation tests were conducted under dry conditions and in reality, water vapor will be present in varying amounts in the feed stream to be purified. This is especially true for the purification of hydrogen since the gas stream comes from a water gas shift reactor. Therefore, it is necessary to establish the gas separation performance of the membranes in the presence of water vapor.

9.2.2 Effect of grafting different functional groups on polyimide membranes

The covalent reaction between the imide and amine groups is a convenient approach to graft different functional groups on the polymer chain. The objective of grafting different functional groups is to enhance the interactions between the gas molecules, in particular CO_2 and the polymer matrix. This may enhance the CO_2 solubility and CO_2/CH_4 solubility selectivity. The introduction of amino-compounds to the polyimide matrix inevitably reduces the polymer free volume due to space-filling effects. To reduce the molecular sieving effects brought about by the reduction in free volume, a polyimide with exceptionally high free volume is chosen the preferred working polymer. A series of aliphatic amino-compounds with different end-cap functional groups will be used for chemical grafting and the CO_2/CH_4 separation performance of the grafted membrane will be performed under dry and wet conditions.

9.2.3 Polyimide/POSS® hybrid membranes for CO_2/CH_4 separation

Polyhedral oligomeric silsesquioxane® (POSS®) is a potential filler for fabricating mixed matrix membranes. The cage size of POSS® is relatively large and is not likely to enhance the molecular sieving capability of the gas separation membranes. However, it may be utilized to enhance the gas permeability. Several commercial polymers including, polyetherimide (e.g. Ultem®), poly(amide-imide) (e.g. Torlon®) and polyimide (e.g. P84® copolyimide) have good intrinsic CO_2/CH_4 selectivity but poor CO_2 permeability. Some preliminary investigations on organic-inorganic hybrid membranes containing POSS as

the dispersed phase and the abovementioned commercial polyimides as the continuous organic matrix have been conducted. The POSS® fillers are grafted to the polyimide chains prior to membrane fabrication for better particle dispersion. Our preliminary data suggests that the use of appropriate POSS® loading with a polymer with suitable inherent properties brings about significant enhancement in the gas permeability while maintaining the gas pair selectivity. This approach will be scaled up to dual-layer hollow fiber membranes and the gas transport properties of the as-spun fibers will be characterized.

9.2.4 Effect of the sulfonation degree on the gas separation performance of poly(ether ether ketone)

Poly(ether ether ketone) (PEEK) is commonly utilized as a membrane material for fuel cell applications and has not been widely used for gas separation. PEEK is a relatively solvent resistance material that is not compatible with common organic solvents. An approach to improve the processability of PEEK is to introduce sulfonic acid groups to the polymer chain. It has been reported that the presence of sulfonic acid groups appreciably alters the gas transport behavior of the membranes, especially in the presence of water vapor. Hence, it is worthwhile to investigate the effect of different sulfonation degree on the gas separation performance. The sulfonation of PEEK introduces anionic sites which may be utilized for further modification. Chemicals with cationic functional groups can be used for grafting or crosslinking to enhance the gas transport properties. Compared to covalent crosslinking (e.g. diamine and diol crosslinking of polyimide), the ionic crosslinking of polymeric membranes for gas separation is less studied.

9.2.5 CO_2-selective polymers based on poly(ethylene oxide) units

Poly(ethylene oxide) (PEO) has been extensively investigated as a material for fabricating CO_2-selective membranes. The strong affinity between the ethylene oxide units and CO_2 accounts for the favorable CO_2 transport. However, one deficiency of pure PEO is its high tendency to crystallize and poor mechanical properties. The formation of crosslinked networks with PEO as the entities have been studied to overcome the shortcomings of PEO. Here, an alternative approach to fabricate crosslinked PEO membranes is proposed. Oligomers comprising of mainly EO units with small amounts of propylene units (PO) will be used in conjunction with an azido-containing compound with multi-reactive sites. The in-situ formation of the crosslinked polymer and the CO_2/H_2 separation performance of the membranes will be examined.